eCAM Evidence-Based Complementary and Alternative Medicine

Natural Bioactives and Phytochemicals Serve in Cancer Treatment and Prevention

Guest Editors: Shun-Fa Yang, Chia-Jui Weng, Gautam Sethi, and Dan-Ning Hu

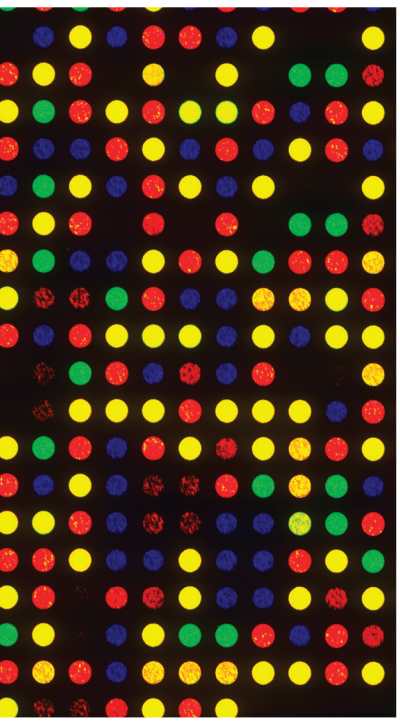

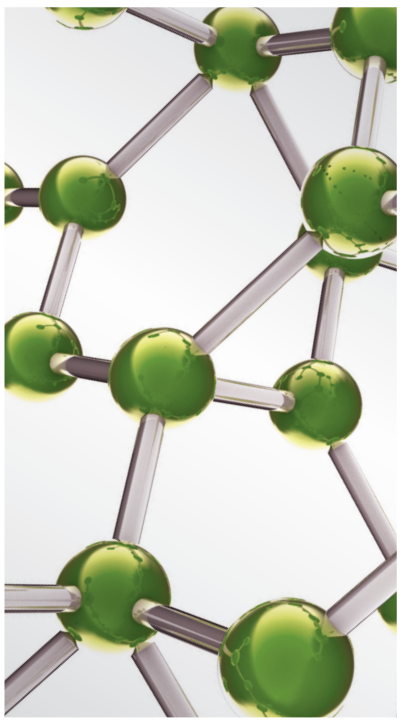


Natural Bioactives and Phytochemicals Serve in Cancer Treatment and Prevention

Evidence-Based Complementary and Alternative Medicine

Natural Bioactives and Phytochemicals Serve in Cancer Treatment and Prevention

Guest Editors: Shun-Fa Yang, Chia-Jui Weng, Gautam Sethi, and Dan-Ning Hu

Editorial Board

Contents

Inhibition of Metastatic Potential in Breast Carcinoma *In Vivo* and *In Vitro* through Targeting VEGFRs and FGFRs, Ming-Hsien Chien, Liang-Ming Lee, Michael Hsiao, Lin-Hung Wei, Chih-Hau Chen, Tsung-Ching Lai, Kuo-Tai Hua, Min-Wei Chen, Chung-Ming Sun, and Min-Liang Kuo
Volume 2013, Article ID 718380, 13 pages

Hindawi Publishing Corporation
Evidence-Based Complementary and Alternative Medicine
Volume 2013, Article ID 698190, 1 page
http://dx.doi.org/10.1155/2013/698190

Editorial

Natural Bioactives and Phytochemicals Serve in Cancer Treatment and Prevention

Shun-Fa Yang,[1,2] Chia-Jui Weng,[3] Gautam Sethi,[4] and Dan-Ning Hu[5]

[1] *Institute of Medicine, Chung Shan Medical University, Taichung 402, Taiwan*
[2] *Department of Medical Research, Chung Shan Medical University Hospital, Taichung 402, Taiwan*
[3] *Graduate Institute of Applied Living Science, Tainan University of Technology, Tainan City 710, Taiwan*
[4] *Department of Pharmacology, Yong Loo Lin School of Medicine, National University of Singapore, Singapore 119077*
[5] *Tissue Culture Center, New York Eye and Ear Infirmary, New York Medical College, New York, NY 10009, USA*

Correspondence should be addressed to Shun-Fa Yang; ysf@csmu.edu.tw

Received 5 December 2013; Accepted 5 December 2013

Natural bioactives or phytochemicals are generally referred to as the compounds that have specific biological activity in human. Studies have shown that natural phytochemicals derived from certain plants have the capability to prevent carcinogenesis. In this special issue, we collected numerous studies which provide novel evidence to support the opinion. For instance, [6]-gingerol prevents disassembly of cell junctions and activities of MMPs in invasive human pancreas cancer cells; butein inhibits angiogenesis of human endothelial progenitor cells; the anticancer effects of sterol fraction come from red algae porphyra dentata; zeaxanthin induces apoptosis in human uveal melanoma cells; and ocotillol enhanced the antitumor activity of doxorubicin. It is therefore believed that the appropriate application of natural bioactives or phytochemicals should be a supplementary and safe way to prevent carcinogenesis and/or to enhance the efficacy of cancer therapy.

Shun-Fa Yang
Chia-Jui Weng
Gautam Sethi
Dan-Ning Hu

Hindawi Publishing Corporation
Evidence-Based Complementary and Alternative Medicine
Volume 2013, Article ID 817674, 9 pages
http://dx.doi.org/10.1155/2013/817674

Research Article

Subtoxic Levels of Apigenin Inhibit Expression and Secretion of VEGF by Uveal Melanoma Cells via Suppression of ERK1/2 and PI3K/Akt Pathways

Shih-Chun Chao,[1,2] Sheng-Chieh Huang,[2] Dan-Ning Hu,[3] and Hung-Yu Lin[1,4]

[1] *Department of Ophthalmology, Show Chwan Memorial Hospital, Changhua 500, Taiwan*
[2] *Institute of Electrical and Computer Engineering, National Chiao Tung University, Hsinchu 30010, Taiwan*
[3] *Tissue Culture Center, The New York Eye and Ear Infirmary, NY 10003, USA*
[4] *Department of Optometry, Yuan Pei University, Hsinchu 30015, Taiwan*

Correspondence should be addressed to Hung-Yu Lin; anthonyhungyulin@hotmail.com

Received 5 September 2013; Accepted 23 September 2013

Academic Editor: Shun-Fa Yang

The effects of apigenin on the expression of VEGF in uveal melanoma cells have not been reported. We studied this effect and relevant signaling pathways in two human uveal melanoma cell lines (SP6.5 and C918). ELISA assay revealed that the constitutive secretion of VEGF by uveal melanoma cells was 21-fold higher than that in normal uveal melanocytes. Apigenin at subtoxic levels (1–5 μM) significantly suppressed the secretion of VEGF in a dose- and time-dependent manner in melanoma cells. VEGF levels in the conditioned culture media from SP6.5 and C918 cell lines treated with 5 μM apigenin for 24 h reduced to 29% and 21% of those in cells not treated with apigenin, respectively. RT-PCR analysis found that apigenin also decreased the expression of VEGF mRNA in melanoma cells. ELISA study of various signal pathways showed that apigenin significantly decreased phosphorylated Akt and ERK1/2 but increased phosphorylated JNK1/2 and p38 MAPK levels in melanoma cells. PI3K/Akt or ERK1/2 inhibitors significantly decreased, but JNK1/2 and p38 MAPK inhibitors did not influence the secretion of VEGF by melanoma cells, suggesting that apigenin suppresses the secretion of VEGF mainly through the inhibition of PI3K/Akt and ERK1/2 pathways.

1. Introduction

Uveal melanoma is the most common primary malignant intraocular tumor in adults in western countries [1]. This malignant tumor develops in one of the most capillary-rich tissues of the body and has a purely hematogenous dissemination. The mortality rate of uveal melanoma, is high because of the frequent occurrence of metastases, mainly in the liver. There is no efficient treatment for metastatic uveal melanoma and most of these patients died within 6 months after the metastasis [2, 3].

Angiogenesis is required for tumor growth and metastasis. VEGF or VEGF A is a vascular endothelial mitogen and stimulator of angiogenesis. VEGF plays a critical role in tumor angiogenesis and in the growth and metastasis of various cancers [4, 5]. It has been reported that uveal melanoma cells have a high constitutive expression and secretion of VEGF [6, 7]. A high serum VEGF level is associated with metastasis of uveal melanoma [8, 9]. Therefore, inhibiting the secretion of VEGF is becoming a target for uveal melanoma therapy [6].

Flavonoids are a family of polyphenolic compounds synthesized by plants with a similar structure and are divided into subclasses, including anthocyanidins, flavanols, flavanones, flavonols, flavones, and isoflavones. Epidemiological and case-control studies have suggested that high intake of various flavonoids from vegetables and fruits were inversely associated with risk of various cancers [10, 11]. Apigenin is a flavonoid belonging to the flavone subgroup and is present in various fruits, vegetables, herbs, and Chinese traditional medications [10, 11]. Apigenin inhibits the growth and invasion of various types of cancer in experimental

animals and in vitro [10, 11]. Recently, it has been reported that apigenin also inhibits the secretion of VEGF in several types of malignant tumor cells [12–21].

The effects of apigenin on the expression and secretion of VEGF by uveal melanoma cells have not been reported. We have developed the methodology for isolation, cultivation, and study of normal human uveal melanocytes, established many uveal melanocyte cell lines, and collected several human uveal melanoma cell lines [22–25]. The purpose of this study was to compare the constitutive secretion of VEGF in uveal melanoma with normal uveal melanocytes, and to investigate the effects of apigenin on the expression and secretion of VEGF by uveal melanoma cells and the relevant signal pathways.

2. Materials and Method

2.1. Reagents. F-12 culture medium, Dulbecco's modified Eagle's medium (DMEM), fetal bovine serum (FBS), phosphate buffered saline (PBS), 0.05% trypsin-0.02% EDTA solution, and gentamicin were purchased from GIBCO (Grand Island, NY, USA). Apigenin, isobutylmethylxanthine, cholera toxin, dimethyl sulfoxide (DMSO), and 3-[4,5-dimethylthiazol-2-yl]-2,5-diphenyltetrazolium bromide (MTT) were purchased from Sigma (St. Louis, MO, USA). Basic fibroblast growth factor was purchased from PeproTech (Rocky Hill, NJ, USA).

2.2. Cell Culture. The constitutive levels of VEGF secretion were tested in three human uveal melanoma cell lines (MP17, SP6.5 and C918) and compared to those in three different human normal uveal melanocyte cell lines. M17 melanoma cell line (isolated from a primary choroidal melanoma patient), and primary cultures of human normal uveal melanocytes (all from the choroid) were established in the Tissue Culture Center of the New York Eye and Ear Infirmary as previously reported [22]. SP6.5 melanoma cell line was isolated from a primary choroidal melanoma patient and was provided by Dr. Guy Pelletier (Research Center of Immunology, Quebec, Canada) [26]. Melanoma cell line C918 was derived from a choroidal melanoma patient with liver metastasis at the University of Iowa and was provided by Dr. Robert Folberg (University of Illinois, Chicago) and Dr. Xiaoliang Leon Xu (Memorial Sloan Kettering Cancer Center, NY) [27]. Both M17 and SP.6.5 cell lines were originated from nonmetastatic uveal melanoma, and C918 is a metastatic and aggressive melanoma cell line [22, 26, 27]. Uveal melanoma cells were cultured in DMEM culture medium with 10% FBS, and uveal melanocytes were cultured in FIC medium with 10% FBS [22]. Cells were incubated at 37°C in a CO_2 regulated incubator in a humidified 95% air/5% CO_2 atmosphere. After cultures reached confluence, cells were detached with trypsin-EDTA solution and passaged. All tissues were obtained with premortem consent in accordance with the laws and regulations in place in the various jurisdictions.

2.3. Comparison of VEGF Secretion between Uveal Melanoma Cells and Normal Melanocytes. Early passages of three cell lines of cultured uveal melanocytes and three cell lines of uveal melanoma (M17, SP6.5 and C918) were plated into 24-well plates at a density of 1×10^5 per well. After 24 h, the culture medium was withdrawn, washed with PBS, and replaced with serum-free culture medium. Conditioned media were collected 24 h later, centrifuged, and the supernatants were stored at −70°C until analysis. All experiments were performed in triplicate.

2.4. MTT Assay for Cell Viability. Uveal melanoma cells were seeded into 96-well plates at a density of 5×10^3 cells per well. Apigenin (1.08 mg) was dissolved in 1 mL DMSO to make a stock solution of 2 mM. The cells in the control group were cultured in medium containing the same levels of DMSO as in the apigenin solution. After 48 h cultured with apigenin, MTT solution (1 mg/mL, 50 μL) was added. After 4 h incubation, the medium and MTT were aspirated and 100 μL of DMSO was added. Optical density of the plates was determined with a microplate reader (Multiskan MCC/340, Fisher Scientific, Pittsburgh, PA, USA) at 540 nm. The optical density in control (untreated) cells was taken as 100% viability. All tests were performed in three independent experiments.

2.5. VEGF Secretion in Uveal Melanoma Cells with Apigenin Stimulation. Uveal melanoma cells (SP6.5 and C918) were plated into 24-well plates at a density of 1×10^5 per well. In the dose-effect study, after 24 h culture, the cultured medium was withdrawn, washed, and replaced with serum-free medium. Apigenin at different concentrations (0, 1.0, 2.0, and 5.0 μM) was added to the media. After 24 h, conditioned media were collected and stored as described above. In the time-effect study, apigenin at 5 μM was added into the culture medium. Conditioned media were collected at 6, 12, and 24 h later and stored as described above. Cultures without apigenin were used as the control. All tests were performed in three independent experiments.

2.6. Measurement of VEGF Levels. The amount of VEGF protein in the conditioned media was determined using the human VEGF (VEGF-A) Quantikine ELISA kit (R&D Systems, Minneapolis, MN, USA) according to the manufacturer's instructions. Optical density was read by using a microplate reader at 450 nm. The amount of VEGF (pg/mL) was calculated from a standard curve. The sensitivity of this kit was 5 pg/mL.

2.7. RNA Isolation and RT-PCR. Uveal melanoma cells (SP6.5) were plated into 6-well plates at a density of 5×10^5. After 24 h, the culture medium was replaced with serum-free culture medium. Apigenin at different concentrations (0, 1.0, 2.0, and 5.0 μM) was added to the media, and cells were collected at 6 h later. After the culture medium was withdrawn, the cultures were washed with cold PBS, and cells were harvested by scraping with a rubber policeman. Cells cultured without apigenin were used as negative controls. After microcentrifuging at 800 ×g for 5 min at 4°C, cell pellets were collected for mRNA extraction. Total RNA was

isolated with the RNeasy PureLink RNA Mini Kit (Life Technology, Carlsbad, CA, USA), according to the manufacturer's instructions. The SuperScript first-strand synthesis system for RT-PCR kit (Invitrogen, Camarillo, CA, USA) was used to perform cDNA synthesis. The PCR primers for glyceraldehyde-3-phosphate dehydrogenase (GAPDH) were TGAACTGAPIGENINGCTCTCCACC, CTGATGTACCAGTTGGGGAA. VEGF primers were AGGGCAGAATCATCACGAAGT, AGGGTCTCGATTGGATGGCA. Both primers were obtained from Invitrogen. The first-strand cDNAs were synthesized from 0.5 μg of total RNA at 50°C for 50 min. PCR amplification was conducted in a GeneAmp PCR system 9700 (Applied Biosystems, Foster City, CA, USA) using the following parameters: first denaturation at 94°C for 5 min followed by 35 cycles of reactions of denaturation at 94°C for 30 s, annealing at 58°C for 45 s, extension at 72°C for 45 s, and last extension on for 5 min at 72°C. After amplification, samples were run on a 1% agarose gel (Invitrogen) in TBE (0.01 M Tris-borate) 0.001 M EDTA (Invitrogen) containing 2.0 μg/mL ethidium bromide (Invitrogen). Bands were visualized and photographed on a UV transilluminator (ChemiDoc XRS System, Bio-Rad, Hercules, CA, USA).

2.8. Phosphorylated Akt, ERK, JNK, and p38 MAPK Assay. Uveal melanoma cells (SP6.5) were seeded into 6-well plates at a density of 1×10^6. After 24 h, apigenin at different concentrations (0, 1.0, 2.0, and 5.0 μM) was added. After 1 h, the cultures were washed with cold PBS, and cells were harvested by scraping with a rubber policeman. Cells cultured without apigenin were used as the negative controls. After microcentrifuging for 5 min at 4°C, pellets were treated with ice-cold Cell Extraction Buffer (Biosource, Carlsbad, CA, USA) with Protease Inhibitor Cocktail (Sigma) and PMSF (Biosource) for 30 min, with subsequent vortexing at 10 min intervals. Cell extractions were microcentrifuged at 13,000 rpm for 10 min at 4°C. The supernatants were collected and stored at −70°C until analysis. Phosphorylated Akt, extracellular signal-regulated kinases 1/2 (ERK1/2), c-Jun N-terminal kinase (JNK1/2), and p38 mitogen-activated protein kinase (MAPK) measurement were performed in triplicate by using phosphorylated Akt, ERK1/2, JNK1/2 and p38 MAPK ELISA kits (Biosource), respectively, according to the protocol outlined by the manufacturer, and were expressed as percentages of the control (cells not exposed to apigenin). The sensitivity of ERK, JNK, and p38 MAPK ELISA kits was 0.8 U/mL and was 1.6 U/mL for Akt ELISA kit.

2.9. Effects of Akt, ERK, JNK and p38 MAPK Inhibitors on Secretion of VEGF by Uveal Melanoma Cells. Uveal melanoma cells were plated into 24-well plates at a density of 1×10^5 cells per well. After 24 h incubation, the medium was changed, and various signal inhibitors were added to the medium separately, including 10 μM of LY294002 (PI3K/Akt inhibitor), UO1026 (ERK inhibitor), SP600125 (JNK inhibitor), and SB203580 (p38 MAPK inhibitor), all from Calbiochem, San Diego, CA, USA. Thirty min later, apigenin was added to the medium at a final concentration of 5 μM. Cells cultured without any signal inhibitor were used as the controls. After 24 h incubation, the conditioned media were collected and stored. The VEGF protein levels in the supernatants were determined using the human VEGF Quantikine ELISA kit as described above. Tests were performed in triplicate.

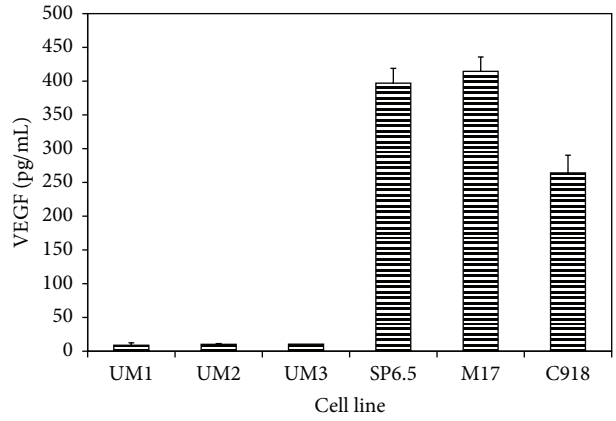

Figure 1: Constitutive secretion of VEGF by human uveal melanoma cells and normal uveal melanocytes. Three different primary cultures of uveal melanocytes (UM1-3) and uveal melanoma cells from 3 different cell lines (SP6.5, M17, and C918) were plated into 24-well plates. After 24 h, culture medium was removed and cultures were washed by PBS. Serum-free culture medium was added and cultured for 24 h. Conditioned media were collected, and the amount of VEGF protein was determined by using the human VEGF Quantikine ELISA kit. VEGF levels in conditioned culture medium were expressed as pg/mL. VEGF levels in culture medium from melanoma cells were significantly higher than that from normal melanocytes ($P < 0.05$). Data are mean ± SD ($n = 3$).

2.10. Statistical Analysis. Statistical significances of difference of means throughout this study were calculated by ANOVA one-way test in comparing data from more than two groups and Student's t-test in comparing data between two groups. The data was analyzed using SPSS statistical software (SPSS Inc., Chicago, IL, USA). A difference at $P < 0.05$ was considered to be statistically significant.

3. Results

3.1. Comparison of VEGF Secretion between Uveal Melanoma Cells and Uveal Melanocytes. VEGF levels in the conditioned culture media from uveal melanoma and uveal melanocytes were measured and compared. In cells cultured with serum-free medium, VEGF levels were 359 ± 43.6 pg/mL and 14.3 ± 3.7 pg/mL in the conditioned media of uveal melanoma cells and uveal melanocytes, respectively (Figure 1). The VEGF levels in the conditioned medium from uveal melanoma cells were 25-fold those from normal uveal melanocytes; the difference was statistically significant ($P < 0.05$). The secretion of VEGF by uveal melanoma cells (1486 ± 243 pg/10^6 cells/24 h) was also significantly greater than that by normal uveal melanocytes (67.4 ± 4.8 pg/10^6 cells/24 h) ($P < 0.05$), indicating that uveal melanoma cells have a much higher

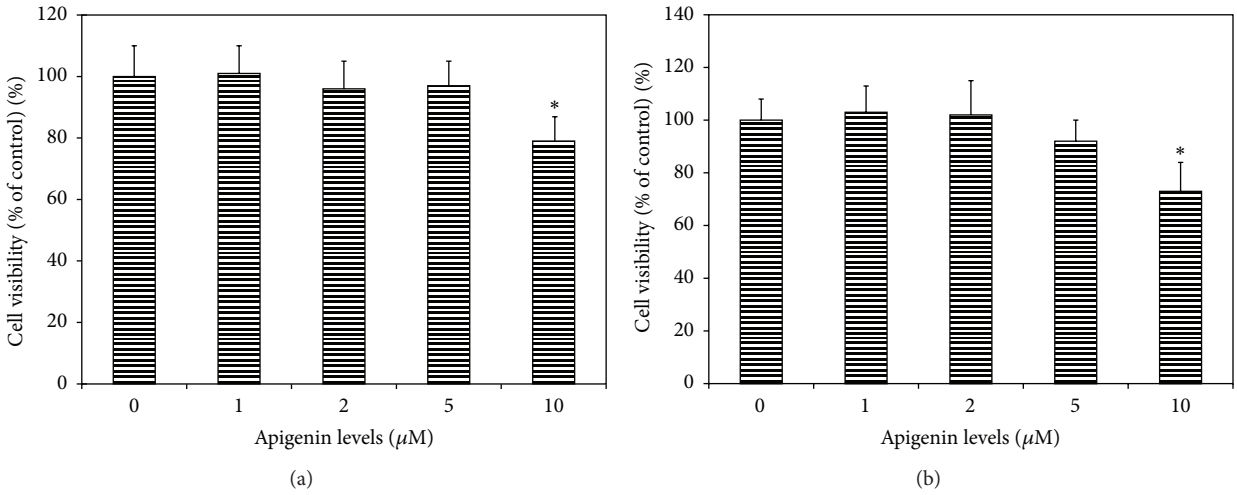

Figure 2: Dose effect of apigenin on cell viability of uveal melanoma cells. Human uveal melanoma cells SP6.5 (a) and C918 (b) were seeded into 96-well plates and treated with apigenin at various doses for 48 h, and cell viability was determined by MTT assay (see Methods). Apigenin at 1–5 μM did not affect, whereas 10 μM apigenin significantly decreased the cell viability of uveal melanoma cells. Data are mean ± SD ($n = 3$). $^{*}P < 0.05$, versus control (cells cultured without apigenin).

constitutively secretion of VEGF (21-fold) as compared with their normal counterparts.

3.2. Effects of Apigenin at Different Levels on Cell Viability of Uveal Melanoma Cells. In uveal melanoma cells (SP6.5 and C918) cultured with apigenin at 1.0–5.0 μM, the reading of MTT test showed no significant difference as compared with cells cultured without apigenin (Figure 2), indicating that apigenin at 5 μM or less did not affect the viability of both cell lines. Cell viability in uveal melanoma cells was decreased only at cells treated with 10 μM apigenin (Figure 2). Therefore, apigenin at 5 μM or less was used for the studies of effects of subtoxic levels of apigenin on the expression and secretion of VEGF from uveal melanoma cells.

3.3. Effects of Apigenin on VEGF Secretion by Uveal melanoma Cells. Apigenin at different levels (1.0, 2.0, and 5.0 μM) significantly decreased the VEGF protein levels in the conditioned medium in a dose-dependent manner (Figure 3). VEGF levels in the conditioned medium from cells (SP6.5) cultured without apigenin were 415 ± 29 pg/mL. VEGF levels in conditioned media from cells cultured with apigenin (1.0, 2.0, and 5.0 μM) for 24 h were 74%, 51%, and 29% of the control values, respectively (Figure 3(a)). The difference of VEGF levels between apigenin treated cells and the controls was statistically significant at all levels of apigenin ($P < 0.05$). Studies in C918 melanoma cell line showed similar results (Figure 3(b)).

Apigenin inhibition of secretion of VEGF by uveal melanoma was also time dependent (Figure 3). VEGF levels in the conditioned media from SP6.5 melanoma cells cultured with apigenin (5.0 μM) for 6, 12, and 24 h were 85%, 54%, and 31% of the control, respectively (Figure 3(c)). The difference of VEGF levels between apigenin treated cells and the controls was statistically significant in cells treated for 6, 12, and 24 h ($P < 0.05$). Studies in C918 melanoma cell line showed similar results (Figure 3(d)).

3.4. Effects of Apigenin on Expression of VEGF mRNA by Uveal Melanoma. The RT- PCR analysis demonstrated that VEGF mRNA was expressed in uveal melanoma cells (SP6.5 cell line) cultured without apigenin (Figure 4). Apigenin decreased VEGF mRNA expression in the uveal melanoma cells in a dose-dependent manner (Figure 4), indicating that apigenin also downregulates the expression of VEGF mRNA in uveal melanoma cells.

3.5. Effects of Apigenin on Phosphorylated Akt, ERK, JNK, and p38 MAPK Levels in Uveal Melanoma Cells. Apigenin treatment (5 μM with 1 h incubation) significantly decreased both phosphorylated Akt and ERK1/2 levels in uveal melanoma cells (SP6.5 cell line) in a dose-dependent manner (Figures 5(a) and 5(b)). On the other hand, phosphorylated JNK1/2 and p38 MAPK levels were significantly increased in apigenin treated uveal melanoma cells in a dose-dependent manner (Figures 5(c) and 5(d)).

3.6. Effects of Various Signal Inhibitors on the Secretion of VEGF by Uveal Melanoma Cells. VEGF protein levels in the conditioned media from uveal melanoma cells (SP6.5 cell line) cultured without any signal inhibitors were 437 ± 36 pg/mL (control). Treatment of cells with LY294002 (PI3K/Akt inhibitor) and UO1026 (ERK inhibitor) significantly decreased VEGF levels in the conditioned media ($P < 0.05$) (Figure 6). VEGF levels in the conditioned media from SP600125 (JNK1/2 inhibitor) and SB203580 (p38 MAPK inhibitor) treated cells did not show significant changes as compared with the control ($P > 0.05$) (Figure 6). These results suggest that VEGF secretion by uveal melanoma cells

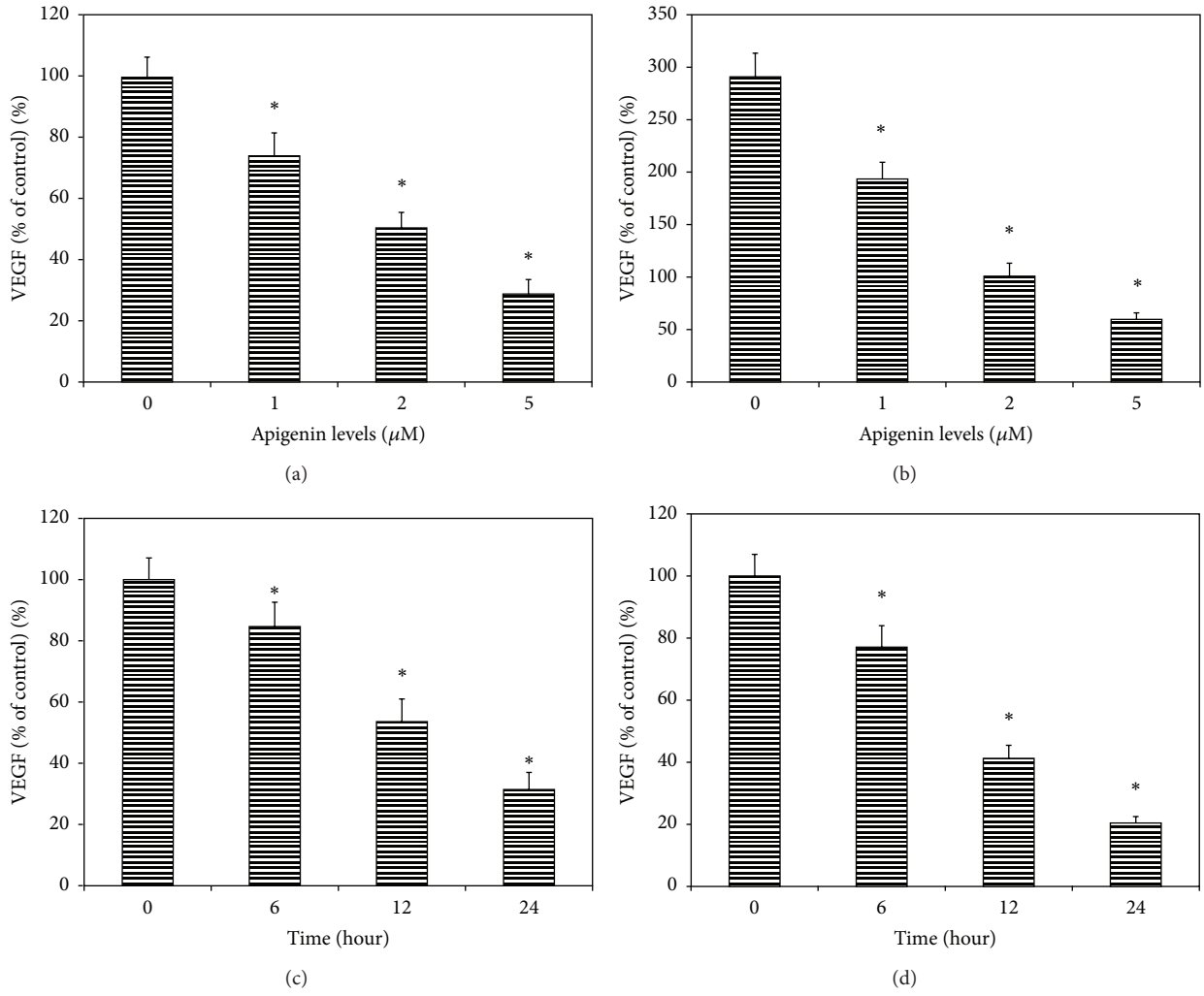

Figure 3: Dose- and time-effects of apigenin on the secretion of VEGF by human uveal melanoma cells. Cells were plated into 24-well plates. In the dose-effect study, apigenin at 0, 1, 2 and 5 μM was added to the culture and incubated for 24 h, (a) SP6.5 cell line and (b) C918 cell line. In the time-effect study, apigenin at 5.0 μM was added and conditioned medium was collected 6, 12 and 24 h later, (c) SP6.5 and (d) C918. The amount of VEGF protein in the conditioned medium was determined by using the human VEGF Quantikine ELISA kit. VEGF levels in the conditioned culture medium were expressed as the percentages of the controls. Apigenin significantly reduced the secretion of VEGF by uveal melanoma cells in a dose- and time-dependent manner. Data are mean ± SD ($n = 3$). $^*P < 0.05$, versus control (cells cultured without apigenin).

is regulated by Akt and ERK1/2 and not by JNK1/2 and p38 MAPK signal pathways.

4. Discussion

Apigenin is a flavonoid belonging to the flavone structural class and chemically known as 4′, 5, 7,-trihydroxyflavone, with molecular formula $C_{15}H_{10}O_5$. Apigenin is abundantly present in common fruits such as grapefruit, plant-derived beverages, and vegetables such as parsley, onions, oranges, tea, chamomile, and wheat sprouts. For centuries, apigenin has been utilized as a traditional or alternative medicine. One of the most common sources of apigenin consumed as single ingredient herbal tea is chamomile, prepared from the dried flowers of *Matricaria chamomilla* [10, 11]. Apigenin is present in various Chinese traditional medications, such as *Achillea millefolium, Apium graveolens, Buddleja officinalis, Cosmos bipinnata, Gingko biloba, Sabina chinensis, Taraxacum officinale, and Thymus serpyllum*, and have been used for the treatment of different diseases [28, 29]. In recent years, apigenin has been increasingly recognized as a cancer chemopreventive agent [10, 11].

Apigenin has gained particular interest in recent years as a beneficial and health promoting agent because of its low intrinsic toxicity and different effects in normal versus cancer cells [10, 11]. It has been reported that apigenin could inhibit the growth of cancers in experimental animal models [10, 11] In vitro studies suggested that apigenin induced apoptosis and inhibited the growth and invasion of various cultured cancer cells, including breast, cervical, colon, lung, ovarian, prostate, gastric, liver, and skin cancer cells [10, 11].

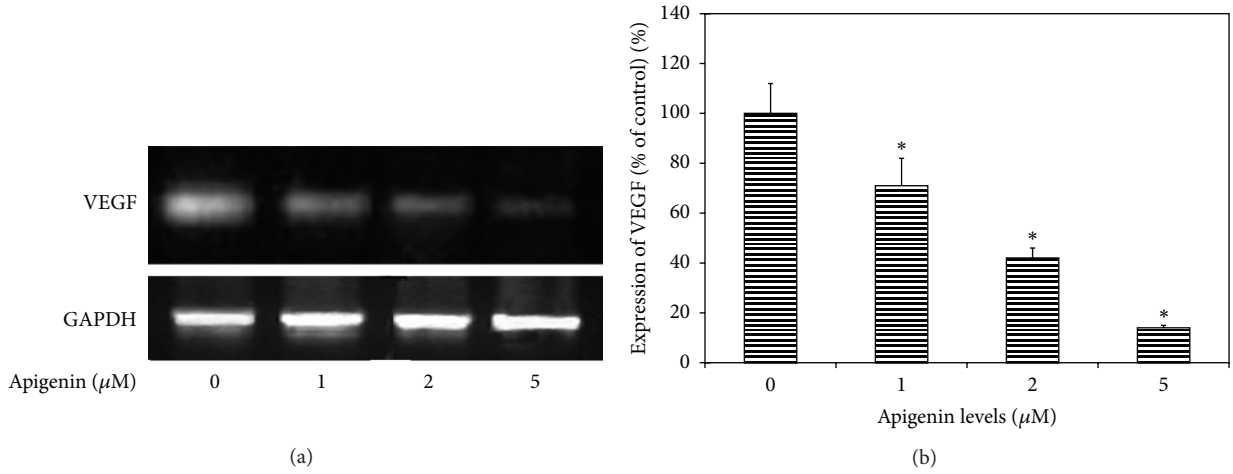

Figure 4: RT-PCR analysis for the effects of apigenin on the expression of VEGF mRNA in uveal melanoma cells. Representative RT-PCR profiles from three experiments showed the mRNA expressions of VEGF by uveal melanoma cells (SP6.5 cell line) exposed to apigenin at 0, 1, 2, and 5 μM (a). After 6 h of culture with or without apigenin, cells were collected, mRNA was extracted, and RT-PCR analysis was performed as described in the text. GAPDH was used as an internal loading control. Apigenin inhibited the expression of VEGF mRNA in uveal melanoma cells in a dose-dependent manner (b).

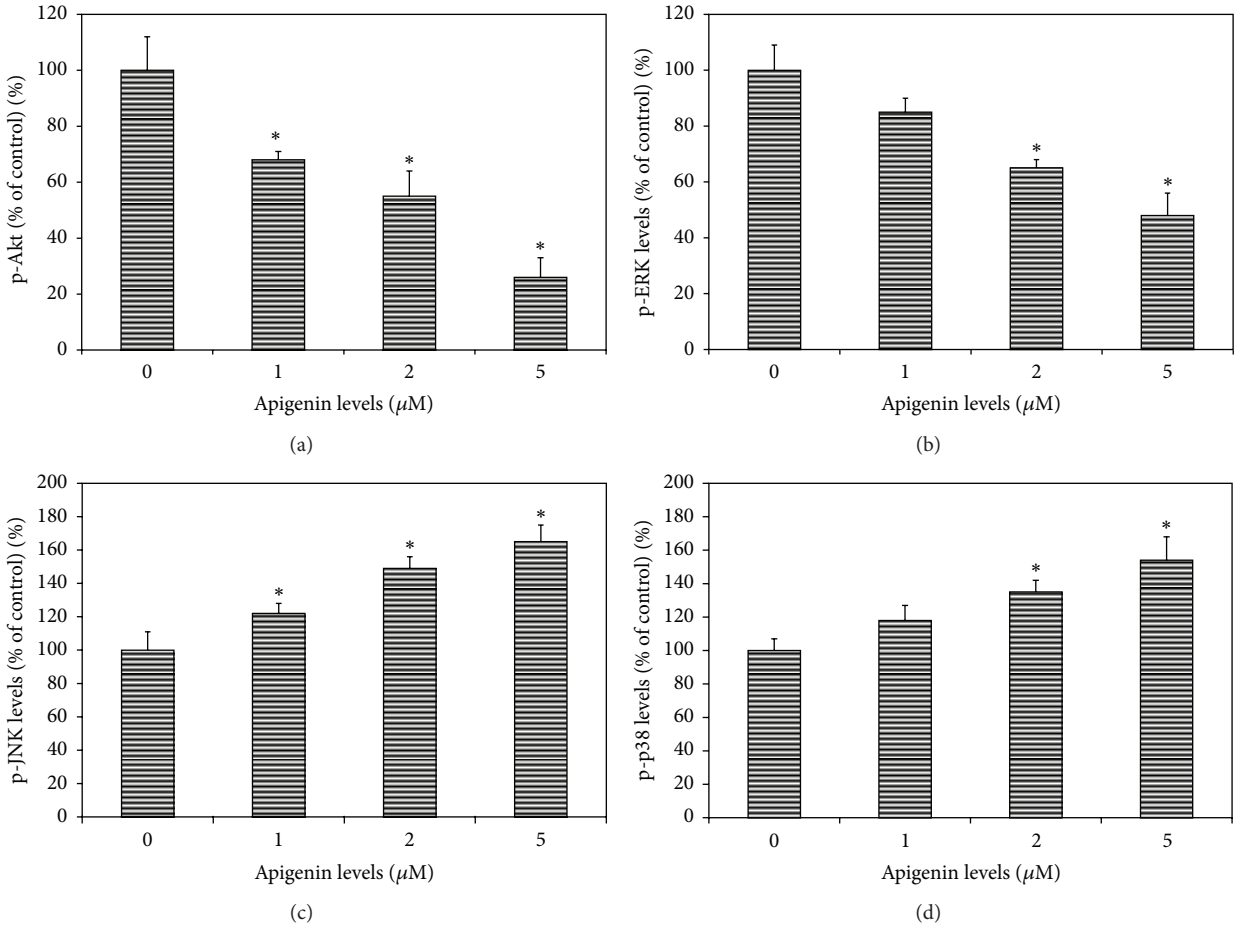

Figure 5: Dose effects of apigenin on phosphorylated Akt, ERK, JNK, and p38 MAPK levels in cultured uveal melanoma cells. Cells (SP6.5) were plated into 24-well plates. After 24 h incubation, apigenin at 0, 1, 2, and 5 μM was added to the medium. Cells were collected 60 min later. The amount of phosphorylated Akt (p-Akt), ERK1/2 (p-ERK), JNK1/2 (p-JNK), and p38 MAPK (p-p38) in cell lysates was measured using the relevant ELISA kits and was expressed as the percentages of the controls (cells cultured without apigenin). Apigenin significantly decreased p-Akt (a) and p-ERK levels (b) and increased p-JNK (c) and p-p38 (d) levels in cell lysates in a dose-dependent manner. Data are mean ± SD ($n = 3$). $^*P < 0.05$, versus control.

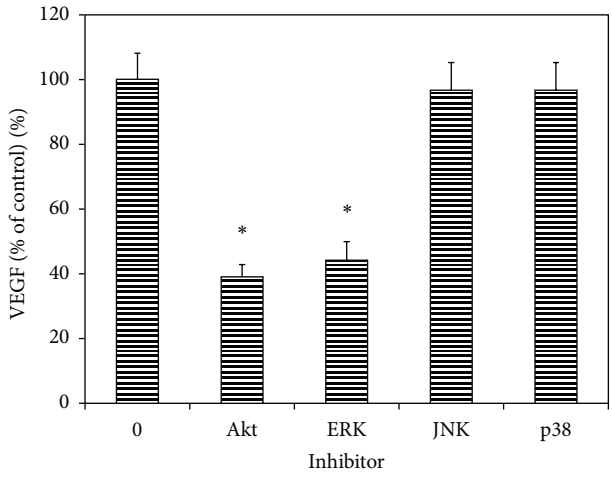

Figure 6: Effects of Akt and MAPK inhibitors on the constitutive secretion of VEGF by uveal melanoma cells. Cells were plated into 24-well plates. Various MAPK and Akt inhibitors were added to the medium separately, including LY294002 (PI3K/Akt inhibitor), UO1026 (ERK inhibitor), SP600125 (JNK inhibitor), and SB203580 (p38 MAPK inhibitor) at a final concentration of 10 μM. After 24 h incubation, culture medium was collected, the VEGF levels were measured with human VEGF Quantikine ELISA kit and expressed as the percentages of the controls (cells cultured without any signal inhibitors). Akt and ERK inhibitors significantly decreased, whereas JNK and p38 inhibitors did not affect the VEGF levels in the conditioned culture medium from uveal melanoma cells. Data are mean ± SD ($n = 3$). $^{*}P < 0.05$, versus control (cells cultured without inhibitor).

Angiogenesis is required for tumor growth and metastasis. VEGF is a critical regulator of tumor vascularization. The VEGF family consists of VEGF or VEGF-A, VEGF-B, VEGF-C, VEGF-D, VEGF-E (viral), and placenta growth factor [4]. VEGF family members signal by binding to members of a group of high-affinity receptors, VEGFR-1, -2, -3 and Neuropilin-1 and -2. VEGF-A binds to VEGFR-1, -2, and Neuropilin-1, and all of them are selectively though not exclusively expressed on vascular endothelium [4]. VEGF modulates tumor vascularization through its potent functions as a stimulator of endothelial cell survival, mitogenesis, migration, differentiation, and self-assembly [4, 5]. It is well established that VEGF is an important component of tumor growth, vascularity, and metastasis. VEGF expression, both in the tumor and in the circulation, is correlated with poor patient prognosis in several types of cancer [4, 5]. Cancer cells constitutively express VEGF proteins without apparent stimuli, which may provide a paracrine mechanism to induce angiogenesis [4, 5]. Therefore, using various drugs that inhibit the expression and secretion of VEGF by cancer cells is becoming a target for cancer therapy.

In uveal melanoma, it has been reported that VEGF mRNA and protein were detected in the tumor tissues [30–32]. VEGF levels were elevated in aqueous humor from uveal melanoma patients [32, 33]. Serum VEGF levels were elevated in uveal melanoma with metastasis [8, 9]. Uveal melanoma cell lines show a very high constitutive expression and secretion of VEGF [6, 7]. All of these results suggest that VEGF plays an important role in the growth, invasion, and metastasis of uveal melanoma.

It has been reported that apigenin suppressed the expression and secretion of VEGF in various cancer cells in vitro, including lung [21], prostate [13–15, 17], liver [18], and ovarian [12, 20] cancers. Apigenin also suppressed the VEGF expression and secretion in various experimental cancer models [16, 21].

The effects of apigenin on the expression of VEGF in uveal melanoma cells have not been reported. The present study found that uveal melanoma cells had a much higher constitutive secretion of VEGF as compared with normal uveal melanocytes, which is consistent with the previous report [7]. Apigenin suppressed the expression and secretion of VEGF in uveal melanoma cells in a dose-dependent manner, which is consistent with the inhibition of VEGF expression and secretion by apigenin in various types of cancer [12–21].

Constitutive activation of the ERK1/2 and PI3K/Akt pathways has been observed in many tumors and plays a very important role in tumor progression [4, 5]. Activation of both signal pathways leads to enhanced VEGF gene transcription [4, 5]. It has been reported that ERK and PI3K/Akt signal pathways are highly activated in uveal melanoma cells constitutively [34–37]. PI3K/Akt signal pathway in uveal melanoma cells also could be regulated by micro-RNA (*miRNA-34a*) [38].

In the present study, apigenin significantly inhibited the activation of ERK1/2 and PI3 K/Akt and increased the activation of JNK1/2 and p38 MAPK pathways in cultured uveal melanoma cells. However, only ERK1/2 and PI3 K/Akt inhibitors significantly reduced the secretion of VEGF by uveal melanoma cells, whereas JNK1/2 and p38 inhibitors did not influence the secretion of VEGF by melanoma cells in the present study. Therefore, it is most probably that apigenin suppresses the expression and secretion of VEGF through the inhibition of ERK1/2 and PI3 K/Akt pathways. This is consistent with the previous reports, which showed that the inhibition of ERK1/2 and/or PI3 K/Akt pathways by apigenin plays an important role in its inhibiting effects on VEGF expression in various malignant tumors [12–14, 17, 21].

5. Conclusion

Apigenin at low and nontoxic levels significantly inhibits the expression and secretion of VEGF by uveal melanoma cells, suggesting that it is worth to study the use of apigenin as a chemopreventive and/or chemotherapeutic agent against uveal melanoma in the future.

Conflict of Interests

There are no commercial relationships existed in the form of financial support or personal financial interest regarding the contents of this paper. This paper has not been published elsewhere and has not been submitted simultaneously for publication elsewhere.

Acknowledgments

The authors thank Dr. Xiaoliang Leon Xu (Memorial Sloan Kettering Cancer Center, New York) for providing C918 melanoma cell line and Dr. Guy Pelletier (Research Center of Immunology, Quebec, Canada) for providing SP6.5 melanoma cell line.

References

[1] D. N. Hu, G. P. Yu, S. A. McCormick, S. Schneider, and P. T. Finger, "Population-based incidence of uveal melanoma in various races and ethnic groups," *American Journal of Ophthalmology*, vol. 140, no. 4, pp. 612–617, 2005.

[2] E. Kujala, T. Mäkitie, and T. Kivelä, "Very long-term prognosis of patients with malignant uveal melanoma," *Investigative Ophthalmology and Visual Science*, vol. 44, no. 11, pp. 4651–4659, 2003.

[3] J. J. Augsburger, Z. M. Corrêa, and A. H. Shaikh, "Effectiveness of treatments for metastatic uveal melanoma," *American Journal of Ophthalmology*, vol. 148, no. 1, pp. 119–127, 2009.

[4] K. Xie, D. Wei, Q. Shi, and S. Huang, "Constitutive and inducible expression and regulation of vascular endothelial growth factor," *Cytokine and Growth Factor Reviews*, vol. 15, no. 5, pp. 297–324, 2004.

[5] R. M. B. Loureiro and P. A. D'Amore, "Transcriptional regulation of vascular endothelial growth factor in cancer," *Cytokine and Growth Factor Reviews*, vol. 16, no. 1, pp. 77–89, 2005.

[6] P. Logan, J. Burnier, and M. N. Burnier Jr., "Vascular endothelial growth factor expression and inhibition in uveal melanoma cell lines," *Ecancermedicalscience*, vol. 7, article 336, 2013.

[7] I. C. Notting, G. S. O. A. Missotten, B. Sijmons, Z. F. H. M. Boonman, J. E. E. Keunen, and G. van der Pluijm, "Angiogenic profile of uveal melanoma," *Current Eye Research*, vol. 31, no. 9, pp. 775–785, 2006.

[8] M. El Filali, G. S. O. A. Missotten, W. Maat et al., "Regulation of VEGF-A in uveal melanoma," *Investigative Ophthalmology and Visual Science*, vol. 51, no. 5, pp. 2329–2337, 2010.

[9] V. Barak, J. Pe'er, I. Kalickman, and S. Frenkel, "VEGF as a biomarker for metastatic uveal melanoma in humans," *Current Eye Research*, vol. 36, no. 4, pp. 386–390, 2011.

[10] S. Shukla and S. Gupta, "Apigenin: a promising molecule for cancer prevention," *Pharmaceutical Research*, vol. 27, no. 6, pp. 962–978, 2010.

[11] D. Patel, S. Shukla, and S. Gupta, "Apigenin and cancer chemoprevention: progress, potential and promise (review)," *International Journal of Oncology*, vol. 30, no. 1, pp. 233–245, 2007.

[12] J. Fang, C. Xia, Z. Cao, J. Z. Zheng, E. Reed, and B. H. Jiang, "Apigenin inhibits VEGF and HIF-1 expression via PI3K/AKT/p70S6K1 and HDM2/p53 pathways," *FASEB Journal*, vol. 19, no. 3, pp. 342–353, 2005.

[13] J. Fang, Q. Zhou, L. Z. Liu et al., "Apigenin inhibits tumor angiogenesis through decreasing HIF-1α and VEGF expression," *Carcinogenesis*, vol. 28, no. 4, pp. 858–864, 2007.

[14] S. Mirzoeva, D. K. Nam, K. Chiu, C. A. Franzen, R. C. Bergan, and J. C. Pelling, "Inhibition of HIF-1 alpha and VEGF expression by the chemopreventive bioflavonoid apigenin is accompanied by Akt inhibition in human prostate carcinoma PC3-M cells," *Molecular Carcinogenesis*, vol. 47, no. 9, pp. 686–700, 2008.

[15] S. Shukla and S. Gupta, "Suppression of constitutive and tumor necrosis factor alpha-induced nuclear factor (NF)-kappaB activation and induction of apoptosis by apigenin in human prostate carcinoma PC-3 cells: correlation with down-regulation of NF-kappaB-responsive genes," *Clinical Cancer Research*, vol. 10, no. 9, pp. 3169–3178, 2004.

[16] B. Mafuvadze, I. Benakanakere, F. R. López Pérez, C. Besch-Williford, M. R. Ellersieck, and S. M. Hyder, "Apigenin prevents development of medroxyprogesterone acetate-accelerated 7,12-dimethylbenz(a)anthracene-induced mammary tumors in sprague-dawley rats," *Cancer Prevention Research*, vol. 4, no. 8, pp. 1316–1324, 2011.

[17] S. Shukla, G. T. MacLennan, P. Fu, and S. Gupta, "Apigenin attenuates insulin-like growth factor-I signaling in an autochthonous mouse prostate cancer model," *Pharmaceutical Research*, vol. 29, no. 6, pp. 1506–1517, 2012.

[18] B. R. Kim, Y. K. Jeon, and M. J. Nam, "A mechanism of apigenin-induced apoptosis is potentially related to anti-angiogenesis and anti-migration in human hepatocellular carcinoma cells," *Food and Chemical Toxicology*, vol. 49, no. 7, pp. 1626–1632, 2011.

[19] L. G. Melstrom, M. R. Salabat, X. Z. Ding et al., "Apigenin down-regulates the hypoxia response genes: HIF-1α, GLUT-1, and VEGF in human pancreatic cancer cells," *Journal of Surgical Research*, vol. 167, no. 2, pp. 173–181, 2011.

[20] H. Luo, B. H. Jiang, S. M. King, and Y. C. Chen, "Inhibition of cell growth and VEGF expression in ovarian cancer cells by flavonoids," *Nutrition and Cancer*, vol. 60, no. 6, pp. 800–809, 2008.

[21] L. Z. Liu, J. Fang, Q. Zhou, X. Hu, X. Shi, and B. H. Jiang, "Apigenin inhibits expression of vascular endothelial growth factor and angiogenesis in human lung cancer cells: implication of chemoprevention of lung cancer," *Molecular Pharmacology*, vol. 68, no. 3, pp. 635–643, 2005.

[22] D. N. Hu, S. A. McCormick, R. Ritch, and K. Pelton-Henrion, "Studies of human uveal melanocytes in vitro: isolation, purification and cultivation of human uveal melanocytes," *Investigative Ophthalmology and Visual Science*, vol. 34, no. 7, pp. 2210–2219, 1993.

[23] D. N. Hu, "Regulation of growth and melanogenesis of uveal melanocytes," *Pigment Cell Research*, vol. 13, no. 8, pp. 81–86, 2000.

[24] D. N. Hu, S. A. McCormick, and D. F. Woodward, "A functional study on prostanoid receptors involved in cultured human iridal melanocyte stimulation," *Experimental Eye Research*, vol. 73, no. 1, pp. 93–100, 2001.

[25] D. N. Hu, K. Wakamatsu, S. Ito, and S. A. McCormick, "Comparison of eumelanin and pheomelanin content between cultured uveal melanoma cells and normal uveal melanocytes," *Melanoma Research*, vol. 19, no. 2, pp. 75–79, 2009.

[26] D. Soulieres, A. Rousseau, J. Deschenes, M. Tremblay, M. Tardif, and G. Pelletier, "Characterization of gangliosides in human uveal melanoma cells," *International Journal of Cancer*, vol. 49, no. 4, pp. 498–503, 1991.

[27] K. J. Daniels, H. C. Boldt, J. A. Martin, L. M. Gardner, M. Meyer, and R. Folberg, "Expression of type VI collagen in uveal melanoma: its role in pattern formation and tumor progression," *Laboratory Investigation*, vol. 75, no. 1, pp. 55–66, 1996.

[28] J. J. Zhou, G. R. Xie, and X. J. Yan, *Phytochemistry of Chinese Traditional Medicine*, Chemical Industry Press, Beijing, China, 2004.

[29] Y. J. Shen, *Pharmacology of Chinese Traditional Medicine*, People's Medical Publishing House, Beijing, China, 2002.

[30] S. R. Boyd, D. S. W. Tan, L. de Souza et al., "Uveal melanomas express vascular endothelial growth factor and basic fibroblast growth factor and support endothelial cell growth," *British Journal of Ophthalmology*, vol. 86, no. 4, pp. 440–447, 2002.

[31] T. G. Sheidow, P. L. Hooper, C. Crukley, J. Young, and J. G. Heathcote, "Expression of vascular endothelial growth factor in uveal melanoma and its correlation with metastasis," *British Journal of Ophthalmology*, vol. 84, no. 7, pp. 750–756, 2000.

[32] G. S. O. Missotten, I. C. Notting, R. O. Schlingemann et al., "Vascular endothelial growth factor A in eyes with uveal melanoma," *Archives of Ophthalmology*, vol. 124, no. 10, pp. 1428–1434, 2006.

[33] S. R. Boyd, D. Tan, C. Bunce et al., "Vascular endothelial growth factor is elevated in ocular fluids of eyes harbouring uveal melanoma: identification of a potential therapeutic window," *British Journal of Ophthalmology*, vol. 86, no. 4, pp. 448–452, 2002.

[34] A. Calipel, F. Mouriaux, A. L. Glotin, F. Malecaze, A. M. Faussat, and F. Mascarelli, "Extracellular signal-regulated kinase-dependent proliferation is mediated through the protein kinase A/B-Raf pathway in human uveal melanoma cells," *Journal of Biological Chemistry*, vol. 281, no. 14, pp. 9238–9250, 2006.

[35] W. Zuidervaart, F. van Nieuwpoort, M. Stark et al., "Activation of the MAPK pathway is a common event in uveal melanomas although it rarely occurs through mutation of BRAF or RAS," *British Journal of Cancer*, vol. 92, no. 11, pp. 2032–2038, 2005.

[36] H. Pópulo, P. Soares, A. S. Rocha, P. Silva, and J. M. Lopes, "Evaluation of the mTOR pathway in ocular (uvea and conjunctiva) melanoma," *Melanoma Research*, vol. 20, no. 2, pp. 107–117, 2010.

[37] V. S. Saraiva, A. L. Caissie, L. Segal, C. Edelstein, and M. N. Burnier Jr., "Immunohistochemical expression of phospho-Akt in uveal melanoma," *Melanoma Research*, vol. 15, no. 4, pp. 245–250, 2005.

[38] D. Yan, X. Zhou, X. Chen et al., "MicroRNA-34a inhibits uveal melanoma cell proliferation and migration through downregulation of c-Met," *Investigative Ophthalmology and Visual Science*, vol. 50, no. 4, pp. 1559–1565, 2009.

Hindawi Publishing Corporation
Evidence-Based Complementary and Alternative Medicine
Volume 2013, Article ID 205082, 12 pages
http://dx.doi.org/10.1155/2013/205082

Research Article

Zeaxanthin Induces Apoptosis in Human Uveal Melanoma Cells through Bcl-2 Family Proteins and Intrinsic Apoptosis Pathway

Ming-Chao Bi,[1] Richard Rosen,[2] Ren-Yuan Zha,[3] Steven A. McCormick,[4,5] E. Song,[1] and Dan-Ning Hu[2,4,5]

[1] *Department of Ophthalmology, The First Hospital of Jilin University, 71 Xinmin Street, Changchun 130021, China*
[2] *Department of Ophthalmology, The New York Eye and Ear Infirmary, New York Medical College, 310 E. 14th Street, New York, NY 10003, USA*
[3] *Department of Oncological Sciences, Tisch Cancer Institute, Icahn School of Medicine at Mount Sinai, New York, NY 10029, USA*
[4] *Tissue Culture Center, The New York Eye and Ear Infirmary, New York Medical College, New York, NY 10003, USA*
[5] *Department of Pathology, The New York Eye and Ear Infirmary, New York Medical College, 310 E. 14th Street, New York, NY 10003, USA*

Correspondence should be addressed to E. Song; songe23@163.com and Dan-Ning Hu; hu2095@yahoo.com

Received 26 July 2013; Accepted 3 September 2013

Academic Editor: Shun-Fa Yang

The cytotoxic effects of zeaxanthin on two human uveal melanoma cell lines (SP6.5 and C918) and related signaling pathways were studied and compared to effects on normal ocular cells (uveal melanocytes, retinal pigment epithelial cells, and scleral fibroblasts). MTT assay revealed that zeaxanthin reduced the cell viability of melanoma cells in a dose-dependent manner (10, 30, and 100 μM), with IC_{50} at 40.8 and 28.7 μM in SP6.5 and C918 cell lines, respectively. Zeaxanthin did not affect the viability of normal ocular cells even at the highest levels tested (300 μM), suggesting that zeaxanthin has a selectively cytotoxic effect on melanoma cells. Zeaxanthin induced apoptosis in melanoma cells as indicated by annexin V and ethidium III flow cytometry. Western blot analysis demonstrated that zeaxanthin decreased the expression of antiapoptotic proteins (Bcl-2 and Bcl-xL) and increased the expression of proapoptotic proteins (Bak and Bax) in zeaxanthin-treated melanoma cells. Zeaxanthin increased mitochondrial permeability as determined by JC-1 fluorescein study. Zeaxanthin also increased the level of cytosol cytochrome c and caspase-9 and -3 activities, but not caspase-8, as measured by ELISA assay or colorimetric assay. All of these findings indicate that the intrinsic (mitochondrial) pathway is involved in zeaxanthin-induced apoptosis in uveal melanoma cells.

1. Introduction

Uveal melanoma is the most common primary intraocular tumor in the adult population, with an incidence of 6-7 cases per million per year in the US [1]. Uveal melanoma has a poor prognosis, with half of uveal melanoma patients dying from their disease within 25 years [2]. The high mortality rate is related to the development of metastasis, which has a strong preference for the liver. Most uveal melanoma patients with liver metastasis die within 6 months [2–4]. Because of the poor prognosis of metastatic uveal melanoma, new therapies are urgently required.

Zeaxanthin is a carotenoid pigment, which belongs to the xanthophyll subclass, having a chemical formula $C_{40}H_{56}O_2$. It is found at high levels in various foods (e.g., egg yolk, corn, and many vegetables and fruits), herbs, and traditional Chinese medications (*Hippophae rhamnoides, Lycium barbarum, Lycium chinense, Lilium hansonii, Cycas revolute,* and *Crocus sativus*) [5, 6]. It has been used in traditional Chinese medicine to treat various diseases and has been tested for its biomedical effects in several experimental disease models, including various cancers [7].

Humans are not capable of synthesizing zeaxanthin, and thus, the zeaxanthin content of the body is entirely

dependent upon dietary intake [8, 9]. Zeaxanthin is present in various tissues and highly concentrated in the central retina (macula) of the eye [10–13]. Zeaxanthin is an antioxidant which also acts as a yellow filter protecting the macula from the blue light. Various observational and interventional studies have suggested that zeaxanthin might modify the risk of age-related macular degeneration (AMD) [14–19]. Therefore, supplementation of zeaxanthin with and without other antioxidants has been used clinically for the prevention and treatment of AMD with variable effects [20, 21].

Epidemiological studies have shown that higher intake and higher blood levels of zeaxanthin appear to be associated with a lower risk of occurrence of various cancers [22–44]. It has also been reported that zeaxanthin may inhibit cell growth or induce apoptosis of several tumor cell lines *in vitro* [45–48].

To our best knowledge, the effect of zeaxanthin on cultured uveal melanoma cells has not been reported previously. The purpose of the present study was to investigate the cytotoxic and apoptosis-inducing effects of zeaxanthin on human uveal melanoma cells *in vitro* compared to those in normal human uveal melanocytes, retinal pigment epithelial (RPE) cells, and fibroblasts. The effects of zeaxanthin on the Bcl-2 family of proteins, mitochondrial transmembrane potential (MTP), cystolic cytochrome c, and the activation of various caspases were also studied to elucidate the signaling pathway involved in zeaxanthin-induced apoptosis of uveal melanoma cells.

2. Materials and Method

2.1. Reagents. F-12 culture medium, Dulbecco's Modified Eagle's Medium (DMEM), fetal bovine serum (FBS), phosphate buffered saline (PBS), 0.05% trypsin-0.02% EDTA solution, and gentamicin were purchased from GIBCO (Grand Island, NY, USA). Isobutylmethylxanthine, cholera toxin, 3-[4,5-dimethylthiazol-2-yl]-2,5-diphenyltetrazolium bromide (MTT), and dimethyl sulfoxide (DMSO) were obtained from Sigma (St. Louis, MO, USA). Basic fibroblast growth factor was obtained from PeproTech (Rocky Hill, NJ, USA). Zeaxanthin was obtained from Dr. Dennis L. Gierhart (Chesterfield, MO, USA). Cytochrome c ELISA kit was purchased from Calbiochem (San Diego, CA, USA). Caspase-8 and -9 colorimetric activity assay kits were purchased from R&D Systems (Minneapolis, MN, USA). Caspase-3 colorimetric assay kits were purchased from Calbiochem.

2.2. Cell Culture. The effects of zeaxanthin were tested in two human choroidal melanoma cell lines (SP6.5 and C918) and compared to effects on three different normal cell lines, human normal uveal melanocytes, fibroblasts, and retinal pigment epithelial (RPE) cells. SP6.5 melanoma cell line was isolated from a primary choroidal melanoma patient and was provided by Dr. Guy Pelletier (Research Center of Immunology, Quebec, Canada) [49]. Melanoma cell line C918 was derived from a choroidal melanoma patient with liver metastasis at the University of Iowa and was provided by Dr. Robert Folberg (University of Illinois, Chicago) and Dr. Xiaoliang Leon Xu (Memorial Sloan Kettering Cancer Center, New York) [50]. C918 is epithelioid in morphology and is a highly invasive, metastatic, and aggressive melanoma cell line [50]. The human uveal melanocytes (isolated from the choroid) and scleral fibroblasts were established in the Tissue Culture Center of the New York Eye and Ear Infirmary as previously reported [51]. The human RPE cell line, ARPE-19, was obtained from American Type Culture Collection (Manassas, VA, USA). All melanoma cells, RPE cells, and fibroblasts were cultured with DMEM, supplemented with 10% FBS and gentamicin (50 μg/mL). Uveal melanocytes were cultured with FIC medium, supplemented with 10% FBS and gentamicin [51]. Cells were incubated at 37°C in a CO_2 regulated incubator in a humidified 95% air/5% CO_2 atmosphere. After cultures reached confluence, cells were detached with trypsin-EDTA solution and passaged. All tissues were obtained with premortem consent in accordance with the laws and regulations in place in the various jurisdictions.

2.3. MTT Assay for Cell Viability. Methods for MTT assay have been described previously [52]. Briefly, cells were seeded into 96-well plates at a density of 5×10^3 cells per well. After 24 h, zeaxanthin was applied to the cultures. Zeaxanthin (6.82 mg) was dissolved in 200 μL DMSO to make a stock solution of 60 mM. Tested cells were treated by different concentrations of zeaxanthin. The cells in the control group were cultured in medium containing the same levels of DMSO as in the zeaxanthin solution. A separate investigation about the effects of the highest DMSO levels (1 : 200) used in this experiment did not show significant differences in the cell viability between the cells with and without DMSO. After 48 h incubation with or without zeaxanthin, culture medium was aspirated and replaced with fresh culture medium. MTT solution (1 mg/mL, 50 μL) was added to each well. After 4 h incubation at 37°C, the medium and MTT were aspirated and the formazan blue that formed in the cells was dissolved in 100 μL of DMSO. Optical density of the 96-well plates was determined with a microplate reader (Multiskan MCC/340, Fisher Scientific, Pittsburgh, PA, USA) at 540 nm. The optical density of formazan formed in control (untreated) cells was taken as 100% viability. The concentration at which cell viability was inhibited by 50% (the 50% inhibitory concentration, IC_{50}) was determined by linear interpolation. All tests were performed in three independent experiments.

To study the time-effect of zeaxanthin on uveal melanoma cells, melanoma cells (C918 cell line) were seeded into 96-well plates at a density of 5×10^3 cells per well and divided into two groups, zeaxanthin-treated group and control group (without treatment of zeaxanthin). After 24 h, zeaxanthin was added to the cultures in the treated groups at final concentrations of 30 μM. At 0, 6, 12, 24, and 48 h after the addition of zeaxanthin; MTT test was performed in both treated and control groups. The results of each treated group were compared to the controls cultured for the same time periods. All tests were performed in three independent experiments.

2.4. Flow Cytometric Detection of Apoptotic Cells. Cell apoptosis was measured using the Apoptotic/Necrotic Cells Detection Kit (Promokine, Heidelberg, Germany) and analyzed by flow cytometry. Uveal melanoma cells (SP6.5 and C918 cell lines) were seeded in 6-well plates at a density of 1.2×10^5 cells per well. After treatment with zeaxanthin (30 μM) for 6 h and 24 h, cells were washed in PBS, detached from the well using trypsin, centrifuged for 5 min to discard supernatant, and resuspended in binding buffer. FITC-annexin V and ethidium homodimer III were added to the suspension and incubated for 15 min at room temperature in darkness. Specimens, containing 1×10^5 cells each, were then analyzed using a Becton Dickinson Flow Cytometer (Becton & Dickinson, Franklin Lakes, NJ, USA). The data were analyzed using Cell Quest V3.3 software and results were reported as percentages of the cell populations.

2.5. Western Blot Analysis for BCL-2 Family Proteins. Uveal melanoma cells (SP6.5 and C918 cell lines) were seeded in 10 cm culture dishes at a density of 6×10^6 cells per dish. Zeaxanthin (30 μM) was added to the medium 24 h later. After being cultured for 24 h, cells were washed in PBS and then scraped from the well, centrifuged for 5 min to discard the supernatant, and finally resuspended in binding buffer. Lysates were prepared by homogenizing cell pellets in lysis buffer. Protein concentrations were determined by the BCA protein assay kit (Novagen, Germany), using bovine serum albumin as the standard. Protein (20 μg) was separated by a precast of 10% SDS-PAGE gel (Invitrogen, Carlsbad, CA, USA) and transferred onto polyvinylidene difluoride membranes. The membranes were blocked with 5% milk for 1 h at room temperature. The membranes were incubated with the primary antibodies of anti-Bak, Bax, Bad, Bcl-2, Bcl-xL (1 : 500 dilution; Santa Cruz Biotechnology, Dallas, TX, USA), and calnexin (1 : 1000 dilution; Abcam, Cambridge, MA, USA) at 4°C overnight. The membranes were then incubated with a secondary antibody (anti-mouse, 1 : 10000 dilution and anti-rabbit, 1 : 6000 dilution) (Sigma) for 1 h at room temperature and the protein was detected using a chemiluminescence method. Chemiluminescent signals were captured using the Las-4000 (Fujifilm, Tokyo, Japan). The signal of each protein was determined using ImageJ software (National Institutes of Health, Bethesda, MD, USA).

2.6. MTP Assessment (JC-1). MTP was assessed using a Mitochondria Staining Kit which employed JC-1 (5,5′,6,6′-tetrachloro-1,1′,3,3′-tetraethylbenzimidazol-carbocyanine iodine), a sensitive fluorescent dye as the probe. Uveal melanoma cells (C918 cell line) were seeded into 8-well chamber slides at a density of 6×10^4 cells/well. After 24 h, cells were treated with 30 μM of zeaxanthin for another 24 h. JC-1 at a final concentration of 10 μM was added and incubated for 15 min at 37°C in the dark. JC-1 and culture medium were aspirated and cells were washed three times. Cells were immediately observed by fluorescence microscopy using dual band-pass filters (at 490 nm excitation and 530 and 590 nm emission). The assay is based on the aggregation of the dye and its fluorescence in the mitochondria. In the undamaged mitochondria, the aggregated dye appears as red fluorescence located in the mitochondria, whereas in cells with damaged MTP, the dye remains as monomers in the cytoplasm with diffuse green fluorescence.

2.7. Cytochrome c Release Assay. Uveal melanoma cells (C918 cell line) were seeded into 6-well plates at a density of 4×10^5 cells/well (4×10^4 cells/cm^2), and 24 h later, zeaxanthin was added at final concentrations of 0, 10, 30, and 100 μM. Cells were harvested at 2 h after the addition of zeaxanthin. Cultures were washed with cold PBS and then scraped from the well. After cell counting and centrifugation at 1,500 rpm for 5 min at 4°C, the cell pellets were collected. Cells were lysed in a cold hypotonic cell lysis buffer (BioSource, Camarillo, CA, USA) and centrifuged at 1000 ×g for 10 min. The supernatant (cytosol and mitochondria) was collected and centrifuged at 10,000 ×g for 20 min. The pellets (mitochondria) and the supernatant (cytosol) were collected separately. The cytochrome c level in the cytosol was measured using a cytochrome c enzyme-linked immunosorbent assay (ELISA) kit and performed in accordance with the manufacturer's instructions. The level of cytochrome c was expressed as a percentage of the controls (cells cultured without zeaxanthin). This was performed in three independent experiments.

2.8. Caspase-3, Caspase-8, and Caspase-9 Colorimetric Assay. Melanoma cells (C918 cell line) were seeded into 6-well plates at a density of 4×10^5 cells/well, and 24 h later zeaxanthin was added at final concentrations of 0, 10, 30, and 100 μM. Two hours after the addition of zeaxanthin, cells were washed with cold PBS and collected. After cell counting and centrifugation at 1,500 rpm for 5 min at 4°C, the cell pellets were collected. Cells were lysed by using the cell extraction buffer (BioSource) with protease inhibitor cocktail (Sigma) and PMSF (BioSource), incubated on ice for 30 min, and vortexed for 30 sec. The lysates were centrifuged at 10,000 rpm for 10 min at 4°C. The supernatant was stored at −70°C until analysis. The caspase-8, caspase-9, and -3 levels in cell lysates were measured using individual specific colorimetric kits, according to the manufacturer's instructions. The optical density was read using a microplate reader (Multiskan EX) at 405 nm. The activities of caspase-8, caspase-9, and caspase-3 were expressed as a percentage of the controls (cells cultured without zeaxanthin). This was performed in three independent experiments.

2.9. Statistics. Statistical significances of difference of means throughout this study were calculated by ANOVA one-way test in comparing data from more than two groups and Student's t-test in comparing data between two groups. The data was analyzed using SPSS statistical software (SPSS Inc., Chicago, IL, USA). A difference at $P < 0.05$ was considered statistically significant.

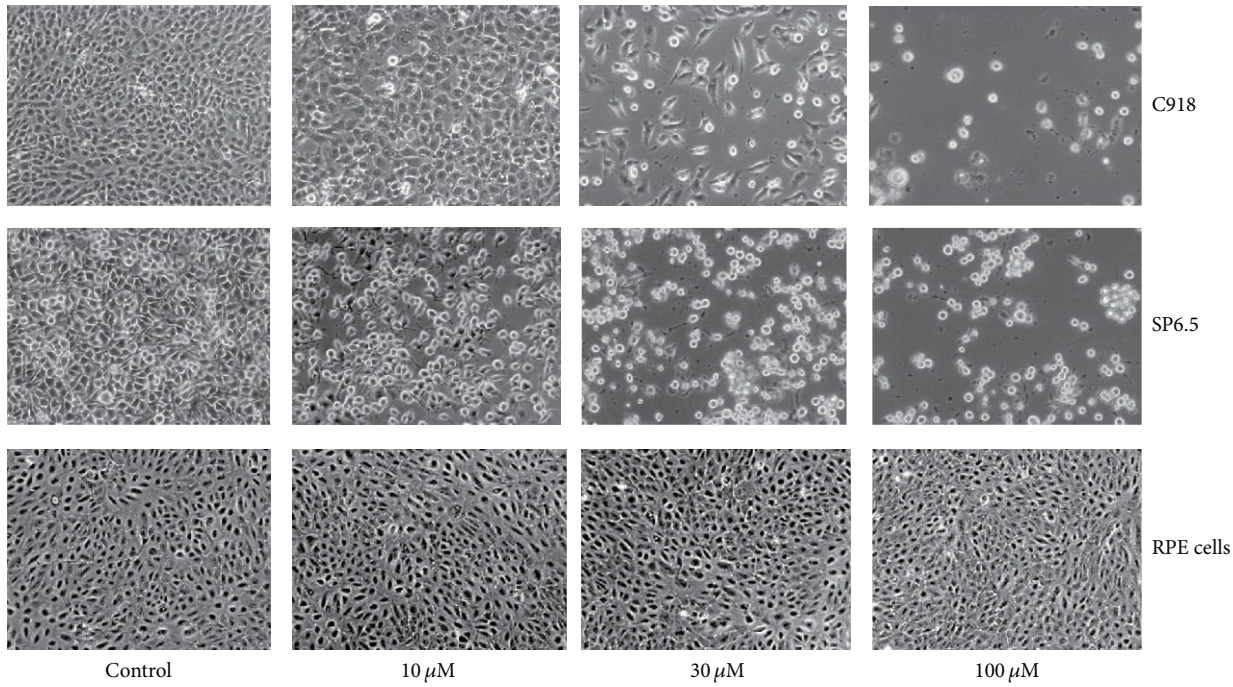

Figure 1: Phase-contrast photomicrograph of uveal melanoma cells and retinal pigment epithelial (RPE) cells treated with various concentrations of zeaxanthin. Human uveal melanoma cells (SP6.5 and C918) or RPE cells were seeded into 24-well plates at density of 8×10^4/well ($4 \times 10^4/cm^2$) and treated with zeaxanthin at 10, 30, and 100 μM levels for 48 h. Zeaxanthin at all treated levels significantly decreased number of viable cells in melanoma cells, whereas, it did not affect the cell viability of RPE cells.

3. Results

3.1. Effects of Zeaxanthin on Cell Viability of Melanoma Cells and Various Normal Cells. Zeaxanthin at 10, 30, 100, and 300 μM levels did not affect the cell viability of cultured human uveal melanocytes, RPE cells, or fibroblasts (Figures 1 and 2).

Zeaxanthin at 10, 30, and 100 μM levels significantly decreased the cell viability of uveal melanoma cells in a dose-dependent manner (Figures 1 and 2). The difference in cell viability between cells treated with and without zeaxanthin at all tested levels (10, 30, and 100 μM) was statistically significant ($P < 0.05$). The IC_{50} dose of zeaxanthin for cultured human uveal melanoma cells (SP6.5 and C918) at 48 h was 40.8 and 28.7 μM, respectively. These results suggested that zeaxanthin at 10–100 μM can selectively reduce the cell viability of melanoma cells without affecting normal uveal melanocytes, fibroblasts, or RPE cells.

Time-effect study showed that zeaxanthin at 30 μM decreased the cell viability of uveal melanoma cells (C918) in a time-dependent manner from 6 to 48 h (data not shown). The difference in cell viability at various time points, between cells treated with and without zeaxanthin, was statistically significant ($P < 0.05$).

3.2. Zeaxanthin-Induced Apoptosis of Melanoma Cells. Uveal melanoma cells cultured with zeaxanthin (30 μM for 6 and 24 h) and without zeaxanthin (controls) were double stained using annexin V and ethidium III and analyzed by flow cytometry. Nonapoptotic cells stained negatively with annexin. Apoptotic cells at early stage were annexin positive and ethidium-III negative, whereas apoptotic cells at advanced stage stained positively with both annexin and ethidium-III. Cells cultured with zeaxanthin for 6 and 24 h showed a significant increase in total apoptotic rate ($P < 0.05$, as compared with cells cultured without zeaxanthin) (Figure 3).

3.3. Western Blot Analysis for Effect of Zeaxanthin on BCL-2 Family Proteins. To assess the involvement of the Bcl-2 family of proteins in zeaxanthin-mediated apoptosis, Bax, Bak, Bad, Bcl-2, and Bcl-xL proteins, were examined in zeaxanthin-treated uveal melanoma cell lines. Western blot analysis revealed that zeaxanthin significantly decreased the expression of Bcl-xL and Bcl-2, antiapoptotic proteins, and increased the expression of Bak, a pro-apoptotic protein, in SP6.5 cells ($P < 0.05$ at zeaxanthin 30 μM). Zeaxanthin significantly decreased the expression of Bcl-xL, an anti-apoptotic protein, and increased the expression of Bax, a proapoptotic protein, in C918 cells ($P < 0.05$ at zeaxanthin 30 μM) (Figure 4).

3.4. Effects of Zeaxanthin on MTP in Melanoma Cells. In cells cultured with JC-1, red fluorescence is attributable to a potential-dependent aggregation of JC-1 in the mitochondria. Green fluorescence, reflecting the monomeric form of JC-1, appeared in the cytosol after mitochondrial membrane

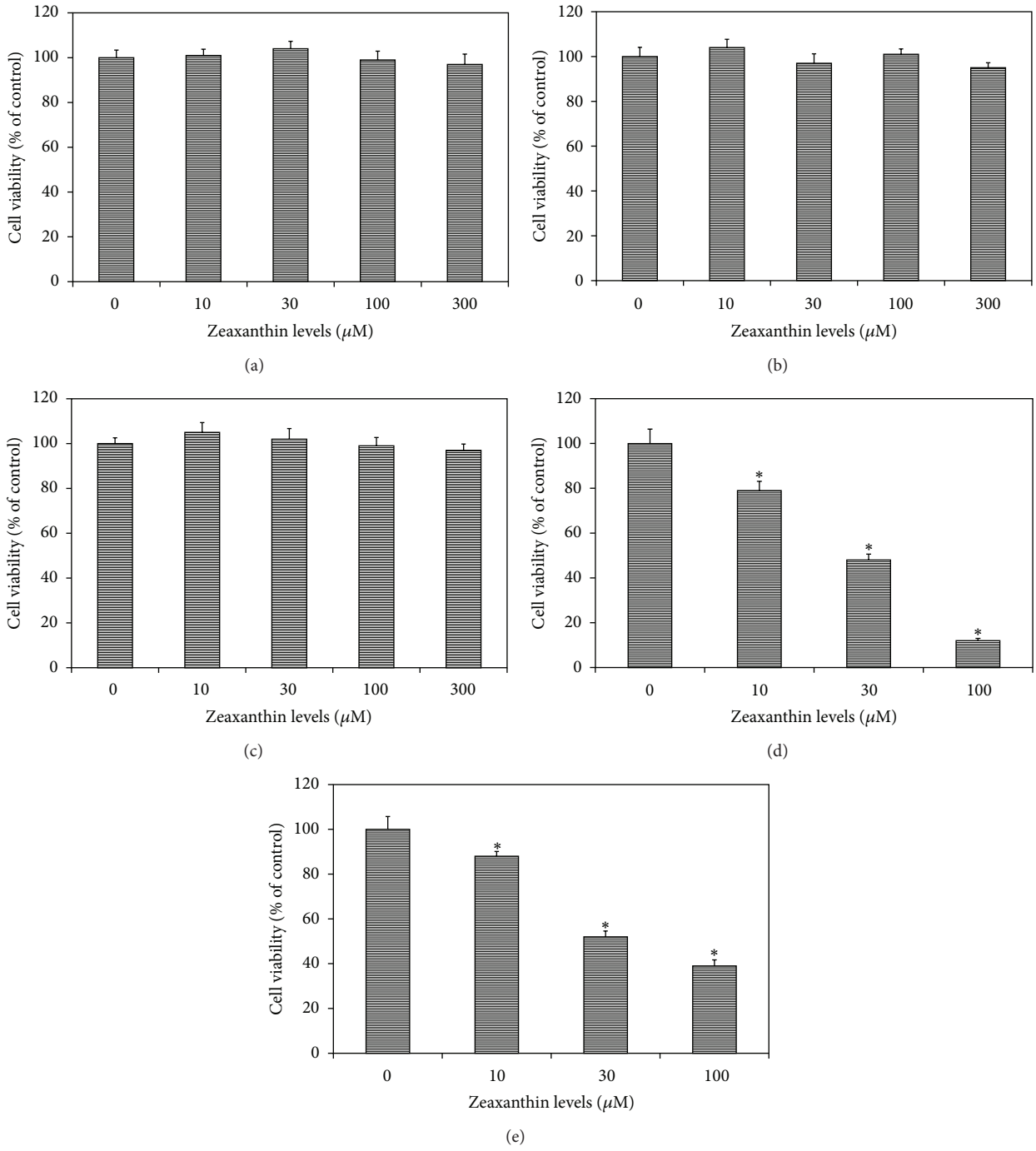

Figure 2: Dose effect of zeaxanthin on cell viability of uveal melanoma cells, uveal melanocytes, retinal pigment epithelial (RPE) cells, and fibroblasts. Human normal uveal melanocytes (a), RPE cells (b), and fibroblasts (c) or uveal melanoma cells C918 (d) and SP6.5 (e) were seeded into 96-well plates and treated with zeaxanthin at various doses for 48 h and cell viability was determined by MTT assay (see Section 2). Zeaxanthin at all tested concentrations selectively reduced the cell viability of uveal melanoma cells, without affecting cell viability of uveal melanocytes, RPE cells, and fibroblasts. Data are mean ± SD ($n = 3$). $^{*}P < 0.05$, versus control (cells cultured without zeaxanthin).

depolarization. As shown in Figure 5, uveal melanoma cells (C918) cultured without zeaxanthin exhibited mainly red fluorescence, indicating a normal MTP. Treatment with zeaxanthin (30 μM) caused a diffuse green staining pattern, representative of damaged MTP (Figure 5).

3.5. Effects of Zeaxanthin on the Release of Cytochrome c into Cytosol. Zeaxanthin increased cytosol cytochrome c levels in melanoma cells in a dose-dependent manner (Figure 6). Cytosol cytochrome c levels in cells treated with 10–100 μM zeaxanthin were significantly increased

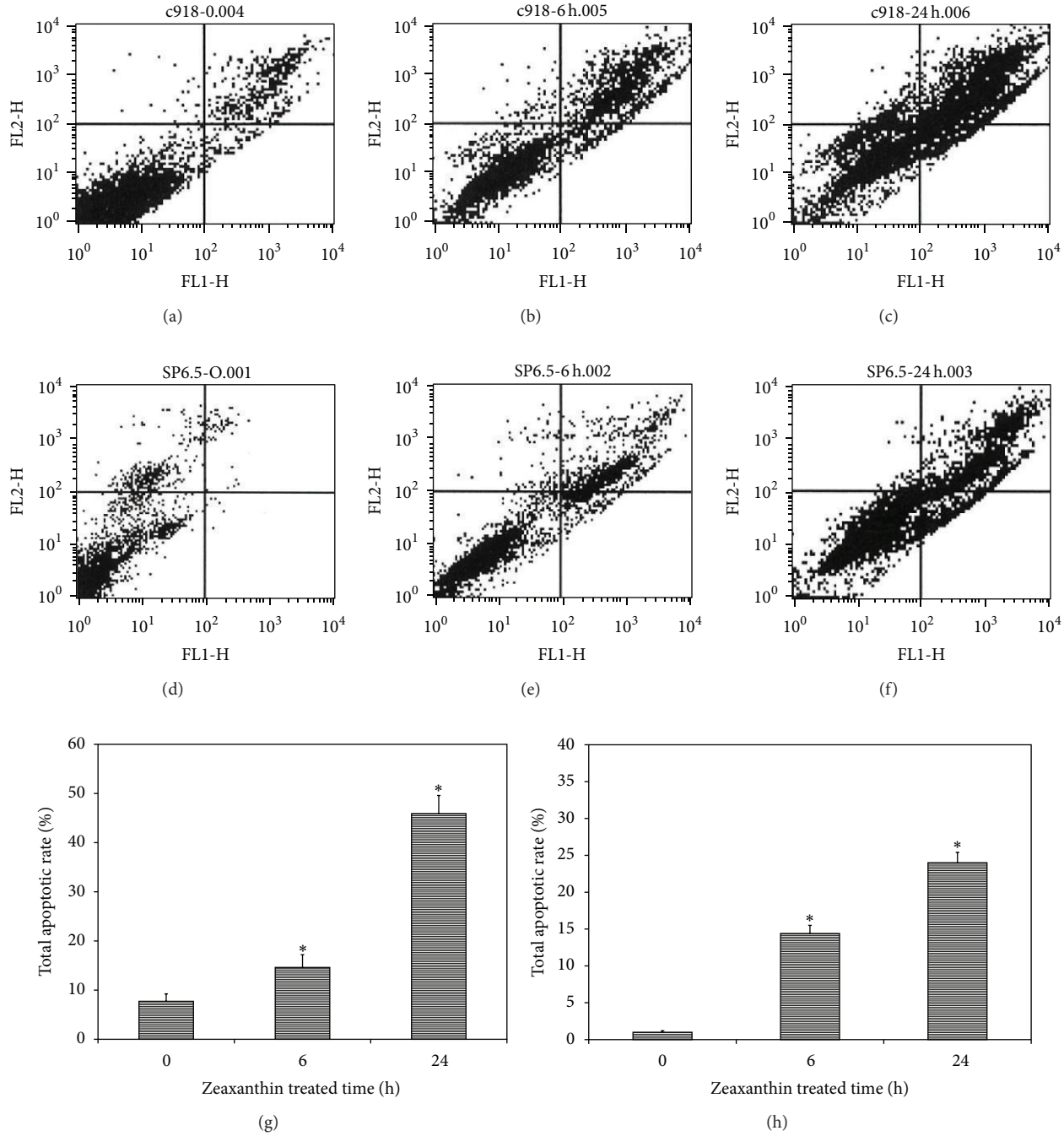

Figure 3: Effect of zeaxanthin on melanoma cell apoptosis as measured by annexin V-FITC/ethidium homodimer III (annexin/EtD III) flow cytometry. Melanoma cells (C918 and SP6.5) were treated by zeaxanthin at 30 μM for 6 and 24 h, and the extent of apoptosis was determined by annexin/EtD III staining and analyzed by flow cytometry (see Section 2). (a)–(f) Annexin and EtD III negative cells are nonapoptotic cells (low left). Annexin positive and EtD III negative cells are in early stage of apoptosis (low right). Annexin and EtD III positive cells are in advanced stage of apoptosis (upper right). (a), (b), and (c) and (d), (e), and (f) are C918 and SP6.5 treated without zeaxanthin and treated with zeaxanthin at 6 and 24 h, respectively. Zeaxanthin significantly increased the rate of total apoptotic cells (the sum of early and advanced stage of apoptotic cells) in C918 (g) and SP6.5 (h). Data are mean ± SD ($n = 3$). $^*P < 0.05$, versus control (cells cultured without zeaxanthin).

($P < 0.05$) as compared with the controls. In cells treated with 100 μM zeaxanthin, cytosol cytochrome c level increased to 3.30-fold of the controls (cells cultured without zeaxanthin).

3.6. Effects of Zeaxanthin on Caspase-3, Caspase-8, and Caspase-9 Activities in Melanoma Cells. Zeaxanthin significantly increased the caspase-3 and -9 activities in melanoma cells (C918) in a dose-dependent manner (Figures 7(a)

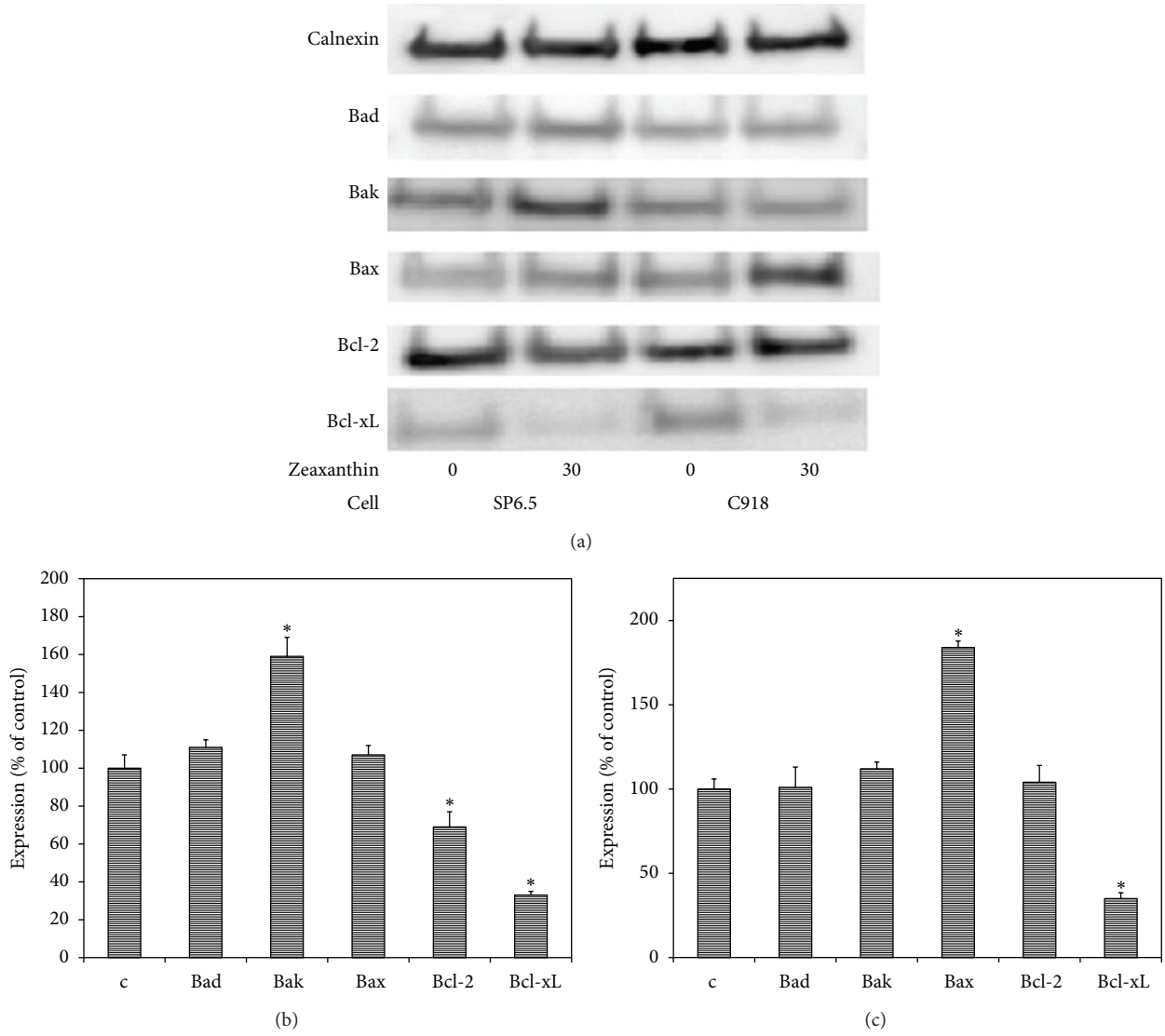

Figure 4: Western blot analysis of effects of zeaxanthin on expression of Bcl-2 family proteins in uveal melanoma cells. C918 and SP6.5 cell lines were treated with zeaxanthin (30 μM) for 24 h. Cellular protein extracts were subjected to western blot analysis and probed with antibodies specific for proapoptosis member proteins (Bad, Bak, and Bax) and antiapoptosis member proteins (Bcl-2 and Bcl-xL). Calnexin was used as an internal loading control. Representative images are shown at (a). Quantitative results are presented at (b) (SP6.5 cell line) and (c) (C918 cell line). Data are mean ± SD ($n = 3$). $^*P < 0.05$, versus control (cells cultured without zeaxanthin).

and 7(c)). Both caspase-3 and -9 activities in uveal melanoma cells treated with 10–100 μM zeaxanthin were very significantly increased ($P < 0.05$). A nearly 5.5-fold increase in caspase-3 and -9 activities was noted in uveal melanoma cells treated with 100 μM zeaxanthin. Zeaxanthin at 10–100 μM did not affect caspase-8 activities of uveal melanoma cells (Figure 7(b)).

4. Discussion

The relationship between the incidence of various malignant tumors and zeaxanthin in the diet or blood has been studied previously. Epidemiological studies showed that high intake and high blood levels of zeaxanthin (alone or combined with lutein) might be associated with a lower risk of occurrence of various malignant tumors, including non-Hodgkin lymphoma [22, 23], cervical [24–28], esophagus [29–31], stomach [31, 32], lung [33–35], breast [34, 36–38, 42], kidney [39], head and neck [40], colon [41, 43] and pancreas [31, 44], cancers.

There were only a few reports on the effects of zeaxanthin on various cancer cells *in vitro* and these studies were tested only in few cancer cell lines. It has been reported that zeaxanthin might inhibit cell growth or cause apoptosis of lymphoma [45], breast cancer [45, 48], colon cancer [47], and neuroblastoma cells *in vitro* [46]. However, the mechanism of zeaxanthin-induced apoptosis has not been studied thoroughly.

To our best knowledge, the relation between the intake and blood levels of zeaxanthin and the incidence of

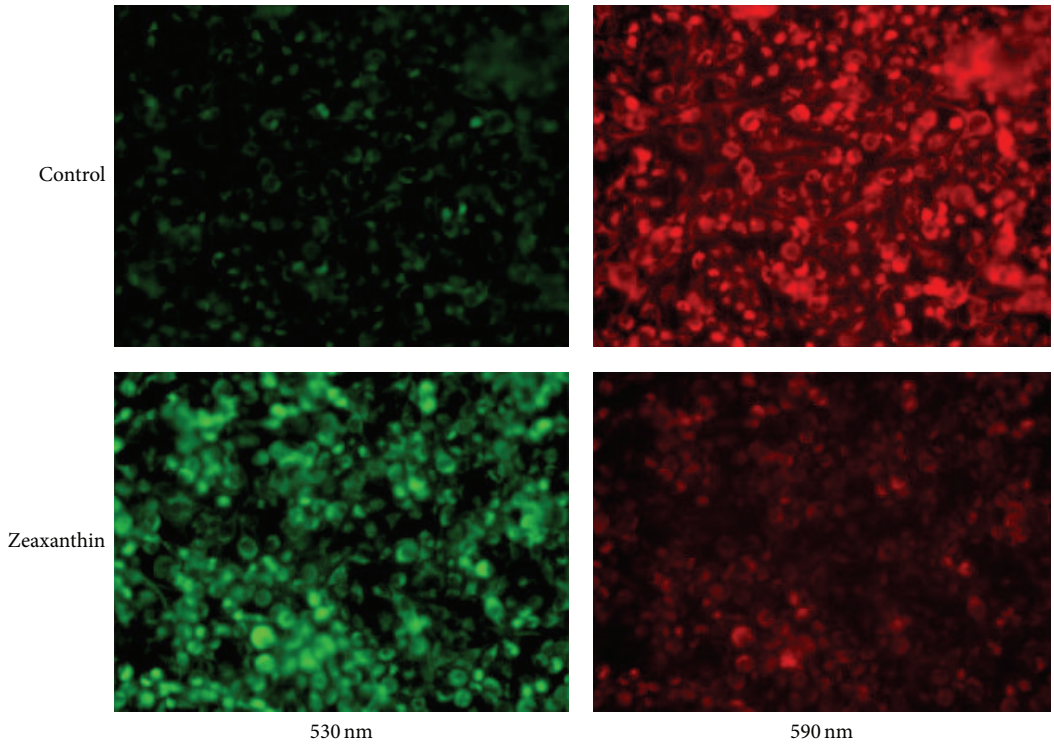

Figure 5: Fluorescence photomicrograph of effects of zeaxanthin on mitochondrial transmembrane potential (MTP) of uveal melanoma cells after JC-1 staining. Melanoma cells (C918) were treated by zeaxanthin at 0 (upper row) and 30 μM (lower row) for 24 h, and the MTP was determined by JC-1 staining (see Section 2). Cells were observed by fluorescence microscopy using dual band-pass filters (at 490 nm excitation and 530 and 590 nm emission). In normal mitochondria, the aggregated dye appears as red fluorescence located in the mitochondria (upper), whereas in cells with damaged MTP, the dye remains as monomers in the cytoplasm with diffuse green fluorescence (lower). The MTP in melanoma cells was observed at 530 nm (left) and 590 mm (right).

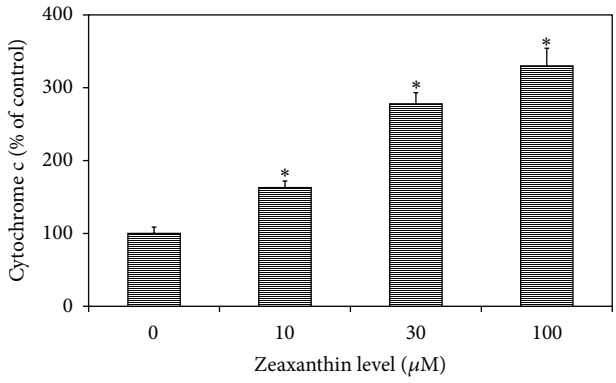

Figure 6: Effects of zeaxanthin-induced cytochrome c activation on human uveal melanoma cells. Uveal melanoma cells (C918) were treated with zeaxanthin at various doses for 2 h. Cells were collected and lysed, and the cytosol was extracted (see Section 2). The cytochrome c level in the cytosol was measured using a cytochrome c enzyme-linked immunosorbent assay kit. Cytosol cytochrome c level in zeaxanthin-treated cells at different concentrations was expressed as percentage of the controls. Zeaxanthin significantly increased the level of cytosol cytochrome c in a dose-dependent manner. Data are mean ± SD ($n = 3$). $^*P < 0.05$, versus control (cells cultured without zeaxanthin).

melanomas and the effect of zeaxanthin on cultured uveal melanoma cells has not been reported previously.

In the present study, zeaxanthin significantly decreased cell viability of two different human melanoma cell lines at concentration of 10–100 μM in a dose-and time-dependent manner. The C918 cell line, which was isolated from a patient with choroidal melanoma and liver metastasis, is epithelioid in morphology and is a highly invasive, metastatic, and aggressive melanoma cell line [50]. C918 is more sensitive to cytotoxic effect of zeaxanthin as compared with the nonmetastatic melanoma cell line (SP6.5), indicating that zeaxanthin may be a promising candidate for prevention and treatment of metastatic uveal melanoma.

The effects of zeaxanthin on human uveal melanoma cells were compared with those in uveal melanocytes, fibroblasts, and RPE cells. Zeaxanthin at lower levels (10 μM) significantly decreased the cell viability of melanoma cells, whereas the viability of these normal cells was not affected. Actually, the cell viability of normal cells was not affected at even the highest tested levels of zeaxanthin (300 μM, which is 30-fold of the minimal toxic levels in melanoma cells), suggesting that zeaxanthin has specific anticancer activity in uveal melanoma cells.

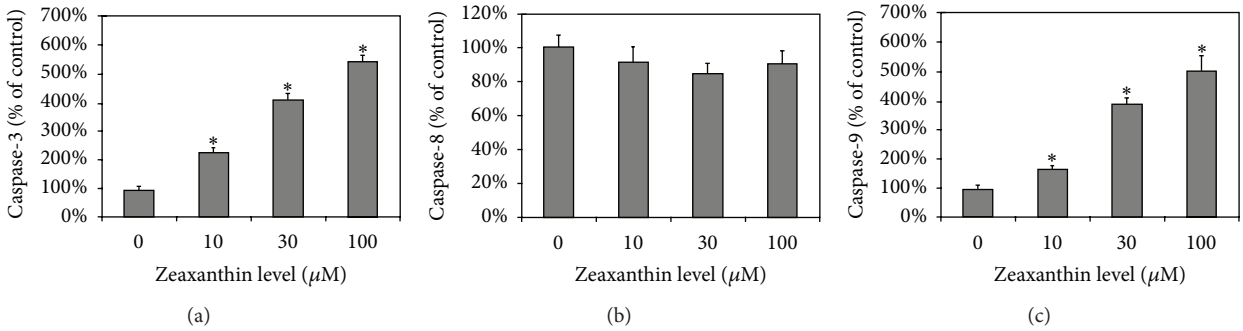

Figure 7: Effects of zeaxanthin on the activation of caspase-3, -8, and -9 in human uveal melanoma cell lines. Uveal melanoma cells (C918) were treated with various concentrations of zeaxanthin (10–100 μM) for 2 h. Cells were collected and lysed (see Section 2). The caspase-3, -8, and -9 in the lysates were measured using relevant caspase colorimetric assay kits. Caspase-3, -8, and -9 levels in zeaxanthin-treated cells at different concentrations were expressed as percentage of the controls. Zeaxanthin significantly increased caspase-3 (a) and caspase-9 (c) activities in a dose-dependent manner, but not caspase-8 activities (b). Data are mean ± SD ($n = 3$). $^{*}P < 0.05$, versus control (cells cultured without zeaxanthin).

Zeaxanthin is a hydrophobic molecule. Once ingested, zeaxanthin enters the liver through the portal vein and is taken up by the hepatocytes, incorporated into water-soluble lipoproteins, transported into the blood, and then transferred to various tissues [8, 9]. The distribution of zeaxanthin is eccentric among different tissues and organs. Ocular tissues have the highest levels of zeaxanthin, especially in the central retina, which can be several hundredfold the level in the serum [9]. The uveal tract also has a high level of zeaxanthin, accounting for up to 30% of the eye's total zeaxanthin content. The RPE and choroid may play a key role in the transport of zeaxanthin from circulating blood to the neural retina [12]. The zeaxanthin levels in mid-peripheral RPE and choroid are equal to 20–30% of the zeaxanthin levels in overlying retina [12]. Supplementation of zeaxanthin significantly increases serum and retina zeaxanthin levels [9–11]. In monkey zeaxanthin supplementation studies, the dietary supplementation of zeaxanthin at 2.2 mg/kg wt/day increased the serum zeaxanthin levels 10-fold [11, 53] and retina zeaxanthin levels from 4- to 9-fold in mid-peripheral and peripheral regions [10, 11]. Actually, supplementation safety dosages of zeaxanthin were far greater than the dosage (2.2 mg/kg wt/day) used in these experiments. One chronic study (52 weeks) in monkeys used 20 mg/kg/day and the dosage used in subacute studies in rats and mice was 50 mg/kg/day. (Gierhart, personal communication). Therefore, while the exact quantitative changes to zeaxanthin levels in uveal tract following supplementation are unknown, it is reasonable to assume that they are also significantly increased and may be comparable to those used in the present *in vitro* studies.

In the present study, the nature of cell death was studied using annexin V-ethidium-III double staining and flow cytometry analysis. An early event in apoptosis is a change in the phospholipid content of the cytoplasmic membrane outer leaflet. Phosphatidylserine (PS) is translocated from the inner to the outer surface of the cell. Annexin V is a phospholipid with a high affinity of PS. Annexin V labeled with fluorescein can bind to PS exposed on the outer leaflet and stain the cell membrane in bright green color [54]. Ethidium-III is a positively charged nucleic acid probe, which is impermeant to cells with intact plasma membrane. In the late stage of apoptosis, the cell membrane is damaged allowing ethidium-III to enter the cell and stain the nuclei producing red fluorescence. In the present study of the cells not treated with zeaxanthin, only very few of them stained with annexin and ethidium-III. Among cells treated with zeaxanthin, annexin-stained cells (indicating apoptotic changes) significantly increased compared to controls. The percentage of apoptotic cells also increased with time, suggesting that zeaxanthin can induce apoptosis of melanoma cells. This is consistent with previous reports which found an apoptosis-induction effect of zeaxanthin in breast cancer, colon cancer, lymphoma, and neuroblastoma cells [45–47].

There are two different apoptosis pathways, one extrinsic and one intrinsic. Extrinsic apoptosis occurs due to the activation of various cell death surface receptors following binding to the relevant ligands. Activated death receptors bind to secondary adaptor proteins which activate caspase-8 leading to a series of downstream events, including subsequent cleavage of caspase-3, and cell apoptosis. Intrinsic apoptosis pathway also called the mitochondrial apoptotic pathway is regulated by the Bcl-2 family of proteins, which includes the anti-apoptotic proteins (Bcl-2, Bcl-xL, etc.), the proapoptotic proteins (Bax and Bak) and the apoptosis initiator proteins (Bad, Bik, etc.). Accumulation of proapoptotic proteins on the mitochondrial outer membrane results in increased mitochondrial membrane permeability, causing the release of cytochrome c into the cytoplasm. Cytochrome c promotes activation of caspase-9, which in turn promotes activation of caspase-3, leading to apoptosis of the tumor cell [55–57].

Very little is known about the mechanism of zeaxanthin-induced apoptosis in malignant tumor cells [48]. In the present study, zeaxanthin reduced the expression of antiapoptotic proteins, Bcl-xL, in the two melanoma cell lines and increased the pro-apoptotic proteins (Bak) in SP6.5 cell line and Bax in C918 cell line. In additional, zeaxanthin decreased

the Bcl-2 in SP6.5 cell lines. All of these results suggest that the zeaxanthin-induced apoptosis effect occurs via the intrinsic cell death pathway and is regulated by Bcl-2 family proteins. This finding is consistent with a previous report which found that zeaxanthin downregulated the expression of Bcl-2 mRNA in breast cancer cells [48].

The effects of zeaxanthin on the mitochondrial apoptosis signal pathway in malignant tumor cells have not been reported previously. In the present study, zeaxanthin significantly increased mitochondria outer membrane permeability as indicated by the mitochondrial staining test. This can lead to release of cytochrome c from mitochondria to cytosol, significantly increasing the cytosol cytochrome c levels, which in turn causes the activation of caspase-9 and -3 and results in the apoptosis. In this study, caspase-8, which plays an important role in the activation of the extrinsic apoptosis pathway, did not increase after exposing the melanoma cells to zeaxanthin. These results suggest that zeaxanthin induces apoptosis in uveal melanoma cells mainly via the intrinsic mitochondrial pathway.

Recently, it has been found that one of zeaxanthin's isomer, mesozeaxanthin [3,3′-dihydro-β,β-carotene], also has antimutagenic and anticarcinogenic potential. Mesozeaxanthin treatment increased survival of mice with 3-methylcholanthrene-induced sarcoma [58, 59].

In summary, zeaxanthin significantly decreased cell viability and induced apoptosis of human uveal melanoma cells without affecting the cell viability of normal cells, suggesting that zeaxanthin has a selective and potent pro-apoptotic effect on human uveal melanoma cells *in vitro*. This effect is mainly through the regulation of Bcl-2 family protein and intrinsic mitochondrial pathway. The potent and selective cytotoxic effects of zeaxanthin on a highly aggressive and metastatic human melanoma cell line (C918 cell line) suggest that zeaxanthin may be a promising agent worth exploring for the treatment of metastatic uveal melanoma.

Acknowledgments

The authors thank Dr. Dennis L. Gierhart for his helpful comments and for providing pure zeaxanthin, Dr. Xiaoliang Leon Xu (Memorial Sloan Kettering Cancer Center, New York) for providing C918 melanoma cell line, and Dr. Guy Pelletier (Research Center of Immunology, Quebec, Canada) for providing SP6.5 melanoma cell line. This work was supported by the National Natural Science Foundation of China (81070736), the Dennis L. Gierhart Charitable Gift Fund; the Bendheim Family Retina Fund, the Estelle Richards Foundation, and the Pathology Fund of New York Eye and Ear Infirmary. Drs. Richard Rosen and Dan-Ning Hu had applied a patent for the use of zeaxanthin in the management of various malignant tumors (PCT/US2013/032422). There are no other commercial relationships existing in the form of financial support or personal financial interest regarding the contents of this paper. This paper has not been published elsewhere and has not been submitted simultaneously for publication elsewhere.

References

[1] D.-N. Hu, G.-P. Yu, S. A. McCormick, S. Schneider, and P. T. Finger, "Population-based incidence of uveal melanoma in various races and ethnic groups," *American Journal of Ophthalmology*, vol. 140, no. 4, pp. 612–617, 2005.

[2] E. Kujala, T. Mäkitie, and T. Kivelä, "Very long-term prognosis of patients with malignant uveal melanoma," *Investigative Ophthalmology and Visual Science*, vol. 44, no. 11, pp. 4651–4659, 2003.

[3] M. J. Jager, J. Y. Niederkorn, and B. R. Ksander, *Uveal Melanoma*, Taylor & Francis, London, UK, 2004.

[4] J. J. Augsburger, Z. M. Corrêa, and A. H. Shaikh, "Effectiveness of treatments for metastatic uveal melanoma," *American Journal of Ophthalmology*, vol. 148, no. 1, pp. 119–127, 2009.

[5] O. Sommerburg, J. E. E. Keunen, A. C. Bird, and F. J. G. M. Van Kuijk, "Fruits and vegetables that are sources for lutein and zeaxanthin: the macular pigment in human eyes," *British Journal of Ophthalmology*, vol. 82, no. 8, pp. 907–910, 1998.

[6] J. J. Zhou, G. R. Xie, and X. J. Yan, *Phytochemistry of Chinese Traditional Medicine*, Chemical Industry Press, Beijing, China, 2004.

[7] Y. J. Shen, *Pharmacology of Chinese Traditional Medicine*, People's Medical Publishing House, Beijing, China, 2002.

[8] S. S. Ahmed, M. N. Lott, and D. M. Marcus, "The macular xanthophylls," *Survey of Ophthalmology*, vol. 50, no. 2, pp. 183–193, 2005.

[9] A. J. Whitehead, J. A. Mares, and R. P. Danis, "Macular pigment: a review of current knowledge," *Archives of Ophthalmology*, vol. 124, no. 7, pp. 1038–1045, 2006.

[10] R. Vishwanathan, M. Neuringer, D. M. Snodderly, W. Schalch, and E. J. Johnson, "Macular lutein and zeaxanthin are related to brain lutein and zeaxanthin in primates," *Nutritional Neuroscience*, vol. 16, no. 1, pp. 21–29, 2013.

[11] E. J. Johnson, M. Neuringer, R. M. Russell, W. Schalch, and D. M. Snodderly, "Nutritional manipulation of primate retinas—III: effects of lutein or zeaxanthin supplementation on adipose tissue and retina of xanthophyll-free monkeys," *Investigative Ophthalmology and Visual Science*, vol. 46, no. 2, pp. 692–702, 2005.

[12] P. S. Bernstein, F. Khachik, L. S. Carvalho, G. J. Muir, D.-Y. Zhao, and N. B. Katz, "Identification and quantitation of carotenoids and their metabolites in the tissues of the human eye," *Experimental Eye Research*, vol. 72, no. 3, pp. 215–223, 2001.

[13] D. M. Snodderly, G. J. Handelman, and A. J. Adler, "Distribution of individual macular pigment carotenoids in central retina of macaque and squirrel monkeys," *Investigative Ophthalmology and Visual Science*, vol. 32, no. 2, pp. 268–279, 1991.

[14] J. M. Seddon, U. A. Ajani, R. D. Sperduto et al., "Dietary carotenoids, vitamins A, C, and E, and advanced age-related macular degeneration," *Journal of the American Medical Association*, vol. 272, no. 18, pp. 1413–1420, 1994.

[15] J. P. SanGiovanni, E. Y. Chew, T. E. Clemons et al., "The relationship of dietary carotenoid and vitamin A, E, and C intake with age-related macular degeneration in a case-control study: AREDS report No. 22," *Archives of Ophthalmology*, vol. 125, no. 9, pp. 1225–1232, 2007.

[16] V. Parisi, M. Tedeschi, G. Gallinaro, M. Varano, S. Saviano, and S. Piermarocchi, "Carotenoids and antioxidants in age-related maculopathy Italian study: multifocal electroretinogram modifications after 1 year," *Ophthalmology*, vol. 115, no. 2, pp. 324–333, 2008.

[17] L. Ma, H. L. Dou, Y. M. Huang et al., "Improvement of retinal function in early age-related macular degeneration after lutein and zeaxanthin supplementation: a randomized, double-masked, placebo-controlled trial," *American Journal of Ophthalmology*, vol. 154, no. 4, pp. 625–634, 2012.

[18] H. P. Y. Sin, D. T. L. Liu, and D. S. C. Lam, "Lifestyle modification, nutritional and vitamins supplements for age-related macular degeneration," *Acta Ophthalmologica*, vol. 91, no. 1, pp. 6–11, 2013.

[19] L. Ho, R. Van Leeuwen, J. C. M. Witteman et al., "Reducing the genetic risk of age-related macular degeneration with dietary antioxidants, zinc, and ω-3 fatty acids. The Rotterdam Study," *Archives of Ophthalmology*, vol. 129, no. 6, pp. 758–766, 2011.

[20] Age-Related Eye Disease Study 2 Research Group, "Lutein + zeaxanthin and omega-3 fatty acids for age-related macular degeneration: the Age-Related Eye Disease Study 2 (AREDS2) randomized clinical trial," *The Journal of the American Medical Association*, vol. 309, no. 19, pp. 2005–2015, 2013.

[21] L. Ma, H.-L. Dou, Y.-Q. Wu et al., "Lutein and zeaxanthin intake and the risk of age-related macular degeneration: a systematic review and meta-analysis," *British Journal of Nutrition*, vol. 107, no. 3, pp. 350–359, 2012.

[22] S. G. Holtan, H. M. O'Connor, Z. S. Fredericksen et al., "Food-frequency questionnaire-based estimates of total antioxidant capacity and risk of non-Hodgkin lymphoma," *International Journal of Cancer*, vol. 131, no. 5, pp. 1158–1168, 2012.

[23] L. E. Kelemen, J. R. Cerhan, and U. Lim, "Vegetables, fruit, and antioxidant-related nutrients and risk of non-Hodgkin lymphoma: a National Cancer Institute-Surveillance, Epidemiology, and End Results population-based case-control study," *American Journal of Clinical Nutrition*, vol. 83, no. 6, pp. 1401–1410, 2006.

[24] H. Cho, M. K. Kim, J. K. Lee et al., "Relationship of serum antioxidant micronutrients and sociodemographic factors to cervical neoplasia: a case-control study," *Clinical Chemistry and Laboratory Medicine*, vol. 47, no. 8, pp. 1005–1012, 2009.

[25] Y.-M. Peng, Y.-S. Peng, J. M. Childers et al., "Concentrations of carotenoids, tocopherols, and retinol in paired plasma and cervical tissue of patients with cervical cancer, precancer, and noncancerous diseases," *Cancer Epidemiology Biomarkers and Prevention*, vol. 7, no. 4, pp. 347–350, 1998.

[26] S.-Y. Tong, J.-M. Lee, E.-S. Song et al., "Functional polymorphism in manganese superoxide dismutase and antioxidant status: their interactions on the risk of cervical intraepithelial neoplasia and cervical cancer," *Gynecologic Oncology*, vol. 115, no. 2, pp. 272–276, 2009.

[27] Y. T. Kim, J. W. Kim, J. S. Choi, S. H. Kim, E. K. Choi, and N. H. Cho, "Relation between deranged antioxidant system and cervical neoplasia," *International Journal of Gynecological Cancer*, vol. 14, no. 5, pp. 889–895, 2004.

[28] M. A. Schiff, R. E. Patterson, R. N. Baumgartner et al., "Serum carotenoids and risk of cervical intraepithelial neoplasia in Southwestern American Indian women," *Cancer Epidemiology Biomarkers and Prevention*, vol. 10, no. 11, pp. 1219–1222, 2001.

[29] S. Franceschi, E. Bidoli, and E. Negri, "Role of macronutrients, vitamins and minerals in the aetiology of squamous-cell carcinoma of the oesophagus," *International Journal of Cancer*, vol. 86, no. 5, pp. 626–631, 2000.

[30] X. X. Ge, M. Y. Xing, L. F. Yu, and P. Shen, "Carotenoid intake and esophageal cancer risk: a meta-analysis," *Asian Pacific Journal of Cancer Prevention*, vol. 14, no. 3, pp. 1911–1918, 2013.

[31] G. Mózsik, G. Rumi, A. Dömötör et al., "Involvement of serum retinoids and Leiden mutation in patients with esophageal, gastric, liver, pancreatic, and colorectal cancers in Hungary," *World Journal of Gastroenterology*, vol. 11, no. 48, pp. 7646–7650, 2005.

[32] M. Jenab, E. Riboli, P. Ferrari et al., "Plasma and dietary carotenoid, retinol and tocopherol levels and the risk of gastric adenocarcinomas in the European prospective investigation into cancer and nutrition," *British Journal of Cancer*, vol. 95, no. 3, pp. 406–415, 2006.

[33] G. W. Comstock, A. J. Alberg, H.-Y. Huang et al., "The risk of developing lung cancer associated with antioxidants in the blood: ascorbic acid, carotenoids, α-tocopherol, selenium, and total peroxyl radical absorbing capacity," *Cancer Epidemiology Biomarkers and Prevention*, vol. 6, no. 11, pp. 907–916, 1997.

[34] T. Tanaka, M. Shnimizu, and H. Moriwaki, "Cancer chemoprevention by carotenoids," *Molecules*, vol. 17, no. 3, pp. 3202–3242, 2012.

[35] C. N. Holick, D. S. Michaud, R. Stolzenberg-Solomon et al., "Dietary carotenoids, serum β-carotene, and retinol and risk of lung cancer in the alpha-tocopherol, beta-carotene cohort study," *American Journal of Epidemiology*, vol. 156, no. 6, pp. 536–547, 2002.

[36] R. M. Tamimi, G. A. Colditz, and S. E. Hankinson, "Circulating carotenoids, mammographic density, and subsequent risk of breast cancer," *Cancer Research*, vol. 69, no. 24, pp. 9323–9329, 2009.

[37] J. F. Dorgan, A. Sowell, C. A. Swanson et al., "Relationships of serum carotenoids, retinol, α-tocopherol, and selenium with breast cancer risk: results from a prospective study in Columbia, Missouri (United States)," *Cancer Causes and Control*, vol. 9, no. 1, pp. 89–97, 1998.

[38] A. H. Eliassen, S. J. Hendrickson, L. A. Brinton et al., "Circulating carotenoids and risk of breast cancer: pooled analysis of eight prospective studies," *Journal of the National Cancer Institute*, vol. 104, no. 24, pp. 1905–1916, 2012.

[39] J. Hu, C. La Vecchia, and E. Negri, "Dietary vitamin C, E, and carotenoid intake and risk of renal cell carcinoma," *Cancer Causes and Control*, vol. 20, no. 8, pp. 1451–1458, 2009.

[40] A. K. Sakhi, S. K. Bøhn, S. Smeland et al., "Postradiotherapy plasma lutein, α-carotene, and β-carotene are positively associated with survival in patients with head and neck squamous cell carcinoma," *Nutrition and Cancer*, vol. 62, no. 3, pp. 322–328, 2010.

[41] M. L. Slattery, J. Benson, K. Curtin, K.-N. Ma, D. Schaeffer, and J. D. Potter, "Carotenoids and colon cancer," *American Journal of Clinical Nutrition*, vol. 71, no. 2, pp. 575–582, 2000.

[42] L. I. Mignone, E. Giovannucci, P. A. Newcomb et al., "Dietary carotenoids and the risk of invasive breast cancer," *International Journal of Cancer*, vol. 124, no. 12, pp. 2929–2937, 2009.

[43] S. Jung, K. Wu, E. Giovannucci et al., "Carotenoid intake and risk of colorectal adenomas in a cohort of male health professionals," *Cancer Causes Control*, vol. 24, no. 4, pp. 705–717, 2013.

[44] R. J. Jansen, D. P. Robinson, R. Z. Stolzenberg-Solomon et al., "Nutrients from fruit and vegetable consumption reduce the risk of pancreatic cancer," *Journal of Gastrointestinal Cancer*, vol. 44, no. 2, pp. 152–161, 2013.

[45] J. Molnár, N. Gyémánt, I. Mucsi et al., "Modulation of multidrug resistance and apoptosis of cancer cells by selected carotenoids," *In Vivo*, vol. 18, no. 2, pp. 237–244, 2004.

[46] M. Maccarrone, M. Bari, V. Gasperi, and B. Demmig-Adams, "The photoreceptor protector zeaxanthin induces cell death in neuroblastoma cells," *Anticancer Research*, vol. 25, no. 6 B, pp. 3871–3876, 2005.

[47] H. C. Kwang, Y. I. K. Song, and D.-U. Lee, "Antiproliferative effects of carotenoids extracted from *Chlorella ellipsoidea* and *Chlorella vulgaris* on human colon cancer cells," *Journal of Agricultural and Food Chemistry*, vol. 56, no. 22, pp. 10521–10526, 2008.

[48] Z. Li, Y. Wang, and B. Mo, "The effects of carotenoids on the proliferation of human breast cancer cell and gene expression of bcl-2," *Chinese Journal of Preventive Medicine*, vol. 36, no. 4, pp. 254–257, 2002.

[49] D. Soulieres, A. Rousseau, J. Deschenes, M. Tremblay, M. Tardif, and G. Pelletier, "Characterization of gangliosides in human uveal melanoma cells," *International Journal of Cancer*, vol. 49, no. 4, pp. 498–503, 1991.

[50] K. J. Daniels, H. C. Boldt, J. A. Martin, L. M. Gardner, M. Meyer, and R. Folberg, "Expression of type VI collagen in uveal melanoma: its role in pattern formation and tumor progression," *Laboratory Investigation*, vol. 75, no. 1, pp. 55–66, 1996.

[51] D.-N. Hu, S. A. McCormick, R. Ritch, and K. Pelton-Henrion, "Studies of human uveal melanocytes in vitro: isolation, purification and cultivation of human uveal melanocytes," *Investigative Ophthalmology and Visual Science*, vol. 34, no. 7, pp. 2210–2219, 1993.

[52] Z. Cui, E. Song, D. N. Hu et al., "Butein induces apoptosis in human uveal melanoma cells through mitochondrial apoptosis pathway," *Current Eye Research*, vol. 37, no. 8, pp. 730–739, 2012.

[53] M. Neuringer, M. M. Sandstrom, E. J. Johnson, and D. M. Snodderly, "Nutritional manipulation of primate retinas—I: effects of lutein or zeaxanthin supplements on serum and macular pigment in xanthophyll-free Rheus monkeys," *Investigative Ophthalmology and Visual Science*, vol. 45, no. 9, pp. 3234–3243, 2004.

[54] M. van Engeland, F. C. Ramaekers, B. Schutte, and C. P. Reutelingsperger, "A novel assay to measure loss of plasma membrane asymmetry during apoptosis of adherent cells in culture," *Cytometry*, vol. 24, no. 2, pp. 131–139, 1996.

[55] G. Kroemer, B. Dallaporta, and M. Resche-Rigon, "The mitochondrial death/life regulator in apoptosis and necrosis," *Annual Review of Physiology*, vol. 60, pp. 619–642, 1998.

[56] D. J. McConkey, "Biochemical determinants of apoptosis and necrosis," *Toxicology Letters*, vol. 99, no. 3, pp. 157–168, 1998.

[57] A. Strasser, S. Cory, and J. M. Adams, "Deciphering the rules of programmed cell death to improve therapy of cancer and other diseases," *EMBO Journal*, vol. 30, no. 18, pp. 3667–3683, 2011.

[58] A. P. Firdous, E. R. Sindhu, V. Ramnath, and R. Kuttan, "Antimutagenic and anti-carcinogenic potential of the carotenoid meso-zeaxanthin," *Asian Pacific Journal of Cancer Prevention*, vol. 11, no. 6, pp. 1795–1800, 2010.

[59] A. P. Firdous, E. R. Sindhu, V. Ramnath, and R. Kuttan, "Anticarcinogenic activity of meso-zeaxanthin in rodents and its possible mechanism of action," *Nutrtion and Cancer*, vol. 65, no. 65, pp. 850–856, 2013.

Hindawi Publishing Corporation
Evidence-Based Complementary and Alternative Medicine
Volume 2013, Article ID 761852, 9 pages
http://dx.doi.org/10.1155/2013/761852

Research Article

[6]-Gingerol Prevents Disassembly of Cell Junctions and Activities of MMPs in Invasive Human Pancreas Cancer Cells through ERK/NF-κB/Snail Signal Transduction Pathway

Sung Ok Kim and Mi Ryeo Kim

Department of Herbal Pharmacology, College of Oriental Medicine, Daegu Haany University, 165 Sang Dong, Suseong gu, Daegu 706-828, Republic of Korea

Correspondence should be addressed to Sung Ok Kim; sokim@dhu.ac.kr

Received 24 May 2013; Revised 15 July 2013; Accepted 14 August 2013

Academic Editor: Dan-Ning Hu

To study the effects of [6]-gingerol, a ginger phytochemical, on tight junction (TJ) molecules, we investigated TJ tightening and signal transduction pathways in human pancreatic duct cell-derived cancer cell line PANC-1. The following methods were utilized: MTT assay to determine cytotoxicity; zymography to examine matrix metalloproteinase (MMP) activities; transepithelial electrical resistance (TER) and paracellular flux for TJ measurement; RT-PCR and immunoblotting for proteins related to TJ and invasion; and EMSA for NF-κB activity in PANC-1 cells. Results revealed that TER significantly increased and claudin 4 and MMP-9 decreased compared to those of the control. TJ protein levels, including zonula occludens (ZO-) 1, occludin, and E-cadherin, increased in [6]-gingerol-treated cells, which correlated with a decrease in paracellular flux and MMP activity. Furthermore, NF-κB/Snail nuclear translocation was suppressed via downregulation of the extracellular signal-regulated kinase (ERK) pathway in response to [6]-gingerol treatment. Moreover, treatment with U0126, an ERK inhibitor, completely blocked NF-κB activity. In conclusion, these findings demonstrate that [6]-gingerol regulates TJ-related proteins and suppresses invasion and metastasis through NF-κB/Snail inhibition via inhibition of the ERK pathway. Therefore, [6]-gingerol may suppress the invasive activity of PANC-1 cells.

1. Introduction

Most natural products target multiple gene products and thus are ideally suited for the prevention and treatment of various chronic diseases, including cancer [1]. Metastasis is considered the major cause of death in patients with cancer. Recently, in various human cancers, including pancreatic cancer, some tight junction (TJ) proteins, including claudins, were determined to be abnormally regulated; thus, they may be promising molecular targets for diagnosis and therapy [2, 3].

TJs are apical intercellular junctional complexes whose general function is the maintenance of epithelial polarity, as well as functioning as selective barriers to molecules such as inhibition of solute and water flow through the paracellular space [4]. TJs are dynamic structures subject to modulation during wound repair, inflammation, and tumor progression. TJs are dysregulated or lost in cancer tissues. Consequently, dysregulation of TJ proteins contributes to cancer progression and metastasis [5].

The rhizome of *Zingiber officinale*, commonly known as ginger, is a globally important spice. The ginger phytochemicals, specifically [6]-gingerol, (5-Hydroxy-1-(4-hydroxy-3-methoxyphenyl)-3-decanone; Figure 1), the major pungent component of ginger, has antioxidant, anti-inflammation, and antitumor promoting activities [6–8]. However, the exact mechanism responsible for the anti-invasiveness and metastasis effects of ginger in pancreatic cancer cells is still unknown. The present research attempts for the first time to address TJ regulation in the anti-invasive effects of ginger in pancreatic cancer (PC) chemotherapy.

PC is one of the most lethal malignant cancers in Western countries, as well as in Korea [6, 7]. PC is characterized by

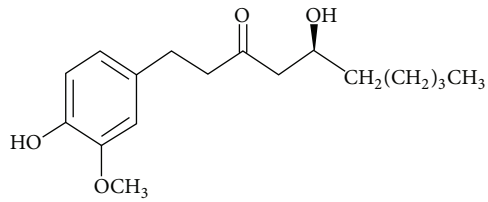

5-Hydroxy-1-(4-hydroxy-3-methoxyphenyl)-3-decanone

Figure 1: Chemical structures of [6]-gingerol.

rapid progression, late clinical presentation, difficulty in early diagnosis, and unresponsiveness to chemotherapy, radiotherapy, and immunotherapy, resulting in low resectability rates after diagnosis, early recurrence after resection, and extremely poor survival rates [8, 9]. At the time of diagnosis, PC normally shows extensive local invasion and/or metastasis, precluding a curative surgical resection. A better understanding of the molecular genetics of pancreatic carcinoma is needed to develop new diagnostic and therapeutic strategies. However, no studies have reported the effect of [6]-gingerol on the cellular and molecular mechanisms of invasion and metastasis related TJs in human pancreatic cancer cells. In this study, we investigated whether [6]-gingerol prevents disruption of the TJ and cancer cell invasion in human pancreatic cancer cells.

2. Material and Methods

2.1. Cell Culture. The human pancreatic cancer cell line PANC-1 was obtained from the American Type Culture Collection (ATCC, Rockville, MD, USA). Cells were cultured in Dulbecco's modified Eagle's medium (DMEM) supplemented with 10% fetal bovine serum (FBS; Gibco-BRL, Grand Island, NY, USA) at 37°C in a humidified atmosphere containing 5% CO_2.

2.2. MTT Assay. For the cell viability assay, cells were plated at 1×10^4 cells/well in a 96-well plate (Nunc, Roskilde, Denmark). After incubation with 0, 5, 10, 15, or 20 μM [6]-gingerol (Sigma-Aldrich, St. Louis, MO, USA) for 24 h, cell viability was determined using a 3-(4,5-dimethylthiazol-2-yl)-2,5-diphenyltetrazolium bromide (MTT) assay, which is based on the conversion of MTT to MTT-formazan by mitochondria. Cells were incubated with 1 mg/mL MTT (Chemicon, Temecula, CA, USA) in phosphate-buffered saline (PBS) for 4 h at 37°C in 5% CO_2. Isopropanol and hydrochloric acid were then added at final concentrations of 50% and 20 mM, respectively. The optical density at 570 nm was determined using an enzyme-linked immunosorbent assay (ELISA) plate reader (MN 3663; Molecular Devices, Sunnyvale, CA, USA) with a reference wavelength of 630 nm.

2.3. Transepithelial Electrical Resistance (TER). The TER is a quantitative measure explaining the barrier integrity of monolayers. The TER value was measured for transport experiments with an epithelial volt-ohm meter (World Precision Instruments, Sarasota, FL, USA). TER measurements were determined to evaluate the barrier-strengthening effect of [6]-gingerol in cells. TERs were obtained at four separate areas of each Transwell and averaged.

2.4. Paracellular Permeability. A PANC-1 transport study was performed to examine the effect of [6]-gingerol on paracellular permeability. Cells were seeded at a density of 6×10^4 cells/cm^2 in 12-well, 0.4 μm inserts (Coaster; Corning, Corning, NY, USA) and grown in DMEM with 10% FBS for 3 days at 37°C, 95% humidity, and 5% CO_2. Cells were washed twice with prewarmed PBS, and [^{14}C] D-mannitol in PBS (0.1 μCi/mL) was then added to the apical compartment. Afterward, the basolateral sample was removed and replaced with fresh PBS at 10, 20, 30, 40, 50, and 60 min. Monolayers were continuously agitated during permeability experiments. [^{14}C] D-mannitol in the samples was quantified using a LS6500TA liquid scintillation counter (Beckman Coulter, Fullerton, CA, USA). The apparent permeability coefficient, Papp (cm/s), for mannitol was determined using the following equation: $\text{Papp} = (V_d/A \bullet D_o) \bullet (dQ/dt)$, where dQ/dt is the flux across the monolayer, V_d is the volume of the donor compartment (0.5 mL), A is the surface area (1 cm^2) of the Transwell membrane, and D_o is the initial concentration of mannitol in the donor compartment.

2.5. MMP Activity. After incubation with [6]-gingerol for 24 h, cell-free culture supernatants were collected and mixed with 2× sample buffer and then subjected to 10% polyacrylamide gel electrophoresis (PAGE) with 0.1% gelatin Novex Zymogram precast gels (Invitrogen, Camarillo, CA, USA). After electrophoresis, gels were washed twice at room temperature for 30 min in 2.5% Triton X-100, subsequently washed in buffer containing 50 mM Tris-HCl, 150 mM NaCl, 5 mM $CaCl_2$, 1 μM $ZnCl_2$, and 0.02% NaN_3 (pH 7.5), and incubated in the same buffer at 37°C for 24 h. Gels were stained with 0.25% (w/v) Coomassie Brilliant Blue G-250 (Bio-Rad Laboratories, Hercules, CA, USA) and then destained in water solution containing methanol and acetic acid, respectively, for 1 h. The gelatinolytic activity was shown as clear bands (area of gelatin degradation) against the blue background of stained gelatin.

2.6. In Vitro Invasion Assay. To determine the effects of [6]-gingerol on PANC-1 cell invasiveness, cells were pretreated with 10 μM [6]-gingerol for 6 h and plated onto the apical side of Matrigel-coated filters with 8 mm pore membranes (Corning) in serum-free medium containing either [6]-gingerol or vehicle solution. Medium containing 20% FBS was placed in the basolateral chamber to act as a chemoattractant. After 72 h, cells on the apical side were wiped off using a Q-tip. Cells on the bottom of the filter were fixed with methanol and stained with hematoxylin and eosin Y and then counted (three fields of each triplicate filter) under an inverted microscope (Nikon, Tokyo, Japan).

2.7. Reverse Transcription-Polymerase Chain Reaction (RT-PCR). Total RNA was prepared using Trizol reagent (Invitrogen) according to the manufacturer's recommendations and

subsequently used for RT-PCR with one step RT-PCR premix (Intron Biotechnology Co., Sungnam, Korea) according to the manufacturer's instructions. PCR was performed in a Mastercycler (Eppendorf, Hamburg, Germany) with primers indicated in Table 1. PCR conditions were as follows: 1 cycle at 94°C for 3 min; 35 cycles at 94°C for 45 s, 58°C for 45 s, and 72°C for 1 min; and 1 cycle at 72°C for 10 min. As a sample loading control and normalization between samples, PCR amplification of the housekeeping gene, glyceraldehydes 3-phosphate dehydrogenase (GAPDH), was included for each run. PCR amplification products were electrophoretically separated on a 1.5% agarose gel and visualized by ethidium bromide (EtBr; Sigma-Aldrich) staining.

2.8. Western Blot Analysis. Immunoblot analysis was performed to analyze protein levels. After pretreatment with the ERK inhibitor U0126 (Calbiochem, Billerica, MA, USA) for 1 h and treatment with/without [6]-gingerol for 24 h, cells were harvested, and then protein was extracted with protein lysis buffer (25 mM Tris-Cl, pH 7.5, 250 mM NaCl, 5 mM ethylendiaminetetracetic acid, 1% Nonidet P-40, protease inhibitor, and phosphatase inhibitor cocktails; Thermo Scientific, Waltham, MA, USA). Quantification of protein concentration was carried out using the Bradford method (Bio-Rad protein assay reagent), and total protein was resuspended in Laemmli sample buffer containing 5% β-mercaptoethanol and heated at 65°C for 10 min. Aliquots containing ~20–50 μg of total cell proteins were resolved on 8–12% sodium dodecyl sulfate (SDS)-PAGE and then transferred onto nitrocellulose membranes (Amersham, Arlington Heights, IL, USA). Membranes were blocked in 5% nonfat milk (w/v) in Tris-buffered saline (TBS) containing 0.05% Tween 20 (TBST) for 1 h at room temperature, and membranes were then subjected to immunoblot analysis with the desired antibodies (Table 2). After overnight incubation at 4°C, membranes were washed in TBST and incubated with the appropriate peroxidase-conjugated secondary antibodies (Santa Cruz Biotechnology, Santa Cruz, CA, USA). Membranes were developed using chemiluminescence according to the enhanced chemiluminescence Western blotting detection reagent (Pierce, Rockford, IL, USA).

2.9. Electrophoretic Mobility Shift Assay (EMSA). Nuclear proteins were extracted using the NE-PER nuclear and cytosolic extraction reagents kit (Pierce) according to the instructions. Synthetic complementary NF-κB binding oligonucleotides (Promega, Madison, WI, USA) were 3-biotinylated using a biotin 3-end DNA labeling kit (Pierce) according to the manufacturer's instructions. Assays were performed using a LightShift electrophoretic mobility shift assay (EMSA) optimization kit (Pierce) according to the manufacturer's protocol.

2.10. Statistical Analysis. All data are presented as the means ± standard deviation (SD). Statistical analyses (Student's t-test and one way analysis of variance, ANOVA) were performed using GraphPad Prism 5 software (GraphPad Software, Inc., La Jolla, CA, USA). Densitometry was performed using L process V2.01 and MultiGauge V2.02 (Fuji Film, Stamford, CT, USA). A value of $^{*}P < 0.05$ was considered to indicate a statistically significant difference. All results presented in the figures in this study were obtained from at least three independent experiments.

3. Results

3.1. Effect of [6]-Gingerol on Cell Viability in PANC-1 Cells. The MTT assay was performed to determine the cytotoxicity of [6]-gingerol on PANC-1 cells with ~0–20 μM [6]-gingerol (Figure 2). Therefore, <20 μM [6]-gingerol was used for treatments in this experiment. Subsequently, [6]-gingerol did not inhibit cell growth compared to that of the control. Cytotoxicity was not observed at concentrations below 20 μM [6]-gingerol.

3.2. [6]-Gingerol Increased Transepithelial Electrical Resistance (TER) in PANC-1 Cells. TER (a measure of TJ formation) values were measured to examine the relationship between TJ tightening and invasive activity of PANC-1 cells treated with [6]-gingerol. As shown in Figure 3(a), incubation of cells with [6]-gingerol substantially increased TER levels in a dose-dependent manner. Using a Matrigel-coated invasion assay, we next examined the question of whether [6]-gingerol decreases cell invasion activity. As shown in Figure 3(b), [6]-gingerol treatment reduced cell invasion through the Matrigel chamber. These results show that the increase in TER values upon treatment with [6]-gingerol indicates an increase in TJ formation and is associated with inhibition of cell invasion in PANC-1 cells.

3.3. [6]-Gingerol Reduced Paracellular Permeability in PANC-1 Cells. To further characterize TJ changes induced by [6]-gingerol, paracellular permeability of PANC-1 monolayers was determined using the permeability marker mannitol. The D-mannitol compound is an inert carbohydrate that is transported only through this paracellular route, that is, through TJs. After 3 days of treatment with or without [6]-gingerol (10 μM), the apparent permeability of mannitol (Papp mannitol) decreased by ~32% compared to that of untreated control cells (Figure 4), confirming that [6]-gingerol exhibits an enhancing effect on TJ formation in human pancreatic cancer cells.

3.4. [6]-Gingerol Suppressed MMP Activity in PANC-1 Cells. To clarify activation of MMPs in PANC-1 cells, zymography was conducted to assess whether [6]-gingerol affects MMP activation. Secretion of MMP-2 and MMP-9 was significantly ($P < 0.05$) inhibited by [6]-gingerol treatment compared with untreated cells (Figure 5). MMP-9 activity was suppressed more than that of MMP-2. This result suggests that [6]-gingerol inhibits the invasiveness of pancreatic cancer cells by decreasing the levels of protease, MMP-2, and MMP-9.

3.5. [6]-Gingerol Regulated the Expression of TJ and Invasion-Related Genes in PANC-1 Cells. To determine whether [6]-gingerol regulates the expression of TJ and invasion-related

Table 1: Oligonucleotides used in RT-PCR.

Genes	Primer sequence
Claudin-4	Sense 5′-TGG ATG AAC TGC GTG GTG CAG-3′
	Antisense 5′-GAG GCG GCC CAG CCG ACG TA-3′
MMP-2	Sense 5′-GGC CCT GTC ACT CCT GAG AT-3′
	Antisense 5′-GGC ATC CAG GTT ATC GGG GA-3′
MMP-9	Sense 5′-CGG AGC ACG GAG ACG GGT AT-3′
	Antisense 5′-TCA AGG GGAAGA CGC ACA GC-3′
ZO-1	Sense 5′-GCT CCT CCC ACC TCG CAC GT-3′
	Antisense 5′-GAC CTG CTG GAG CAT AGG GCT G-3′
Occludin	Sense 5′-TCAGGGAATATCCACCTATCACTTCAG-3′
	Antisense 5′-CATCAGCAGCAGCCATGTACTCTTCAC-3′
E-cadherin	Sense 5′-GAA CAG CAC GTA CAC AGC CCT-3′
	Antisense 5′-GCA GAA GTG TCC CTG TTC CAG-3′
GAPDH	Sense 5′-CGG AGT CAA CGG ATT TGG TCG TAT-3′
	Antisense 5′-AGC CTT CTC CAT GGT GGT GAA GAC-3′

Table 2: List of antibodies used in Western blot.

Antibody	Company	Dilution
Claudin-4	Invitrogen	1 : 500
MMP-2	Santa Cruz Biotechnology	1 : 500
MMP-9	Santa Cruz Biotechnology	1 : 500
ZO-1	Invitrogen	1 : 1000
Occludin	Invitrogen	1 : 1000
E-cadherin	Invitrogen	1 : 1000
Snail	Abcam	1 : 1000
NF-κB	Santa Cruz Biotechnology	1 : 1000
pERK	Cell Signaling	1 : 1000
ERK	Cell Signaling	1 : 1000
β-actin	Santa Cruz Biotechnology	1 : 1000
Lamin B	Santa Cruz Biotechnology	1 : 1000

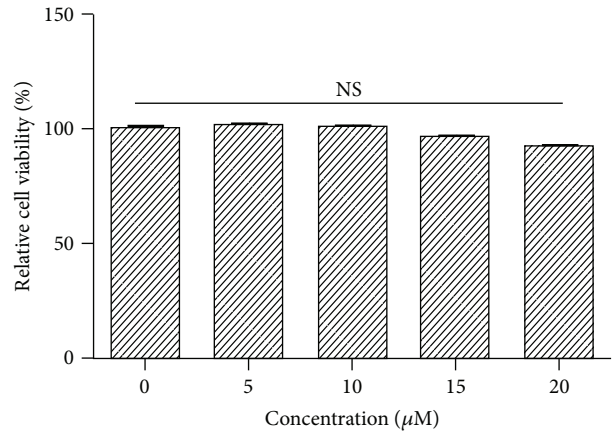

Figure 2: Effect of [6]-gingerol on cell viability in PANC-1 cells. Cells were seeded onto 96-well plates and grown for 1 day. Media containing the compounds were added after 24 h, and cell numbers were quantified using the MTT assay. Data represent the mean ± SD from three independent experiments. Statistical analysis (one-way ANOVA) was performed using GraphPad Prism 5. NS, no significance versus the untreated control.

genes, RT-PCR and Western blot analysis were conducted in PANC-1 cells with or without [6]-gingerol. As shown in Figures 6(a) and 6(b), claudin 4 and MMP-9 expression decreased in [6]-gingerol-treated cells compared to untreated cells. Inversely, the mRNA and protein levels of ZO-1, occludin, and E-cadherin increased upon treatment with [6]-gingerol. These results suggest that [6]-gingerol can restore the levels of claudin protein and that TJ may suppress metastasis and invasion.

3.6. [6]-Gingerol Inhibited the Invasion of PANC-1 Cells by a Decrease in NF-κB/Snail Activity. As shown in Figure 7(a), protein levels of NF-κB/Snail in the cytosolic fraction were significantly downregulated in [6]-gingerol-treated cells compared to those of the control. The degradation of IkB was also inhibited by [6]-gingerol. However, the nuclear translocation of NF-κB and Snail significantly ($P < 0.05$) decreased in cells. Inhibition of Snail, a transcription factor, increased the expression of E-cadherin, a regulator of TJ, in cells. An inverse relationship between the expression of these genes was also observed. Activation of NF-κB in the nucleus was also inhibited by [6]-gingerol treatment. MAPK is known as an upstream regulator of NF-κB. Consequently, additional testing was necessary to elucidate the signaling pathway that regulates NF-κB activity upon treatment with [6]-gingerol, which inhibited Snail in PANC-1 cells. Western blot analysis revealed that [6]-gingerol-treated cells suppressed ERK phosphorylation compared to that of the control (Figure 7(b)). These results demonstrate that Snail expression was inhibited by [6]-gingerol through suppression of NF-κB activation via a decrease in ERK phosphorylation. As shown in Figure 7(b), treatment with U0126, an ER-specific inhibitor, confirmed the suppression of Snail and NF-κB expression through inhibition of ERK phosphorylation, suggesting that inhibition of ERK by [6]-gingerol regulates NF-κB activity.

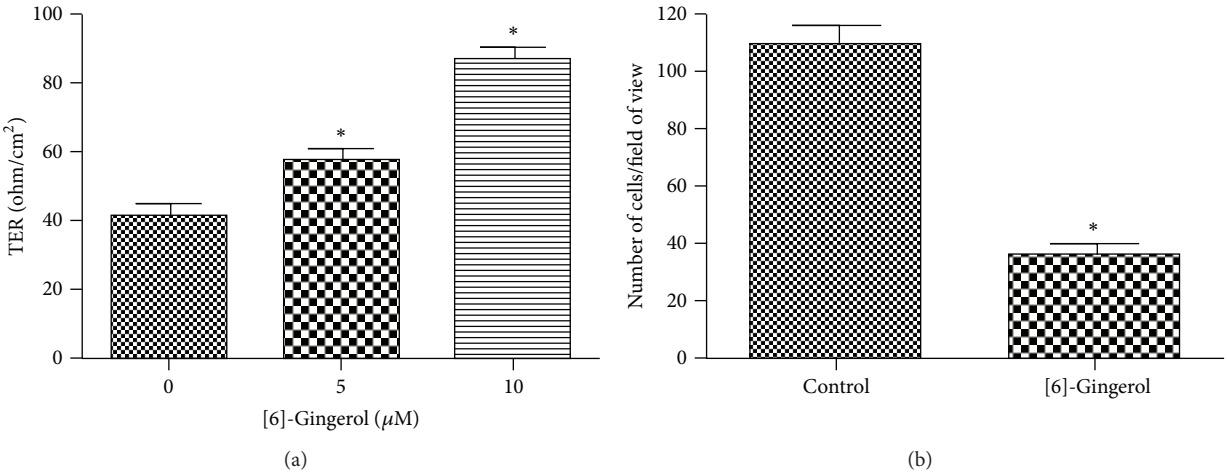

Figure 3: Effect of [6]-gingerol on TER value and cell invasion in PANC-1 cells. (a) Cells were plated onto 12-well polyester membrane Transwells (1 cm^2 surface area, 0.4-mm pore size; Costar) and grown in media. The compound was added to both the apical and basolateral compartments in triplicate. TER values were measured using an epithelial volt-ohm meter. (b) Cells were grown on the apical side of a Matrigel-coated filter chamber in the presence of the compound in serum-free media. Medium including 20% FBA as a chemoattractant was placed in the basolateral chamber. After 3 days, cells were fixed and stained and then counted. Data represent the mean ± SD from three independent experiments. Statistical analyses (one-way ANOVA and Student's t-test) were performed using GraphPad Prism 5. $^*P < 0.05$ versus the untreated control.

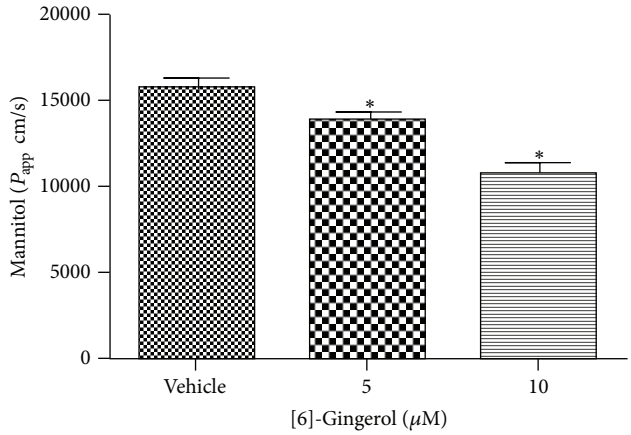

Figure 4: Effect of [6]-gingerol on paracellular permeability in PANC-1 cells. Cells grown on Transwells were treated for 3 days. At time 0, PBS (0.5 mL) containing [^{14}C] mannitol (0.1 μCi/mL) was added to the apical compartment. The amount of mannitol transported across the monolayer was determined by counting the samples in a liquid scintillation counter (LS 6500; Beckman Coulter). Data represent the mean ± SD from three independent experiments. Statistical analysis (one-way ANOVA) was performed using GraphPad Prism 5. $^*P < 0.05$ versus the untreated control.

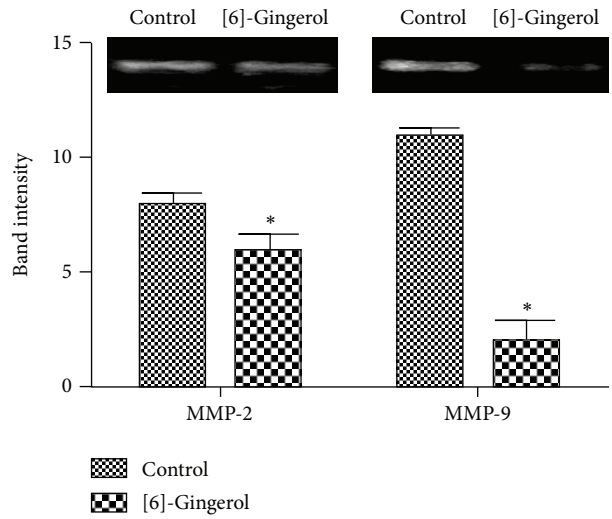

Figure 5: Effect of [6]-gingerol on MMP activity in PANC-1 cells. Cells were cultured in the absence or presence of the compound for 24 h. Cell-free medium was collected and MMP activity was measured by gelatin zymography. Protease activity was quantified by densitometry using L Process and MultiGauge software and normalized relative to the control and background. Data represent the mean ± SD from three independent experiments. Statistical analysis (Student's t-test) was performed using GraphPad Prism 5. $^*P < 0.05$ versus the untreated control.

4. Discussion

Ginger has been used in traditional Oriental medicine and contains gingerol, shogaol, paradol, zingerone, zingiberene, curcumene, and farnesene and so forth [10, 11]. Gingerols have been reported to exhibit many interesting pharmacological and physiological functions, including antipyretic, cardiotonic, chemopreventive, anti-inflammatory, and antioxidant properties[12–14].

Metastasis is the main reason of death in patients with cancer and is a multistep process involving invasion and migration. In cancer, breakdown of the extracellular matrix and basement membrane via activation of MMPs and tissue remodeling via the loss the TJ in turn promote tumor cell migration. Here, we present a new paradigm for the

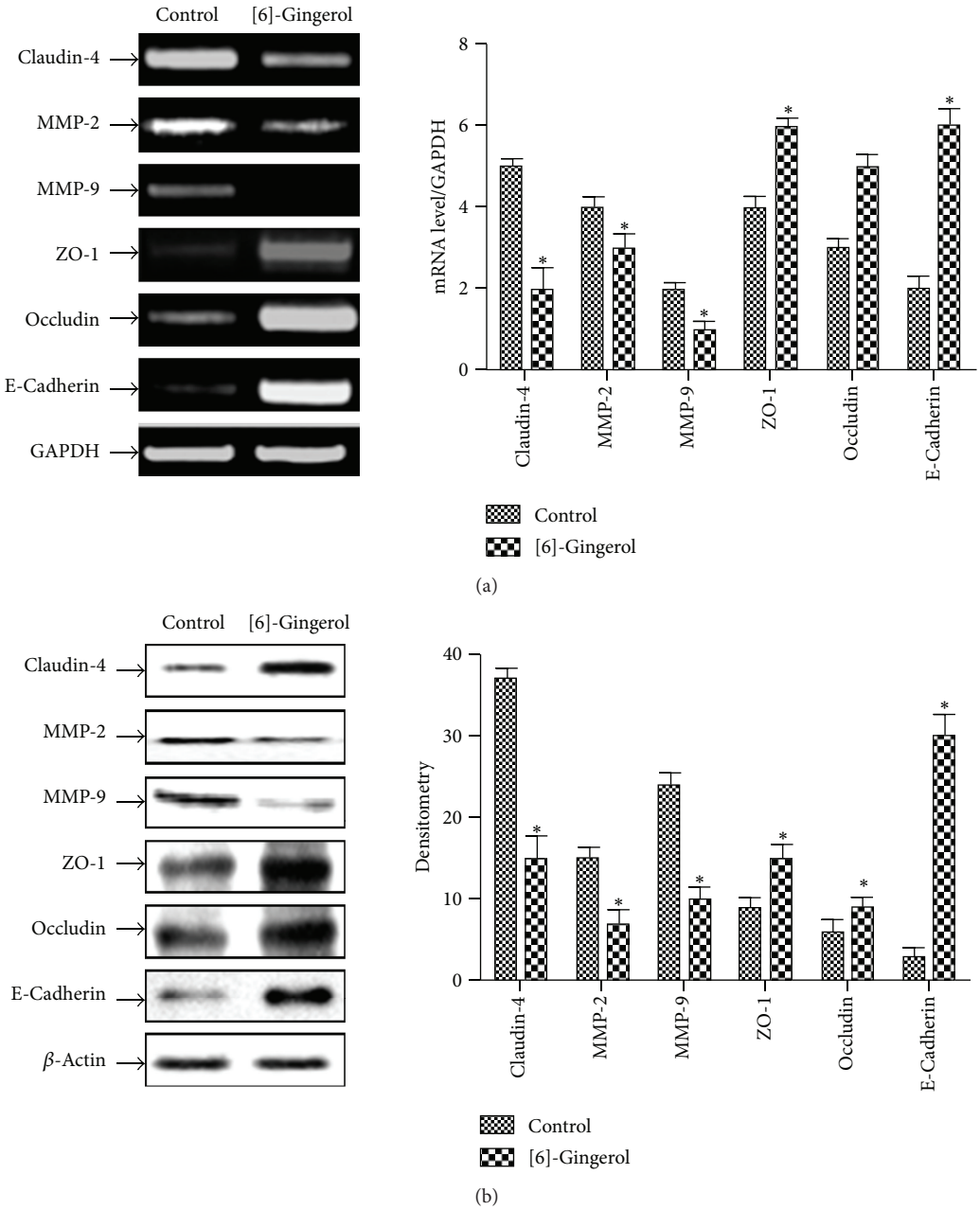

Figure 6: Effect of [6]-gingerol on TJ-related gene expression in PANC-1 cells. (a) Cells were treated with [6]-gingerol for 24 h. Total RNAs were extracted and reverse transcribed. cDNAs were subjected to PCR, and products were observed by 1.5% agarose gel electrophoresis and visualized by staining with EtBr. GAPDH was used as an internal control. (b) Cells cultured under the same conditions were lysed, and equal amounts of cell protein were resolved by SDS-PAGE and transferred to a nitrocellulose membrane. Western blotting was then performed with the proper antibodies and an enhanced ECL detection system. Actin was used as an internal control. Band intensities in the immunoblots were quantified by densitometry using L Process and MultiGauge software. Band intensities were normalized relative to the internal control and background, respectively. Data represent the mean ± SD from three independent experiments. Statistical analysis (Student's t-test) was performed using GraphPad Prism 5. $^{*}P < 0.05$ versus the untreated control.

prevention of PC metastasis through the restoration of TJs in PC cells by the natural compound [6]-gingerol. However, the antimetastatic effects of [6]-gingerol, a major phenolic compound derived from ginger, are unknown in PC cells. The aim of this study was to examine the effect of [6]-gingerol on PC metastasis and investigate the intracellular signaling pathways involved.

First, MTT assays were performed to confirm that [6]-gingerol treatment was not cytotoxic. The effects of [6]-gingerol on TER and paracellular permeability of PC cells were then investigated using the PANC-1 cell line. Our study indicated that [6]-gingerol tightened TJ formation and thus suppressed paracellular permeability compared to that of untreated cells. Soler et al. [15] demonstrated that the TER

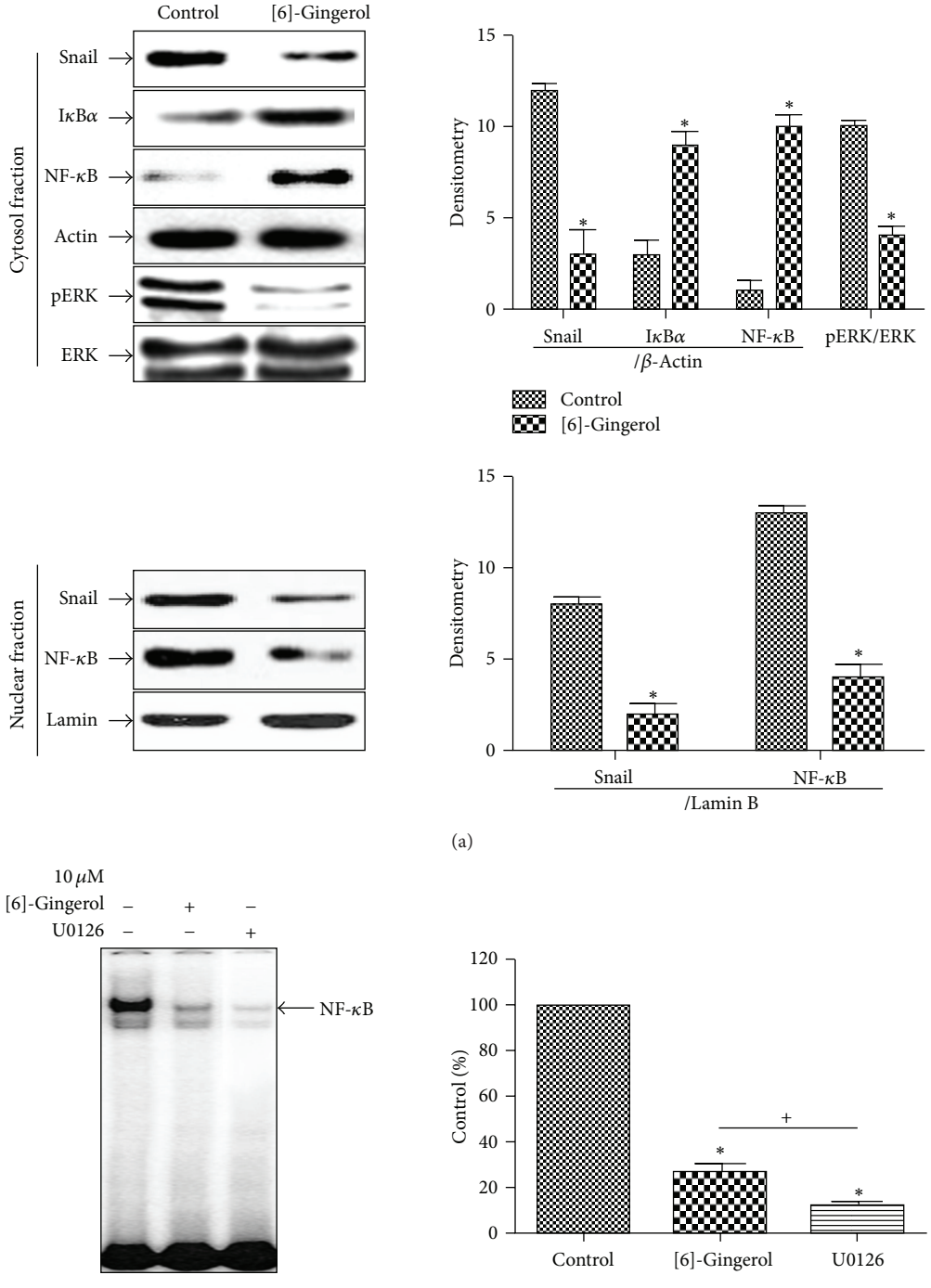

FIGURE 7: Effect of [6]-gingerol on the DNA-binding activity of NF-κB in PANC-1 cells. (a) Nuclear and cytosolic extracts were prepared using the NE-PER nuclear and cytoplasmic extraction kit from PANC-1 cells treated with [6]-gingerol for 24 h. Western blotting was then performed on each fraction. Actin was used as an internal control for, the cytosolic fraction, and lamin was applied as an internal control for the nuclear fraction. (b) Cells cultured under the same conditions were pretreated for 30 min with U0126, an ERK inhibitor. Cells were then tested for the DNA-binding activity of NF-κB by EMSA. Band intensities in the immunoblots were quantified by densitometry using L Process and MultiGauge software. Band intensities were normalized relative to the internal control and background. Data represent the mean ± SD from three independent experiments. Statistical analyses (Student's t-test and one-way ANOVA) were performed using GraphPad Prism 5. $^{*}P < 0.05$ versus the untreated control. $^{+}P < 0.05$, [6]-gingerol compared with U0126-treated cells.

of colon carcinoma tissue was significantly lower than that of normal colon tissue and concurrently that the transepithelial paracellular permeability of colon carcinomas was higher than that in normal colon epithelial tissue, confirming the loss of TJs. Gumbiner [16] reported that the paracellular transport of ions and small solutes are regulated by TJs. Schneeberger and Lynch [17] determined that TJs are involved either directly or indirectly with TJ plaque proteins to coordinate diverse functions such as the regulation of paracellular solute permeability, cell proliferation, cell polarity, and tumor suppression. Therefore, these reports support that [6]-gingerol exhibits significant activity on two measures of metastatic potential, motility, and invasiveness in human PC cells.

The protein components of TJs have been identified, in particular those of the claudin family, which include transmembrane proteins and their extracellular domains. They then interact with that of other claudin proteins of adjacent cells to regulate paracellular permeability [2]. A critical regulator of TJs, ZO-1, was reduced or lost by 69% in breast cancers analyzed [18]. Claudin-1, -3, and -4 are overexpressed in colorectal tumor tissues [19]. Additionally, claudin-3 and -4 have also been shown to be overexpressed in cancers including gastric, ovarian, and pancreatic cancers [2, 20–23]. A German group reported that the ectopic expression of claudin-4 in pancreatic cancer cells reduced their invasive potential both *in vitro* and *in vivo* [2]. These reports strongly suggest that claudins may act as promising targets for antimetastatic cancer therapeutics [5]. The reports described above indicate that claudins are dysregulated in many types of cancers and that the nature of the dysregulation is highly cancer type specific. E-cadherin, an adherent junction protein and type I transmembrane glycoprotein [24], is also known to regulate TJ formation [25]. The loss of E-cadherin and Snail overexpression is correlated with tumor grade and stage [26], nodal metastasis, and tumor recurrence and predicts a poor outcome in patients with various cancers [27–29]. In this study, we showed that [6]-gingerol in PC cells inhibited TJ proteins and mRNA levels, claudin-4, ZO, and occludin. The increase in E-cadherin and decrease in Snail were also regulated by [6]-gingerol. These observations suggest that [6]-gingerol may bode well for its therapeutic use as an antimetastatic therapeutic in human pancreatic cancer.

MMPs are proteolytic enzymes that are highly expressed in various malignant tumors. Inhibition of MMPs could be an effective strategy to prevent tumor cell invasion and metastasis. As MMPs are important regulators of tumor progression and metastasis, they have been identified as candidate prognostic markers. Activated MMPs degrade type IV collagen (a major constituent of the basement membrane), thereby increasing cell mobility [30, 31]. Durlik and Gardian found that MMP-9 is activated only in higher tumor grades of human pancreatic cancer [32]. Dhawan et al. reported that the ectopic overexpression of claudin-1 in a colon adenocarcinoma cell line increased the activity of MMP-2 and MMP-9, which play important roles in cell invasion [33]. These reports support our findings showing that the natural compound [6]-gingerol plays inhibitory roles in metastasis and invasiveness of human pancreatic cancer cells.

The transcription factor NF-κB plays a critical role in metastasis and invasion signaling pathways [34]. Also, the transcription factor Snail translocates into the nucleus in metastatic human cancer [35]. In the current study, we found that [6]-gingerol inhibited the nuclear translocation of Snail, which is regulated by NF-κB. Inhibition of Snail and MMP-9 could be the mechanism of [6]-gingerol-induced inhibition of cancer cell metastasis. We further investigated the effect of [6]-gingerol on MAPK pathways. We found that [6]-gingerol inhibited ERK phosphorylation, which was also confirmed by the U0126 inhibitor. Therefore, [6]-gingerol modulated the suppression of ERK phosphorylation, suggesting that [6]-gingerol-suppressed metastasis is associated with NF-κB/Snail via the ERK pathway in PANC-1 cells.

5. Conclusion

In conclusion, we present data demonstrating that a natural compound, [6]-gingerol, can strengthen TJs and regulate the expressions of TJ-related proteins in human pancreatic cancer cells and that it is also a potent inhibitor of NF-κB activation. Thus, our study will greatly enhance our understanding of the role of TJs and their composite proteins in human pancreatic cancer metastasis. However, further studies are needed to elucidate whether [6]-gingerol can suppress tumor metastasis and invasion *in vivo* and further potentiate chemotherapy effects.

Conflict of Interests

All the authors confirm that there is no conflict of interests.

Authors' Contribution

Sung Ok Kim and Mi Ryeo Kim contributed equally to this work.

Acknowledgments

This work was supported by the National Research Foundation of Korea (NRF) and Grant funded by the Korea government (MSIP) (no. 2012-0009400).

References

[1] B. Sung, S. Prasad, V. R. Yadav, and B. B. Aggarwal, "Cancer cell signaling pathways targeted by spice-derived nutraceuticals," *Nutrition and Cancer*, vol. 64, no. 2, pp. 173–197, 2013.

[2] P. Michl, C. Barth, M. Buchholz et al., "Claudin-4 expression decreases invasiveness and metastatic potential of pancreatic cancer," *Cancer Research*, vol. 63, no. 19, pp. 6265–6271, 2003.

[3] Z. E. Karanjawala, P. B. Illei, R. Ashfaq et al., "New markers of pancreatic cancer identified through differential gene expression analyses: claudin 18 and annexin A8," *American Journal of Surgical Pathology*, vol. 32, no. 2, pp. 188–196, 2008.

[4] J. M. Anderson and C. M. Van Itallie, "Tight junctions and the molecular basis for regulation of paracellular permeability," *American Journal of Physiology*, vol. 269, no. 4, pp. G467–G475, 1995.

[5] P. J. Morin, "Claudin proteins in human cancer: promising new targets for diagnosis and therapy," *Cancer Research*, vol. 65, no. 21, pp. 9603–9606, 2005.

[6] A. Jemal, R. Siegel, J. Xu, and E. Ward, "Cancer statistics, 2010," *CA Cancer Journal for Clinicians*, vol. 60, no. 5, pp. 277–300, 2010.

[7] K. W. Jung, Y. J. Won, H. J. Kong et al., "Cancer statistics in Korea: incidence, mortality, survival and prevalence in 2010," *Cancer Research and Treatment*, vol. 45, no. 1, pp. 1–14, 2013.

[8] S. S. Devesa, W. J. Blot, B. J. Stone, B. A. Miller, R. E. Tarone, and J. F. Fraumeni Jr., "Recent cancer trends in the United States," *Journal of the National Cancer Institute*, vol. 87, no. 3, pp. 175–182, 1995.

[9] World Cancer Research Fund & American Institute for Cancer Research, "1997 World Cancer Research Fund & American Institute for Cancer Research," *Food, Nutrition and the Prevention of Cancer*: A Global Perspective American Institute for Cancer Research, Washington, DC, USA, 1997.

[10] B. White, "Ginger: an overview," *American Family Physician*, vol. 75, no. 11, pp. 1689–1691, 2007.

[11] Y. Shukla and M. Singh, "Cancer preventive properties of ginger: a brief review," *Food and Chemical Toxicology*, vol. 45, no. 5, pp. 683–690, 2007.

[12] R. C. Lantz, G. J. Chen, M. Sarihan, A. M. Sólyom, S. D. Jolad, and B. N. Timmermann, "The effect of extracts from ginger rhizome on inflammatory mediator production," *Phytomedicine*, vol. 14, no. 2-3, pp. 123–128, 2007.

[13] Y.-J. Surh, "Molecular mechanisms of chemopreventive effects of selected dietary and medicinal phenolic substances," *Mutation Research*, vol. 428, no. 1-2, pp. 305–327, 1999.

[14] B. H. Ali, G. Blunden, M. O. Tanira, and A. Nemmar, "Some phytochemical, pharmacological and toxicological properties of ginger (Zingiber officinale Roscoe): a review of recent research," *Food and Chemical Toxicology*, vol. 46, no. 2, pp. 409–420, 2008.

[15] A. P. Soler, R. D. Miller, K. V. Laughlin, N. Z. Carp, D. M. Klurfeld, and J. M. Mullin, "Increased tight junctional permeability is associated with the development of colon cancer," *Carcinogenesis*, vol. 20, no. 8, pp. 1425–1431, 1999.

[16] B. M. Gumbiner, "Breaking through the tight junction barrier," *Journal of Cell Biology*, vol. 123, no. 6, pp. 1631–1633, 1993.

[17] E. E. Schneeberger and R. D. Lynch, "The tight junction: a multifunctional complex," *American Journal of Physiology*, vol. 286, no. 6, pp. C1213–C1228, 2004.

[18] K. B. Hoover, S.-Y. Liao, and P. J. Bryant, "Loss of the tight junction MAGUK ZO-1 in breast cancer: relationship to glandular differentiation and loss of heterozygosity," *American Journal of Pathology*, vol. 153, no. 6, pp. 1767–1773, 1998.

[19] S. S. De Oliveira, I. M. De Oliveira, W. De Souza, and J. A. Morgado-Díaz, "Claudins upregulation in human colorectal cancer," *FEBS Letters*, vol. 579, no. 27, pp. 6179–6185, 2005.

[20] S. C. Cunningham, F. Kamangar, M. P. Kim et al., "Claudin-4, mitogen-activated protein kinase kinase 4, and stratifin are markers of gastric adenocarcinoma precursor lesions," *Cancer Epidemiology Biomarkers and Prevention*, vol. 15, no. 2, pp. 281–287, 2006.

[21] L. B. A. Rangel, R. Agarwal, T. D'Souza et al., "Tight junction proteins claudin-3 and claudin-4 are frequently overexpressed in ovarian cancer but not in ovarian cystadenomas," *Clinical Cancer Research*, vol. 9, no. 7, pp. 2567–2575, 2003.

[22] S. L. Kominsky, M. Vali, D. Korz et al., "Clostridium perfringens enterotoxin elicits rapid and specific cytolysis of breast carcinoma cells mediated through tight junction proteins claudin 3 and 4," *American Journal of Pathology*, vol. 164, no. 5, pp. 1627–1633, 2004.

[23] H. Long, C. D. Crean, W.-H. Lee, O. W. Cummings, and T. G. Gabig, "Expression of Clostridium perfringens enterotoxin receptors claudin-3 and claudin-4 in prostate cancer epithelium," *Cancer Research*, vol. 61, no. 21, pp. 7878–7881, 2001.

[24] R. W. McLachlan and A. S. Yap, "Not so simple: the complexity of phosphotyrosine signaling at cadherin adhesive contacts," *Journal of Molecular Medicine*, vol. 85, no. 6, pp. 545–554, 2007.

[25] C. M. Van Itallie and J. M. Anderson, "Claudins and epithelial paracellular transport," *Annual Review of Physiology*, vol. 68, pp. 403–429, 2006.

[26] P. Cowin, T. M. Rowlands, and S. J. Hatsell, "Cadherins and catenins in breast cancer," *Current Opinion in Cell Biology*, vol. 17, no. 5, pp. 499–508, 2005.

[27] M. J. Blanco, G. Moreno-Bueno, D. Sarrio et al., "Correlation of Snail expression with histological grade and lymph node status in breast carcinomas," *Oncogene*, vol. 21, no. 20, pp. 3241–3246, 2002.

[28] C.-W. Cheng, P.-E. Wu, J.-C. Yu et al., "Mechanisms of inactivation of E-cadherin in breast carcinoma: modification of the two-hit hypothesis of tumor suppressor gene," *Oncogene*, vol. 20, no. 29, pp. 3814–3823, 2001.

[29] S. E. Moody, D. Perez, T.-C. Pan et al., "The transcriptional repressor Snail promotes mammary tumor recurrence," *Cancer Cell*, vol. 8, no. 3, pp. 197–209, 2005.

[30] N. Voorzanger-Rousselot and P. Garnero, "Biochemical markers in oncology—part 1: molecular basis—part 2: clinical uses," *Cancer Treatment Reviews*, vol. 33, no. 3, pp. 230–283, 2007.

[31] S. D. Mason and J. A. Joyce, "Proteolytic networks in cancer," *Trends in Cell Biology*, vol. 21, no. 4, pp. 228–237, 2011.

[32] M. Durlik and K. Gardian, "Metalloproteinase 2 and 9 activity in the development of pancreatic cancer," *Polish Journal of Surgery*, vol. 84, no. 8, pp. 377–382, 2012.

[33] P. Dhawan, A. B. Singh, N. G. Deane et al., "Claudin-1 regulates cellular transformation and metastatic behavior in colon cancer," *Journal of Clinical Investigation*, vol. 115, no. 7, pp. 1765–1776, 2005.

[34] S. Shishodia and B. B. Aggarwal, "Nuclear factor-kappaB activation mediates cellular transformation, proliferation, invasion angiogenesis and metastasis of cancer," *Cancer Treatment and Research*, vol. 119, pp. 139–173, 2004.

[35] S. Prasad, V. R. Yadav, C. Sundaram et al., "Crotepoxide chemosensitizes tumor cells through inhibition of expression of proliferation, invasion, and angiogenic proteins linked to proinflammatory pathway," *Journal of Biological Chemistry*, vol. 285, no. 35, pp. 26987–26997, 2010.

Hindawi Publishing Corporation
Evidence-Based Complementary and Alternative Medicine
Volume 2013, Article ID 493869, 10 pages
http://dx.doi.org/10.1155/2013/493869

Research Article

In Vitro and *In Vivo* Anticancer Effects of Sterol Fraction from Red Algae *Porphyra dentata*

Katarzyna Kazłowska,[1] Hong-Ting Victor Lin,[1,2] Shun-Hsien Chang,[1] and Guo-Jane Tsai[1,2]

[1] *Department of Food Science, National Taiwan Ocean University, 2 Pei-Ning Road, Keelung 20224, Taiwan*
[2] *Center for Marine Bioenvironment and Biotechnology, National Taiwan Ocean University, 2 Pei-Ning Road, Keelung 20224, Taiwan*

Correspondence should be addressed to Guo-Jane Tsai; b0090@ntou.edu.tw

Received 25 March 2013; Accepted 5 June 2013

Academic Editor: Chia-Jui Weng

Porphyra dentata, an edible red macroalgae, is used as a folk medicine in Asia. This study evaluated *in vitro* and *in vivo* the protective effect of a sterol fraction from *P. dentata* against breast cancer linked to tumor-induced myeloid derived-suppressor cells (MDSCs). A sterol fraction containing cholesterol, β-sitosterol, and campesterol was prepared by solvent fractionation of methanol extract of *P. dentata in silica* gel column chromatography. This sterol fraction *in vitro* significantly inhibited cell growth and induced apoptosis in 4T1 cancer cells. Intraperitoneal injection of this sterol fraction at 10 and 25 mg/kg body weight into 4T1 cell-implanted tumor BALB/c mice significantly inhibited the growth of tumor nodules and increased the survival rate of mice. This sterol fraction significantly decreased the reactive oxygen species (ROS) and arginase activity of MDSCs in tumor-bearing mice. Therefore, the sterol fraction from *P. dentata* showed potential for protecting an organism from 4T1 cell-based tumor genesis.

1. Introduction

Breast cancers constitute one of the most serious problems in oncology, and in many countries breast cancer is a leading cause of death among women [1]. As the breast cancer phenotype progresses, survival factors that inhibit apoptotic cell death are expressed [2, 3]. In addition, the pathophysiology of breast cancer has linked it to tumor-induced myeloid derived-suppressor cells (MDSCs), and MDSCs pose a serious barrier to effective T cell immunotherapy against cancer [4].

Tumor-induced immune suppression is widespread among patients and experimental animals that display malignant tumors [5]. Multiple mechanisms have been suggested as the possible cause of tumor-induced immune suppression, with MDSCs (previously called immature myeloid cells) [6] being a major contributor [3]. In mice, MDSCs are characterized as Gr-1$^+$CD11b$^+$ cell phenotype and are thus also called Gr-1$^+$CD11b$^+$ cells [7]. Myeloid lineage differentiation antigen Gr-1 (also known as Ly6G) is expressed on myeloid precursor cells and granulocytes and transiently on monocytes [6]. Tumor growth is associated with systemic expansion of Gr-1$^+$ myeloid cells with the CD11b antigen. The CD11b antigen is also known as αM-integrin, and is a marker for myeloid cells of the macrophage lineage [8]. The quantity of these suppressor cells is positively correlated to malignancy, which suggests that MDSCs play a role in tumor invasion and metastasis [7]. MDSCs in the bone marrow and spleen are significantly overproduced in tumor-bearing mice [7]. The expansion of MDSCs is promoted by expansion factors produced by tumor cells, through stimulation of myelopoiesis and the inhibition of differentiation of mature myeloid cells [3].

Some studies have suggested that MDSCs are potent inhibitors of antitumor immunity in secondary lymphoid organs and may facilitate tumor progression by inactivating antigen-specific T cells [6, 9]. MDSCs in tumor-bearing hosts may generate reactive oxygen species (ROS) to suppress antigen-specific cell responses [6, 10]. ROS inhibition can completely abrogate the suppressive effect of MDSCs [6]. MDSC suppression has also been implicated in reduced bioavailability of L-arginine [9, 11–13]. This effect is the result of enhanced activity of arginase, which hydrolyzes L-arginine to L-ornithine and urea. The reduction of L-arginine is thought to affect multiple key biological processes in T

cells, including proliferation, expression of the T cell receptor complex, and the development of memory [9]. Zea et al. [9] showed that cytokines of interleukin 4 (IL-4) and IL-13 upregulate arginase activity of MDSCs, thereby increasing the suppressive function of MDSCs. *In vivo* studies have shown that blocking arginase eliminated the suppressor function of MDSCs and induced an antitumor effect of T cells [9, 13].

In vitro, 4T1 cells grow as adherent epithelial type and are characterized as murine mammary carcinoma cells [14]. The 4T1 cell line is an estrogen-nonresponsive [15] and transplantable tumor cell line that is tumorigenic in NOD/SCID and BALB/c mice. It multiplies rapidly, resulting in highly metastatic tumors in the lung, liver, lymph nodes, and brain while the primary tumor is growing *in situ* [4]. This tumor closely imitates human breast cancer and provides an animal model for Stage IV human breast cancer [2].

Algal remedies from the *Porphyra* species, commonly known as red seaweeds, are emerging as popular agents for cancer-related therapy [16, 17]. Various sterol components have been identified in the *Porphyra* species, including campesterol, cholesterol, 22-dehydrocholesterol, desmosterol, fucosterol, β-sitosterol, and stigmasterol [18–20]. Several of these components have been shown to exhibit antitumor activity [21]. In eastern Asian countries, *Porphyra dentata* (Bangiaceae) has been used for centuries in the preparation of folk medicine [22, 23]. This study investigated the anti-breast-cancer effects of *P. dentata* using the 4T1 breast cell line *in vitro* and 4T1 implanted mice *in vivo*. We analyzed the presence of effective compositions of sterols and attempted to explain the underlying mechanism related to MDSC to account for these anticancer effects.

2. Materials and Methods

2.1. Plant Materials and Chemicals. Marine red alga, *P. dentata*, was collected in Taiwan and authenticated as described previously [22]. Unless otherwise stated, chemicals and reagents were purchased from Sigma Aldrich (St. Louis, MO, USA). These included aprotinin, L-arginine, campesterol, cholesterol, desmosterol, dichlorodihydrofluorescein diacetate (DCFDA), dimethyl sulfoxide (DMSO), 3-(4,5-dimethylthiazol-2-yl)-2,5-diphenyltetrazolium bromide (MTT), EDTA (ethylenediaminetetraacetate), α-isonitrosopropiophenone, N-(1-naphthyl) ethylenediamine, leupeptin, phenyl methyl sulfonyl fluoride, β-sitosterol, stigmasterol, sulfanilamide, taxol, tris, triton X-100, and urea. We obtained catalase, arginase inhibitor N^W-hydroxy-nor-L-arginine (nor-NOHA), and phorbol-12-myristate-13-actetate (PMA) from Calbiochem (Calbiochem, San Diego, CA). Fetal bovine serum (FBS), EDTAx4Na (tetrasodium EDTA), HEPES buffer, 2-β-mercaptoethanol, nonessential amino acids, penicillin/streptomycin, sodium pyruvate, Dulbecco's Modified Eagle's Medium (DMEM), PBS, and RPMI 1640 were purchased from Gibco (Rockville, MD, USA). From BD Biosciences (San Diego, CA, USA) we obtained a fluorescein isothiocyanate (FITC) Annexin V Apoptosis Detection Kit I, propidium iodide (PI), and the antibodies, namely, anti-mouse $Gr1^+$-FITC (Clone: RB6-8C5; Catalog number: 553126) and anti-mouse $CD11b^+$-PE (Clone: M1/70; Catalog number: 553311). A protein assay kit (Bradford reagent) was purchased from Bio-Rad Laboratories (Richmond, CA, USA). All solvents and chemicals used in this study were of HPLC grade.

2.2. Extraction and Fractionation of Plant. Crude extract of *P. dentata* soaked in methanol was prepared as described previously [22]. A freeze-dry powder of the methanolic crude extract (18 g) was fractionated on a chromatographic column filled with silica gel particles. The first fractionation was eluted with 1 L of hexane (fraction 1; F1), followed by 2.5 L of dichloromethane (fraction 2; F2), 3 L of ethyl acetate (fraction 3; F3), 4 L of acetone (fraction 4; F4), and 4 L of methanol (fraction 5; F5). The various obtained fractions were concentrated in a rotary evaporator to dryness and were then weighed and stored in a freezer (−80°C) until use.

2.3. Cell Line Maintenance. The 4T1 breast cancer cell line was obtained from the American Type Culture Collection (ATCC) and was maintained using standard cell culture techniques. The cells were cultured in a "4T1 medium" [24] comprising DMEM supplemented with 0.2% (w/v) $NaHCO_3$, 10% (v/v) FBS, and 1% (w/v) penicillin/streptomycin; the culture was maintained at 37°C, 95% humidity, and 5% CO_2. The subcultures were performed every 3 days. The cells were detached using 0.05% (w/v) trypsin with 0.53 mM EDTAx4Na for 5 min at 37°C in a humidified incubator. The cell count for each subculture was determined using a hemacytometer (Marienfeld, Long Isand, NY, USA).

2.4. Cytotoxic Effects of Samples on 4T1 Cells. The 4T1 cells (1×10^6 cells/mL) were incubated with 4T1 medium containing DMSO (control), various concentrations of methanolic crude extract (100, 200, and 400 μg/mL), or fractions of F1, F2, F3, F4, and F5 (25, 50, and 100 μg/mL in each case) for 48 h. The cells were then subjected to MTT assays [22]. The relative cell viability (%) was defined as 100 multiplied by the ratio of the OD490 value of the cells treated with extract or fraction, over the OD490 value of the control cells.

2.5. In Vitro Effect of Sample on Apoptosis and Necrosis of 4T1 Cells. The 4T1 cells (1×10^6 cells/mL) were incubated in the 4T1 medium containing various concentrations of F2 fraction for 48 h. The cell undergoing apoptosis or necrosis was determined using FITC Annexin V Apoptosis Detection Kit I and PI exclusion in a FACS-based assay, according to the manufacturer's protocol (BD Biosciences, San Diego, CA, USA). Briefly, the reacted 4T1 cell suspension was mixed with 1 μL of FITC Annexin V staining solution and left for 7 min. Thereafter, 1 μL of PI solution was added and reacted for 15 s in the dark. Flow cytometric analysis was performed immediately.

2.6. Mouse Maintenance. Thirty female BALB/c mice (5 wk old) were purchased from National Laboratory Animal Center (NLAC) in Taiwan. They were fed *ad libitum* for 1 wk and were then divided randomly into 5 groups of 6 animals each.

The groups were as follows: a naive group of tumor-free mice, a control group of tumor-bearing mice that did not receive treatment, and 3 experimental groups of tumor-bearing mice that received the sample treatments at 3 dosage levels. For the survival rate analysis, another 30 female BALB/c mice (5 wk old) were divided in the same manner. The 6 mice in each group were housed in a cage at 25°C and were libitum fed and observed daily. Approval for this study was issued by the Institutional Animal Care Board of National Taiwan Ocean University, and the mice were handled and euthanized according to the board's guidelines.

2.7. 4T1 Breast Tumor Model. The experimental mice were injected with 100 μL of syngeneic breast cancer 4T1 cell suspension (5×10^6 cells/mL). The injection was delivered subcutaneously (s.c.) into the mammary fat pads of the mice. Three hours after the tumor engraftment, the experimental mice (3 groups) were intraperitoneally (i.p.) injected with 20 μL of sample at dosages of 5, 10, or 25 mg/kg/day. The negative control group (naive mice) and the control group (tumor-bearing mice) were injected with DMSO (a carrier). The mice were injected every 3 d over 18 consecutive days.

Tumor growth was assessed morphometrically, using a caliper, and tumor volumes were calculated from the formula V (mm^3) = L_1 (major axis) × L_2^2 (minor axis)/2 [25]. After the indicated time, the mice were sacrificed on frozen CO_2. Gross pathology of animals was performed, abnormalities were noted, and images were obtained to document the results. Tumor tissues were isolated and weighed on a microbalance and then stored in cytotoxic media on ice until further *ex vivo* analysis. The cytotoxic media comprised 1 mM nonessential amino acids, 10 mM hepes buffer, 50 μM 2-β-mercaptoethanol, 1% (v/v) sodium pyruvate, 2.0 g/L $NaHCO_3$, and 100 U/mL penicillin/streptomycin in RPMI 1640.

2.8. Splenocyte Isolation. The suspensions of splenic cells were prepared according to the method of Nelson et al. [26]. The cell suspensions were washed once with media and the pellet was resuspended in erythrolysis buffer (7.47 g/L NH_4Cl, 2.29 g/L $KHCO_3$, 0.22 μm filtrated, pH 7.2). Erythrolysis was performed at 37°C for 10 min in a water bath. Thereafter, the cells were washed twice with phosphate buffer saline (PBS) and filtered through a cell strainer (40 μm, BD) to remove conglomerated or dead cell debris.

2.9. FACS Analysis of MDSC Surface Proteins in Splenocytes. Splenocytesat 1×10^6 cells/well in a 96-well V bottom plate (Hartenstein) were spun down. Cells were resuspended in 50 μL FACS buffer (1% v/v FBS, 0.05% w/v NaN_3 in PBS) containing the selected antibody cocktail (fluorescence-conjugated antibodies Gr-1^+-FITC and $CD11b^+$-PE) and were then incubated at 4°C in the dark for 30 min. After staining, the cells were washed twice with FACS buffer and were resuspended in 500 μL FACS buffer. A single stain was performed for each antibody present in the staining cocktail. After staining, the cells were analyzed using a BD FACSCanto II flow cytometer with FACSDiva software (BD Biosciences, San Diego, CA, USA). The instrument was thresholded on a forward angle light scatter (FS), and signals from FS and orthogonal light scatter (SS) were collected using a linear scale. Two colors of fluorescence were collected using logarithmic amplification, with the optical filters set at approximately 525 nm (on FL1 channel for FITC fluorochrome detection) and approximately 575 nm (on FL2 channel for PE fluorochrome detection).

2.10. Single-Cell Sorting of MDSC Fraction. Splenocytes were stained with fluorescence-labeled antibodies and sorted with a BD FACSAria II flow cytometer using FACSDiva software (BD Biosciences, San Diego, CA, USA). The MDSCs were freshly collected for assays of ROS production and arginase activity.

2.11. ROS Detection Assay. DCFDA, a cell-permanent dye sensitive to oxidation by ROS, was used to determine oxidative stress in the MDSCs isolated from the spleens of BALB/c mice [6]. We labeled 100 μL of MDSCs (2×10^6 cells/mL) in PBS using 1 μL DCFDA (2 μM) for 15 min at 37°C; thereafter, the cells were washed twice with PBS. The oxidized DCFDA-labeled cells were quantified in a green channel (FL1) of fluorescence by flow cytometry.

2.12. Arginase Activity Assay. Arginase activity was measured using the method of Chang et al. [27] with some modifications. To prepare cell lysates for arginase activity assay, the sorted MDSCs were rinsed twice with ice-cold Dulbecco PBS and then suspended in 300 μL of lysis buffer containing 50 mM Tris-HCl (pH 7.5), 0.1 mM EDTA, 1 mg/mL leupeptin, 1 mg/mL aprotinin, 0.1 mM phenylmethylsulfonyl fluoride, and 0.4% Triton X-100. Finally, cells were lysed for 10 min in the lysis buffer and the arginase activity in the cell lysate was measured. In brief, cell lysate (5 μg/50 μL ddH_2O) was added to 50 μL of Tris-HCl (50 mM; pH 7.5) containing 10 mM $MnCl_2$. The arginase in MDSCs was then activated by heating the mixture at 55°C for 10 min. The hydrolysis reaction of L-arginine by arginase was performed by coincubating the activated arginase with 50 μL of L-arginine (0.5 M, pH 9.7) at 37°C for 1 h. Thereafter, 400 μL of the acid solution (95% H_2SO_4 : 85% H_3PO_4 : H_2O = 1 : 3 : 7) was added to stop the reaction. For colorimetric determination of urea, 25 μL α-isonitrosopropiophenone (9% in absolute ethanol) was added. The mixture was heated at 100°C for 45 min and quickly cooled to 25°C. After being kept in the dark at 25°C for 10 min, the absorbance at 550 nm was determined using a microplate reader (lQuantTM, BIO-TEK Instrument Inc., Winooski, VT). The amount of urea produced was calculated from the standard curve and prepared as described but using urea (mg/mL) instead of cell lysate for the arginase activity assay.

2.13. Identification of Sterols Using a High-Performance Liquid Chromatography Evaporative Light Scattering Detector (HPLC-ELSD). The HPLC-ELSD system consisted of a pump PU-1580 obtained from Jasco (Tokyo, Japan), a Mightysil RP-18 (H) column (250 × 4.5 mm) preceded by an Asahipak GS-2G 7B guard column (50 × 7.6 mm) (Shodex, Showa Denko, Tokyo, Japan), and an ELSD ZAM 3000 (Schambeck

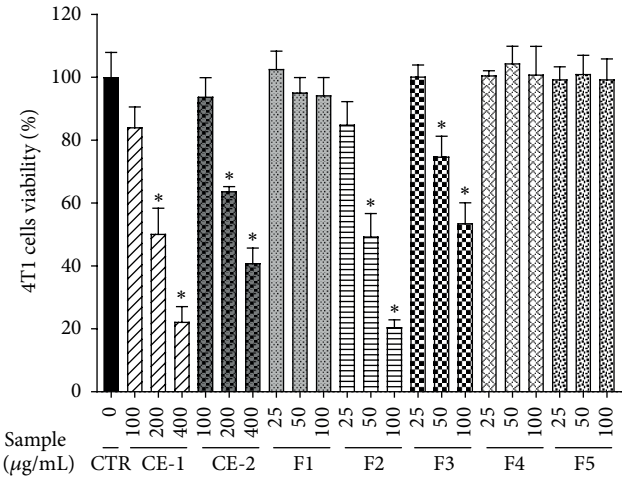

Figure 1: Effect of *P. dentata* methanolic crude extract (CE-1) and dichloromethane (DCM) crude extract (CE-2) as well as F1 (hexane), F2 (DCM), F3 (ethyl acetate), F4 (acetone), and F5 (methanol) fractions of CE-1 on the viability of tumor 4T1 cells. The 4T1 cells were incubated with DMEM containing DMSO (control), CE-1, CE-2, or indicated fractions for 48 h at indicated concentrations. The cells were subjected to MTT assays. The relative cell viability (%) was defined as 100 multiplied by the ratio of the OD490 value of the cells treated with sample over the OD490 value of the control cells. Data are expressed as mean ± S.D. ($n = 3$).

SFD GmbH, Bad Honnef, Germany). The temperatures for the column oven and detector nebulizer were 40°C and 80°C, respectively. Samples were injected through a CO-150 sampler with a 20 μL sample loop (Rheodyne, Cotati, CA, USA). The mobile phase was a mixture of methanol and deionized water at a ratio of 95 : 5 with a flow-rate of 1 mL/min. Commercially supplied campesterol, desmosterol, β-sitosterol, and cholesterol were used as calibration standards for this system. Chrome Manager 5.8 software from Analytical Based Development Center (Taichung, Taiwan) was used for online data monitoring and analysis.

2.14. Statistical Analysis. Survival curves were generated using Sigma-Plot software; the Kaplan-Meier method [28] and the logrank test [29] were used to compare mean survival. All other analyses were performed using Student's t-test and the results were expressed as means ± standard deviation (SD). Differences were considered significant at $P < 0.05$.

3. Results

3.1. Effects of Sterol Fraction of P. dentata on Proliferation and Apoptosis in 4T1 Cells. The cytotoxic effects of the methanol crude extract (CE-1) of *P. dentata* and various solvent fractions (F1–F5) of CE-1 on 4T1cells were investigated. As shown in Figure 1, cell viability decreased in a dose-dependent manner in samples of CE-1, F2, and F3. Cell viability was significantly decreased after treatment with CE-1 (200 or 400 μg/mL), F2 (50 or 100 μg/mL), or F3 (50 or 100 μg/mL). Samples of F1, F4, and F5 did not affect cell viability. Furthermore, F2 was found to have the highest cytotoxic effect on 4T1 cell proliferation. Therefore, F2 was selected for testing in the following experiments.

The sterol components in F2 were determined by HPLC-ELSD after comparing the retention time (T_R) of individual peaks with the T_R library of sterol standards for cholesterol, β-sitosterol, and campesterol. The data were analyzed under the same HPLC conditions (Figure 2). The three major peaks in F2 had retention times of 10.2 min (Peak 1), 12.0 min (Peak 2), and 13.1 min (Peak 3) (Figure 2(a)), which were equivalent to those of cholesterol ($T_R = 10.2$ min), β-sitosterol ($T_R = 12.0$ min), and campesterol ($T_R = 13.1$ min), respectively (Figure 2(b)). The relative weight percentages for cholesterol, β-sitosterol, and campesterol in F2 were 15%, 55%, and 30%, respectively.

The dose effects of F2 on 4T1 cell proliferation and apoptosis were further investigated. As shown in Figure 3, the proliferation of 4T1 cells was inhibited by the sample (F2) in dose- and time-dependent manner. The proliferation percentage of 4T1 cells was significantly decreased by a dose of 50 μg/mL of F2, compared with the control cells. The proliferation percentage in treated 4T1 cells was 63.3% compared with the control cells at 24 h; by 48 h it had reduced further to 31.1%. Based on the data shown in Figure 3, the sample concentrations required to achieve 50% inhibition of cell proliferation at 24 h and 48 h were calculated as 76.2 and 48.3 μg/mL, respectively.

PI and annexin V dual staining enables the identification of live cells (using annexin V^- and PI^-); early membrane damage (using annexin V^+ and PI^-); and apoptotic, necrotic, or necrotic membrane-disrupted cells (using annexin V^+ and PI^+). To determine if the ability of the sample to inhibit proliferation was connected with apoptosis in 4T1 cells, dual staining of annexin V and PI for cells undergoing necrosis-apoptosis was performed at 48 h (Figure 4). Less than 5% of 4T1 cells in control were dual positive for annexin V and PI (Figure 4). In the presence of the sample at dosages of 25 to 100 μg/mL, the percentage of apoptotic cells (white bar) and apoptotic-necrotic cells (black bar) gradually increased from 22% to 50% and from 10% to 20%, respectively. In the presence of 200 μg/mL of the sample, the percentage of apoptotic-necrotic cells increased to 70%, and the apoptotic cell percentage decreased to 15%. The remaining 15% of events showed nonstained viable cells (Figure 4). In this assay, taxol, a clinical chemotherapy drug for breast and ovarian cancer, was used as a positive control. Administering taxol at a dosage of 10 μg/mL induced cell apoptosis at a level of 40% (white bar) and apoptosis-necrosis at 22% (black bar) (Figure 4).

3.2. Antitumor Effects of Sterol Fraction of P. dentata In Vivo. The 4T1 cell-implanted tumor mice were i.p. injected with sample every 3 d over 18 consecutive days. Changes in the body weights and tumor sizes of mice were monitored. After the animals were sacrificed, the primary tumor nodules were isolated and weighed. On day 18 of the experiment, the body weight of tumor-bearing mice in groups that were treated with the sample was significantly decreased, compared with the tumor-bearing control group, for all 3 dosage levels (Figure 5(a)). As shown in Figure 5(b), tumor nodules developed by day 3 in tumor-bearing control mice, whereas

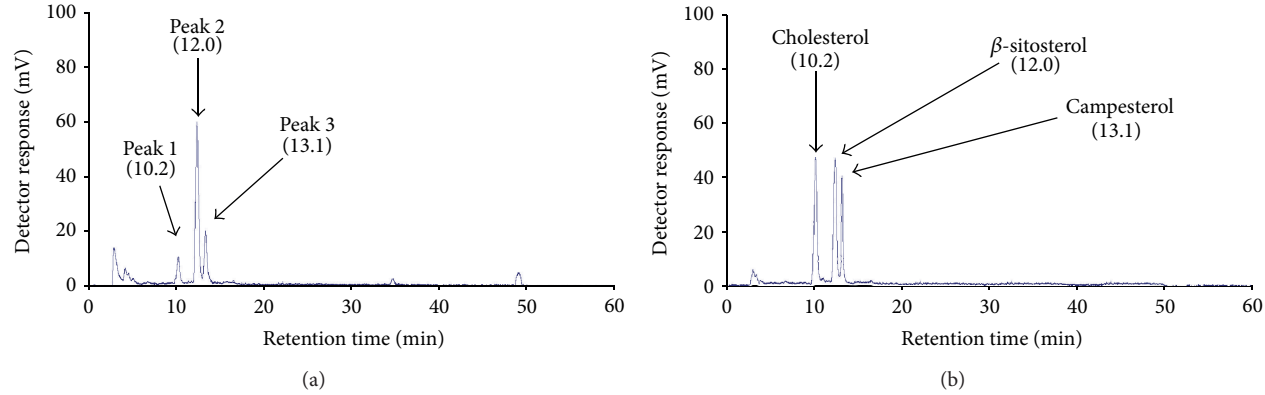

Figure 2: HPLC-ELSD chromatograms of *Porphyra dentata* F2 fraction (a) and a mixture of standards (cholesterol, β-sitosterol, and campesterol) (b). The retention time (T_R) of each major peak (Peak 1, Peak 2, and Peak 3) present in F2 fraction and each standard is shown in parentheses and on a time scale. Conditions for HPLC-ELSD: column, Mightysil RP-18 (H) column (250 × 4.5 mm); column temperature, 40°C; mobile phase, 95% methanol in water; flow rate: 1 mL/min; ELSD detector nebulizer temperature, 80°C.

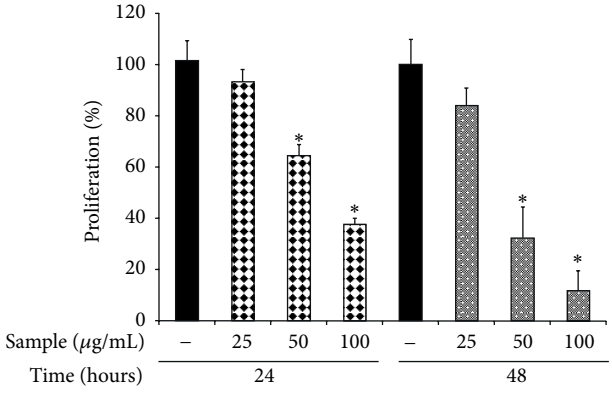

Figure 3: Effect of *Porphyra dentata* F2 fraction on viability of 4T1 cells. The 4T1 cells were incubated in DMEM culture containing 10% FBS and sample at indicated concentrations for 24 h and 48 h. Thereafter, the cells were subjected to MTT assay. The proliferation percentage (%) was defined as 100 multiplied by the ratio of the OD_{490} value of the cells treated with sample over the OD_{490} value of the control cells. Data are expressed as mean ± S.D. ($n = 3$).

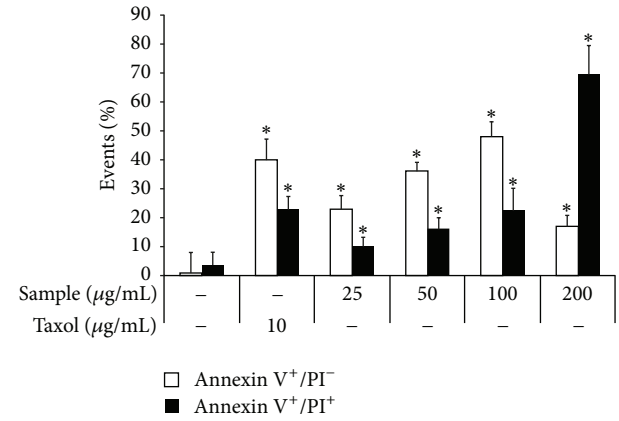

Figure 4: Simultaneous *in vitro* detection of apoptosis (annexin V staining) and necrosis (PI staining) of 4T1 cells treated with *P. dentata* F2 fraction. The 4T1 cells were incubated in DMEM culture containing 10% FBS and F2 sample at indicated concentrations for 48 h. Taxol (10 μg/mL) was used as a positive control. The relative cell population (%) undergoing a solely apoptotic (annexin V positive) pathway is shown by an open bar square; cells undergoing necrotic-apoptotic pathway (annexin V and PI double positive) are shown by a closed black bar square. Data are expressed as mean ± S.D. ($n = 3$).

tumor nodules were barely detectable on days 3 and 6 in tumor-bearing mice that were treated with sample at a dose of 25 mg/kg. On day 18, the volume and mass of 4T1 tumors were significantly larger in the control group than in the tumor-bearing group treated with the sample at dosages of 10 and 25 mg/kg ($P < 0.05$) (Figures 5(c) and 5(d)). By contrast, on day 18 no significant difference was noted in tumor size between the control mice and mice treated with a low dose of the sample (5 mg/kg) (Figures 5(b) and 5(c)). Increased survival benefits were observed in the sample-treated groups (Figure 5(e)). All 6 mice in the tumor-bearing control group died within 33 days, whereas mice treated with sample at a dose of 25 mg/kg survived significantly longer, at 43 days ($P = 0.039$). Overall, these results showed that the sterol fraction of *P. dentata* effectively retarded tumorgenesis and increased mouse survival (Figure 5).

3.3. Sterol Fraction of P. dentata Did Not Affect Gr-1$^+$CD11b$^+$ Myeloid Cell Expansion. The effect of the sterol fraction of *P. dentata* on the percentage of MDSC in splenocytes of tumor-bearing mice was investigated. The MDSCs were labeled with fluorescence-conjugated antibodies Gr-1$^+$-FITC and CD11b$^+$-PE and were then detected using flow cytometry. On Day 18, the percentage of splenic MDSCs in tumor-bearing control mice was markedly elevated by 36% compared with naive tumor-free mice (4%) (Figure 6). By contrast, mice treated with dosages of 5 or 25 mg/kg of sample did not show significant changes in the MDSC induction level, compared with tumor-bearing control mice (Figure 6). This result suggested that the sterol fraction of *P. dentata* did not inhibit MDSC induction pathways in BALB/c mice.

3.4. Sterol Fraction of P. dentata Decreased ROS Levels in Purified MDSCs. The ROS levels in MDSCs isolated from

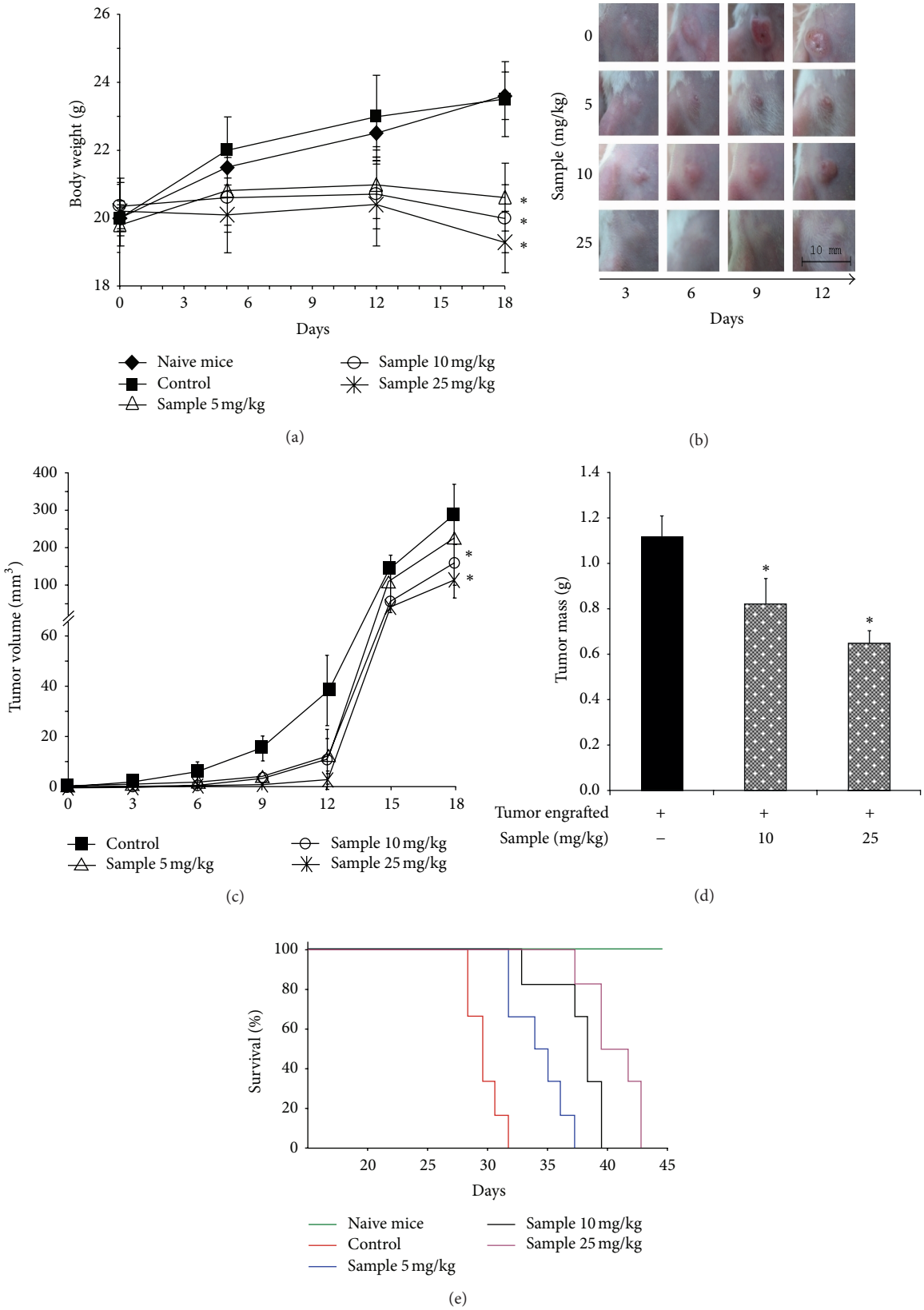

Figure 5: Inhibitory effect of *P. dentata* F2 fraction on 4T1 tumor-cell-engrafted mice. The 4T1 cells were subcutaneously engrafted (5×10^5 cells suspended in 0.1 mL of PBS) in the nipples of BALB/c female mice. The following parameters were measured: (a) body weight, (b) photo for tumor growth status, (c) primary tumor volume, (d) primarytumor mass, and (e) survival rate. The data are representative of one experiment with 6 mice in each group. Naive mice and control mice were i.p. treated with DMSO only.

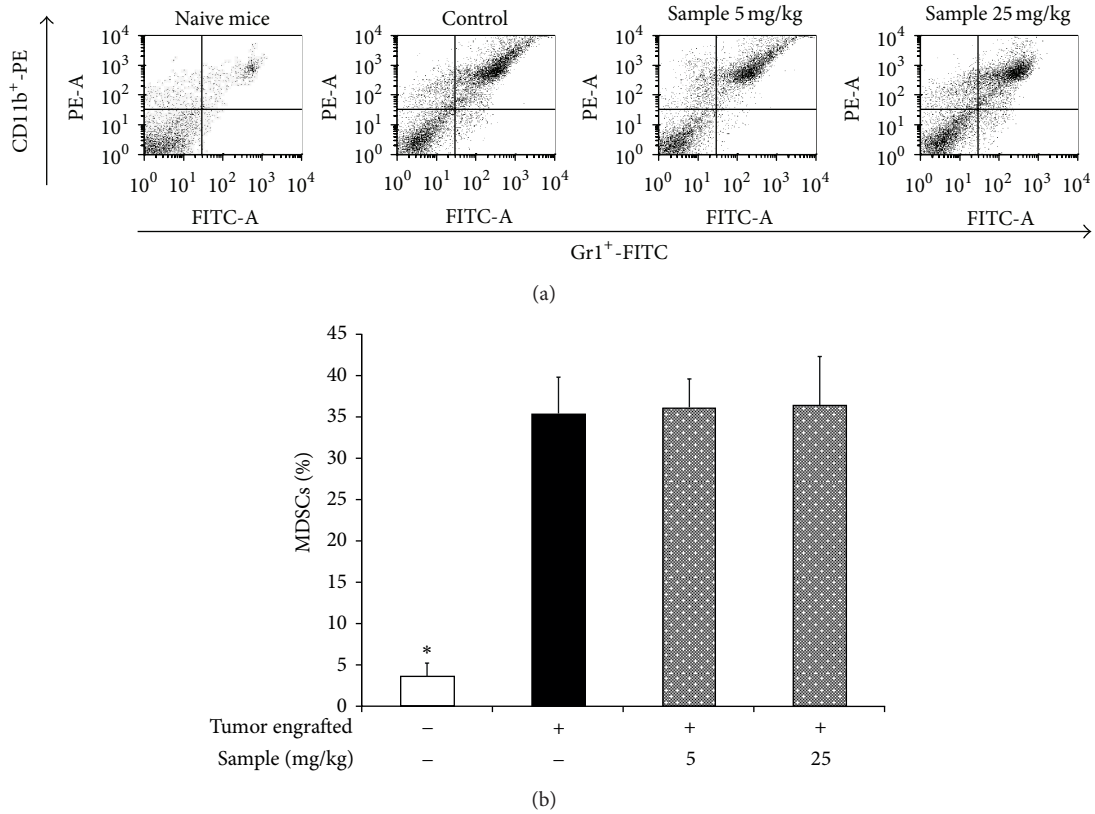

Figure 6: The induction of MDSCs in female BALB/c mice treated with or without *P. dentata* F2 fraction. The 4T1 cells were subcutaneously engrafted in the mice. A typical dot plot of splenic MDSCs level is shown in (a). The percentage of MDSCs detected in the spleen of mice bearing 4T1 tumors is shown in (b). The data are representative of one experiment, with 3 mice from each group.

BALB/c mice using an oxidation-sensitive fluorescent dye, DCFDA, are shown in Figure 7. *In vivo*, MDSCs from tumor-bearing control mice exhibited 10 times more ROS-positive cells than MDSCs from tumor-free mice (Figure 7(a)). The mean fluorescence intensity (MFI) values represent the ROS content. These values were 65 ± 3 and 777 ± 68 for naive MDSCs and tumor-bearing control MDSCs, respectively. By contrast, the MFI values for MDSCs from tumor-bearing mice treated with the sample at dosages of 5 and 25 mg/kg were 621 ± 84 and 265 ± 50, respectively; both of which were significantly lower than the MFI values for MDSCs from the control group (Figure 7(a)). *In vitro*, the purified MDSCs from tumor-bearing control mice were treated with various stimuli, including catalase (a ROS-quenching agent), PMA (a ROS induction agent), nor-NOHA (an arginase inhibitor), and sample. As expected, the *in vitro* ROS level in untreated control MDSCs (MFI 776 ± 47) was similar to the *in vivo* MDSC level in the tumor-bearing control group (777 ± 68, Figure 7(a)). Treatment with catalase or nor-NOHA decreased the ROS level significantly to MFI 336 ± 67 and MFI 70 ± 3, respectively. By contrast, the ROS level of MDSCs treated with ROS-inducing PMA increased 2-fold (MFI 1556 ± 120). Similarly, the ROS levels of MDSCs treated *in vitro* with the sample at dosages of 5 and 25 μg/mL were significantly decreased, with MFI values being 271 ± 66 and 72 ± 15, respectively (Figure 7(b)). Overall, the sterol fraction of *P. dentata* decreased ROS in a dose-dependent manner in MDSCs both *in vivo* and *in vitro* (Figure 7).

3.5. Sterol Fraction of P. dentata Inhibited Arginase Activity of MDSCs In Vivo. Arginase activity is an important contributor to MDSC suppressive activity. Thus, the arginase activity in MDSCs from naive, control, and sample-treated mice was measured to determine whether the arginase activity of MDSCs was modulated *in vivo* by our sample. As shown in Figure 8, the arginase activity (expressed as urea level) in control MDSCs was 4-fold higher than that in naive MDSCs. No significant difference was found in arginase activity between the control MDSCs and cells treated with the sample (5 mg/kg). However, arginase activity (1.9 mg/mL of urea) in MDSCs from mice treated with sample (25 mg/kg) was significantly lower ($P < 0.05$) than that of the control (2.6 mg/mL of urea) (Figure 8).

4. Discussion

Porphyra dentata is an edible seaweed that is widely cultivated in Taiwan. Our previous study examined the anti-inflammatory effect of *P. dentata* methanolic crude extract on iNOS-implicated diseases in lipopolysaccharide-challenged mouse macrophages [22]. The current study showed for the first time that dichloromethane solvent fraction (F2) of

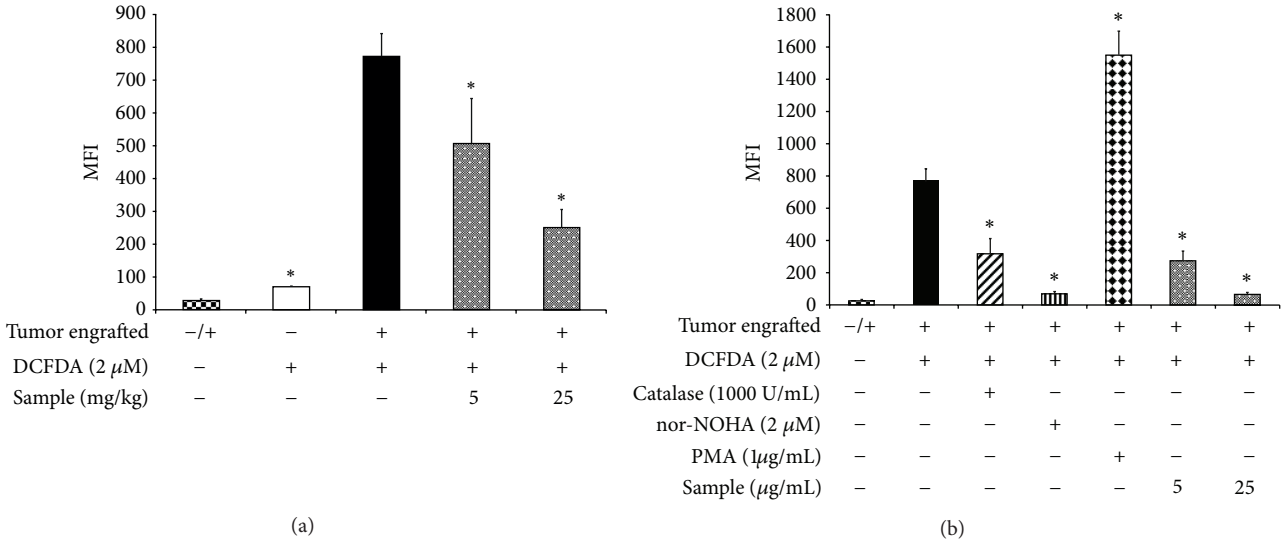

Figure 7: *In vivo* effect of *P. dentata* F2 fraction (a) and *in vitro* effect of F2 fraction and various agents (b) on ROS production by MDSCs. *In vivo*, tumor-bearing BALB/c mice were i.p. injected with F2 fraction at dosages of 5 and 25 mg/kg body weight. MDSCs were isolated from tumor-bearing control mice and F2-treated mice as described in Section 2 and their ROS productions were measured. *In vitro*, MDSCs isolated from the tumor-bearing control mice were incubated first with F2 fraction or the tested agent; thereafter, ROS production was measured. Where the stimulating agent PMA was used, MDSCs were incubated at 37°C for 5 min with 1 μg/mL PMA and then washed with cold PBS. To block ROS production *in vitro*, MDSCs were incubated with catalase, arginase inhibitor (nor-NOHA), or F2 fraction at 37°C for 10 min. The oxidative-sensitive dye DCFDA was used to measure ROS production by the cells. MDSCs were incubated with 2 μM DCFDA for 15 min at 37°C and then washed twice with PBS. The intensity of fluorescence was measured by flow cytometry. Data were obtained from one experiment, with 4 individual mice from each group. Measurements were obtained in duplicate and the mean fluorescence intensity (MFI) was calculated for MDSCs in each group, for both *in vivo* and *in vitro* treatments.

the crude extract of *P. dentata* displays anti-breast-cancer activities.

Phytochemical analysis showed that our biologically active sample was composed of cholesterol and phytosterols (β-sitosterol and campesterol) (Figure 2). Recent findings from a number of studies have shown that foods containing phytosterols, such as β-sitosterol either alone or in combination with campesterol, may protect animals from the risk of various tumors [21, 30–32]. Phytosterols exert anticancer actions by inhibition of carcinogen production, cancer cell proliferation, angiogenesis, invasion and metastasis, and induction of apoptosis of cancer cells [33]. Similarly, probably because of the presence of β-sitosterol and campesterol, our sample inhibited proliferation of breast cancer cells *in vitro* (Figure 3) and caused an apoptotic-necrotic effect in the cells (Figure 4). Furthermore, treatment with the sample effectively reduced the tumor size of 4T1 implanted cells and prolonged survival of the mice (Figure 5).

Previous research has established that MDSCs play a key role in tumorgenesis [9, 11]. The expansion of MDSCs in bone marrow of tumor-bearing hosts is governed largely by factors produced by tumor cells, which results in an accumulation of MDSCs in the secondary lymphoid organs (spleen and lymph nodes) [3]. This process occurs through the stimulation of myelopoiesis and inhibition of the differentiation of mature myeloid cells [3, 34]. Similar expansion, although not inhibited by the sterol fraction of *P. dentata*, was observed in splenic MDSCs of tumor-bearing mice that either did or did not receive the sample treatments (Figure 6). In the presence of appropriate cytokines, MDSCs differentiate into mature myeloid cells [35]. Such differentiation is blocked in the presence of tumor-cell-conditioned media or in tumor-bearing hosts [35]. Overall, our study might indicate that tumor-derived factors that induced expansion of MDSCs were unaffected by the sterol fraction of *P. dentata*. This would suggest other mechanisms of action on MDSC resulting in the inhibition of breast cancer tumorgenesis.

The T cell immunosuppressive functions of MDSCs act through the release of short-lived soluble mediators such as ROS [6, 10] and arginase activity [12, 13]. Arginase catalyzes the conversion of L-arginine to urea and L-ornithine [8]. Recent data showed that there is a close correlation between the availability of L-arginine and the regulation of T cell proliferation [12, 13]. The high expression of arginase activity by MDSCs favors their direct inhibition on T-cell function [8, 11]. Serafini et al. [36] found that a phosphodiesterase-5 inhibitor, sildenafil, could downregulate the expression of arginase by MDSCs and, accordingly, inhibit the suppressive function of MDSCs in growing tumors. In this study the sterol fraction of *P. dentata* significantly decreased the ROS production (Figure 7(a)) and arginase activity (Figure 8) of MDSCs in 4T1 tumor-cell-engrafted mice *in vivo*. Accordingly, this fraction could down-regulate suppressive activity of MDSCs and decrease the tumor size (Figure 5). In addition, L-arginine is also used by nitric oxide synthase for nitric oxide (NO) generation [3]. Boucher et al. [37] showed that a low

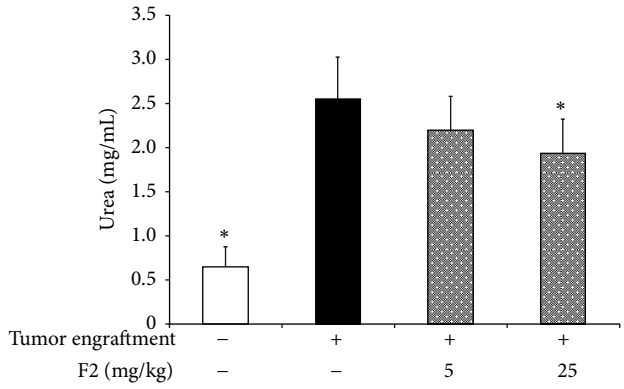

FIGURE 8: Arginase activity of MDSCs in naive mice, tumor-bearing control mice, and tumor-bearing mice treated with *P. dentata* F2 fraction. The splenic MDSCs were isolated from various groups of BALB/c mice and were lysed for 10 min in the lysis buffer and the arginase activity (shown as urea production) in the cell lysate was measured, as described in Section 2. Data were obtained from one experiment, with 3 mice from each group, and expressed as mean ± S.D.

concentration of L-arginine resulted in low NO generation and high production of superoxide ion ($^{\bullet}O_2^-$). In this study, the high arginase activity in tumor-derived MDSCs in control mice (Figure 8) might have lowered the level of L-arginine, which resulted in increasing of $^{\bullet}O_2^-$, one of ROS (Figures 6(a) and 6(b)) and undetectable NO (data not shown). *In vitro* the addition of an arginase inhibitor, Nor-NOHA, in MDSCs might cause the high level of L-arginine that can be used for NO production and, finally, significantly decreased ROS production (Figure 7(b)).

5. Conclusion

This study was the first to screen and isolate the *P. dentata* fraction (F2 fraction) and to examine its potent anti-cancer activity. These anti-cancer effects probably result from the presence of β-sitosterol and campesterol. This sterol containing fraction reduced tumorgenesis and increased the survival rate of 4T1-engrafted mice; we suggest 2 likely mechanisms for this effect. First, the sample might cause the apoptosis of 4T1 cells. The other possible mechanism is that the sample might down-regulate the suppressive activity of MDSCs by affecting their ROS accumulation and arginase activity. This inhibition would be consistent with the use of *Porphyra dentata* as a folk medicine to treat inflammatory disorders and also for breast cancer.

Acknowledgments

The authors gratefully acknowledge the financial support for this study received from the National Science Council of Taiwan, China, (NSC98-2313-B-019-010-MY3), and the Center of Marine Bioenvironment and Biotechnology, National Taiwan Ocean University (NTOU-RD-AA- 2013-102012).

References

[1] L. Giacinti, P. P. Claudio, M. Lopez, and A. Giordano, "Epigenetic information and estrogen receptor alpha expression in breast cancer," *Oncologist*, vol. 11, no. 1, pp. 1–8, 2006.

[2] T. Luo, J. Wang, Y. Yin et al., "(-)-Epigallocatechin gallate sensitizes breast cancer cells to paclitaxel in a murine model of breast carcinoma," *Breast Cancer Research*, vol. 12, no. 1, article R8, 2010.

[3] B. A. Pulaski and S. Ostrand-Rosenberg, "Mouse 4T1 breast tumor model," in *Current Protocols in Immunology*, chapter 20, unit 20.22, 2001.

[4] D. I. Gabrilovich and S. Nagaraj, "Myeloid-derived suppressor cells as regulators of the immune system," *Nature Reviews Immunology*, vol. 9, no. 3, pp. 162–174, 2009.

[5] P. Sinha, V. K. Clements, S. K. Bunt, S. M. Albelda, and S. Ostrand-Rosenberg, "Cross-talk between myeloid-derived suppressor cells and macrophages subverts tumor immunity toward a type 2 response," *Journal of Immunology*, vol. 179, no. 2, pp. 977–983, 2007.

[6] S. Kusmartsev, Y. Nefedova, D. Yoder, and D. I. Gabrilovich, "Antigen-specific inhibition of CD8+ T cell response by immature myeloid cells in cancer is mediated by reactive oxygen species," *Journal of Immunology*, vol. 172, no. 2, pp. 989–999, 2004.

[7] L. Yang, J. Huang, X. Ren et al., "Abrogation of TGF beta signaling in mammary carcinomas recruits Gr-1+CD11b+ myeloid cells that promote metastasis," *Cancer Cell*, vol. 13, no. 1, pp. 23–35, 2008.

[8] P. Serafini, I. Borrello, and V. Bronte, "Myeloid suppressor cells in cancer: recruitment, phenotype, properties, and mechanisms of immune suppression," *Seminars in Cancer Biology*, vol. 16, no. 1, pp. 53–65, 2006.

[9] A. H. Zea, P. C. Rodriguez, M. B. Atkins et al., "Arginase-producing myeloid suppressor cells in renal cell carcinoma patients: a mechanism of tumor evasion," *Cancer Research*, vol. 65, no. 8, pp. 3044–3048, 2005.

[10] C. A. Corzo, M. J. Cotter, P. Cheng et al., "Mechanism regulating reactive oxygen species in tumor-induced myeloid-derived suppressor cells," *Journal of Immunology*, vol. 182, no. 9, pp. 5693–5701, 2009.

[11] A. C. Ochoa, A. H. Zea, C. Hernandez, and P. C. Rodriguez, "Arginase, prostaglandins, and myeloid-derived suppressor cells in renal cell carcinoma," *Clinical Cancer Research*, vol. 13, no. 2, part 2, pp. 721s–726s, 2007.

[12] P. C. Rodriguez, M. S. Ernstoff, C. Hernandez et al., "Arginase I-producing myeloid-derived suppressor cells in renal cell carcinoma are a subpopulation of activated granulocytes," *Cancer Research*, vol. 69, no. 4, pp. 1553–1560, 2009.

[13] P. C. Rodriguez, D. G. Quiceno, J. Zabaleta et al., "Arginase I production in the tumor microenvironment by mature myeloid cells inhibits T-cell receptor expression and antigen-specific T-cell responses," *Cancer Research*, vol. 64, no. 16, pp. 5839–5849, 2004.

[14] K. Tao, M. Fang, J. Alroy, and G. G. Gary, "Imagable 4T1 model for the study of late stage breast cancer," *BMC Cancer*, vol. 8, article 228, 2008.

[15] C. L. Banka, C. V. Lund, M. T. N. Nguyen, A. J. Pakchoian, B. M. Mueller, and B. P. Eliceiri, "Estrogen induces lung metastasis through a host compartment-specific response," *Cancer Research*, vol. 66, no. 7, pp. 3667–3672, 2006.

[16] T. Ichihara, H. Wanibuchi, T. Taniyama et al., "Inhibition of liver glutathione S-transferase placental form-positive foci development in the rat hepatocarcinogenesis by *Porphyra tenera* (Asakusa-nori)," *Cancer Letters*, vol. 141, no. 1-2, pp. 211–218, 1999.

[17] Y. Okai, K. Higashi-Okai, Y. Yano, and S. Otani, "Identification of antimutagenic substances in an extract of edible red alga, *Porphyra tenera* (Asadusa-nori)," *Cancer Letters*, vol. 100, no. 1-2, pp. 235–240, 1996.

[18] D. R. Idler, A. Saito, and P. Wiseman, "Sterols in red algae (Rhodophyceae)," *Steroids*, vol. 11, no. 4, pp. 465–473, 1968.

[19] M. Plaza, A. Cifuentes, and E. Ibáñez, "In the search of new functional food ingredients from algae," *Trends in Food Science and Technology*, vol. 19, no. 1, pp. 31–39, 2008.

[20] D. I. Sánchez-Machado, J. López-Hernández, P. Paseiro-Losada, and J. López-Cervantes, "An HPLC method for the quantification of sterols in edible seaweeds," *Biomedical Chromatography*, vol. 18, no. 3, pp. 183–190, 2004.

[21] A. B. Awad and C. S. Fink, "Phytosterols as anticancer dietary components: evidence and mechanism of action," *Journal of Nutrition*, vol. 130, no. 9, pp. 2127–2130, 2000.

[22] K. Kazłowska, T. Hsu, C.-C. Hou, W.-C. Yang, and G.-J. Tsai, "Anti-inflammatory properties of phenolic compounds and crude extract from *Porphyra dentata*," *Journal of Ethnopharmacology*, vol. 128, no. 1, pp. 123–130, 2010.

[23] T. Kimiya, K. Ohtani, S. Satoh et al., "Inhibitory effects of edible marine algae extracts on degranulation of RBL-2H3 cells and mouse eosinophils," *Fisheries Science*, vol. 74, no. 5, pp. 1157–1165, 2008.

[24] M. Engeland, S. M. van den Eijnde, T. Aken et al., "Detection of apoptosis in ovarian cells in vitro and in vivo using the annexin v-affinity assay," *Methods in Molecular Medicine*, vol. 39, pp. 669–677, 2001.

[25] S. A. duPre' and K. W. Hunter Jr., "Murine mammary carcinoma 4T1 induces a leukemoid reaction with splenomegaly: association with tumor-derived growth factors," *Experimental and Molecular Pathology*, vol. 82, no. 1, pp. 12–24, 2007.

[26] D. A. Nelson, M. D. Tolbert, S. J. Singh, and K. L. Bost, "Expression of neuronal trace amine-associated receptor (Taar) mRNAs in leukocytes," *Journal of Neuroimmunology*, vol. 192, no. 1-2, pp. 21–30, 2007.

[27] C.-I. Chang, J. C. Liao, and L. Kuo, "Macrophage arginase promotes tumor cell growth and suppresses nitric oxide-mediated tumor cytotoxicity," *Cancer Research*, vol. 61, no. 3, pp. 1100–1106, 2001.

[28] J. M. Bland and D. G. Altman, "Statistics notes: survival probabilities (the Kaplan-Meier method)," *British Medical Journal*, vol. 317, no. 7172, p. 1572, 1998.

[29] J. M. Bland and D. G. Altman, "Statistics notes: the logrank test," *British Medical Journal*, vol. 328, no. 7447, p. 1073, 2004.

[30] R. L. von Holtz, C. S. Fink, and A. B. Awad, "β-Sitosterol activates the sphingomyelin cycle and induces apoptosis in LNCaP human prostate cancer cells," *Nutrition and Cancer*, vol. 32, no. 1, pp. 8–12, 1998.

[31] A. B. Awad, A. Downie, C. S. Fink, and U. Kim, "Dietary phytosterol inhibits the growth and metastasis of MDA-MB-231 human breast cancer cells grown in SCID mice," *Anticancer Research*, vol. 20, no. 2, pp. 821–824, 2000.

[32] A. B. Awad, C. S. Fink, H. Williams, and U. Kim, "*In vitro* and *in vivo* (SCID mice) effects of phytosterols on the growth and dissemination of human prostate cancer PC-3 cells," *European Journal of Cancer Prevention*, vol. 10, no. 6, pp. 507–513, 2001.

[33] T. A. Woyengo, V. R. Ramprasath, and P. J. H. Jones, "Anticancer effects of phytosterols," *European Journal of Clinical Nutrition*, vol. 63, no. 7, pp. 813–820, 2009.

[34] C. A. Corzo, T. Condamine, L. Lu et al., "HIF-1α regulates function and differentiation of myeloid-derived suppressor cells in the tumor microenvironment," *Journal of Experimental Medicine*, vol. 207, no. 11, pp. 2439–2453, 2010.

[35] S. Kusmartsev and D. I. Gabrilovich, "Inhibition of myeloid cell differentiation in cancer: the role of reactive oxygen species," *Journal of Leukocyte Biology*, vol. 74, no. 2, pp. 186–196, 2003.

[36] P. Serafini, K. Meckel, M. Kelso et al., "Phosphodiesterase-5 inhibition augments endogenous antitumor immunity by reducing myeloid-derived suppressor cell function," *Journal of Experimental Medicine*, vol. 203, no. 12, pp. 2691–2702, 2006.

[37] J. L. Boucher, C. Moali, and J. P. Tenu, "Nitric oxide biosynthesis, nitric oxide synthase inhibitors and arginase competition for L-arginine utilization," *Cellular and Molecular Life Sciences*, vol. 55, no. 8-9, pp. 1015–1028, 1999.

Hindawi Publishing Corporation
Evidence-Based Complementary and Alternative Medicine
Volume 2013, Article ID 639083, 10 pages
http://dx.doi.org/10.1155/2013/639083

Research Article

Coniferyl Ferulate, a Strong Inhibitor of Glutathione S-Transferase Isolated from Radix *Angelicae sinensis*, Reverses Multidrug Resistance and Downregulates P-Glycoprotein

Chang Chen,[1] Chuanhong Wu,[1] Xinhua Lu,[2] Zhiyong Yan,[3] Jian Gao,[4] Hui Zhao,[5] and Shaojing Li[1]

[1] *Institute of Chinese Materia Medica, China Academy of Chinese Medical Sciences, Beijing 100700, China*
[2] *New Drug Research and Development Centre of North China Pharmaceutical Group Corporation, Hebei 050015, China*
[3] *College of Life Science and Engineering, Southwest Jiaotong University, Chengdu 610031, China*
[4] *College of Pharmaceutical Science, Hebei University, Baoding, Hebei 071002, China*
[5] *China Academy of Chinese Medical Sciences, Beijing 100700, China*

Correspondence should be addressed to Shaojing Li; shaojingli2004@126.com

Received 16 May 2013; Accepted 24 June 2013

Academic Editor: Shun-Fa Yang

Glutathione S-transferase (GST) is the key enzyme in multidrug resistance (MDR) of tumour. Inhibition of the expression or activity of GST has emerged as a promising therapeutic strategy for the reversal of MDR. Coniferyl ferulate (CF), isolated from the root of *Angelica sinensis* (Oliv.) Diels (Radix *Angelicae sinensis*, RAS), showed strong inhibition of human placental GST. Its 50% inhibition concentration (IC_{50}) was 0.3 μM, which was greater than a known GSTP1-1 inhibitor, ethacrynic acid (EA), using the established high-throughput screening model. Kinetic analysis and computational docking were used to examine the mechanism of GST inhibition by CF. Computational docking found that CF could be fully docked into the gorge of GSTP1-1. The further exploration of the mechanisms showed that CF was a reversible noncompetitive inhibitor with respect to GSH and CDNB, and it has much less cytotoxicity. Apoptosis and the expression of P-gp mRNA were evaluated in the MDR positive B-MD-C1 (ADR+/+) cell line to investigate the MDR reversal effect of CF. Moreover, CF showed strong apoptogenic activity and could markedly decrease the overexpressed P-gp. The results demonstrated that CF could inhibit GST activity in a concentration-dependent manner and showed a potential MDR reversal effect for antitumour adjuvant therapy.

1. Introduction

Chemotherapeutics provide the most effective treatment modality for metastatic cancer. However, resistance to anticancer chemotherapy remains a serious obstacle in cancer treatment. Primary and acquired resistance of tumour cells to anticancer drugs are major causes of the limited efficacy of chemotherapy [1, 2]. Tumours may be intrinsically drug resistant or develop resistance during treatment; a phenomenon that is known as multidrug resistance (MDR). Acquired resistance is particularly a problem as tumours not only become resistant to the drugs originally used in treatment but also become cross-resistant to other drugs [3].

Glutathione S-transferases (GSTs, EC 2.5.1.18) are a superfamily of Phase II detoxification enzymes that catalyse the conjugation of glutathione (GSH) to a wide variety of endogenous and exogenous electrophilic compounds including chemotherapeutic agents [4]. GSTs are present in human tissues and have been subdivided into at least eight gene-independent classes named Alpha, Pi, Mu, Theta, Zeta, Omega, Sigma, and Kappa. Resistant cells often have increased detoxification of compounds mediated by high levels of GSH and GST [5]. Evidence suggests that the GST isozymes may have additional functions beyond their catalytic role [6]. These roles might include protecting the cells from death, detoxifying chemotherapeutic agents, and

inducing drug resistance by inactivating chemotherapeutic compounds via GSH conjugation [7]. Among these isoenzymes, overexpression of GSTP1-1 was found to be correlated with the resistance of some chemotherapeutic agents in human tumour cells including colon, stomach, pancreas, uterine cervix, breast, lung cancers, melanoma, and lymphoma [8, 9]. The activity of GST appears to be an important factor contributing to the resistance of tumour.

However, MDR to cancer chemotherapy is complex and may involve multiple mechanisms. Notably, a combination of mechanisms, rather than a sole mechanism, has often been observed in the resistance to antineoplastic drugs. A close correlation between the high activity of GSTP1-1 and overexpression of P-glycoprotein (P-gp) has often been found simultaneously in many MDR cell lines [10]. P-gp is a classical ABC transporter (the gene product of *ABCB1*/*MDR1*) and acts as an ATP-dependent active efflux pump for chemotherapeutic agents. P-gp-mediated MDR appears to be a major feature in drug resistance [11–13]. Moreover, GSTP1-1 displays an additional antiapoptotic activity based on a protein-protein interaction with the c-Jun N-terminal kinase (JNK), a key enzyme in the apoptotic cascade [14], by which GST inhibitors seem to indirectly inhibit the abnormal expression of P-gp. Therefore, the therapeutic use of GST inhibitors is viable suggestions as MDR reversing agents to improve the efficacy of chemotherapy. Ethacrynic acid (EA) [15], an active diuretic, was one of the first generation of GST inhibitors to be utilised as chemosensitiser [16]. Since then, a variety of GST inhibitors focused on the substrate-binding site of the GST isozyme or glutathione analogue have currently been examined and found to modulate drug resistance by sensitising tumour cells to anticancer drugs [4, 17, 18]. Unfortunately, most of them, including EA, have not fared well in clinical trials due to poor efficacy and side effects [19].

Development of MDR reversing agents with higher activity and lower toxicity is a promising strategy in the battle against MDR as this approach could result in the enhanced efficacy of anticancer compounds. Natural products might be important sources as potential chemosensitising agents with greater inhibition of the activity of GST. However, only a few inhibitors of GSTP1-1 from natural products, such as quinine [20], thonningianin A [21], quercetin [22], curcumin [23], and plant phenols [24], have been demonstrated to antagonise MDR in preclinical trials.

The natural resources of Chinese medicine materials are abundant and diverse. In addition, these medicines have relatively few side effects in long-term clinical use. Accordingly, they should be good candidates for a new generation of GST inhibitors to modulate MDR. In this study, a high-throughput screening (HTS) model was established to screen for inhibitors of GST from natural Chinese herbs. Using this approach, a compound isolated from the roots of *Angelica sinensis* (Oliv.) Diels (Radix *Angelicae sinensis*, RAS) was found to be a strong inhibitor of GST.

This compound was also investigated in inhibitory kinetic and computational docking to evaluate its mechanism of GST inhibition and the structure-activity relationship. Apoptosis analysis and a reverse transcription-polymerase chain reaction (RT-PCR) assay for P-gp/MDR1 expression in an Adriamycin-resistant human endometrial cancer cell line were also utilised to evaluate the ability of the compound to reverse MDR. The primary aim of this study was to provide natural source for the discovery of new drug candidate with MDR reversing activity.

2. Materials and Methods

2.1. Chemicals and Reagents. GST (mainly GSTP1-1, from human placenta), glutathione (GSH), 1-chloro-2, 4-dinitrobenzene (CDNB), RPMI-1640, 3′-(4,5-dimethylthiazol-2-yl)-2,5-diphenyl tetrazolium bromide (MTT), ethacrynic acid (purity ≥ 98%), RNase A, propidium iodide, and Adriamycin (purity ≥ 98%) were obtained from Sigma (St Louis, MO, USA). Coniferyl ferulate standard (purity ≥ 98%) was purchased for structure identification from Chengdu Herbpurify CO., LTD, Chengdu, China (QC number A-001-120726). TRIzol reagent and a RT-PCR assay kit were from Life Technologies (Carlsbad, California, USA). All other chemicals were from Beijing Chemical Co., Beijing, China. All the chemicals used were of analytical grade.

2.2. Cell Lines and Cell Culture. Human lung carcinoma A549 cells and human endometrial carcinoma B-MD-C1 cells were maintained in Dulbecco's modified Eagle's medium (DMEM, Life Technologies, Carlsbad, California, USA), supplemented with 10% foetal bovine serum (Takara Bio, Shimogyo-ku, Kyoto, Japan) and antibiotics (100 U/mL penicillin and 100 μg/mL streptomycin). The drug-resistant cell line B-MD-C1 (ADR+/+) was a gift from Professor Baoen Shan; the cell line's multidrug resistance was maintained by culturing the cells at in 5 μg/mL Adriamycin.

2.3. Plant Materials. RAS was collected in 2008 from the Gansu province of China, as identified by Professor Lanping Guo of the Institute of Chinese Materia Medica, China Academy of Chinese Medical Sciences. A voucher specimen (20080705024) was deposited in the Herbarium of the Institute of Chinese Materia Medica, China Academy of Chinese Medical Sciences.

2.4. Extraction and Isolation. The isolation procedure for the studied compound was as follows. Briefly, dried RAS (10 kg) was ground into farina and extracted with 95% EtOH (100 L). After the insoluble farina was removed, the EtOH was evaporated under reduced pressure to give a viscous residue. The viscous residue was suspended in water and extracted with petroleum ether. The petroleum ether extract (400 g) was partitioned between petroleum ether and 80% MeOH, and the 80% MeOH layer (260 g) was chromatographed on a silica gel column (100 × 460 mm, 160–200 mesh). The column was eluted with a gradient of *n*-hexane/acetone from 90 : 10 to 10 : 90 to obtain seven fractions according to TLC detection. The fraction containing the compound was further separated by silica gel (column: 36 × 460 mm, 260~300 mesh, chloroform/acetone from 100 : 0 to 0 : 100), Sephadex LH20 column chromatography (column: 26 × 920 mm eluted with MeOH), and preparative HPLC (Phenomenex C18 column (21.2 × 250 mm, 10 μm, 100 Å, Kromasil), eluted with 55%

CH_3CN-H_2O) to give the test compound (249.0 mg). The compound was identical to one known compound, coniferyl ferulate (CF) [25]. Its purity was more than 95% by HPLC. The structure of the compound (Figure 1) was elucidated by analysis of mass spectrometry (MS) and ^1H, ^{13}C NMR data and confirmed with authentic sample (QC no. A-001-120726, Chengdu Herbpurify CO., LTD, Chengdu, China) spectra data of isolated compound CF as shown in supporting information in Supplementary Material available online at http://dx.doi.org/10.1155/2013/639083.

2.5. Enzyme Activity Assay. The inhibition studies using GST from human placenta were carried out at 37°C using the established HTS method in which GSH and CDNB are used as substrates [26]; GSH was used at 5 mM, and CDNB was used at 0.1 mM. One microlitre of the purified CF (final concentration from 0.1 μM to 100 μM) or positive control (final concentration from 0.1 μM to 1 mM) dissolved in DMSO was added to the reaction mixture (10 μL of GST, approximately 0.0018 units) dissolved in 50 mM potassium phosphate buffer (pH 7.4) in a 384-well plate. After incubation of a certain amount of GST and CF at 37°C for 30 min with GSH and CDNB, the change in absorbance at 340 nm was monitored to measure the product GSH conjugate formation with a spectrophotometer (Spectra Max M5, Molecular Devices, USA).

2.6. Enzyme Inhibitory Kinetics. Enzyme kinetic experiments were performed to elucidate the interaction of human GSTs with CF in detail. Firstly, the initial rate of the enzyme was analysed by measuring the formation of catalysate at 340 nm. The reaction was carried out at 37°C for 5 min after preincubating GST with various concentrations of CF for 5 min. Furthermore, a plot of v (μM/mL/min) versus [E] was obtained with different CF or EA concentrations (0%, 20%, and 50% inhibition rate to GST) and different GST concentrations of 0.0075–0.18 U/mL to distinguish between reversible and irreversible inhibition. A Hanes plot of v versus [S] was performed at GSH concentrations from 0.07 to 2.24 mM or CDNB concentrations from 0.5 to 44.1 μM, with CF at concentrations of 0, 0.25, and 0.5 μM.

2.7. Computational Docking Methods. Computational docking was performed with FlexX software in SBVS (rational drug design v7.0, Tripos Inc.). The protein data bank (PDB) file 2GSS and the cocrystal format of the inhibitor, EA, in the active site of GST (human GSTP1-1) were optimised and used. EA was selected as a reference ligand structure which was a fixed conformation docked into the active site of the enzyme. The flexible docking conformations of EA were then created with 30 docking conformation options. Each conformation was energy-minimised using a molecular mechanics program. All ligands were predicted based on the active sites being within a 6.5 Å radius from the bound ligand. Water and metals not involved in binding were removed from the protein. The docking scores in GSTP1-1 were employed and elucidated in detail.

2.8. Cytotoxic Activity by MTT Assay. The wild-type human endometrial cancer B-MD-C1 cells or the multidrug-resistant

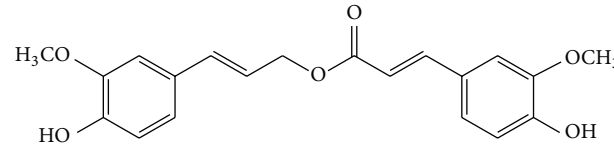

Figure 1: Structure of CF isolated from the Chinese herb RAS.

B-MD-C1 (ADR+/+) cells were plated in quadruplicate (6×10^3 cells per well) and incubated in the presence of different concentrations of positive control EA (10 μM–200 μM) and CF (4.12 μM–3 mM) for 48 h. The cytotoxic activity and dose response of EA and CF to these cell lines were determined using the MTT assay. Normalised data were plotted graphically as percentages of viable cells. Each study was performed in triplicate and repeated three times.

2.9. Flow Cytometry Apoptosis Analysis. Flow cytometry was used to evaluate the effect of CF on apoptosis of the multidrug-resistant B-MD-C1 (ADR+/+) cells treated with Adriamycin. Briefly, B-MD-C1 (ADR+/+) cells (1×10^7/mL) were incubated with CF at various concentrations or positive control EA (40 μm) for 48 h, and then the medium was replaced with fresh medium in the presence of Adriamycin (5 μg/mL). The B-MD-C1 (ADR+/+) cells only treated with Adriamycin were used as a control. After incubation for 24 h at 37°C, the cells were collected and fixed in 70% cold ethanol (−20°C) overnight. The cell suspensions were washed twice with phosphate-buffered saline (PBS) and resuspended in phosphate-buffered saline containing 1% foetal calf serum. RNA in the fixed cells was digested with RNase A (0.5 mg/mL) at 37°C for 1 h. Finally, the cells were centrifuged at 1000 revolutions/min for 5 min. The cells were resuspended with binding buffer and stained with propidium iodide (2.5 μg/mL) at room temperature for 15 min. The samples were measured by flow cytometry with CellQuest software (Becton Dickinson, San Jose, CA, USA).

2.10. MDR1 Gene Expression by RT-PCR. MDR1 gene expression levels were evaluated by RT-PCR assay on the B-MD-C1 and B-MD-C1 (ADR+/+) cells described above. Total cellular RNA was isolated using the TRIzol reagent (Life Technologies). First-strand cDNA synthesis was performed using a kit (Life Technologies). The primers used for the analysis of MDR1 were sense 5′-TCGTAGGAGTATCCGTGGAT-3′ and antisense 5′-CATTGGCGAGCCTGGTAG-3′ (455 bp); β-actin was used as an internal standard (sense primer 5′-AGCCCTTTCTCAAGGACCAC-3′ and antisense primer 5′-GCACTTTCTCCGCAGTTTCC-3′; 312 bp). The amplification reaction was carried out with 2 μL of cDNA product for 35 cycles with each cycle consisting of 95°C for 30 sec, 55°C for 30 sec, and 72°C for 30 sec, followed by a final 5 min elongation at 72°C. The final RT-PCR products were visualised by ultraviolet illumination after electrophoresis through 1.5% agarose gel, with 0.5 mg/mL ethidium bromide at 50 V at 2 h, and scanned using Kodak gel analysis software. RNA amounts were normalised against the β-actin mRNA levels. EA (40 μM) was also used as the positive control in this assay.

2.11. Statistical Analysis. Data were expressed as the means ± SD and analysed statistically using Student's *t*-test. The results were considered to be statistically significant when $P < 0.05$.

3. Results

3.1. The Inhibitory Activity of CF on GST. As shown in Figure 2, the inhibitory activity of CF on GST was investigated in the established HTS assay model. EA was chosen as a positive control that inhibited GST, with an IC_{50} value of 4.89 μM (see Figure 2). Notably, CF showed the stronger inhibition of GST (mainly GST-pi, from human placenta) in a concentration-dependent manner. The 50% inhibitory concentration (IC_{50}) of CF was approximately 0.3 μM. Moreover, the inhibitory kinetics and the associated binding mode were investigated because they may provide an exploitable mechanism for developing potent drugs with desirable properties. The kinetic analysis of the mechanism of inhibition to GST by CF was investigated by varying either GSH or CDNB concentration. The results showed that the inhibition of GST by CF might be reversible (Figure 3). Figure 4 shows the Hanes plots with various concentrations of GSH or CDNB. The results of the Hanes plots indicated that CF inhibited GST noncompetitively (Michaelis constant [K_m] remained unchanged, whereas the maximum rate of clearance [V_{max}] decreased) with respect to GSH and CDNB. Therefore, CF was likely to act as a reversible noncompetitive inhibitor of GST.

3.2. Computational Docking for CF. In order to gain an insight into the structural basis by which CF exerts its inhibitory activity on GST, the active site of GST was analysed using the GST-EA complex, and molecular docking studies were performed on CF using the PDB file 2GSS as a reference structure. The computational docking method was used with FlexX software to dock CF into the active site of GST. This method demonstrated that CF might insert into the enzyme molecule active cavity but not bind to the active site. A compound with a high-scoring conformation would display a high inhibitory activity on GST, and the computational docking scoring conformations were consistent with the results of the high-throughput screening. CF's hydroxyl oxygen atoms in the phenyl ring formed a hydrogen bond with active site amino acid TYR7. Methoxy oxygen atoms in the same phenyl ring also formed a hydrogen bond with active site amino acid TYR106. In addition, hydroxyl, hydrogen atoms in another phenyl ring formed a hydrogen bond with the carbonyl oxygen atom of active site amino acid VAL35. The conformation score was −11.0. The reference compound, EA, has a side chain carbonyl oxygen atom that forms a hydrogen bond with active site amino acid TYR108. The carboxyl oxygen atom forms a hydrogen bond with active site amino acid LEU52. The conformation score for the ethacrynic acid interaction is −13.3 (Figure 5).

3.3. The Cytotoxic Activities of CF. The cytotoxic activity of CF and positive control EA were analysed using the MTT assay. It was demonstrated that CF (3 mM or less) had no obvious influence on the proliferation of B-MD-C1 and B-MD-C1 (ADR+/+) cells (the inhibition rate of 3 mM was below 30%), while EA showed more potent inhibition of cell growth and induction of cell death than CF in these two cells (the inhibition rate of 60 μM was above 45%). Our data showed that CF hardly had any cytotoxic effect on the wild-type B-MD-C1 and the B-MD-C1 (ADR+/+) cells when its dose was less than 3 mM (Table 1). However, from the results, greater than 40 μM of EA seemed to affect cell viability, whereas 100 μM EA significantly decreased viable cells and showed the inhibition rate of close to 100%. Considering the low cytotoxicity, 5, 10, and 20 μM CF and 40 μM EA were chosen as reversal agents in our further study.

3.4. The Reversal Effect of CF on Cancer MDR Cell Lines

3.4.1. The Effect of CF on Apoptosis. To further investigate the reversal effect of CF on cancer MDR cell lines, its effects were determined on apoptosis of B-MD-C1 (ADR+/+) cells by flow cytometry. After the cells were exposed to 5 μg/mL Adriamycin together with various concentrations of CF or 40 μM EA for 48 h, a distinct sub-G1 peak, the apoptotic fraction, was observed in the cells compared with the control (Table 2, Figure 6). B-MD-C1 (ADR+/+) cells showed gradual arrest in the G(1)/S phase with the increasing doses of CF. Apoptosis induced by CF markedly increased the proportion of cells in G1-phase, decreased the proportion of cells in S-phase, and decreased cell survival. The apoptosis-inducing capacity of CF was much stronger than the positive control EA in this assay.

3.4.2. The Effect of CF on P-gp Expression Level. RT-PCR analysis of the expression level of P-gp in the studied groups further revealed the effect of CF on reversing MDR in MDR-positive cells (Figure 7(a), lane 1). MDR1/P-gp was significantly increased with exposure to Adriamycin (Figure 7(a), lane 2). This increased level of MDR1/P-gp with exposure to Adriamycin was found to be reversed to normal levels by treatment with various concentrations of CF (Figure 7(a), lanes 3, 4, and 5), and the P-gp levels were significantly decreased in groups pretreated with Adriamycin and CF at various concentrations compared with the group only treated with Adriamycin ($P < 0.01$, Figure 7(b)). CF seemed to be more potent in the inhibition of P-gp expression than the positive control EA.

4. Discussion

Conventional cancer chemotherapy is seriously limited by MDR commonly exhibited by tumour cells. MDR has been recognised as an important type of resistance that can be due to various mechanisms. These various mechanisms might explain why treatment regimens that combine multiple agents with different targets are less effective than expected [11, 27, 28].

Of these mechanisms, one of the most frequently encountered mechanisms for the acquisition of MDR by tumour cells is the induction and activation of efflux transporter proteins. P-gp is commonly accepted as one of the best characterized transporters responsible for the multidrug resistance phenotype exhibited by cancer cells. Most of the researchers

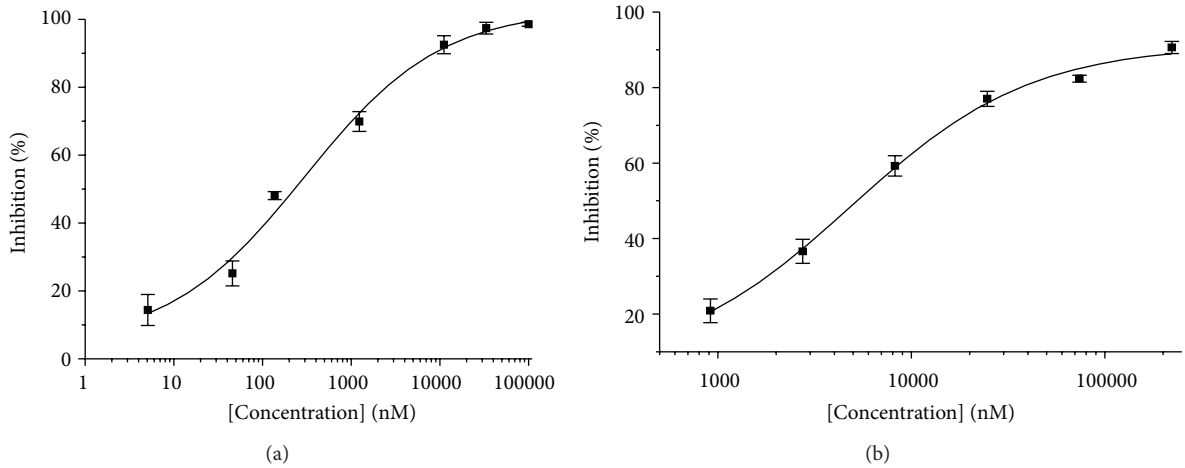

Figure 2: After incubation of GST and CF at 37°C for 30 min with 5 mM GSH and 0.1 mM CDNB, the rate of product formation was monitored by measuring the change in absorbance at 340 nm. The 50% inhibitory concentrations (IC_{50}) were (a) CF, 0.30 μM and (b) EA, 4.89 μM, as a positive control.

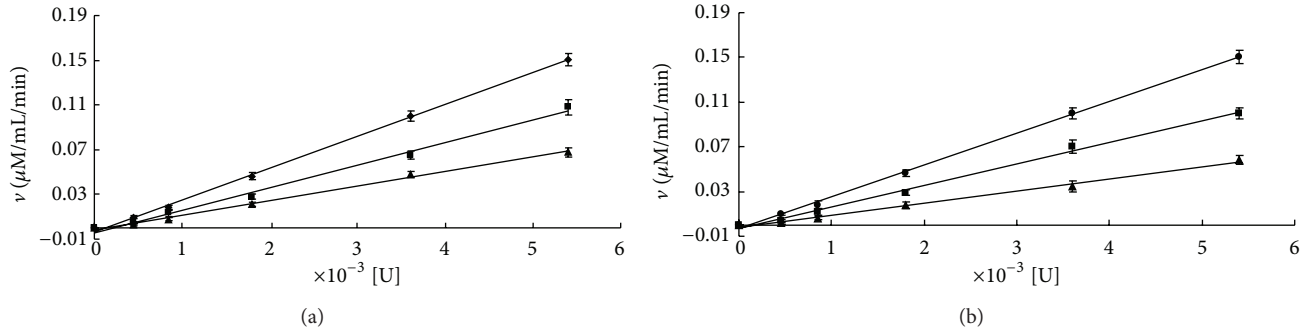

Figure 3: Kinetics plot of CF and EA to GST. The reaction was carried out at 37°C for 5 min after preincubating GST with CF for 5 min. A plot of v (μM/mL/min) versus [E] was obtained for GST concentrations from 0.0075 to 0.18 U/mL. Kinetics plots of inhibition to GST at 0%, 20%, and 50% IC for (a) CF (0 μM, 0.25 μM, and 0.5 μM) and (b) EA (0 μM, 2 μM, and 5 μM). Each point shows the mean ± SD of triplicate experiments.

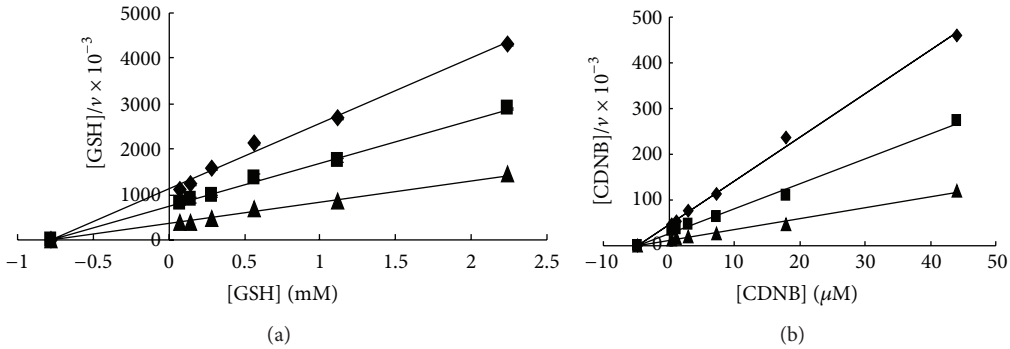

Figure 4: (a) A Hanes plot of v versus [S] for GSH. The reaction was carried out at 37°C for 5 min after preincubating GST with CF for 5 min. A Hanes plot of v versus [S] was created for GSH concentrations from 0.07 to 2.24 mM. (b) A Hanes plot of v versus [S] was created for CDNB concentrations from 0.5 to 44.1 μM. The CF concentrations were 0 μM, 0.25 μM, and 0.5 μM.

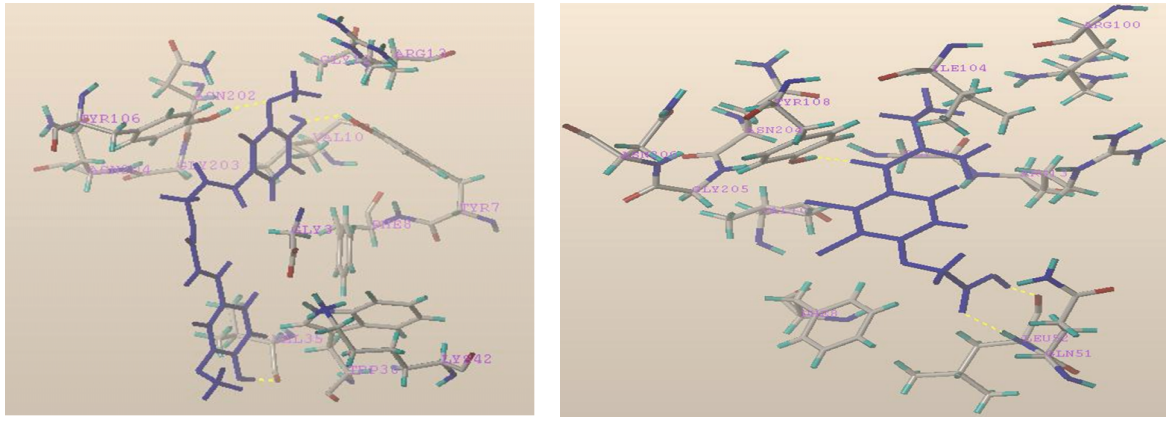

(a) (b)

Figure 5: Computational docking with PDB file 2GSS as a reference structure. (a) CF hydroxyl oxygen atoms in a phenyl ring formed a hydrogen bond with active site amino acid TYR7. Methoxy oxygen atoms in the same phenyl ring formed a hydrogen bond with active site amino acid TYR106. Hydroxyl hydrogen atoms in another phenyl ring formed a hydrogen bond with the carbonyl oxygen atom of VAL35 in the active site. The conformation score was −11.0. (b) Ethacrynic acid's carbonyl oxygen atom forms a hydrogen bond with active site amino acid TYR108. The carboxyl oxygen atom forms a hydrogen bond with active site amino acid LEU52, and the hydroxyl oxygen atom forms a hydrogen bond with active site amino acid GLN51. The conformation score is −13.3.

Table 1: The inhibitory effect of CF and positive control EA on the proliferation of B-MD-C1 and multidrug-resistant B-MD-C1 (ADR+/+) cells ($\overline{X} \pm$ SD, $n = 3$, 48 h).

CF (μM)	Inhibitory rate (%)		EA (μM)	Inhibitory rate (%)	
	B-MD-C1	B-MD-C1 (ADR +/+)		B-MD-C1	B-MD-C1 (ADR+/+)
3000	27.39 ± 4.70	22.67 ± 7.49	200	99.29 ± 5.68	99.89 ± 7.76
1000	18.62 ± 2.87	10.72 ± 3.21	100	99.52 ± 7.49	94.68 ± 10.23
333.33	5.07 ± 0.20	6.33 ± 0.35	80	78.72 ± 4.53	85.56 ± 5.62
111.11	5.30 ± 1.45	5.42 ± 2.20	60	53.30 ± 6.40	45.61 ± 4.43
37.04	2.56 ± 0.51	3.86 ± 0.49	40	6.56 ± 0.89	5.09 ± 1.35
12.35	1.36 ± 0.41	2.56 ± 0.27	20	4.01 ± 1.18	2.14 ± 1.28
4.12	1.02 ± 0.35	2.11 ± 0.45	10	3.02 ± 0.86	1.34 ± 0.57

Table 2: Flow cytometry data for the effect of CF on apoptosis of B-MD-C1 (ADR+/+) cells ($\overline{X} \pm$ SD, $n = 3$).

Treatment	G1%	S%	Apoptosis (%)
Control	57.30 ± 7.26	41.87 ± 7.39	4.82 ± 1.38
EA, 40 μM	76.63 ± 4.23*	6.07 ± 3.86*	16.83 ± 4.69*
CF, 5 μM	78.77 ± 3.48*	0*	17.13 ± 3.52*
10 μM	80.43 ± 5.00*	0*	21.73 ± 3.36*
20 μM	81.20 ± 5.15*	0*	39.40 ± 5.20*

Values are presented as the mean ± SD ($n = 3$). *$P < 0.01$ versus control.

pay more attention to find molecules that can directly block the activity of P-gp, which is a common step and a well-accepted strategy to reverse MDR phenotype [29]. However, the characteristic structures of the P-gp, such as multiple active binding sites, too large protein molecule (consists of 12 transmembrane domains, and two cytoplasmic ATP-binding domains), make it so difficult to evaluate activity in vitro and find more effective single-target candidate compound. And as an important transporter protein, it is believed that P-gp may play a significant role in the processes of drug absorption, distribution, metabolism, and excretion and may protect the healthy human body against toxic xenobiotics by excreting these compounds into the bile, urine, and the intestinal lumen and by preventing their accumulation in the brain. P-gp is also closely related with the drug-metabolizing enzymes, such as CYP 3A4 [30]. So developing drug candidate which is a possible strong P-gp modulator may most likely cause the potential side effects [28].

Cancer cells can also acquire resistance by overexpressing GSTs that may increase detoxification and circumvent the cytotoxic action of antitumour drugs. In particular, a number of chemotherapy agents currently used in cancer therapy are known to be substrates of GSTs [31], and it has been clearly shown that overexpression of GSTs in tumours is closely linked to the development and expression of MDR [4]. The GST superfamily, particularly the P1-class GST (GSTP1-1), is frequently overexpressed in various human cancers. GST is obviously a key resistance factor for anticancer drugs and has become the focus of extensive pharmaceutical research in an attempt to generate more efficient anticancer

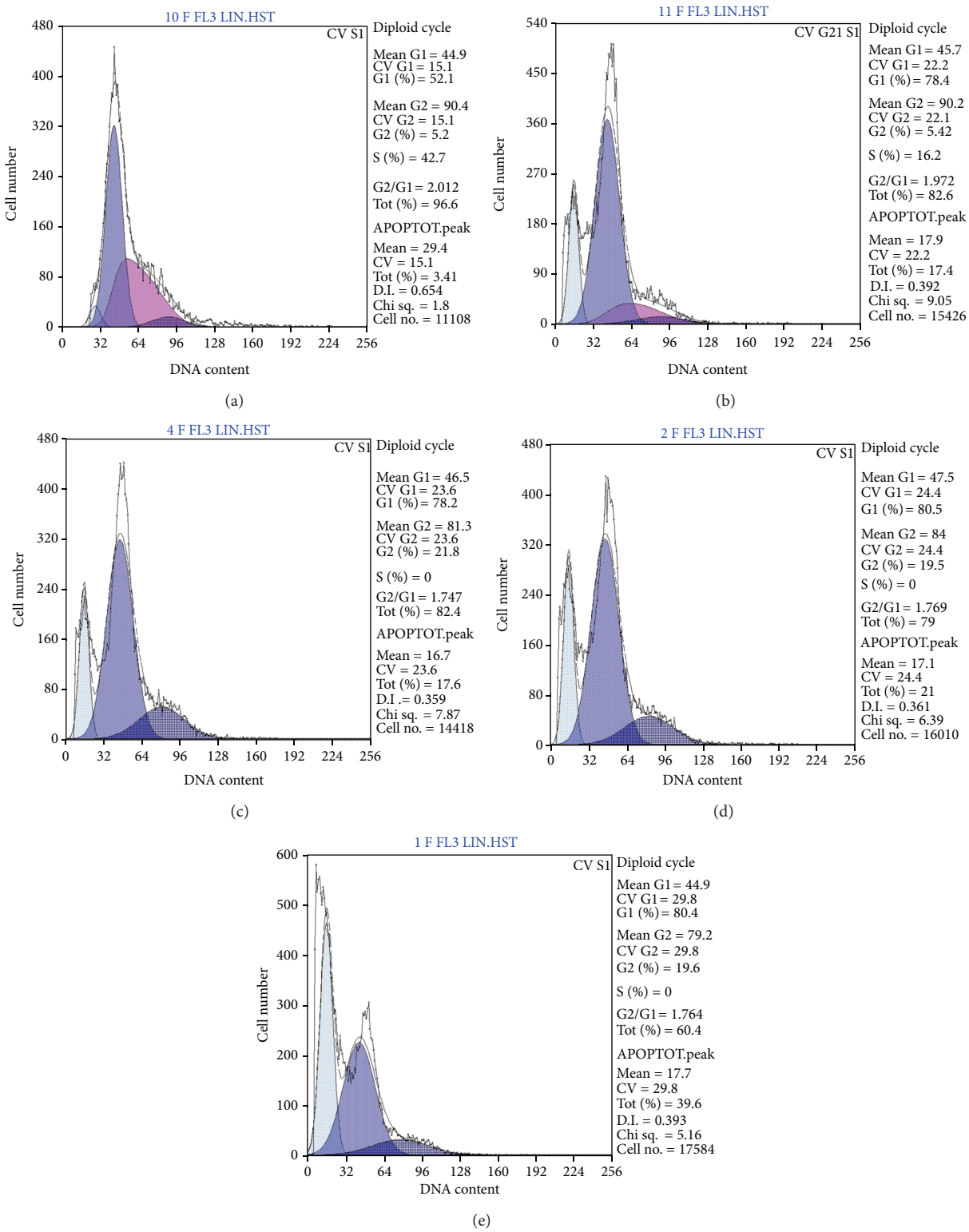

Figure 6: Flow cytometry results for the effect of CF on apoptosis of B-MD-C1 (ADR+/+) cells induced by Adriamycin. (a) Control; (b) EA concentration of 40 μM; CF concentrations of (c) 5 μM, (d) 10 μM, and (e) 20 μM.

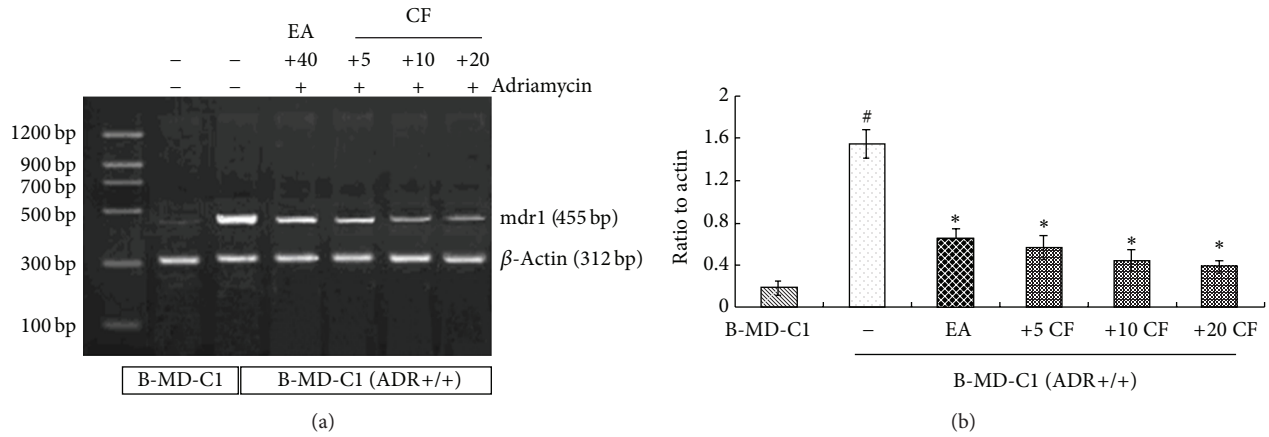

Figure 7: Effect of CF on MDR1 expression in B-MD-C1 (ADR+/+) cells. Cells were incubated with various concentrations of CF (5 μM, 10 μM, and 20 μM) or Adriamycin (5 μg/mL) for 48 h. EA (40 μM) as positive control. MDR1 bands were noted in (a). Densitometric analysis is shown in (b). $^{\#}P < 0.01$ B-MD-C1 versus B-MD-C1 (ADR+/+), $^{*}P < 0.01$ compound (+)/Adriamycin (+) versus compound (−)/Adriamycin (+) group. All the data shown are representative of three independent experiments.

agents [32]. Therefore, GST is a valuable target for the development of inhibitors that could be used to increase chemotherapeutic efficiency and to address MDR. Moreover, accumulating studies suggest that MDR is closely correlated with the combination action of the high level of GSTs and overexpression of P-gp and the increased GST activity could influence the expression of P-gp via several signal pathways. GSTP1-1 activity and P-gp levels were often found higher in the chemotherapy-resistant cancer cell lines, such as the B-MD-C1 cell line treated with Adriamycin compared to the sensitive cells. Exposure to Adriamycin rapidly increased GST activity and P-gp expression in the resistant cells [33, 34]. So it could be a better way to find new MDR reversal agents by screening for inhibitors of GST, which can indirectly regulate P-gp, rather than having a direct effect on the P-gp.

Natural products should be a noteworthy resource for the generation of potential MDR reversal agents that have higher levels of inhibition of GST. However, the GST inhibitors from natural sources have not been well studied, only a few natural components have been examined in clinical trials, and their efficacy has been less than expected. There is our interest in finding the strong GST inhibitors from natural products and then observing the effect of the active compound on reversing MDR. RAS, known as Chinese Angelica, is the root of *Angelica sinensis* (Oliv.) Diels, which has been used in traditional Chinese medicine (TCM) for more than 2000 years [35]. It has been mostly used as one of the herbal ingredients in prescriptions of TCM to treat gynaecological diseases. However, more and more studies show that RAS has a variety of pharmacological activities, including antitumour activity [36, 37].

Two ligustilide compounds isolated from RAS have been reported to be the inhibitors of GST in a previous study from our laboratory [26]. In this study, another compound, CF, also isolated from RAS, showed a stronger GST inhibitory effect than the positive control EA. EA is one of the first generation GST inhibitors that was utilised as a classical MDR reversal agent, and it inhibits GST-Alpha, -Mu, and -Pi by binding directly to the substrate binding site of these isozymes. In addition, EA inhibits GST by depleting its cofactor, GSH, via conjugation of the Michael addition intermediate to the thiol group of GSH [15, 38, 39]. An enzyme inhibitory kinetic analysis was conducted in some detail to clarify the mechanism of inhibition of GST by CF. The results gave the hint that the inhibitory binding site of CF might not be the catalytic sites. CF did not compete with GSH for the GSH-binding site (G-site) nor did it compete with CDNB for the CDNB-binding site (H-site). These effects suggested that CF induced conformational changes and hence made enzyme inactivation. The kinetic characteristics showed a valuable property of CF.

This study also investigated the structure-activity relationship and the molecule's binding mode to understand the pharmacologic action of this compound. Docking is one of the most commonly used techniques in drug design. It is used for both identifying correct poses of a ligand in the binding site of a protein as well as for the estimation of the interactions between potential drugs and the target proteins. In this work, a docking analysis using FlexX, combined with the HTS of human GST inhibitors, was employed to identify the effect of the inhibitor on the structure-activity relationship. It was found that CF could be fully docked into the gorge of GSTP1-1 and that hydrogen bond interactions could be an important factor to the binding affinity of CF in the active cavity. In addition, these interactions might be important for the inhibition of GST through a conformation change.

Moreover, in order to clarify whether CF itself could make the influence on the growth of the test tumour cells, the cytotoxicity assays were performed on the MDR phenotype B-MD-C1 (ADR+/+) and wild-type B-MD-C1 cell lines. The results showed much less cytotoxicity with CF treatment alone compared to EA alone. Based on the high GST inhibitory activity and the low cytotoxicity, the further apoptosis analysis by flow cytometry and RT-PCR analysis of MDR1 gene expression had been implemented to evaluate the MDR reversal effect of CF. The B-MD-C1 (ADR+/+) cells

presented the typical acquired Adriamycin resistance with the features of high activity of GST and overexpression of P-gp. The flow cytometry data demonstrated a strong apoptogenic activity when the cells were treated with a certain concentration of Adriamycin and CF together. CF, in a concentration-dependent manner, significantly induced apoptosis in the B-MD-C1 (ADR+/+) cells and altered the phase distribution of cell cycle. RT-PCR analysis showed that the overexpression of P-gp when the cells exposed to Adriamycin was markedly decreased by CF. CF might inhibit the P-gp expression and thus increase the intracellular Adriamycin accumulation. It was of interest that CF seemed to show much stronger effect of Adriamycin resistance reversal than the positive control EA in our study.

5. Conclusions

In conclusion, we demonstrated the strong GST inhibitory activity and the action mechanism of CF, the component from the Chinese medicine RAS. These studies add powerful novel evidence that RAS was a potential source to provide an effective MDR reversal agent for cancer. The compound CF could also be used as a promising lead compound for chemosensitization that was able to indirectly regulate P-gp expression via modulation of GST activity with the possible lower adverse effect and warrants further investigation in antitumour adjuvant therapy.

Conflict of Interests

The authors declare that they have no conflict of interests.

Authors' Contribution

Chang Chen and Chuanhong Wu contributed equally to this work.

Acknowledgments

This work was supported by grants from the National Natural Science Foundation of China (no. 30901976 and no. 81274133) and the Major Scientific and Technological Special Project for "Significant New Drugs Creation" (no. 2012ZX09103201-055).

References

[1] M. Sun, X. Xu, Q. Lu, Q. Pan, and X. Hu, "Schisandrin B: a dual inhibitor of P-glycoprotein and multidrug resistance-associated protein 1," *Cancer Letters*, vol. 246, no. 1-2, pp. 300–307, 2007.

[2] W.-F. Fong, C. Wang, G.-Y. Zhu, C.-H. Leung, M.-S. Yang, and H.-Y. Cheung, "Reversal of multidrug resistance in cancer cells by Rhizoma Alismatis extract," *Phytomedicine*, vol. 14, no. 2-3, pp. 160–165, 2007.

[3] D. B. Longley and P. G. Johnston, "Molecular mechanisms of drug resistance," *Journal of Pathology*, vol. 205, no. 2, pp. 275–292, 2005.

[4] D. M. Townsend and K. D. Tew, "The role of glutathione-S-transferase in anti-cancer drug resistance," *Oncogene*, vol. 22, no. 47, pp. 7369–7375, 2003.

[5] M. J. Ruiz-Gómez, A. Souviron, M. Martínez-Morillo, and L. Gil, "P-glycoprotein, glutathione and glutathione S-transferase increase in a colon carcinoma cell line by colchicine," *Journal of Physiology and Biochemistry*, vol. 56, no. 4, pp. 307–312, 2000.

[6] C. J. Henderson, K. J. Ritchie, A. McLaren, P. Chakravarty, and C. R. Wolf, "Increased skin papilloma formation in mice lacking glutathione transferase GSTP," *Cancer Research*, vol. 71, no. 22, pp. 7048–7060, 2011.

[7] M. Schultz, S. Dutta, and K. D. Tew, "Inhibitors of glutathione S-transferases as therapeutic agents," *Advanced Drug Delivery Reviews*, vol. 26, no. 2-3, pp. 91–104, 1997.

[8] G. Zhao, T. Yu, R. Wang, X. Wang, and Y. Jing, "Synthesis and structure-activity relationship of ethacrynic acid analogues on glutathione-s-transferase P1-1 activity inhibition," *Bioorganic and Medicinal Chemistry*, vol. 13, no. 12, pp. 4056–4062, 2005.

[9] K. D. Tew, A. Monks, L. Barone et al., "Glutathione-associated enzymes in the human cell lines of the National Cancer Institute Drug Screening Program," *Molecular Pharmacology*, vol. 50, no. 1, pp. 149–159, 1996.

[10] M. Volm, M. Kastel, J. Mattern, and T. Efferth, "Expression of resistance factors (P-glycoprotein, glutathione S-transferase-π, and topoisomerase II) and their interrelationship to proto-oncogene products in renal cell carcinomas," *Cancer*, vol. 71, no. 12, pp. 3981–3987, 1993.

[11] R. Pérez-Tomás, "Multidrug resistance: retrospect and prospects in anti-cancer drug treatment," *Current Medicinal Chemistry*, vol. 13, no. 16, pp. 1859–1876, 2006.

[12] D. Xu, Q. Lu, and X. Hu, "Down-regulation of P-glycoprotein expression in MDR breast cancer cell MCF-7/ADR by honokiol," *Cancer Letters*, vol. 243, no. 2, pp. 274–280, 2006.

[13] I. Utz, V. Gekeler, W. Ise et al., "Protein kinase C isoenzymes, p53, accumulation of rhodamine 123, glutathione-S-transferase, topoisomerase II and MRP in multidrug resistant cell lines," *Anticancer Research*, vol. 16, no. 1, pp. 289–296, 1996.

[14] V. Adler, Z. Yin, S. Y. Fuchs et al., "Regulation of JNK signaling by GSTp," *EMBO Journal*, vol. 18, no. 5, pp. 1321–1334, 1999.

[15] A. Sau, F. Pellizzari Tregno, F. Valentino, G. Federici, and A. M. Caccuri, "Glutathione transferases and development of new principles to overcome drug resistance," *Archives of Biochemistry and Biophysics*, vol. 500, no. 2, pp. 116–122, 2010.

[16] G. Zhao, T. Yu, R. Wang, X. Wang, and Y. Jing, "Synthesis and structure-activity relationship of ethacrynic acid analogues on glutathione-s-transferase P1-1 activity inhibition," *Bioorganic and Medicinal Chemistry*, vol. 13, no. 12, pp. 4056–4062, 2005.

[17] A. Hall, C. N. Robson, I. D. Hickson, A. L. Harris, S. J. Proctor, and A. R. Cattan, "Possible role of inhibition of glutathione S-transferase in the partial reversal of chlorambucil resistance by indomethacin in a Chinese hamster ovary cell line," *Cancer Research*, vol. 49, no. 22, pp. 6265–6268, 1989.

[18] J. M. Ford, W. N. Hait, S. A. Matlin, and C. C. Benz, "Modulation of resistance to alkylating agents in cancer cell by gossypol enantiomers," *Cancer Letters*, vol. 56, no. 1, pp. 85–94, 1991.

[19] H. Lage, "An overview of cancer multidrug resistance: a still unsolved problem," *Cellular and Molecular Life Sciences*, vol. 65, no. 20, pp. 3145–3167, 2008.

[20] S. Mukanganyama, M. Widersten, Y. S. Naik, B. Mannervik, and J. A. Hasler, "Inhibition of glutathione S-transferases by antimalarial drugs possible implications for circumventing anticancer drug resistance," *International Journal of Cancer*, vol. 97, no. 5, pp. 700–705, 2002.

[21] M. A. Gyamfi, I. I. Ohtani, E. Shinno, and Y. Aniya, "Inhibition of glutathione S-transferases by thonningianin A, isolated from the African medicinal herb, *Thonningia sanguinea*, in vitro," *Food and Chemical Toxicology*, vol. 42, no. 9, pp. 1401–1408, 2004.

[22] J. J. Van Zanden, O. B. Hamman, M. L. P. S. Van Iersel et al., "Inhibition of human glutathione S-transferase P1-1 by the flavonoid quercetin," *Chemico-Biological Interactions*, vol. 145, no. 2, pp. 139–148, 2003.

[23] A. Duvoix, F. Morceau, S. Delhalle et al., "Induction of apoptosis by curcumin: mediation by glutathione S-transferase P1-1 inhibition," *Biochemical Pharmacology*, vol. 66, no. 8, pp. 1475–1483, 2003.

[24] M. Das, S. V. Singh, H. Mukhtar, and Y. C. Awasthi, "Differential inhibition of rat and human glutathione S-transferase isoenzymes by plant phenols," *Biochemical and Biophysical Research Communications*, vol. 141, no. 3, pp. 1170–1176, 1986.

[25] M. A. Metwally, R. M. King, and H. Robinson, "An acetylenic epoxide and a ferulate from Coreopsis longula," *Phytochemistry*, vol. 24, no. 1, pp. 182–183, 1985.

[26] F. Huang, S. Li, X. Lu, A. Liu, G. Du, and G. Shi, "Two glutathione S-transferase inhibitors from Radix *Angelicae sinensis*," *Phytotherapy Research*, vol. 25, no. 2, pp. 284–289, 2011.

[27] X.-H. Wang, D.-Z. Jia, Y.-J. Liang et al., "Lgf-YL-9 induces apoptosis in human epidermoid carcinoma KB cells and multidrug resistant KBv200 cells via reactive oxygen species-independent mitochondrial pathway," *Cancer Letters*, vol. 249, no. 2, pp. 256–270, 2007.

[28] G. Szakács, J. K. Paterson, J. A. Ludwig, C. Booth-Genthe, and M. M. Gottesman, "Targeting multidrug resistance in cancer," *Nature Reviews Drug Discovery*, vol. 5, no. 3, pp. 219–234, 2006.

[29] G. Lehne, "P-glycoprotein as a drug target in the treatment of multidrug resistant cancer," *Current Drug Targets*, vol. 1, no. 1, pp. 85–99, 2000.

[30] A. Palmeira, F. Rodrigues, E. Sousa, M. Pinto, M. H. Vasconcelos, and M. X. Fernandes, "New uses for old drugs: pharmacophore-based screening for the discovery of P-glycoprotein inhibitors," *Chemical Biology and Drug Design*, vol. 78, no. 1, pp. 57–72, 2011.

[31] H. A. A. M. Dirven, B. Van Ommen, and P. J. Van Bladeren, "Glutathione conjugation of alkylating cytostatic drugs with a nitrogen mustard group and the role of glutathione S-transferases," *Chemical Research in Toxicology*, vol. 9, no. 2, pp. 351–360, 1996.

[32] T. Nakajima, T. Takayama, K. Miyanishi et al., "Reversal of multiple drug resistance in cholangiocarcinoma by the glutathione S-transferase-π-specific inhibitor O1-hexadecyl-γ-glutamyl-S-benzylcysteinyl-D-phenylglycine ethylester," *Journal of Pharmacology and Experimental Therapeutics*, vol. 306, no. 3, pp. 861–869, 2003.

[33] M. Volm, M. Kastel, J. Mattern, and T. Efferth, "Expression of resistance factors (P-glycoprotein, glutathione S-transferase-π, and topoisomerase II) and their interrelationship to proto-oncogene products in renal cell carcinomas," *Cancer*, vol. 71, no. 12, pp. 3981–3987, 1993.

[34] J. Liu, H. Chen, D. S. Miller et al., "Overexpression of glutathione S-transferase II and multidrug resistance transport proteins is associated with acquired tolerance to inorganic arsenic," *Molecular Pharmacology*, vol. 60, no. 2, pp. 302–309, 2001.

[35] G.-H. Lu, K. Chan, Y.-Z. Liang et al., "Development of high-performance liquid chromatographic fingerprints for distinguishing Chinese Angelica from related umbelliferae herbs," *Journal of Chromatography A*, vol. 1073, no. 1-2, pp. 383–392, 2005.

[36] C.-C. Hsieh, W.-C. Lin, M.-R. Lee et al., "Dang-Gui-Bu-Xai-Tang modulated the immunity of tumor bearing mice," *Immunopharmacology and Immunotoxicology*, vol. 25, no. 2, pp. 259–271, 2003.

[37] C. C. Quan, J. Lee, W. Jin et al., "Cytotoxic constituents from *Angelicae sinensis* Radix," *Archives of Pharmacal Research*, vol. 30, no. 5, pp. 565–569, 2007.

[38] T. P. Mulder, W. H. Peters, T. Wobbes, B. J. Witteman, and J. B. Jansen, "Measurement of glutathione S-transferase P1-1 in plasma: pitfalls and significance of screening and follow-up of patients with gastrointestinal carcinoma," *Cancer*, vol. 80, no. 5, pp. 873–880, 1997.

[39] A. J. Oakley, M. Lo Bello, A. P. Mazzetti, G. Federici, and M. W. Parker, "The glutathione conjugate of ethacrynic acid can bind to human pi class glutathione transferase P1-1 in two different modes," *FEBS Letters*, vol. 419, no. 1, pp. 32–36, 1997.

Hindawi Publishing Corporation
Evidence-Based Complementary and Alternative Medicine
Volume 2013, Article ID 423164, 10 pages
http://dx.doi.org/10.1155/2013/423164

Research Article

Berberine Reduces the Metastasis of Chondrosarcoma by Modulating the $\alpha v\beta 3$ Integrin and the PKCδ, c-Src, and AP-1 Signaling Pathways

Chi-Ming Wu,[1] Te-Mao Li,[1] Tzu-Wei Tan,[2,3] Yi-Chin Fong,[1,4] and Chih-Hsin Tang[2,3,5]

[1] *School of Chinese Medicine, China Medical University, Taichung 404, Taiwan*
[2] *Graduate Institute of Basic Medical Science, China Medical University, No. 91, Hsueh-Shih Road, Taichung 404, Taiwan*
[3] *Department of Pharmacology, School of Medicine, China Medical University, Taichung 404, Taiwan*
[4] *Department of Orthopaedics, China Medical University Hospital, Taichung 404, Taiwan*
[5] *Department of Biotechnology, College of Health Science, Asia University, Taichung 413, Taiwan*

Correspondence should be addressed to Chih-Hsin Tang; chtang@mail.cmu.edu.tw

Received 4 June 2013; Accepted 16 July 2013

Academic Editor: Shun-Fa Yang

Chondrosarcoma is a primary malignant bone cancer, with a potent capacity to invade locally and cause distant metastasis, especially to the lungs. Patients diagnosed with chondrosarcoma have poor prognosis. Berberine, an active component of the Ranunculaceae and Papaveraceae families of plant, has been proven to induce tumor apoptosis and to prevent the metastasis of cancer cells. However, the effects of berberine in human chondrosarcoma are largely unknown. In this study, we found that berberine did not induce cell apoptosis in human primary chondrocytes and chondrosarcoma cells. However, at noncytotoxic concentrations, berberine reduced the migration and invasion of chondrosarcoma cancer cells. Integrins are the major adhesive molecules in mammalian cells and have been associated with the metastasis of cancer cells. We also found that incubation of chondrosarcoma cells with berberine reduced mRNA transcription for, and cell surface expression of, the $\alpha v\beta 3$ integrin, with additional inhibitory effects on PKCδ, c-Src, and NF-κB activation. Thus, berberine may be a novel antimetastasis agent for the treatment of metastatic chondrosarcoma.

1. Introduction

Chondrosarcomas are a heterogeneous group of neoplasms that are characterized by the production of cartilage matrix by tumor cells. They are uncommon, malignant, and lethal primary bone tumors that may occur at any age between 10 and 80 years. Approximately two-thirds of the affected patients are males [1], and the tumor usually appears on the scapula, sternum, ribs, or pelvis [2]. Clinically, surgical resection remains the primary mode of therapy for chondrosarcoma. There is a high incidence of fatality associated with this mesenchymal malignancy due to the absence of an effective adjuvant therapy, and therefore, it is important to explore novel remedies [3].

Tumor invasion and metastasis are the main biological characteristics of cancer cells [4]. Mortality in cancer patients principally results from the metastatic spread of cancer cells to distant organs. Tumor metastasis is a highly complex, multistep process, which includes changes in cell-cell adhesion properties [4]. Because integrins expressed on the surface of a cell determine whether the cell can adhere to and survive in a particular microenvironment, the matching of integrins and ligands plays a key role in metastasis [5]. Integrins are a family of transmembrane glycoprotein adhesion receptors that play central roles in the biology of metazoans by controlling cell adhesion, migration, differentiation, and apoptosis. Integrins form heterodimers of α- and β-subunits [6]. There are at least 19 α-subunits and 8 β-subunits that can associate to form 25 unique integrin heterodimers [7, 8]. Integrins play an important role in many extracellular matrix (ECM) proteins such as collagens, fibronectin, laminin, osteopontin, and vitronectin [9]. In addition, they have been implicated in

the metastasis of chondrosarcomas and lung, breast, bladder, and colon cancers [10–13]. The $\alpha v\beta 3$ integrin, in particular, has been reported in chondrosarcoma progression, with effects on angiogenesis, survival, and invasion [14, 15]. *In vitro* studies have also found that the $\alpha v\beta 3$ integrin facilitated chondrosarcoma migration and invasion through several ECM substrates and transendothelial migration [16].

Berberine, an active component of the Ranunculaceae and Papaveraceae families of plant, is part of the well-studied group of naturally occurring isoquinoline alkaloids. It has been suggested that the beneficial properties of berberine may also have an effect on other diseases such as diabetes, hypertension, arrhythmia, and gastrointestinal diseases [17]. A recent study has shown its potential chemotherapeutic efficacy against cancers [18]. In addition, berberine has been reported to reduce the metastasis of human gastric cancer, prostate cancer, and breast cancer [19–21]. However, the effects of berberine in the metastasis of human chondrosarcoma cells are largely unknown. Here, we report that berberine inhibits the migration and invasion of human chondrosarcoma cells. In addition, the downregulation of the $\alpha v\beta 3$ integrin through protein kinase C (PKC)δ, c-Src, and AP-1 is involved in berberine-reduced cell motility. Therefore, our data provide evidence that berberine may be an antimetastatic agent for the treatment of metastasic chondrosarcoma.

2. Experimental Section

2.1. Materials. Protein A/G beads, rabbit polyclonal antibodies specific for p-c-Jun, and c-Jun were purchased from Santa Cruz Biotechnology (Santa Cruz, CA, USA). The pSV-β-galactosidase vector and luciferase assay kit were purchased from Promega (Madison, MA). All other chemicals were purchased from Sigma-Aldrich (St. Louis, MO, USA).

2.2. Cell Culture. The human chondrosarcoma cell line JJ012 was kindly provided by the laboratory of Dr. Sean P. Scully (University of Miami School of Medicine, Miami, FL, USA) [22]. Cells were cultured in Dulbecco's Modified Eagle's Medium (DMEM)/α-MEM supplemented with 10% fetal bovine serum (FBS). The human chondrosarcoma cell line SW1353 was obtained from the American Type Culture Collection. These cells were cultured in DMEM supplemented with 10% FBS. All cells were maintained at 37°C in a humidified atmosphere of 5% CO_2.

To establish primary cultures, chondrocytes were isolated from articular cartilage, as previously described [23]. The cells were grown in plastic cell culture dishes in 95% air-5% CO_2, in DMEM supplied with 20 mM HEPES, 10% heat-inactivated FBS, 2 mM-glutamine, 100 U/mL penicillin, and 100 μg/mL streptomycin.

2.3. MTT Assay. Cell viability was determined with a 3-(4,5-dimethylthiazol-2-yl)-2,5-diphenyltetrazolium bromide (MTT) assay. After being treated with berberine for 24 or 48 h, the cultures were washed with phosphate-buffered saline (PBS). Then, MTT (0.5 mg/mL) was added to each well, and the mixture was incubated at 37°C for 2 h. To dissolve formazan crystals, the culture medium was replaced with an equal volume of DMSO. After the mixture was shaken at room temperature for 10 min, the absorbance of each well was determined at 550 nm by using a microplate reader (Bio-Tek, Winooski, VT, USA).

2.4. TUNEL Assay. Cell apoptosis was examined through a terminal deoxynucleotidyl transferase-mediated deoxyuridine triphosphate nick-end labeling (TUNEL) assay performed using the BD ApoAlert DNA Fragmentation Assay Kit. Cells were incubated with berberine for 24 h, then trypsinized, fixed with 4% paraformaldehyde, and permeabilized with 0.1% Triton-X-100 in 0.1% sodium citrate. After being washed, the cells were incubated with the reaction mixture for 60 min at 37°C. The stained cells were then analyzed with a flow cytometer.

2.5. Caspase 3 Activity Assay. This assay is based on the ability of an active enzyme to cleave a chromophore from the enzyme substrate Ac-DEVD-pNA. Cell lysates were prepared and incubated with anti-caspase 3. Immunocomplexes were incubated with the peptide substrate in assay buffer (100 mM NaCl, 50 mM 4-(2-hydroxyethyl)-1-piperazine-ethanesulphonic acid [HEPES], 10 mM dithiothreitol, 1 mM EDTA, 10% glycerol, and 0.1% 3-[(3-cholamidopropyl) dimethylammonio]-1-propanesulfonate (CHAPS), pH 7.4) for 2 h at 37°C. The release of *p*-nitroaniline was monitored at 405 nm. The results are the percent change in activity compared to the untreated control.

2.6. Migration and Invasion Assay. The migration assay was performed using Transwell inserts (Costar, NY; 8 mm pore size) in 24-well dishes. For the invasion assay, filters were precoated with 30 μL Matrigel basement membrane matrix (BD Biosciences, Bedford, MA) for 30 min. The following procedures were the same for both migration and invasion assays. After treatment with berberine (0, 1, 3, 10, and 30 μM) for 24 h, cells were harvested and seeded to Transwell at 1×10^4 cells/well in serum-free medium, and then incubated for 24 h at 37°C in 5% CO_2. Cells were then fixed in 3.7% formaldehyde for 5 min and stained with 0.05% crystal violet in PBS for 15 min. Cells on the upper side of the filters were removed with cotton-tipped swabs, and the filters were washed with PBS. Cells on the underside of the filters were examined and counted under a microscope. Each experiment was performed in triplicate and repeated at least three times.

2.7. Wound-Healing Migration Assay. For the wound-healing migration assay, cells were seeded on 12-well plates at a density of 1×10^5 cells/well in culture medium. Twenty-four hours after seeding, the confluent monolayer of culture was scratched with a fine pipette tip, and migration was visualized by microscope. The rate of wound closure was observed at the indicated time.

2.8. Flow Cytometric Analysis. Human chondrosarcoma cells were grown in 6-well dishes, and then washed with PBS

and detached using trypsin at 37°C. Cells were fixed for 10 min in PBS containing 3.7% paraformaldehyde, rinsed in PBS and incubated with mouse anti-human $\alpha v\beta 3$ integrin (1 : 100) (BD Biosciences, CA, USA) for 1 h at 4°C. Cells were then washed in PBS, and incubated with fluorescein isothiocyanate-conjugated goat anti-mouse secondary IgG (1 : 100; Leinco Technologies, St Louis, MO) for 45 min at 4°C. After a final rinse, cells were analyzed using a FACSCalibur flow cytometer and CellQuest software (BD Biosciences, CA).

2.9. Western Blot Analysis. Cellular lysates were prepared, and proteins were resolved by SDS-PAGE [24, 25]. Proteins were then transferred to Immobilon polyvinylidene fluoride membranes. The blots were blocked with 4% bovine serum albumin for 1 h at room temperature and probed with rabbit anti-human antibodies against p-c-Jun or c-Jun (1 : 1000) for 1 h at room temperature (Santa Cruz, CA). After three washes, the blots were incubated with peroxidase-conjugated donkey anti-rabbit secondary antibody (1 : 1000) for 1 h at room temperature. The blots were visualized with enhanced chemiluminescence by using X-OMAT LS film (Eastman Kodak, Rochester, NY).

2.10. Kinase Activity Assay. PKCδ and c-Src activities were assessed with a PKC kinase activity assay kit (Assay Designs, Inc., Ann Arbor, MI) and a c-Src kinase activity assay kit (Abnova, Corp., Taipei, Taiwan). The kinase activity kits are based on a solid-phase ELISA that uses a specific synthetic peptide as substrate for PKCδ or c-Src, and a polyclonal antibody that recognizes the phosphorylated form of the substrate.

2.11. Quantitative Real-Time PCR. Total RNA was extracted from chondrosarcoma cells by using a TRIzol kit (MDBio, Taipei, Taiwan). Reverse transcription was performed using 1 μg of total RNA and an oligo(dT) primer [26]. Quantitative real-time PCR (qPCR) was carried out using a TaqMan One-step PCR Master Mix (Applied Biosystems, CA, USA). Total cDNA (100 ng) was added to each 25 μL reaction mixture with sequence-specific primers and TaqMan probes. All target gene primers and probes were purchased commercially, including those for GAPDH as an internal control (Applied Biosystems). qPCR was carried out in triplicate with a StepOnePlus (Applied Biosystems) sequence detection system. The cycling conditions were 10 min at 95°C, followed by 40 cycles of 95°C for 15 s, and 60°C for 60 s. To calculate the cycle number at which the transcript was detected (C_T), the threshold was set above the nontemplate control background and within the linear phase of target gene amplification.

2.12. Reporter Gene Assay. The chondrosarcoma cells were transfected with AP-1 reporter plasmid by using Lipofectamine 2000 according to the manufacturer's recommendations. Twenty-four hours after transfection, the cells were treated with inhibitors for 30 min. Next, berberine or vehicle was added for 24 h. Cell extracts were then prepared, and luciferase and β-galactosidase activities were measured.

2.13. Statistical Analysis. Data are presented as mean ± standard error of the mean (SEM). Statistical analysis of the two samples was performed using the Student's t-test. Statistical comparisons of more than two groups were performed using one-way analysis of variance with Bonferroni's post hoc test. In all cases, $P < 0.05$ was considered significant.

3. Results

3.1. Berberine Did Not Induce Cell Death in Primary Chondrocytes and Human Chondrosarcoma Cells. It has been reported that berberine increases death in human cancer cells [18]. We therefore investigated whether berberine induced cell death in human chondrosarcoma cells. The cytotoxic effect of berberine in chondrosarcoma cells was examined by MTT assay. Stimulation of chondrosarcoma cells (JJ012 and SW1353) for 24 or 48 h did not affect cell viability (Figures 1(a) and 1(b)). Furthermore, berberine also did not affect the cell viability of normal primary chondrocytes (Figure 1(c)). Next, we examined whether berberine induced cell apoptosis in human chondrosarcoma cells by TUNEL staining and caspase 3 activity assays. However, incubation of cells with berberine did not enhance TUNEL expression (Figures 1(d)–1(f)). Berberine also did not affect caspase 3 activity in normal chondrocyte or chondrosarcoma cell lines (Figures 1(g)–1(i)). These data indicate that berberine did not induce cell death in human primary chondrocytes and chondrosarcoma cells. Therefore, we used this berberine concentration range for all subsequent experiments

3.2. Berberine Reduces Cell Migration, Wound-Healing Migration, and Cell Invasion in Human Chondrosarcoma Cells. The role of berberine in reducing the metastasis of human cancers has been previously documented [19–21]. Therefore, we next checked whether berberine inhibits cell motility in chondrosarcoma cancer cells. The results from the Transwell migration assay showed that incubation of chondrosarcoma cells with berberine (1–30 μM) dramatically decreased migration in both chondrosarcoma cell lines (Figures 2(a) and 2(b)). The wound-scratching assay also revealed that berberine reduced wound-healing activity in chondrosarcoma cells (Figures 2(c) and 2(d)). In addition, incubation of cells with berberine thwarted the ability of chondrosarcoma cells to invade through a Matrigel basement membrane matrix (Figures 2(e) and 2(f)). These results suggest that berberine suppresses cell migration and invasion in human chondrosarcoma cells.

3.3. Berberine Reduces Cell Motility in Chondrosarcoma Cells by Inhibiting the Expression of the $\alpha v\beta 3$ Integrin. Upregulation of the $\alpha v\beta 3$ integrin has been known to increase the metastasis of human chondrosarcomas [27]. We therefore hypothesized that the $\alpha v\beta 3$ integrin may be involved in berberine-mediated inhibition of migration in human chondrosarcoma cells. We found that incubation of chondrosarcoma cells with berberine reduced the mRNA expression of αv and β3 integrin in a concentration-dependent manner (Figures 3(a) and 3(b)). Similarly, stimulation of cells with

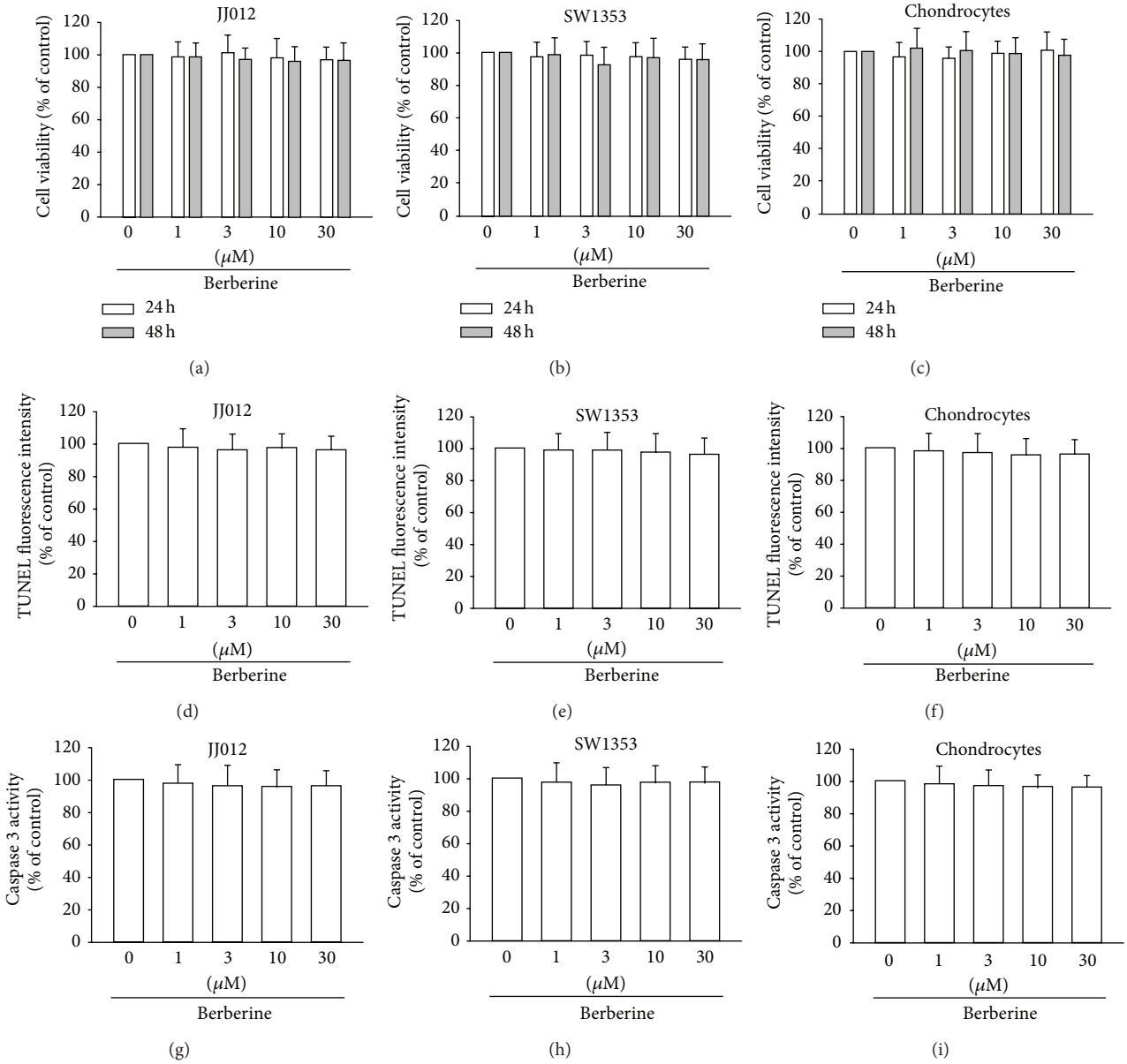

Figure 1: Berberine did not induce cell apoptosis in human chondrocytes and chondrosarcoma cells. ((a)–(c)) Cells were incubated with various concentrations of berberine for 24 or 48 h, and cell viability was examined by MTT assay. ((d)–(f)) Cells were incubated with berberine for 24 h; TUNEL-positive cells were examined by flow cytometry. ((g)–(i)) Cells were incubated with berberine for 24 h, and caspase 3 activity was examined using caspase 3 ELISA kit. Results are expressed as the mean ± S.E.M.*, $P < 0.05$ compared with control.

berberine inhibited the cell surface expression of the $\alpha v\beta 3$ integrin (Figures 3(c) and 3(d)). These data suggest that berberine reduces the metastasis of chondrosarcoma cells by inhibiting the expression of $\alpha v\beta 3$ integrin.

3.4. Berberine Reduces the Activity of the PKCδ and c-Src Signaling Pathways. PKCδ-dependent c-Src activation has been reported to mediate the metastasis of human oral cancer cells [28]. After the inhibitory effects of berberine on cell migration and integrin expression were revealed, the effects of berberine on the expression of the PKCδ and c-Src pathways were investigated. Stimulation of chondrosarcoma cells with berberine reduced PKCδ kinase activity in a concentration-dependent manner (Figures 4(a) and 4(b)). Furthermore, berberine also reduced c-Src kinase activity in chondrosarcoma cells (Figures 4(c) and 4(d)). Therefore, berberine appears to act through a signaling pathway involving PKCδ and c-Src to inhibit cell migration in human chondrosarcoma cells.

3.5. AP-1 Is Involved in Berberine-Mediated Metastasis in Chondrosarcoma Cells. AP-1 was found to be involved in the expression of the $\alpha v\beta 3$ integrin and the metastasis of chondrosarcoma [16]. So, the role of berberine of AP-1

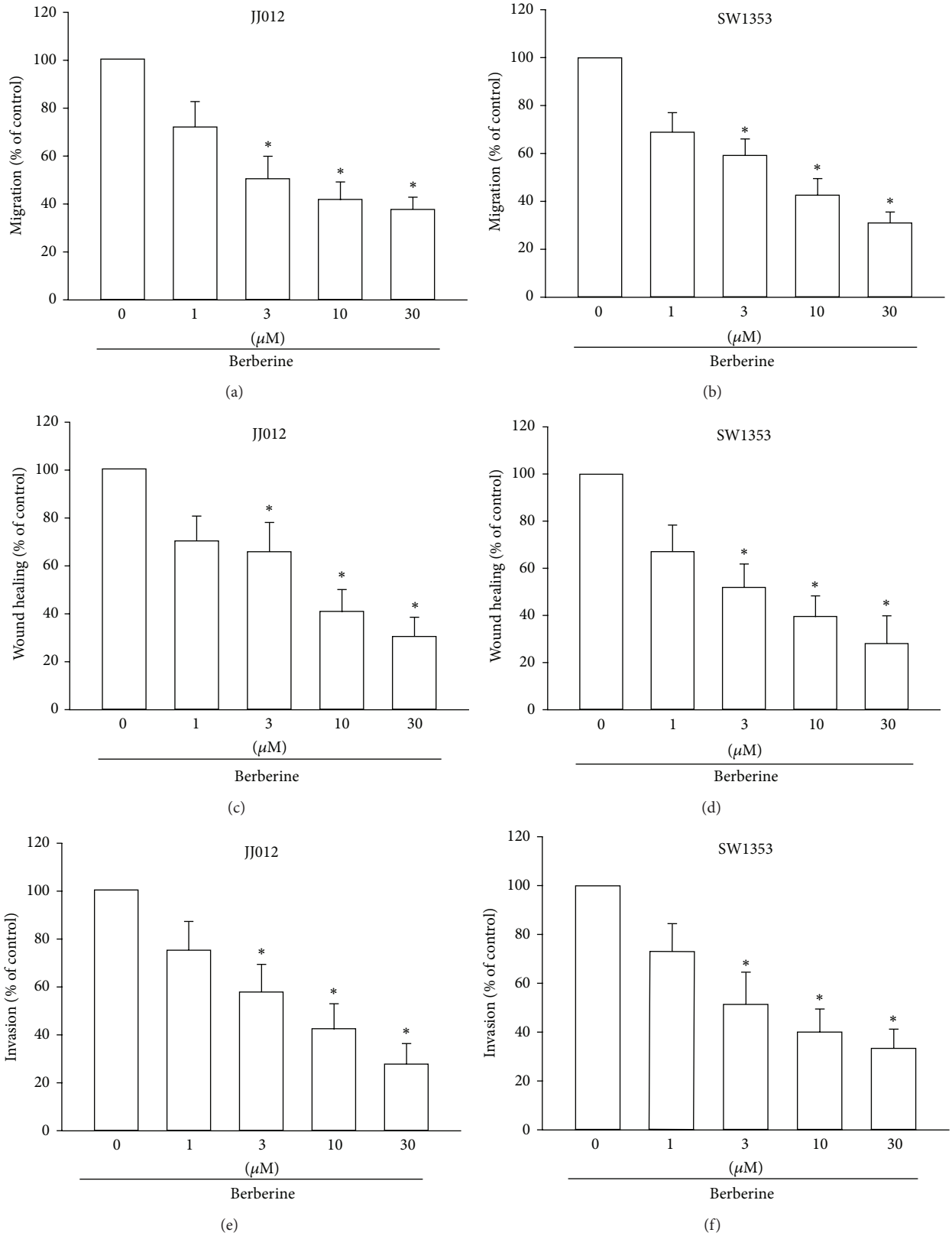

Figure 2: Berberine inhibits migration and invasion of human chondrosarcoma cells. ((a)–(f)) Cells were incubated with various concentrations of berberine for 24 h; cell migration and invasion were examined through Transwell, wound healing, and invasion assays. Results are expressed as the mean ± S.E.M.*, $P < 0.05$ compared with control.

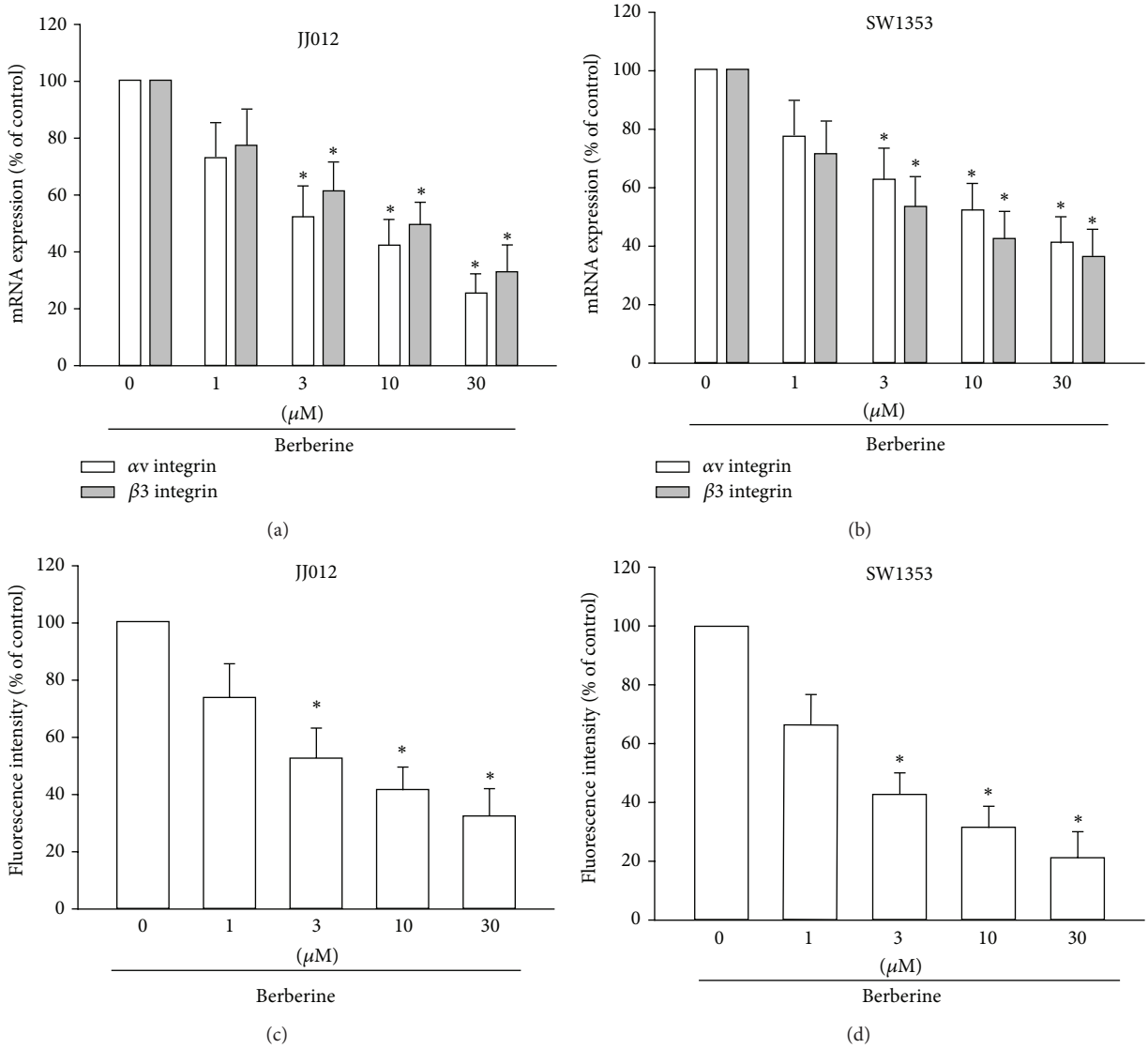

Figure 3: Berberine inhibits expression of the $\alpha v\beta 3$ integrin in chondrosarcoma cells. ((a)–(d)) Cells were incubated with various concentrations of berberine for 24 h; mRNA and cell surface expression of $\alpha v\beta 3$ integrin were examined by qPCR and flow cytometry. Results are expressed as the mean ± S.E.M.*, $P < 0.05$ compared with control.

activation in chondrosarcoma cells was examined. We found that stimulation of cells with berberine inhibited the phosphorylation of p-c-Jun (Figures 5(a) and 5(b)). AP-1 activation was further evaluated by analyzing AP-1 luciferase activity. Cells were transiently transfected with AP-1 luciferase as an indicator of AP-1 activation. We found that berberine reduced AP-1-luciferase activity (Figures 5(c) and 5(d)), implying that AP-1 is involved in berberine-reduced metastasis in chondrosarcoma cells.

4. Discussion

Chondrosarcoma is a rare but deadly form of bone cancer. It is the second most common type of bone cancer, accounting for nearly 26% of all bone cancers [29]. The metastatic potential of conventional chondrosarcomas correlates well with the histologic tumor grade because of the relatively indolent growth rates of many low- and moderate-grade chondrosarcomas; approximately 15% of all metastatic disease-related deaths occur more than 5 years after initial diagnosis [30]. Therefore, it is important to develop effective adjuvant therapy to prevent chondrosarcoma metastasis. Berberine has various biological applications for disease, with properties that are antidiabetes, antihypertension, antiarrhythmia, and antigastrointestinal disease [17]. Berberine also has been reported to diminish the metastatic potential of human cancer cells [31]. However, the antimetastasic effects of berberine on chondrosarcoma cells are mostly unknown. In the current study, we found that, at noncytotoxic concentrations (0–30 μM), berberine reduced cell motility in human chondrosarcoma cells. Furthermore, berberine did not increase cell death in primary chondrocytes. We found that

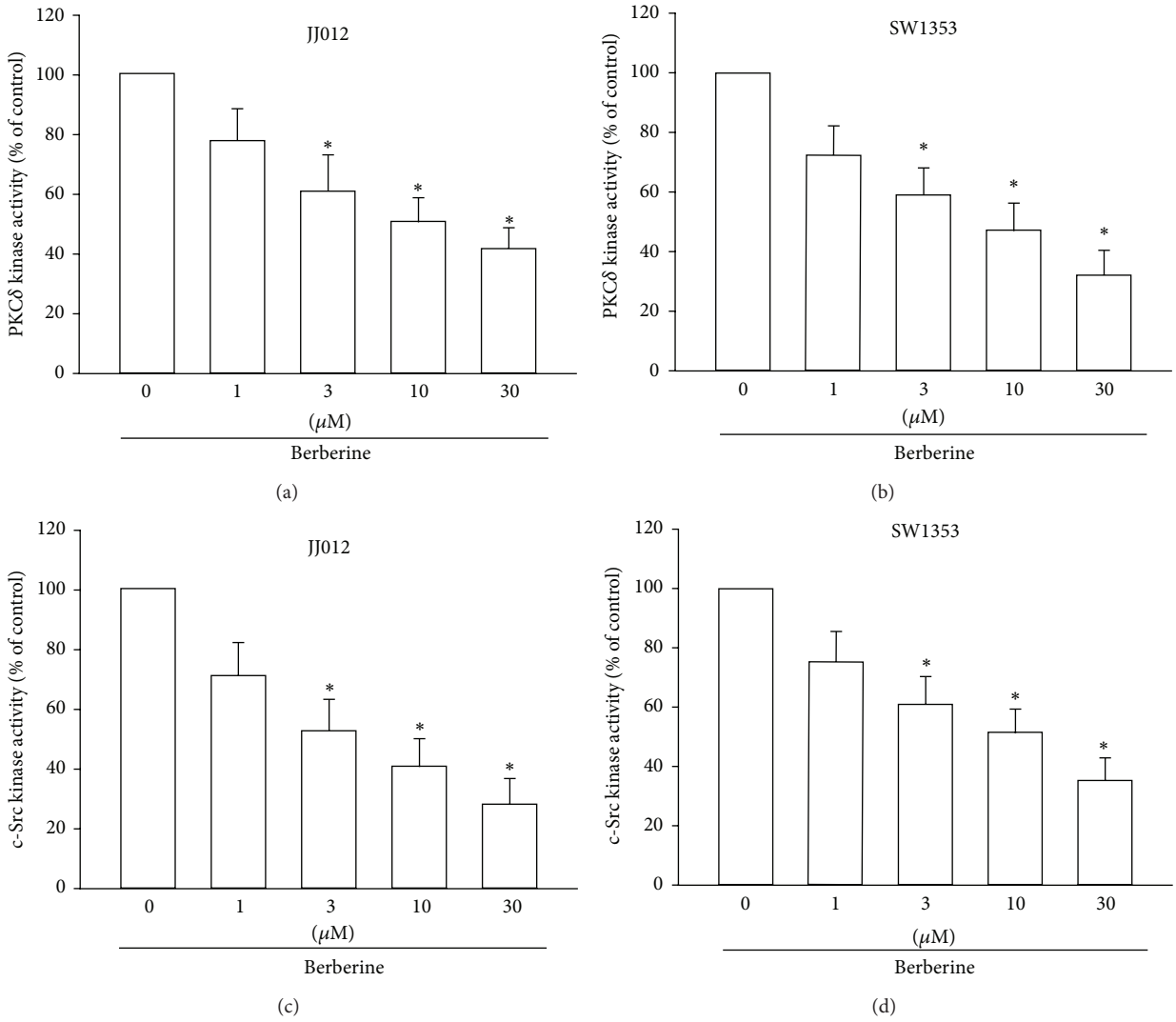

Figure 4: PKCδ and c-Src signaling pathways are involved in the berberine response of human chondrosarcoma cells. ((a) and (b)) Cells were incubated with various concentrations of berberine for 24 h; PKCδ kinase activity was examined by use of the PKCδ kinase activity kit. ((c) and (d)) Cells were incubated with various concentrations of berberine for 24 h; c-Src kinase activity was examined by use of the c-Src kinase activity kit. Results are expressed as the mean ± S.E.M.*, $P < 0.05$ compared with control.

the downregulation of the $\alpha v\beta 3$ integrin through the PKCδ, c-Src, and AP-1 pathways is involved in berberine-reduced cancer migration. In this study, we identified berberine as a potential lead base, with good pharmacological properties, on antimetastasic activity in human chondrosarcoma cells.

Integrins, which link the extracellular matrix to intracellular signaling molecules, regulate a number of cellular processes, including adhesion, signaling, motility, survival, gene expression, growth, and differentiation [32, 33]. Inhibition of $\alpha v\beta 3$ integrin by disintegrin or $\alpha v\beta 3$ integrin antibody reduced the metastasis of human cancer cells [34, 35]. Therefore, reducing the expression of $\alpha v\beta 3$ integrin is a good target for the treatment of the metastasis of human cancer cells. Here, we reported that berberine reduced the mRNA expression of αv and $\beta 3$ integrin. In addition, incubation of chondrosarcoma cells with berberine diminished the cell surface expression of $\alpha v\beta 3$ integrin. These results indicate that berberine reduces chondrosarcoma metastasis through the downregulation of $\alpha v\beta 3$ integrin expression.

PKC isoforms have been characterized at the molecular level and have been found to mediate several cellular molecular responses [36]. Of the isoforms, PKCδ has been shown to mediate tumor migration and metastasis [28, 37]. In our study, we found that, depending on dosage, berberine reduced PKCδ kinase activity in chondrosarcoma cells. These results, therefore, suggest that PKCδ is involved in the berberine-mediated cell motility of chondrosarcoma cells. Our results provide evidence that berberine downregulates cell motility and $\alpha v\beta 3$ integrin expression in human chondrosarcoma cancer cells by way of the PKCδ signaling pathway.

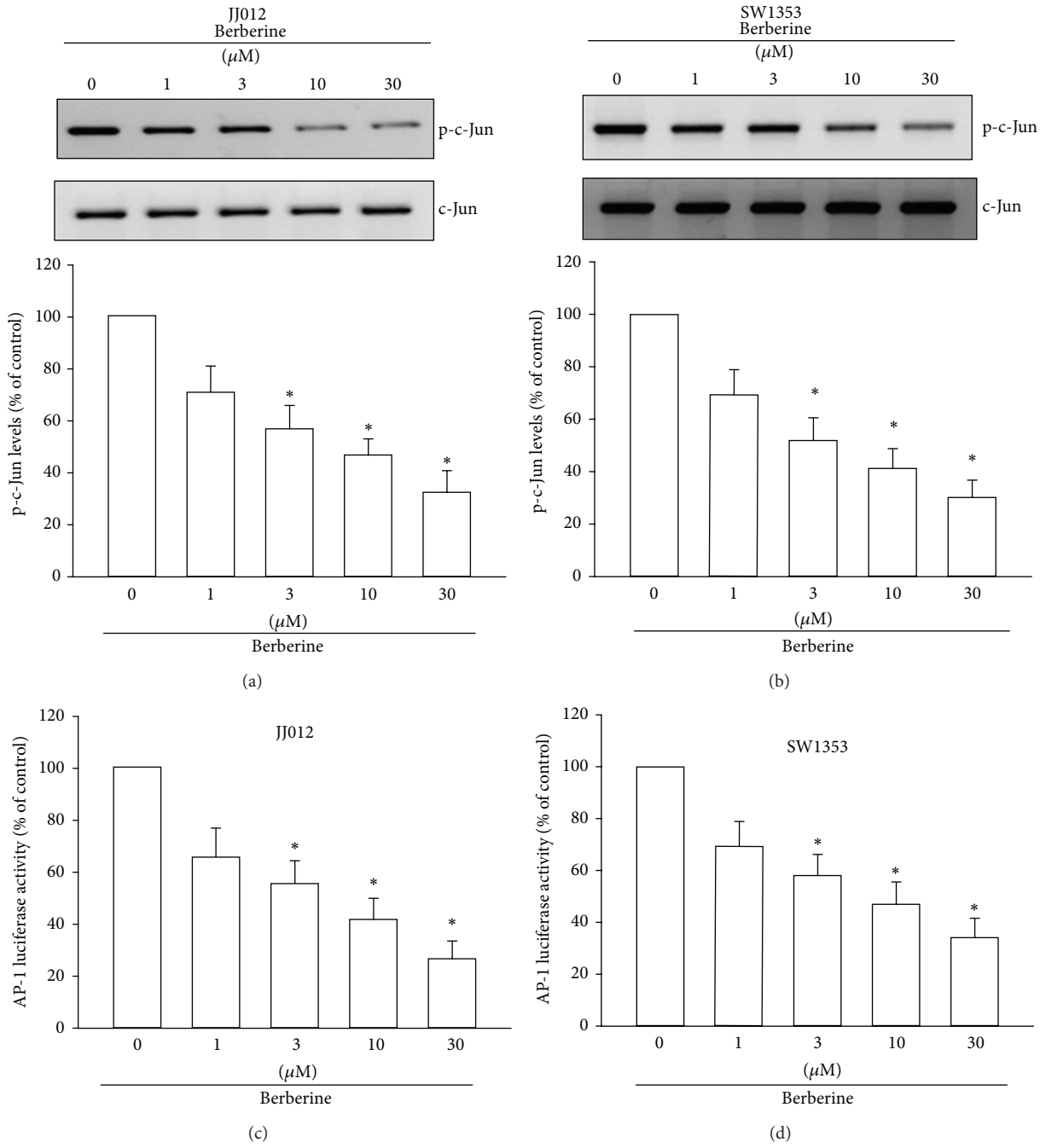

Figure 5: AP-1 mediates the response of human chondrosarcoma cells to berberine. ((a) and (b)) Cells were incubated with various concentrations of berberine for 24 h; p-c-Jun expression was examined by Western blotting. ((c) and (d)) Cells were incubated with various concentrations of berberine for 24 h; AP-1 activity was examined through AP-1 luciferase activity assay. Results are expressed as the mean ± S.E.M.*, $P < 0.05$ compared with control.

Because PKCδ-dependent c-Src activation mediates tumor migration and invasion [28, 37], we examined the potential role of PKCδ-dependent c-Src in the signaling pathway of berberine-reduced cell motility. Treatment of chondrosarcoma cells with berberine also eliminated c-Src kinase activity, indicating the involvement of PKCδ-dependent c-Src activation in berberine-inhibited expression of the $\alpha v\beta 3$ integrin and in the metastasis of human chondrosarcoma cells.

The transcription factors of the Jun and Fos families bind to the AP-1 sequence. These nuclear proteins interact with the AP-1 site as Jun homodimers or Jun-Fos heterodimers that are formed by protein dimerization through their leucine zipper motifs. A variety of growth factors stimulates cancer metastasis via signal-transduction pathways that converge to activate the AP-1 complex of transcription factors [38]. The results of this study show that AP-1 activation contributes to berberine-inhibited migration and metastasis in human

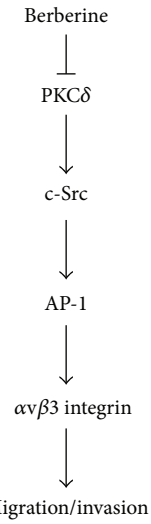

Figure 6: Schematic presentation of the signaling pathways involved in berberine-inhibited metastasis of human chondrosarcoma. Berberine inhibits the migration and invasion of human chondrosarcoma cells by modulating the $\alpha v\beta 3$ integrin through PKCδ, c-Src, and AP-1 signaling pathway.

chondrosarcoma cells. We found that berberine reduced the phosphorylation of c-Jun. In addition, using transient transfection with AP-1 luciferase as an indicator of AP-1 activity, we found that berberine reduced the activity of AP-1 luciferase. Our data indicate that AP-1 activation might play an important role in cell migration and the metastasis of human chondrosarcoma cells. A variety of growth factor stimulate cancer metastasis via signal-transduction pathways that converge to activate NF-κB complex of transcription factors [39]. NF-κB has been reported to regulate the metastasis of human chondrosarcoma [40]. However, we did not examine the role of NF-κB in berberine-inhibited metastasis of human chondrosarcoma in the current study. Therefore, whether NF-κB mediated berberine-inhibited metastasis needs further examination.

It has been recommended that drugs made from natural products play a dominant role in pharmaceutical care. Natural products are important sources of potential agents of cancer chemotherapy and metastasis [41]. The present study showed that berberine inhibits the migration and invasion of human chondrosarcoma cancer cells and that the downregulation of $\alpha v\beta 3$ integrin through the PKCδ, c-Src, and AP-1 pathways is involved in carrying out berberine-mediated effects (Figure 6). The evidence signals that berberine may show beneficial effects in reducing the metastatic activity of human chondrosarcoma cells.

Conflict of Interests

All the authors have no financial or personal relationships with other people or organizations that could inappropriately influence their work.

Authors' Contribution

Chi-Ming Wu and Te-Mao Li equally contributed to this work.

Acknowledgment

This study was supported by Grants from the National Science Council of Taiwan (NSC99-2320-B-039-003-MY3; 100-2320-B-039-028-MY3).

References

[1] R. Barnes and M. Catto, "Chondrosarcoma of bone," *The Journal of Bone and Joint Surgery (British Volume)*, vol. 48, no. 4, pp. 729–764, 1966.

[2] D. Pescador, J. Blanco, C. Corchado et al., "Chondrosarcoma of the scapula secondary to radiodermatitis," *International Journal of Surgery Case Reports*, vol. 3, no. 4, pp. 134–136, 2012.

[3] J. Yuan, C. M. Dutton, and S. P. Scully, "RNAi mediated MMP-1 silencing inhibits human chondrosarcoma invasion," *Journal of Orthopaedic Research*, vol. 23, no. 6, pp. 1467–1474, 2005.

[4] S. S. Liu, X. M. Chen, H. X. Zheng, S. L. Shi, and Y. Li, "Knockdown of Rab5a expression decreases cancer cell motility and invasion through integrin-mediated signaling pathway," *Journal of Biomedical Science*, vol. 18, no. 1, article 58, 2011.

[5] S. M. Weis and D. A. Cheresh, "αv integrins in angiogenesis and cancer," *Cold Spring Harbor Perspectives in Medicine*, vol. 1, no. 1, Article ID a006478, 2011.

[6] F. G. Giancotti and G. Tarone, "Positional control of cell fate through joint integrin/receptor protein kinase signaling," *Annual Review of Cell and Developmental Biology*, vol. 19, pp. 173–206, 2003.

[7] Y. Wang, S. Shenouda, S. Baranwal et al., "Integrin subunits α5 and α6 regulate cell cycle by modulating the chk1 and Rb/E2F pathways to affect breast cancer metastasis," *Molecular Cancer*, vol. 10, article 84, 2011.

[8] S. J. Shattil, C. Kim, and M. H. Ginsberg, "The final steps of integrin activation: the end game," *Nature Reviews Molecular Cell Biology*, vol. 11, no. 4, pp. 288–300, 2010.

[9] Z. Wang, J. Bryan, C. Franz, N. Havlioglu, and L. J. Sandell, "Type IIB procollagen NH2-propeptide induces death of tumor cells via interaction with integrins $\alpha v\beta 3$ and $\alpha v\beta 5$," *The Journal of Biological Chemistry*, vol. 285, no. 27, pp. 20806–20817, 2010.

[10] C. Heyder, E. Gloria-Maercker, W. Hatzmann, B. Niggemann, K. S. Zanker, and T. Dittmar, "Role of the β1-integrin subunit in the adhesion, extravasation and migration of T24 human bladder carcinoma cells," *Clinical and Experimental Metastasis*, vol. 22, no. 2, pp. 99–106, 2005.

[11] E. C. Seales, G. A. Jurado, B. A. Brunson, J. K. Wakefield, A. R. Frost, and S. L. Bellis, "Hypersialylation of β1 integrins, observed in colon adenocarcinoma, may contribute to cancer progression by up-regulating cell motility," *Cancer Research*, vol. 65, no. 11, pp. 4645–4652, 2005.

[12] K. Takenaka, M. Shibuya, Y. Takeda et al., "Altered expression and function of β1 integrins in a highly metastatic human lung adenocarcinoma cell line," *International Journal of Oncology*, vol. 17, no. 6, pp. 1187–1194, 2000.

[13] C. H. Tang, Y. T. Keng, and J. F. Liu, "HMGB-1 induces cell motility and $\alpha 5\beta 1$ integrin expression in human chondrosarcoma cells," *Cancer Letters*, vol. 322, no. 1, pp. 98–106, 2012.

[14] C. Y. Lee, M. J. Su, C. Y. Huang et al., "Macrophage migration inhibitory factor increases cell motility and up-regulates $\alpha v\beta 3$ integrin in human chondrosarcoma cells," *Journal of Cellular Biochemistry*, vol. 113, no. 5, pp. 1590–1598, 2012.

[15] T. H. Lai, Y. C. Fong, W. M. Fu, R. S. Yang, and C. H. Tang, "Stromal cell-derived factor-1 increase $\alpha v\beta 3$ integrin expression and invasion in human chondrosarcoma cells," *Journal of Cellular Physiology*, vol. 218, no. 2, pp. 334–342, 2009.

[16] C. Y. Lee, C. Y. Huang, M. Y. Chen, C. Y. Lin, H. C. Hsu, and C. H. Tang, "IL-8 increases integrin expression and cell motility in human chondrosarcoma cells," *Journal of Cellular Biochemistry*, vol. 112, no. 9, pp. 2549–2557, 2011.

[17] M. Tillhon, L. M. Guaman Ortiz, P. Lombardi, and A. I. Scovassi, "Berberine: new perspectives for old remedies," *Biochemical Pharmacology*, vol. 84, no. 10, pp. 1260–1267, 2012.

[18] C. V. Diogo, N. G. Machado, I. A. Barbosa, T. L. Serafim, A. Burgeiro, and P. J. Oliveira, "Berberine as a promising safe anticancer agent—is there a role for mitochondria?" *Current Drug Targets*, vol. 12, no. 6, pp. 850–859, 2011.

[19] W. Tang, Y. Nakamura, M. Tsujimoto et al., "Heparanase: a key enzyme in invasion and metastasis of gastric carcinoma," *Modern Pathology*, vol. 15, no. 6, pp. 593–598, 2002.

[20] I. Lerner, L. Baraz, E. Pikarsky et al., "Function of heparanase in prostate tumorigenesis: potential for therapy," *Clinical Cancer Research*, vol. 14, no. 3, pp. 668–676, 2008.

[21] J. B. Maxhimer, C. E. Pesce, R. A. Stewart, P. Gattuso, R. A. Prinz, and X. Xu, "Ductal carcinoma in situ of the breast and heparanase-1 expression: a molecular explanation for more aggressive subtypes," *Journal of the American College of Surgeons*, vol. 200, no. 3, pp. 328–335, 2005.

[22] J. A. Block, S. E. Inerot, S. Gitelis, and J. H. Kimura, "Synthesis of chondrocytic keratan sulphate-containing proteoglycans by human chondrosarcoma cells in long-term cell culture," *Journal of Bone and Joint Surgery A*, vol. 73, no. 5, pp. 647–658, 1991.

[23] K. M. Tong, C. P. Chen, K. C. Huang et al., "Adiponectin increases MMP-3 expression in human chondrocytes through AdipoR1 signaling pathway," *Journal of Cellular Biochemistry*, vol. 112, no. 5, pp. 1431–1440, 2011.

[24] C. H. Tang, C. J. Hsu, and Y. C. Fong, "The CCL5/CCR5 axis promotes interleukin-6 production in human synovial fibroblasts," *Arthritis and Rheumatism*, vol. 62, no. 12, pp. 3615–3624, 2010.

[25] C. Y. Huang, S. Y. Chen, H. C. Tsai, H. C. Hsu, and C. H. Tang, "Thrombin induces epidermal growth factor receptor transactivation and CCL2 expression in human osteoblasts," *Arthritis and Rheumatism*, vol. 64, no. 10, pp. 3344–3354, 2012.

[26] H. E. Tzeng, C. H. Tsai, Z. L. Chang et al., "Interleukin-6 induces vascular endothelial growth factor expression and promotes angiogenesis through apoptosis signal-regulating kinase 1 in human osteosarcoma," *Biochemical Pharmacology*, vol. 85, no. 4, pp. 531–540, 2013.

[27] C. H. Hou, R. S. Yang, S. M. Hou, and C. H. Tang, "TNF-α increases $\alpha v\beta 3$ integrin expression and migration in human chondrosarcoma cells," *Journal of Cellular Physiology*, vol. 226, no. 3, pp. 792–799, 2011.

[28] S. F. Yang, M. K. Chen, Y. S. Hsieh et al., "Prostaglandin E2/EP1 signaling pathway enhances intercellular adhesion molecule 1 (ICAM-1) expression and cell motility in oral cancer cells," *The Journal of Biological Chemistry*, vol. 285, no. 39, pp. 29808–29816, 2010.

[29] H. D. Dorfman and B. Czerniak, "Bone cancers," *Cancer*, vol. 75, no. 1, pp. 203–210, 1995.

[30] Y. C. Fong, W. H. Yang, S. F. Hsu et al., "2-methoxyestradiol induces apoptosis and cell cycle arrest in human chondrosarcoma cells," *Journal of Orthopaedic Research*, vol. 25, no. 8, pp. 1106–1114, 2007.

[31] J. Tang, Y. Feng, S. Tsao, N. Wang, R. Curtain, and Y. Wang, "Berberine and Coptidis Rhizoma as novel antineoplastic agents: a review of traditional use and biomedical investigations," *Journal of Ethnopharmacology*, vol. 126, no. 1, pp. 5–17, 2009.

[32] J. Park, K. Singha, S. Son et al., "A review of RGD-functionalized nonviral gene delivery vectors for cancer therapy," *Cancer Gene Therapy*, vol. 19, no. 11, pp. 741–748, 2012.

[33] M. Deb, D. Sengupta, and S. K. Patra, "Integrin-epigenetics: a system with imperative impact on cancer," *Cancer and Metastasis Reviews*, vol. 31, no. 1-2, pp. 221–234, 2012.

[34] H. Boukerche, Z. Z. Su, C. Prevot, D. Sarkar, and P. B. Fisher, "mda-9/syntenin promotes metastasis in human melanoma cells by activating c-Src," *Proceedings of the National Academy of Sciences of the United States of America*, vol. 105, no. 41, pp. 15914–15919, 2008.

[35] C. H. Liang, S. Y. Chiu, I. L. Hsu et al., "α-catulin drives metastasis by activating ILK and driving an $\alpha v\beta 3$ integrin signaling axis," *Cancer Research*, vol. 73, no. 1, pp. 428–438, 2013.

[36] B. C. Berk, M. B. Taubman, E. J. Cragoe Jr., J. W. Fenton II, and K. K. Griendling, "Thrombin signal transduction mechanisms in rat vascular smooth muscle cells: calcium and protein kinase C-dependent and -independent pathways," *The Journal of Biological Chemistry*, vol. 265, no. 28, pp. 17334–17340, 1990.

[37] H. S. Yu, T. H. Lin, and C. H. Tang, "Bradykinin enhances cell migration in human prostate cancer cells through B2 receptor/PKCδ/c-Src dependent signaling pathway," *Prostate*, vol. 73, no. 1, pp. 89–100, 2013.

[38] B. W. Ozanne, H. J. Spence, L. C. McGarry, and R. F. Hennigan, "Transcription factors control invasion: AP-1 the first among equals," *Oncogene*, vol. 26, no. 1, pp. 1–10, 2007.

[39] D. Sliva, "Signaling pathways responsible for cancer cell invasion as targets for cancer therapy," *Current Cancer Drug Targets*, vol. 4, no. 4, pp. 327–336, 2004.

[40] C. M. Wu, T. M. Li, S. F. Hsu et al., "IGF-I enhances $\alpha 5\beta 1$ integrin expression and cell motility in human chondrosarcoma cells," *Journal of Cellular Physiology*, vol. 226, no. 12, pp. 3270–3277, 2011.

[41] J. M. Pezzuto, "Plant-derived anticancer agents," *Biochemical Pharmacology*, vol. 53, no. 2, pp. 121–133, 1997.

Hindawi Publishing Corporation
Evidence-Based Complementary and Alternative Medicine
Volume 2013, Article ID 376123, 12 pages
http://dx.doi.org/10.1155/2013/376123

Research Article

Emodin and Aloe-Emodin Suppress Breast Cancer Cell Proliferation through ERα Inhibition

Pao-Hsuan Huang,[1] Chih-Yang Huang,[2,3] Mei-Chih Chen,[1,4] Yueh-Tsung Lee,[1,5] Chia-Herng Yue,[1,6] Hsin-Yi Wang,[1,7] and Ho Lin[1,4,8,9]

[1] *Department of Life Sciences, National Chung Hsing University, Taichung 40227, Taiwan*
[2] *Department of Health and Nutrition Biotechnology, Asia University, Taichung 41354, Taiwan*
[3] *Graduate Institute of Basic Medical Science, China Medical University, Taichung 40402, Taiwan*
[4] *Department of Urology, University of Texas Southwestern Medical Center, Dallas, TX 75390, USA*
[5] *Department of Surgery, Chang Bing Show Chwan Memorial Hospital, Changhua 50544, Taiwan*
[6] *Department of Surgery, Tungs' Taichung MetroHarbor Hospital, Taichung 43304, Taiwan*
[7] *Department of Nuclear Medicine, Taichung Veterans General Hospital, Taichung 40705, Taiwan*
[8] *Department of Agricultural Biotechnology Center, National Chung Hsing University, Taichung 40227, Taiwan*
[9] *Graduate Institute of Rehabilitation Science, China Medical University, Taichung 40402, Taiwan*

Correspondence should be addressed to Ho Lin; hlin@dragon.nchu.edu.tw

Received 25 April 2013; Accepted 6 June 2013

Academic Editor: Gautam Sethi

The anthraquinones emodin and aloe-emodin are abundant in rhubarb. Several lines of evidence indicate that emodin and aloe-emodin have estrogenic activity as phytoestrogens. However, their effects on estrogen receptor α (ERα) activation and breast cancer cell growth remain controversial. The goal of this study is to investigate the effects and molecular mechanisms of emodin and aloe-emodin on breast cancer cell proliferation. Our results indicate that both emodin and aloe-emodin are capable of inhibiting breast cancer cell proliferation by downregulating ERα protein levels, thereby suppressing ERα transcriptional activation. Furthermore, aloe-emodin treatment led to the dissociation of heat shock protein 90 (HSP90) and ERα and increased ERα ubiquitination. Although emodin had similar effects to aloe-emodin, it was not capable of promoting HSP90/ERα dissociation and ERα ubiquitination. Protein fractionation results suggest that aloe-emodin tended to induce cytosolic ERα degradation. Although emodin might induce cytosolic ERα degradation, it primarily affected nuclear ERα distribution similar to the action of estrogen when protein degradation was blocked. In conclusion, our data demonstrate that emodin and aloe-emodin specifically suppress breast cancer cell proliferation by targeting ERα protein stability through distinct mechanisms. These findings suggest a possible application of anthraquinones in preventing or treating breast cancer in the future.

1. Introduction

Many phytochemicals derived from plants, including anthraquinone, have been reported to have anticancer potential. The anthraquinone derivatives emodin (1,3,8-trihydroxy-6-methylanthraquinone) and aloe-emodin (1,8-dihydroxy-3-hydroxyl-methylanthraquinone) are the main bioactive components of rhubarb (*Rheum palmatum*), which has been used in traditional Chinese medicine [1]. Aloe-emodin is also abundant in the leaves of the common plant *Aloe vera* [2]. Emodin has been widely investigated for its antibacterial [3], anti-inflammatory [4], and antiproliferative effects in several types of cancer [1]. Notably, emodin may downregulate androgen receptor (AR) and lead to the inhibition of prostate cancer cell growth [5], suggesting that anthraquinone derivatives might modulate steroid receptor activity. Several lines of evidence indicate that emodin and aloe-emodin have estrogenic activity and modulate breast cancer cell proliferation as phytoestrogen compounds [6, 7]. However, the pharmacological effects

and molecular mechanisms of emodin and aloe-emodin in estrogen receptor α (ERα) modulation and breast cancer cell growth remain elusive.

Breast cancer is a common malignancy with high lethality in women. Because ERα activation plays an important role in the initiation, development, and progression of breast cancer, estrogen replacement therapy is the most common strategy to suppress breast cancer progression [8]. By mimicking the structure of estrogen, synthetic estrogen-like compounds are used to compete for the binding of endogenous estrogen with ERα and therefore inhibit ERα-dependent growth of breast cancer cells [9, 10]. However, synthetic estrogens have side effects that increase the risk of cancer development due to unselective estrogenic action [11]. Although the potency of natural phytoestrogens is generally lower than that of synthetic estrogens in terms of estrogenic action, natural phytoestrogens are relatively safer with fewer side effects [12]. Therefore, studies investigating the effects and molecular mechanisms of natural herbal medicines that contain phytoestrogens as potential treatments to breast cancer are of interest.

We found that the inhibition of proliferation by emodin and aloe-emodin was ERα-dependent in breast cancer cell lines. Importantly, aloe-emodin treatment promotes ERα protein degradation by repressing the association of ERα and heat shock protein 90 (HSP90). Moreover, the dissociated ERα is ubiquitinated and targeted for proteasome-dependent degradation in the cytosol. The findings for aloe-emodin are distinct from those for emodin. Based on the above observations, these two anthraquinones could potentially be used as specific phytoestrogens to treat breast cancer.

2. Materials and Methods

2.1. Cell Lines and Cell Culture. The human breast cancer cell lines MCF-7 and MDA-MB-453 were obtained from the Bioresource Collection and Research Center (BCRC), Food Industry Research and Development Institute, Taiwan. MCF-7 cells were grown in minimum essential medium (Gibco, Carlsbad, CA, USA) containing 10% fetal bovine serum (Gibco), 1.5 g/L $NaHCO_3$, 0.1 mM nonessential amino acids (Gibco), 1 mM sodium pyruvate (Gibco), and 1% penicillin-streptomycin (Sigma, St. Louis, MO, USA). MDA-MB-453 cells were maintained in Dulbecco's modified Eagle's medium (Gibco) supplemented with 10% fetal bovine serum, 1.5 g/L $NaHCO_3$, and 1% penicillin-streptomycin. All cells were incubated at 37°C in a humidified atmosphere with 5% CO_2.

2.2. Cell Viability Assay. Cells were incubated for 24 hours after attachment. Cell numbers were calculated by direct counting of cells, excluding cells that stained positive for 0.2% trypan blue stain (Sigma, St. Louis, MO, USA) [13]. Cells were treated with different concentrations of aloe-emodin or emodin (ChromaDex, Irvine, CA, USA) for the indicated number of days, and then, the 3-(4,5-dimethylthiazol-2-yl)-2, 5-diphenyltetrazolium bromide (MTT, Sigma, St. Louis, MO, USA) assay was used to quantify cell proliferation. The MTT stock solution (5 mg/mL) was diluted to 0.5 mg/mL with complete culture medium, and 0.1 mL was added to each well. The yellow MTT was converted to blue formazan by living cells, a reaction that is dependent on mitochondrial enzyme activity. After using DMSO to dissolve the blue formazan, the absorbance of converted MTT could be measured at 570 nm λ [14].

2.3. Cell Fractionation and Western Blot Analysis. Cells were collected using a rubber scraper and homogenized with Na_3VO_4 diluted in PBS (1 : 100). After centrifugation, cells were resuspended with lysis buffer as previously described [15–19], and protease inhibitor cocktail (Roche Applied Science, Mannheim, Germany) was added, followed by incubation on ice for 45 minutes. The cell lysate was centrifuged, and the supernatant was collected as total protein extract. The protein extract was mixed with sample buffer and boiled for 10 minutes. Then, western blotting was performed as previously described [19, 20]. Briefly, SDS-polyacrylamide gel electrophoresis (SDS-PAGE) was performed, and proteins were transferred from the SDS-PAGE gel onto a polyvinylidene fluoride (PVDF) membrane. Primary antibodies were incubated with the membrane overnight, and horseradish peroxidase- (HRP-) conjugated secondary antibodies (Jackson ImmunoResearch Laboratory, West Grove, PA, USA) were applied. The ECL (western lighting chemiluminescence reagent plus, PerkinElmer Life Sciences, Shelton, CT, USA) reaction was performed, and the membranes were exposed to X-ray films to visualize protein staining (Fujifilm, Tokyo, Japan). Antibodies directed against the following proteins were used in this study: poly(ADP-ribose) polymerase (PARP, 06-557, Upstate Biotechnology, Lake Placid, NY, USA), α-tubulin (05-829, Upstate Biotechnology), ERα (sc-543 and sc-8005, Santa Cruz Biotechnology, Santa Cruz, CA, USA), cyclin D1 (sc-20044, Santa Cruz Biotechnology), HSP 90 α/β (sc-59577, Santa Cruz Biotechnology), ubiquitin (sc-8017, Santa Cruz Biotechnology), and β-actin (MAB1501, Millipore, Temecula, CA, USA). The quantification software used was MCID Image Analysis Evaluation.

2.4. Immunoprecipitation. Cell lysate was extracted in lysis buffer, and immunoprecipitation was performed as previously described [19]. Briefly, the beads/antibody precipitated complex was prepared by mixing Protein G Mag Sepharose Xtra beads (GE Healthcare, Waukesha, WI, USA) and specific antibody at 10 μg : 1 μg for 2 h at room temperature. Cell lysates were mixed with beads/antibody for 12 h at 4°C, and protein was isolated by precipitation under magnetic attraction with three rounds of PBST washes. The precipitated proteins were analyzed by western blotting after denaturation following dilution in sample buffer and boiling for 10 minutes.

2.5. Quantitative Real-Time PCR. Total RNA was extracted from cells using a Miniprep Purification Kit (Genemark, Taipei, Taiwan), and reverse transcription-PCR was performed using a High-Capacity cDNA Reverse Transcription Kit (Applied Biosystems, Foster City, CA, USA) following the standard procedures recommended by the manufacturer. For reverse transcription, 2 μg of total RNA was used as the

first-strand cDNA template for the subsequent amplification procedure. The following primers were used to amplify the cDNAs: ERα (5′-TGGAGATCTTCGACATGCTG-3′ and 5′-TCCAGAGACTTCAGGGTGCT-3′) [21] and *β-actin* (5′-TTGCCGACAGGATGCAGAA-3′ and 5′-GCCGATCCACACGGAGTACT-3′). cDNA and primers were mixed within FastStart Universal SYBR Green Master (Roche Applied Science) and measured using a real-time PCR instrument (Applied Biosystems). Data presented by Ct values were analyzed and adjusted relative to levels of the *β-actin* housekeeping gene.

2.6. Transfection and Reporter Assays. Cells were plated for at least 24 h and had reached 80% confluency prior to transfection. Expression plasmid was premixed within Lipofectamine 2000 Reagent (Invitrogen, Carlsbad, CA, USA) according to the manufacturer's instructions. The liposome/plasmid complex was transfected into MCF-7 cells incubated with Opti-MEM (Gibco) for 6 h, and then culture medium was added for exogenous protein expression. The pCMV5-ERα expression plasmid was kindly provided by Professor Chih-Yang Huang, Graduate Institute of Basic Medical Science, China Medical University, Taichung, Taiwan. A reporter assay was performed to detected ERα transcriptional activity after cells were transfected with 3×ERE-containing-promoter luciferase reporter gene (pGL2-TK-3 × ERE, gift from Dr. Chih-Yang Huang, China Medical University, Taichung, Taiwan) and internal control pSV-β-galactosidase expression plasmid (gift from Dr. Jeremy J. W. Chen, National Chuang Hsing University, Taichung, Taiwan). Reporter gene luciferase production was performed using the Dual-Light System (Applied Biosystems), and measurements were performed using a 1420 Multilabel Counter VICTOR^3 instrument (PerkinElmer Life Sciences). The raw data were normalized to β-galactosidase activity to control for varying transfection efficiencies [19].

2.7. Statistics. All values are presented as the mean ± standard error of the mean (SEM). In all cases, Student's *t*-test was used to assess the results of cell proliferation and reporter assays. A difference between two means was considered statistically significant when $P < 0.05$.

3. Results

3.1. ERα Is Important for the Growth Inhibition Induced by Emodin and Aloe-Emodin. The effects of different concentrations (0, 6, 12.5, 25, 50, or 100 μM) of emodin and aloe-emodin on the growth of the ERα-positive breast cancer cell line MCF-7 were determined by cell number counting (0–6 days) and MTT assays (4 days). Emodin and aloe-emodin treatment led to dose-dependent suppression of MCF-7 growth (Figures 1(a) and 1(b)). Notably, 12.5 μM or higher concentrations of aloe-emodin had stronger effects on MCF-7 growth compared to the same dosage of emodin. MTT assays showed significant inhibition of MCF-7 proliferation in a dose-dependent manner following emodin treatment at concentrations of 25 to 100 μM (Figure 1(c)) and of aloe-emodin treatment at concentrations of 6 to 100 μM (Figure 1(d)). Whereas emodin was more effective against the ERα-negative breast cancer cell line MDA-MB-453 than against MCF-7 (Figure 1(e)), the inhibitory effects of aloe-emodin on the growth of MDA-MB-453 was moderate compared to the effects on MCF-7 cells (Figure 1(f)). In which, 25 μM of aloe-emodin was not able to affect MDA-MB-453 cell proliferation (Figure 1(f)), while 25 μM of emodin significantly reduced that cell proliferation (Figure 1(e)) implies that the effects of aloe-emodin might be associated with ERα and distinct to emodin. To further investigate whether ERα was involved in the inhibitory effects of the emodin and aloe-emodin treatments, the effects of emodin and aloe-emodin on the growth of MCF-7 with or without ERα overexpression were investigated. Following a 25 μM treatment with emodin (Figure 1(g)) or aloe-emodin (Figure 1(h)), the ERα-overexpressing cells were more sensitive to drug treatments compared to control cells. Similar results were also observed in another ERα-positive cell line, T47D (data not shown). These data indicate that ERα protein plays an important role in the emodin- and aloe-emodin-induced suppression of breast cancer cell proliferation, although the potency of these two compounds are slightly different.

3.2. Emodin and Aloe-Emodin Decrease ERα Protein Levels in a Time- and Dose-Dependent Manner. ERα activation is triggered by estrogen and promotes the initiation and progression of breast cancer [22, 23]. ERα protein levels were detected following treatment with various dosages of emodin or aloe-emodin (0–100 μM, Figures 2(a) and 2(c)) for different time intervals (0–48 h, Figures 2(b) and 2(d)). The quantitative results were provided in the lower panels of the accompanying figures. The data suggest that emodin and aloe-emodin triggered a decrease in ERα protein level in a time- and dose-dependent manner.

3.3. Emodin and Aloe-Emodin Decrease Both Nuclear and Cytosolic ERα and Inhibit ERα Activation. Because ERα protein levels were affected by emodin and aloe-emodin, the activation status of ERα was investigated. Fractionation of cellular protein was performed and indicated that emodin and aloe-emodin repressed both the nuclear and cytosolic distribution of ERα protein (upper panels in Figures 3(a) and 3(b)). The quantitative results are presented in the lower panels of Figures 3(a) and 3(b). Additionally, cytosolic ERα was more sensitive to treatment than nuclear ERα. An ERα reporter assay was performed in MCF-7 cells. The data showed that aloe-emodin significantly inhibited ERα-targeted promoter activity in a dose-dependent manner (Figure 3(d)). Compared to aloe-emodin, emodin in high dosages (25–100 μM) moderately inhibited ERα activation, whereas low dosages of emodin (6 and 12.5 μM) tended to increase ERα activation. Furthermore, the expressions of ERα downstream genes might be affected by those two compounds. Figures 3(e) and 3(f) were the evidence indicating that the protein expression of cyclin D1 which is one of ERα-regulated protein was indeed decreased by treatments of 25 μM emodin or 25 μM aloe-emodin for 48 h.

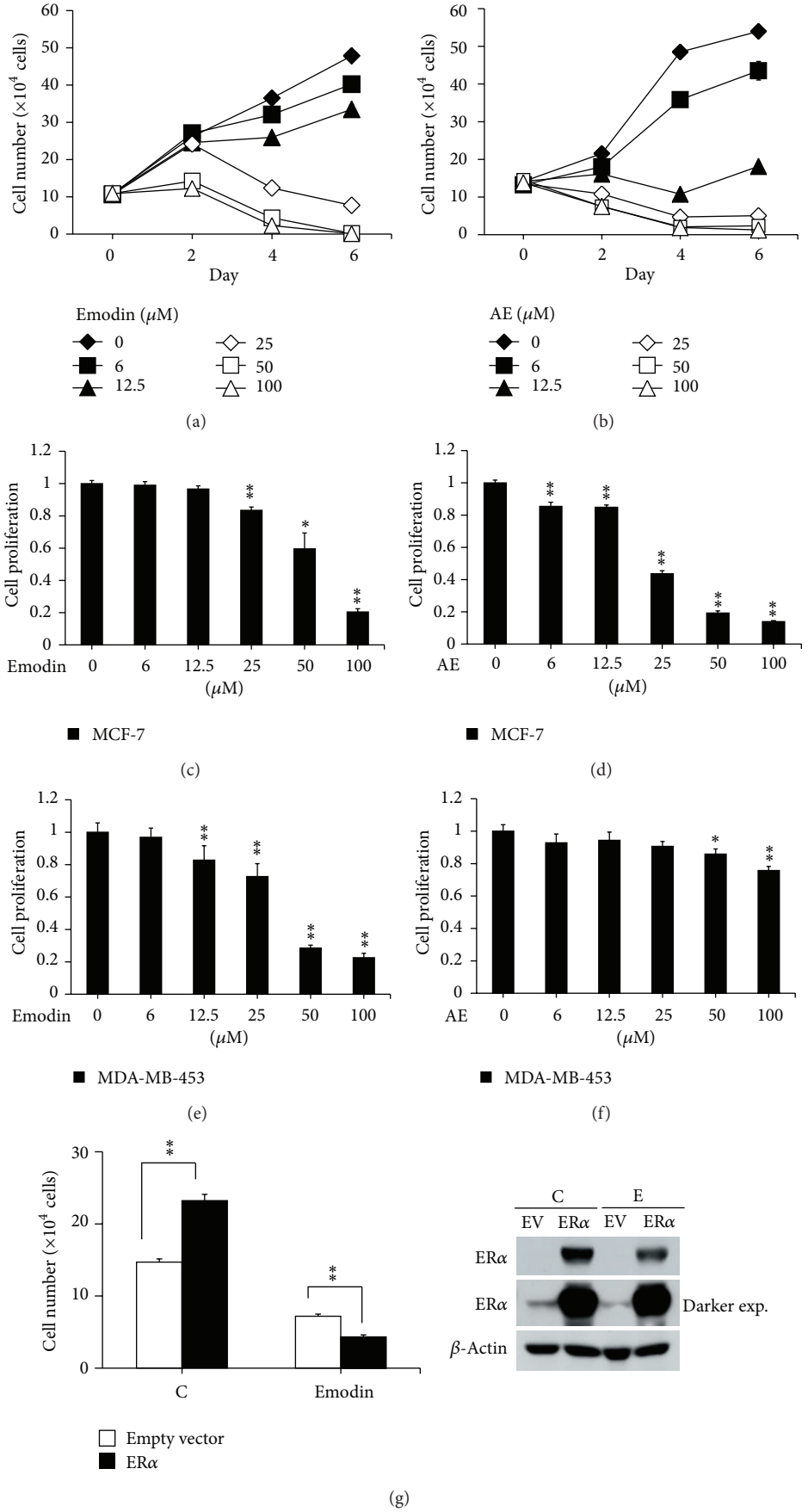

Figure 1: Continued.

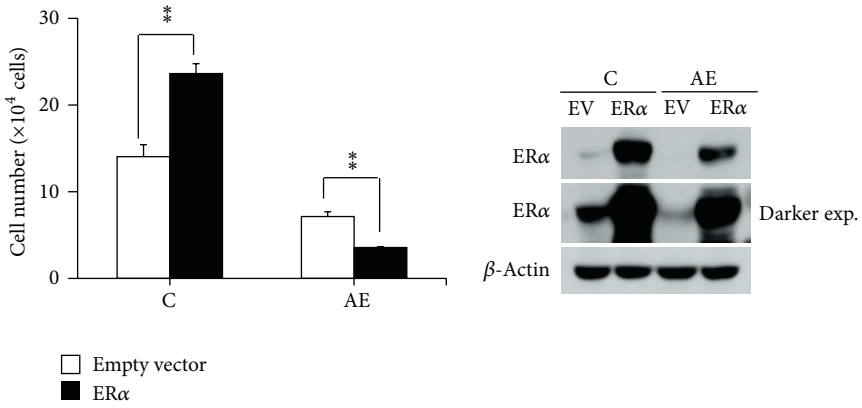

(h)

Figure 1: Emodin and aloe-emodin inhibit breast cancer cell growth. MCF-7 cells were treated with various concentrations of emodin (a) or aloe-emodin (b) for 0 to 6 days. Cell numbers were calculated by trypan blue staining. (c–f) MCF-7 and MDA-MB-453 cells were treated with various concentrations of emodin or aloe-emodin for 4 days. Cell proliferation was determined by an MTT assay. The control cell proliferation rate was set at 1. MCF-7 cells were transiently transfected with empty vector or pCMV5-ERα and treated with 25 μM emodin (g) or aloe-emodin (h) for 4 days. The transfected efficiencies of ERα overexpression and cell numbers were detected by western blotting and trypan blue staining, respectively. The results were presented as the mean ± SEM. * and ** correspond to $P < 0.05$ and $P < 0.01$, respectively, versus the control group or empty vector group.

3.4. Emodin and Aloe-Emodin Treatment Leads to Decreased ERα Protein through Proteasomal Degradation. Because ERα protein levels were affected by both emodin and aloe-emodin in the previous experiments, the gene expression and protein stability of ERα were investigated. First, ERα messenger RNA expression was detected by quantitative real-time PCR following treatment. We found that treatments of 25 μM emodin and 25 μM aloe-emodin for 24 h did not have a significant effect compared to the control group (Figure 4(a)). Second, because ubiquitin-proteasome-dependent degradation is the main process involved in ERα proteolysis [23], the proteasome inhibitor MG132 was used to prevent ERα protein degradation, and drug effects can be observed. The results of this experiment indicated that MG132 could rescue ERα degradation after emodin or aloe-emodin treatment (Figures 4(b) and 4(c)). These findings suggest that the decreased ERα protein levels observed following emodin or aloe-emodin treatment resulted from proteasome degradation.

3.5. Aloe-Emodin Promotes the Dissociation of ER and Heat Shock Protein 90 and Causes ERα Ubiquitination. ERα is processed by ubiquitination after disassociating from heat shock protein 90 (HSP90) [24]. Using immunoprecipitation in the presence of MG132 to prevent protein degradation, we found that aloe-emodin apparently blocked the protein interaction between ERα and HSP90 (Figure 5(a)); however, the effect induced by emodin was not as significant (Figure 5(b)). The quantitative graphs were provided in the lower panels of accompanying figures. Subsequently, ERα ubiquitination following drug treatment was investigated by detecting the levels of ubiquitinated ERα in drug-treated cell extracts following MG132 administration. The data indicated that aloe-emodin treatment enhanced ubiquitin-conjugated ERα levels, and protein degradation was prevented by MG132 treatment regardless of whether ERα or ubiquitin was immunoprecipitated first (Figure 5(c)). Although emodin slightly promoted ERα/HSP90 dissociation (Figure 5(b)), no increase in ERα ubiquitination was observed following emodin treatment (Figure 5(d)). The related quantitative results were shown in the lower panels. It suggests that ubiquitination was not required for emodin-induced ERα degradation by proteasome. These results indicate that aloe-emodin specifically reduces ERα protein levels by promoting ERα ubiquitination, which results in proteasome-dependent degradation.

3.6. Comparison of Emodin/Aloe-Emodin and Estrogen on ERα Behaviors. Ligand binding by estrogen or estrogen-like molecules promotes ERα transactivation, during which ERα first dissociates from HSP90 in the cytoplasm and then translocates into the nucleus [8]. Because the effects of aloe-emodin and emodin on the ERα ubiquitination process are distinct (Figure 5), it is of interest to understand how the effects of these two compounds compare to those of estrogen to mediate ERα behavior. Immunoprecipitation experiment results indicate that aloe-emodin had similar effects to synthetic estrogen (estradiol benzoate (EB)) on ERα/HSP90 dissociation (Figure 6(a)), whereas emodin did not (Figure 5(b)). However, in contrast to EB treatment, aloe-emodin treatment led to a decrease in the nuclear and cytoplasmic levels of ERα protein. Furthermore, the decrease in ERα protein levels following aloe-emodin treatment was blocked by MG132, suggesting that aloe-emodin promotes ERα degradation (Figure 6(b)). Comparing the data in Figure 3(b), we suggest that aloe-emodin preferentially induces ERα degradation in the cytoplasm of breast cancer cells. Interestingly, nuclear ERα was increased by emodin treatment, and protein degradation was prevented by MG132 (Figure 6(c)), suggesting that although emodin

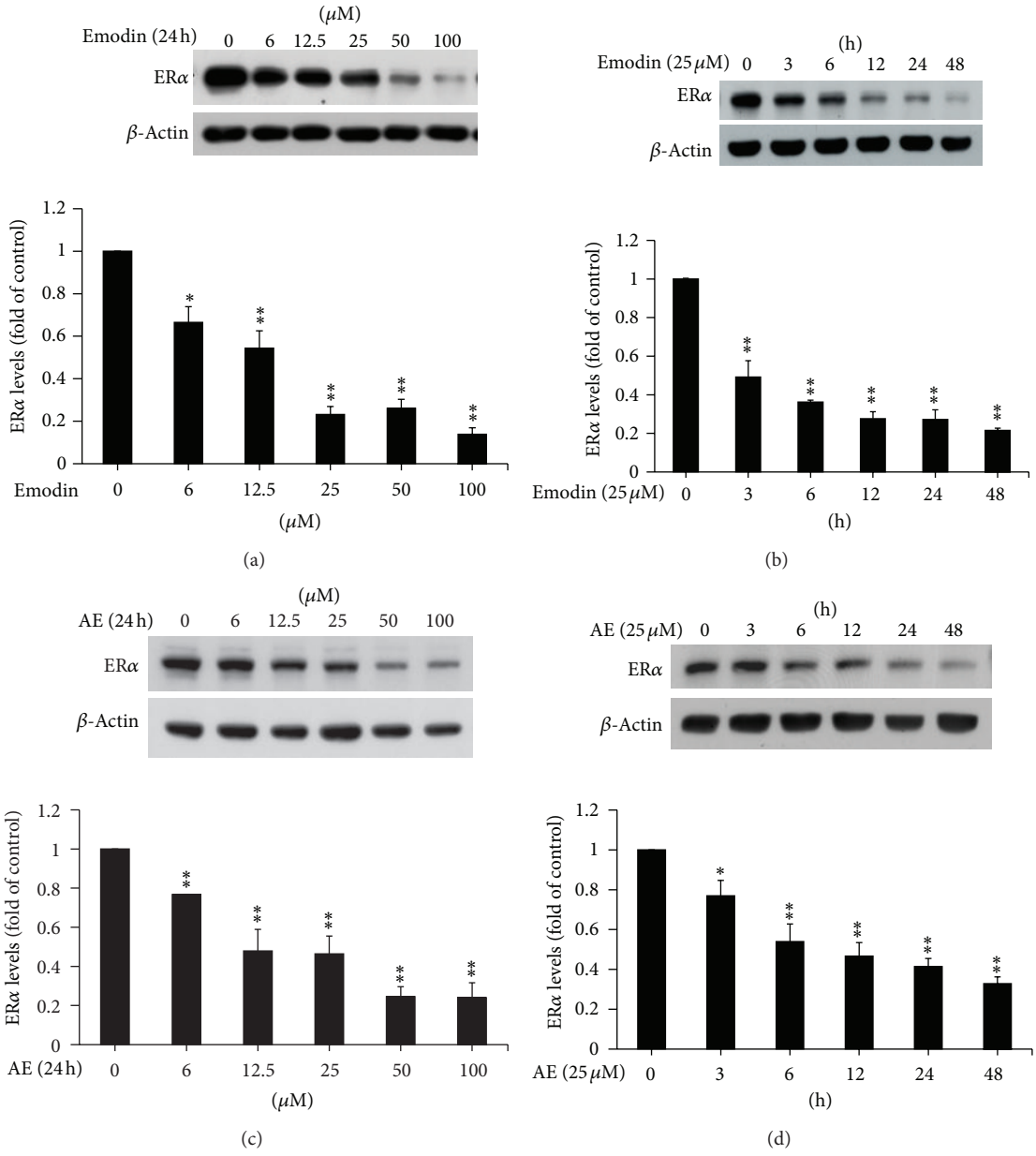

Figure 2: Emodin and aloe-emodin reduce ERα protein levels. MCF-7 cells were treated with emodin or aloe-emodin in a dose-dependent manner for 24 h (a, c) and via a time course using 25 μM of the drug (b, d). ERα protein levels were detected by western blotting. β-Actin was used as an internal control. The quantification of ERα levels is presented as fold increase or decrease compared to control levels and was evaluated in three independent experiments. The results were presented as the mean ± SEM. * and ** correspond to $P < 0.05$, and $P < 0.01$, respectively, versus the control group.

induces ERα degradation in both the nucleus and cytoplasm (compared to Figure 3(a)), it seems that emodin is able to promote ERα translocation into the nucleus, which is in contrast to the actions of aloe-emodin. This might explain why low concentrations of emodin showed slight stimulation in the ERα reporter assay (Figure 3(c)). Taken together, these results demonstrate that aloe-emodin induces the dissociation of ERα/HSP90 and subsequently promotes ERα ubiquitin-proteasome-dependent degradation in the cytoplasm, thereby inhibiting ERα translocation into nucleus, where ERα would otherwise be activated as a positive modulator.

4. Discussion

Breast cancer is a common malignancy in women, and estrogen plays an important role in early cancer development [25]. Estrogen, which usually denotes 17β-estradiol (E2), binds to its primary receptor ERα and stimulates ERα transcriptional activity to regulate downstream gene expression and cell

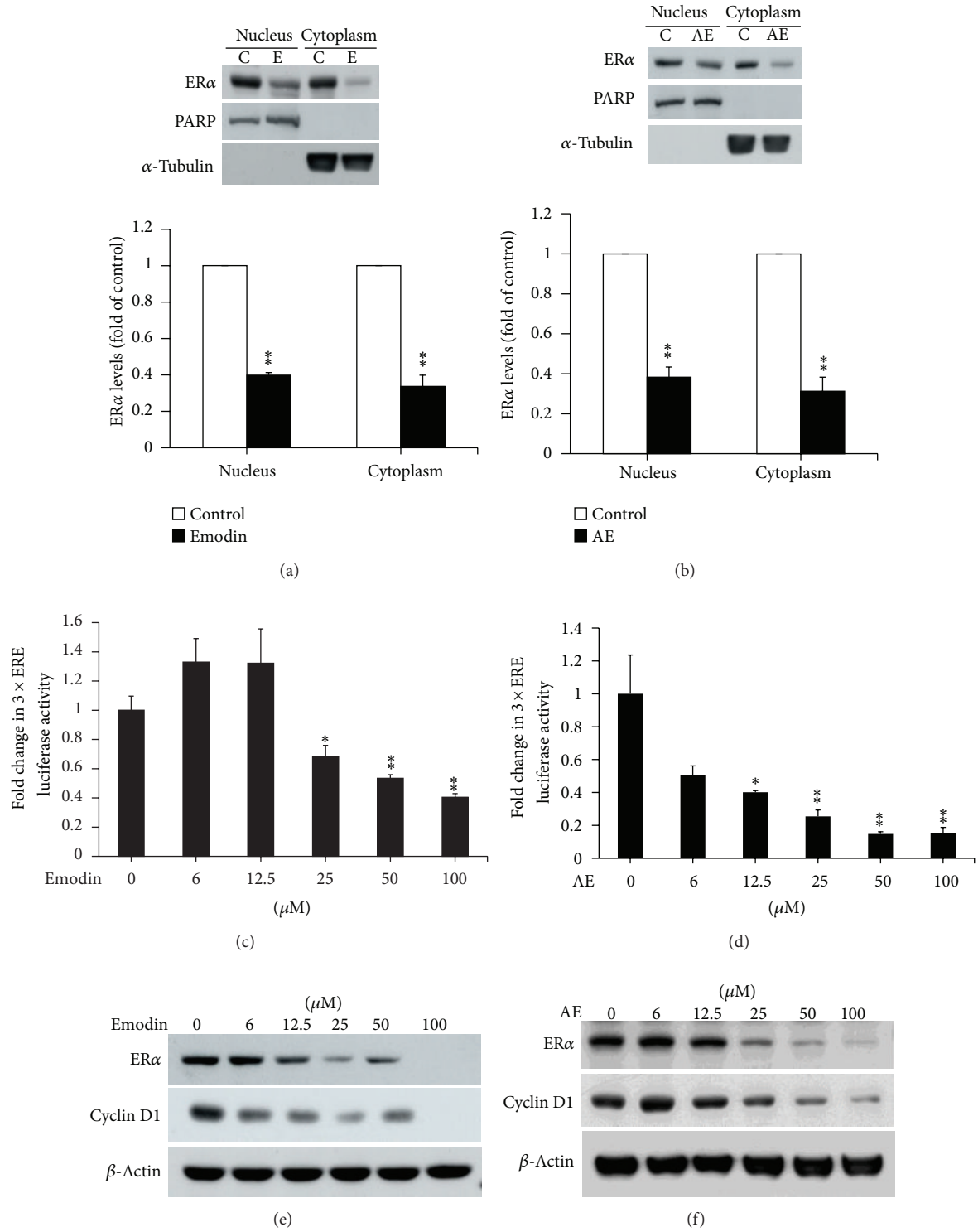

Figure 3: Emodin and aloe-emodin diminish both nuclear and cytoplasmic ERα levels and transcriptional activity. MCF-7 cells were treated with 25 μM emodin (a) or aloe-emodin (b) for 24 h prior to cell lysis and protein fractionation as described in Section 2. ERα protein was detected by western blotting, and PARP and α-tubulin served as markers for the nuclear and cytoplasmic fractions, respectively. The quantification of ERα levels was presented as fold increase or decrease relative to controls and was evaluated in three independent experiments. The effects of emodin (c) and aloe-emodin (d) on ERα activation were evaluated using a 3 × ERE- (estrogen-responsive element-) containing luciferase reporter assay in MCF-7 cells for 48 h. β-galactosidase expression served as the internal control. The data were presented as the fold change compared to control levels (0 μM). The results were presented as the mean ± SEM. * and ** correspond to $P < 0.05$ and $P < 0.01$, respectively, versus control group. MCF-7 cells were treated with emodin (e) or aloe-emodin (f) in a dose-dependent manner for 48 h, and the expressions of ERα-regulated protein cyclin D1 were detected by western blotting.

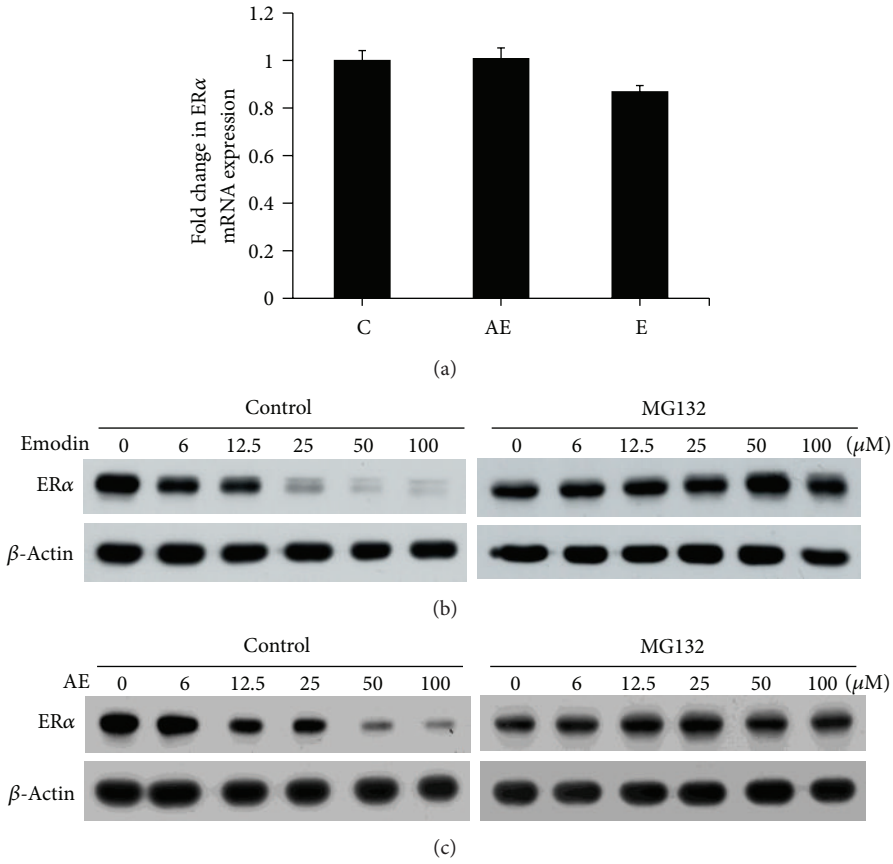

Figure 4: Emodin and aloe-emodin decrease ERα protein levels by promoting protein degradation. (a) MCF-7 cells were treated with 25 μM of emodin or aloe-emodin for 24 h prior to quantitative real-time PCR to assess ERα mRNA expression. Data were presented as the fold change compared to control levels. The experiments were performed in triplicate, and each condition was replicated four times within each experiment. The results are presented as the mean ± SEM. (b, c) MCF-7 cells were treated with various concentrations of emodin or aloe-emodin in the presence of MG132 (proteasome inhibitor, 5 μM) for 24 h. ERα protein levels were detected by western blotting. β-Actin was used as an internal control.

growth [26, 27]. Tamoxifen is designed to interfere with E2 binding and thus block ERα transcriptional activity to treat ERα-dependent diseases such as breast cancer [28]. However, alternative compounds that are safer and associated with fewer side effects than Tamoxifen are desired. Numerous studies suggest that phytoestrogens possess organ-specific estrogenic and antiestrogenic effects [29]. Phytoestrogens mainly consist of isoflavones, such as genistein and daidzein, and are used in the treatment of menopausal symptoms as well as breast cancer [30, 31]. In this study, we provide evidence indicating that two phytoestrogens, emodin and aloe-emodin, might significantly inhibit the proliferation of ERα-positive breast cancer cells through ERα degradation. Although both drugs had dose-responsive effects on inhibiting proliferation of breast cancer cells, low doses (25 μM or less) of aloe-emodin could not affect proliferation of ERα-negative cells (Figure 1(f)). Therefore, 25 μM of drugs were utilized in other experiments (Figure 3 to Figure 6). Interestingly, both compounds had inhibitory effects on ERα, but they utilized different inhibitory mechanisms. Aloe-emodin inhibited ERα activation through HSP90/ERα dissociation and ubiquitin-dependent degradation, whereas emodin did not share the same molecular pathway. Therefore, these findings illustrate that emodin and aloe-emodin might serve as estrogen receptor modulators with different molecular mechanisms. The therapeutic application of these two compounds should be investigated further in the future.

Anthraquinones are phytoestrogens that have been demonstrated to possess anticancer properties through the inhibition of cell proliferation, the induction of apoptosis, and the prevention of metastasis [1]. The effects of the anthraquinone derivatives emodin and aloe-emodin have been extensively investigated in several cancer types through studies on their signaling targets. Emodin has been reported to sensitize Her2/neu-overexpressing lung cancer cells to chemotherapeutic treatments and to suppress Her2/neu-overexpressing breast cancer growth by inhibiting tyrosine kinase activity [32–34]. Notably, emodin has been shown to downregulate androgen receptor (AR) and inhibit prostate cancer growth [5], suggesting that there is a connection between anthraquinone derivatives and steroid receptor in hormone-related cancers. Although the estrogenic ability of emodin is higher than that of aloe-emodin, as determined by ERα binding studies, the antiproliferation effect

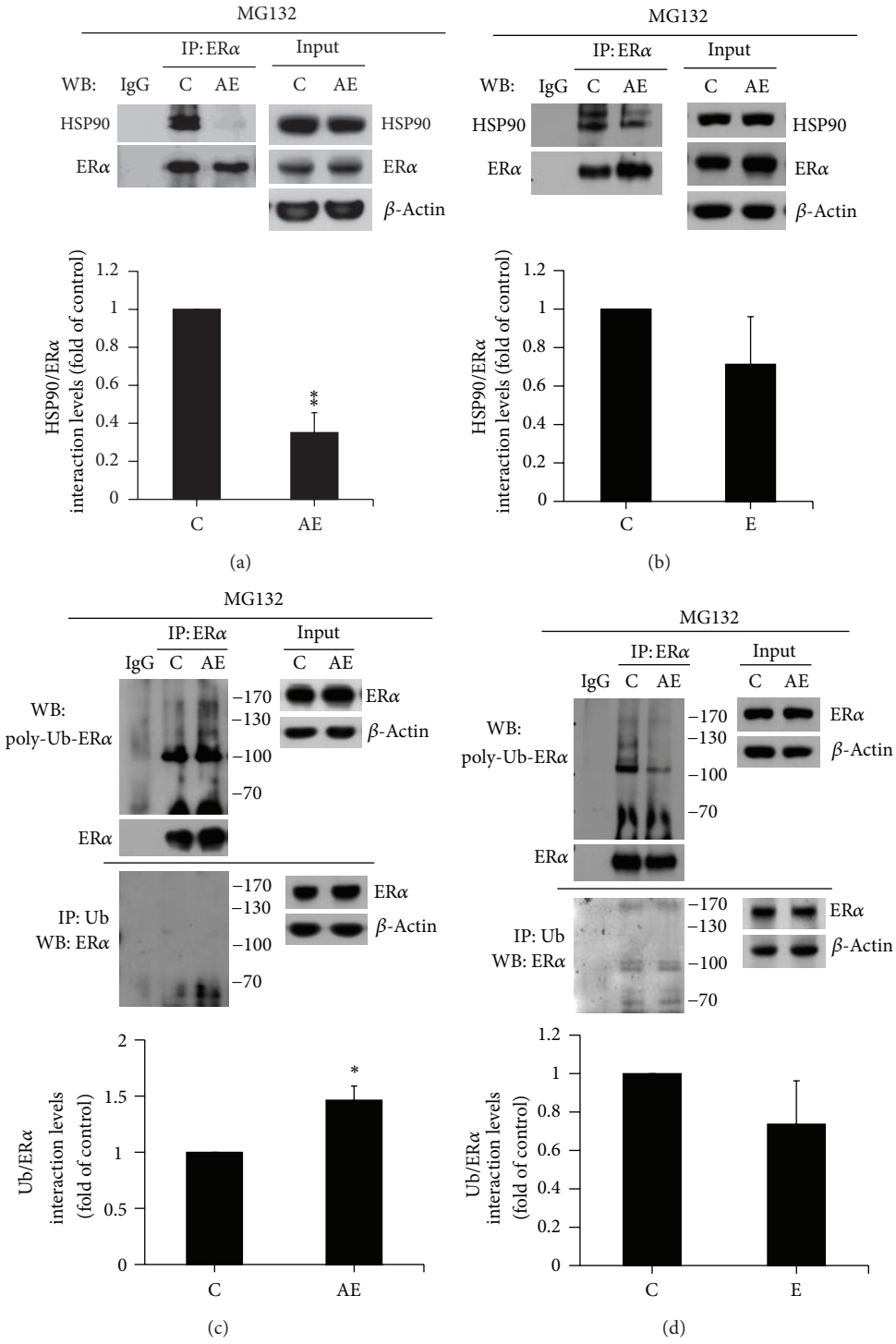

Figure 5: Only aloe-emodin promotes the dissociation of HSP90/ERα and subsequent ERα ubiquitination. The interaction between ERα and HSP90 in MCF-7 cells following 25 μM treatment of aloe-emodin (a) or emodin (b) in the presence of MG132 (5 μM) for 24 h was evaluated by ERα immunoprecipitation followed by western blotting for HSP90 with specific antibodies. The ubiquitin-conjugated ERα levels in MCF-7 cells following 25 μM treatment of aloe-emodin (c) and emodin (d) in the presence of MG132 (5 μM) were examined by immunoprecipitation with anti-ERα or antiubiquitin antibodies followed by western blotting. The lysates were used in the western blotting experiments to indicate protein levels. Immunoprecipitation by IgG served as a negative control. β-Actin served as an internal control for western blotting. The quantitative data were obtained from the results of three times immunoprecipitation experiments and presented as fold change of control. The quantitative graphs were presented as the mean ± SEM. * and ** correspond to $P < 0.05$ and $P < 0.01$, respectively, versus the control group.

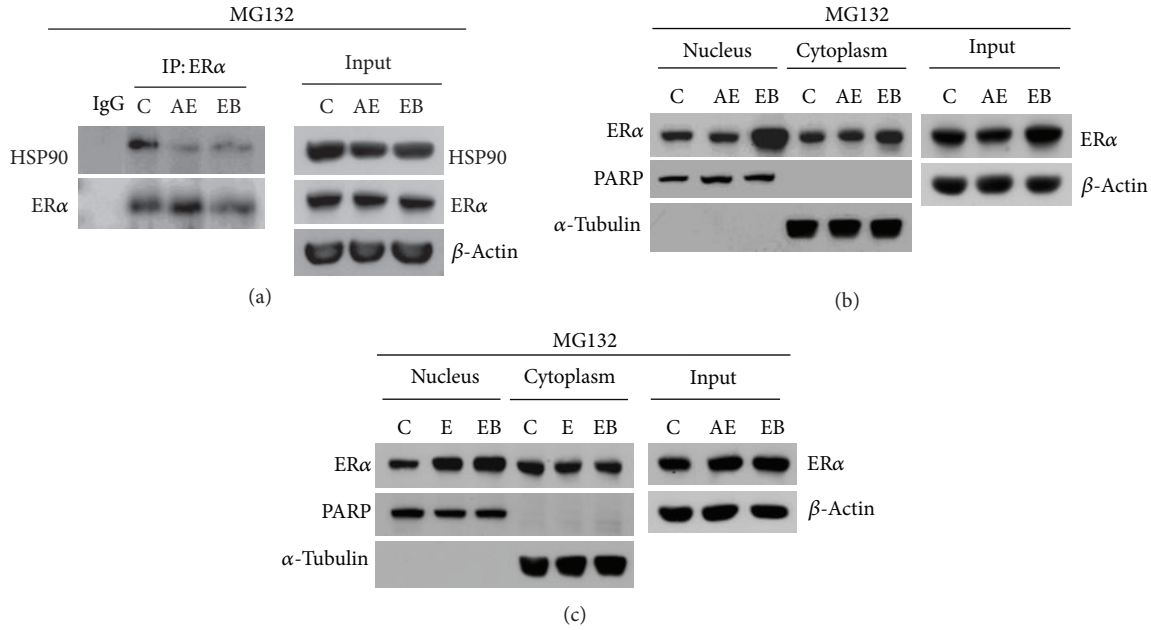

Figure 6: Effects of aloe-emodin and emodin on ERα subcellular distribution in comparison to EB. (a, b) MCF-7 cells were treated with aloe-emodin (25 μM) or estradiol benzoate ((EB) 10 nM) in the presence of MG132 (5 μM) for 24 h. The interaction between HSP90 and ERα was evaluated by ERα immunoprecipitation followed by western blotting of HSP90 with specific antibodies. Immunoprecipitation by IgG served as a negative control. The fractionation of cellular proteins was performed, and ERα protein was detected by western blotting. (c) MCF-7 cells were treated with emodin (25 μM) or EB (10 nM) in the presence of MG132 (5 μM) for 24 h. The fractionation of cellular proteins was performed, and ERα protein was detected by western blotting. PARP and α-tubulin served as markers for the nuclear and cytoplasmic fractions, respectively. The lysates were used in the western blotting experiments to indicate protein levels. β-Actin served as an internal control for western blotting.

of aloe-emodin is more efficient than that of emodin in breast cancer cells [7]. Kang et al. also showed that the cytotoxicity of aloe-emodin is higher in ERα-positive cells than in ERα-negative cells [7]. These observations suggest that aloe-emodin might be a stronger inhibitor of ERα-positive cancer cell growth than emodin.

The goal of this study was to investigate the differences between emodin and aloe-emodin in their efficiency and mechanism of blocking breast cancer cell growth. Our data showed that aloe-emodin is a more potent growth inhibitor than emodin and has a unique mechanism for the growth inhibition of breast cancer cells. MCF-7 cell growth was abolished following treatment with 12.5 μM aloe-emodin for 6 days, and only 50% of cells survived at 25 μM aloe-emodin treatment for 4 days (Figure 1(b)). Although a previous study suggested that the IC_{50} of aloe-emodin is 12.6 ± 0.83 μg/mL (approximately 46 μM) on MCF-7 cells [7], the IC_{50} of aloe-emodin in our system was only approximately 25 μM (Figure 1(d)). With regard to side effects on normal cells, the previous report indicated that 25 μM aloe-emodin is a more significant proliferation inhibitor in human skin epidermoid carcinoma cells than in noncancerous cells [35]. However, aloe-emodin did not significantly affect the proliferation of MDA-MB-453 ERα-negative cells (Figure 1(f)). The overexpression of ERα in MCF-7 cells increased the sensitivity to aloe-emodin treatment (Figure 1(h)). These results are consistent with previous findings that aloe-emodin has a higher cytotoxic potential to MCF-7 (ERα-positive) cells than to MDA-MB-231 (ERα-negative) cells [7]. A low dosage (10 μM) of aloe-emodin [6] showed that both cell growth (Figures 1(b) and 1(d)) and ERα activation (Figure 3(d)) were significantly repressed by aloe-emodin in a dose-dependent manner, even at low dosages (6 μM). Additionally, aloe-emodin treatment reduced ERα protein levels not only in total lysates (Figures 2(c) and 2(d)) but also in nuclear and cytoplasmic fractions (Figure 3(b)). In the nuclear and cytoplasmic fractions, the impact of aloe-emodin treatment on cytoplasmic ERα levels seems stronger than that on nuclear ERα levels (Figure 3(b)). As shown in Figures 2 and 4, we conclude that the decrease in ERα levels induced by aloe-emodin was due to protein degradation. This correlates with ERα proteasome-dependent degradation because of the observed elevation in ubiquitin-conjugated levels (Figure 5(c)). Interestingly, the dissociation of ERα and HSP90 was increased by aloe-emodin treatment (Figure 5(a)), and ERα released from HSP90 protection was subjected to ubiquitination for degradation rather than translocation to the nucleus for activation (Figure 6(b)). These phenomena are similar to the actions of antiestrogens such as ICI 164384, ICI 182780, and RU 58668, which may induce ERα degradation and result in rapid turnover [24]. As a ligand with an inhibitory effect on ERα, we suggest that aloe-emodin might qualify as an estrogen receptor modulator to negatively regulate ERα activity and inhibit breast cancer cell growth.

The effect of emodin was also investigated in this study. Although the inhibitory effects of emodin on breast cancer growth and ERα activation were similar to those of aloe-emodin, the molecular mechanism of emodin inhibition was unexpectedly distinct. In Figures 1(a) and 1(c), the inhibitory potency of emodin on MCF-7 cell growth was lower than that of aloe-emodin (Figures 1(b) and 1(d)). Interestingly, emodin significantly suppressed cell proliferation of the ERα-negative cell line MDA-MB-453 (Figure 1(e)). Because emodin may act as a tyrosine kinase inhibitor by inhibiting the binding of Her2/neu and HSP90, thereby depleting Her2/neu via proteasomal degradation [36], it is possible that emodin might differ in its effect on the growth of MDA-MB-453 cells (which are characterized by Her2 overexpression) in ERα-independent regulation in comparison to aloe-emodin. Like aloe-emodin, emodin targeted ERα by proteasomal degradation (Figures 2 and 4); however, the degradation pathway was independent of HSP90/ERα dissociation and ubiquitination (Figures 5(b) and 5(d)). Although the ubiquitin-proteasome degradation is an important process for modulation of many proteins, recent studies demonstrate that the proteasome-dependent protein degradation possibly goes through ubiquitination-independent pathway [37, 38]. Previous reports indicate that the estrogenic activity of emodin is higher than that of aloe-emodin [6, 7]. Our ERE reporter assay results showed that emodin induced the inhibition of ERα activation only at high dosages (over 25 μM, Figure 3(c)), whereas the aloe-emodin data showed inhibitory effects starting at low dosages (6 μM, Figure 3(d)). Notably, emodin treatment led to a slight increase in ERα activation at 6 and 12.5 μM, which differed from the aloe-emodin treatment results (Figure 3(c)). Unlike aloe-emodin, emodin treatment elevated nuclear ERα protein levels in the presence of MG132, similar to the effects of estradiol benzoate (EB) treatment (Figure 6(c)). Taken together with the data in Figure 3(a), we suggest that emodin, using a distinct mechanism from aloe-emodin, might cause ERα shuttling into the nucleus and subsequently promote nuclear ERα degradation through ubiquitination-independent pathway, whereas cytoplasmic ERα is less affected. This hypothesis is similar to previous studies indicating that the chemical structure of the ligand directly affects the nuclear fate and protein turnover rate of ERα independently of transcriptional regulation [39]. These observations suggest that the essential difference between emodin and aloe-emodin lies in the mechanism of ERα regulation and Her2 inhibition.

In conclusion, we provide evidence showing that the anticancer mechanisms of the anthraquinone derivatives emodin and aloe-emodin are mediated via an ERα-dependent pathway in breast cancer cells. Although emodin and aloe-emodin display distinct differences in efficiency and ERα activation mechanism on breast cancer cell growth, both compounds are potential selectively therapeutic treatments for breast cancer.

Abbreviations

ERα: Estrogen receptor α
HSP90: Heat shock protein 90
AE: Aloe-emodin
E: Emodin.

Conflict of Interests

The authors declare that they have no conflict of interests.

Acknowledgments

The authors thank Dr. H. C. Chen, Dr. T. H. Lee, Dr. Y. M. Liou, Dr. J. W. Chen, and Dr. H. C. Cheng (National Chung Hsing University, Taiwan) for technical support. This work was supported by the following Grants: NSC100-2320-B-005-002 and NSC101-2320-B-005-004-MY3 from the Taiwan National Science Council (to H. Lin); Taichung Veterans General Hospital/National Chung Hsing University Joint Research Program (TCVGH-NCHU1017607 and TCVGH-NCHU1027606); Chang Bing Show Chwan Memorial Hospital Research Grant (CBBC001, to Y.-T. Lee); and the Taiwan Ministry of Education under the Aiming for the Top University plan.

References

[1] Q. Huang, G. Lu, H.-M. Shen, M. C. M. Chung, and N. O. Choon, "Anti-cancer properties of anthraquinones from rhubarb," *Medicinal Research Reviews*, vol. 27, no. 5, pp. 609–630, 2007.

[2] A. Dutta, S. Bandyopadhyay, C. Mandal, and M. Chatterjee, "Aloe vera leaf exudate induces a caspase-independent cell death in *Leishmania donovani* promastigotes," *Journal of Medical Microbiology*, vol. 56, no. 5, pp. 629–636, 2007.

[3] H.-H. Wang and J.-G. Chung, "Emodin-induced inhibition of growth and DNA damage in the *Helicobacter pylori*," *Current Microbiology*, vol. 35, no. 5, pp. 262–266, 1997.

[4] C.-H. Chang, C.-C. Lin, J.-J. Yang, T. Namba, and M. Hattori, "Anti-inflammatory effects of emodin from *Ventilago leiocarpa*," *American Journal of Chinese Medicine*, vol. 24, no. 2, pp. 139–142, 1996.

[5] T.-L. Cha, L. Qiu, C.-T. Chen, Y. Wen, and M.-C. Hung, "Emodin down-regulates androgen receptor and inhibits prostate cancer cell growth," *Cancer Research*, vol. 65, no. 6, pp. 2287–2295, 2005.

[6] H. Matsuda, H. Shimoda, T. Morikawa, and M. Yoshikawa, "Phytoestrogens from the roots of *Polygonum cuspidatum* (Polygonaceae): structure-requirement of hydroxyanthraquinones for estrogenic activity," *Bioorganic and Medicinal Chemistry Letters*, vol. 11, no. 14, pp. 1839–1842, 2001.

[7] S. C. Kang, C. M. Lee, E. S. Choung et al., "Anti-proliferative effects of estrogen receptor-modulating compounds isolated from *Rheum palmatum*," *Archives of Pharmacal Research*, vol. 31, no. 6, pp. 722–726, 2008.

[8] F. Acconcia and R. Kumar, "Signaling regulation of genomic and nongenomic functions of estrogen receptors," *Cancer Letters*, vol. 238, no. 1, pp. 1–14, 2006.

[9] S. Ali and R. C. Coombes, "Endocrine-responsive breast cancer and strategies for combating resistance," *Nature Reviews Cancer*, vol. 2, no. 2, pp. 101–112, 2002.

[10] C. K. Osborne, "Tamoxifen in the treatment of breast cancer," *The New England Journal of Medicine*, vol. 339, no. 22, pp. 1609–1618, 1998.

[11] G. A. Colditz, S. E. Hankinson, D. J. Hunter et al., "The use of estrogens and progestins and the risk of breast cancer in postmenopausal women," *The New England Journal of Medicine*, vol. 332, no. 24, pp. 1589–1593, 1995.

[12] H. Adlercreutz and W. Mazur, "Phyto-oestrogens and Western diseases," *Annals of Medicine*, vol. 29, no. 2, pp. 95–120, 1997.

[13] M. C. Chen, C. Y. Huang, S. L. Hsu et al., "Retinoic acid Induces apoptosis of prostate cancer DU145 cells through Cdk5 overactivation," *Evidence-Based Complementary and Alternative Medicine*, vol. 2012, Article ID 580736, 11 pages, 2012.

[14] H. Lin and P. S. Wang, "Inhibitory effects of digoxin on testosterone production in rat Leydig cells," *Adaptive Medicine*, vol. 4, pp. 165–172, 2012.

[15] H. Lin, T.-Y. Lin, and J.-L. Juang, "Abl deregulates Cdk5 kinase activity and subcellular localization in *Drosophila* neurodegeneration," *Cell Death and Differentiation*, vol. 14, no. 3, pp. 607–615, 2007.

[16] H. Lin, M.-C. Chen, C.-Y. Chiu, Y.-M. Song, and S.-Y. Lin, "Cdk5 regulates STAT3 activation and cell proliferation in medullary thyroid carcinoma cells," *Journal of Biological Chemistry*, vol. 282, no. 5, pp. 2776–2784, 2007.

[17] H. Lin, M.-C. Chen, and C.-T. Ku, "Cyclin-dependent kinase 5 regulates steroidogenic acute regulatory protein and androgen production in mouse Leydig cells," *Endocrinology*, vol. 150, no. 1, pp. 396–403, 2009.

[18] H. Lin, J.-L. Juang, and P. S. Wang, "Involvement of Cdk5/p25 in digoxin-triggered prostate-cancer cell apoptosis," *Journal of Biological Chemistry*, vol. 279, no. 28, pp. 29302–29307, 2004.

[19] F.-N. Hsu, M.-C. Chen, M.-C. Chiang et al., "Regulation of androgen receptor and prostate cancer growth by cyclin-dependent kinase 5," *Journal of Biological Chemistry*, vol. 286, no. 38, pp. 33141–33149, 2011.

[20] M.-C. Chen, S.-W. Wang, S.-F. Kan, S.-C. Tsai, Y.-C. Wu, and P. S. Wang, "Stimulatory effects of propylthiouracil on pregnenolone production through upregulation of steroidogenic acute regulatory protein expression in rat granulosa cells," *Toxicological Sciences*, vol. 118, no. 2, Article ID kfq302, pp. 667–674, 2010.

[21] M. Dalvai and K. Bystricky, "Cell cycle and anti-estrogen effects synergize to regulate cell proliferation and er target gene expression," *PLoS One*, vol. 5, no. 6, Article ID e11011, 2010.

[22] N. Heldring, A. Pike, S. Andersson et al., "Estrogen receptors: how do they signal and what are their targets," *Physiological Reviews*, vol. 87, no. 3, pp. 905–931, 2007.

[23] Y. Miyoshi, K. Murase, M. Saito, M. Imamura, and K. Oh, "Mechanisms of estrogen receptor-α upregulation in breast cancers," *Medical Molecular Morphology*, vol. 43, no. 4, pp. 193–196, 2010.

[24] M. Fan, A. Park, and K. P. Nephew, "CHIP (carboxyl terminus of Hsc70-interacting protein) promotes basal and geldanamycin-induced degradation of estrogen receptor-α," *Molecular Endocrinology*, vol. 19, no. 12, pp. 2901–2914, 2005.

[25] R. A. Walker, "Oestrogen receptor and its potential role in breast cancer development," *The Journal of Pathology*, vol. 188, no. 3, pp. 229–230, 1999.

[26] D. J. Mangelsdorf, C. Thummel, M. Beato et al., "The nuclear receptor super-family: the second decade," *Cell*, vol. 83, no. 6, pp. 835–839, 1995.

[27] J. M. Hall, J. F. Couse, and K. S. Korach, "The multifaceted mechanisms of estradiol and estrogen receptor signaling," *Journal of Biological Chemistry*, vol. 276, no. 40, pp. 36869–36872, 2001.

[28] V. C. Jordan, "Tamoxifen (ICI46,474) as a targeted therapy to treat and prevent breast cancer," *British Journal of Pharmacology*, vol. 147, no. 1, pp. S269–S276, 2006.

[29] A. L. Murkies, G. Wilcox, and S. R. Davis, "Phytoestrogens," *Journal of Clinical Endocrinology and Metabolism*, vol. 83, no. 2, pp. 297–303, 1998.

[30] E. Nikander, A. Kilkkinen, M. Metsä-Heikkilä et al., "A randomized placebo-controlled crossover trial with phytoestrogens in treatment of menopause in breast cancer patients," *Obstetrics and Gynecology*, vol. 101, no. 6, pp. 1213–1220, 2003.

[31] Y. Imai, S. Tsukahara, S. Asada, and Y. Sugimoto, "Phytoestrogens/flavonoids reverse breast cancer resistance protein/ABCG2-mediated multidrug resistance," *Cancer Research*, vol. 64, no. 12, pp. 4346–4352, 2004.

[32] H. Jayasuriya, N. M. Koonchanok, R. L. Geahlen, J. L. McLaughlin, and C.-J. Chang, "Emodin, a protein tyrosine kinase inhibitor from *Polygonum cuspidatum*," *Journal of Natural Products*, vol. 55, no. 5, pp. 696–698, 1992.

[33] L. Zhang, C.-J. Chang, S. S. Bacus, and M.-C. Hung, "Suppressed transformation and induced differentiation of HER-2/neu-overexpressing breast cancer cells by emodin," *Cancer Research*, vol. 55, no. 17, pp. 3890–3896, 1995.

[34] L. Zhang and M.-C. Hung, "Sensitization of HER-2/neu-overexpressing non-small cell lung cancer cells to chemotherapeutic drugs by tyrosine kinase inhibitor emodin," *Oncogene*, vol. 12, no. 3, pp. 571–576, 1996.

[35] T.-H. Chou and C.-H. Liang, "The molecular effects of Aloe-Emodin (AE)/liposome-AE on human nonmelanoma skin cancer cells and skin permeation," *Chemical Research in Toxicology*, vol. 22, no. 12, pp. 2017–2028, 2009.

[36] Y.-Y. Yan, L.-S. Zheng, X. Zhang et al., "Blockade of Her2/neu binding to Hsp90 by emodin azide methyl anthraquinone derivative induces proteasomal degradation of Her2/neu," *Molecular Pharmaceutics*, vol. 8, no. 5, pp. 1687–1697, 2011.

[37] Y. Murakami, S. Matsufuji, T. Kameji et al., "Ornithine decarboxylase is degraded by the 26S proteasome without ubiquitination," *Nature*, vol. 360, no. 6404, pp. 597–599, 1992.

[38] G. Asher and Y. Shaul, "p53 proteasomal degradation: poly-ubiquitination is not the whole story," *Cell Cycle*, vol. 4, no. 8, pp. 1015–1018, 2005.

[39] S. Kocanova, M. Mazaheri, S. Caze-Subra, and K. Bystricky, "Ligands specify estrogen receptor alpha nuclear localization and degradation," *BMC Cell Biology*, vol. 11, article 98, 2010.

Hindawi Publishing Corporation
Evidence-Based Complementary and Alternative Medicine
Volume 2013, Article ID 468537, 8 pages
http://dx.doi.org/10.1155/2013/468537

Research Article

Ocotillol Enhanced the Antitumor Activity of Doxorubicin via p53-Dependent Apoptosis

Hongbo Wang,[1] Pengfei Yu,[1] Jing Bai,[1] Jianqiao Zhang,[1] Liang Kong,[1] Fangxi Zhang,[1,2] Guangying Du,[1] Shiqian Pei,[1] Lixia Zhang,[3] Yongtao Jiang,[1] Jingwei Tian,[1] and Fenghua Fu[1]

[1] *Key Laboratory of Molecular Pharmacology and Drug Evaluation, Ministry of Education of China, School of Pharmacy, Yantai University, Yantai 264005, China*
[2] *State Key Laboratory of Long-Acting and Targeting Drug Delivery Technologies, Luye Pharma Group Ltd., Yantai 264003, China*
[3] *Center of Basic Medicine, Binzhou Medical College, Yantai 264005, China*

Correspondence should be addressed to Jingwei Tian; tianjingwei@luye.cn and Fenghua Fu; fufenghua@sohu.com

Received 15 March 2013; Revised 23 May 2013; Accepted 28 May 2013

Academic Editor: Gautam Sethi

The use of doxorubicin (Dox) was severely constrained by dose-dependent side effects, which might be attenuated by combining a "sensitizer" to decrease its cumulative dosage. In this study, it was investigated whether ocotillol could enhance the antiproliferation activity of Dox. MTT assays and xenograft tumor model were firstly conducted to evaluate the effect of ocotillol on the antitumor activity of Dox. Flow cytometry and Hoechst staining assays were then performed to assess cell apoptosis. Western blot and real-time PCR were finally used to detect the expression of p53 and its target genes. Our results showed ocotillol to enhance Dox-induced cell death in p53 wild-type cancer cells. Compared with Dox alone, Dox with ocotillol (Dox-O) could induce much more cell apoptosis and activate p53 to a much greater degree, which in turn markedly increased expression of proapoptosis genes. The enhanced cytotoxic activity was partially blocked by pifithrin-α, which might be through attenuating the increased apoptosis. Furthermore, ocotillol significantly increased the antitumor activity of Dox in A549 xenograft tumor in nude mice. These findings indicated that ocotillol could potentiate the cytotoxic effect of Dox through p53-dependent apoptosis and suggested that coadministration of ocotillol with Dox might be a potential therapeutic strategy.

1. Introduction

Cancer was one of the leading causes of death in the world [1], and chemotherapy, rather than surgery or radiotherapy, remained the most effective strategy for prolonging survival and improving cancer patients' quality of life [2, 3]. Doxorubicin (Dox) was a potential chemotherapeutic agent, and its use was part of several standard regimens for different cancers [4, 5]. Although Dox had been shown to exert robust antitumor activity, its effectiveness was often restricted by drug-resistance and dose-dependent side effects, especially the Dox-induced cardiomyopathy [5, 6]. Therefore, novel combination chemotherapeutic strategy, in which one novel compound was added to increase the therapeutic index of Dox, would definitely benefit the cancer patients.

The mechanisms of action of Dox in inducing apoptosis in cancer cells via p53 activation had been widely investigated [7]. As the gatekeeper of the genome, the tumor repressor p53 was rapidly activated upon Dox-induced DNA damage and functioned as a transcription factor in regulating downstream target genes, such as *PUMA*, *PIG3*, and *BAX* [8, 9]. The novel compounds, which could potentiate the p53 activation after cotreatment with Dox, might work as one "sensitizer" to reduce the "toxic dosage" to "subtoxic dosage" for Dox and prevent the lethal cardiomyopathy. Indeed, several agents, such as IFN-α, inorganic phosphate, and curcumin, were reported to potentiate the antitumor activity of Dox via p53 activation [10–12].

Natural sources, including plants, microorganisms, and halobiotics, provide rich resources for discovery of novel

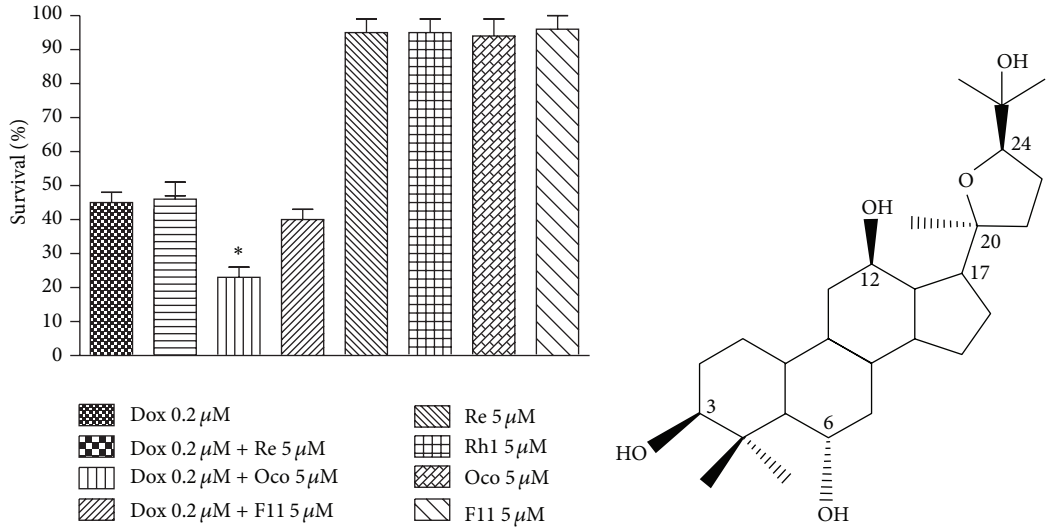

(a) (b)

Figure 1: The effects of four ginsenosides on the cytotoxic activity of Dox in A549 cells. (a) A549 cells were seeded into 96-well plate and treated with Dox (0.2 μM), ginsenoside (5 μM), or the combination as indicated for 72 h. The cell viability was detected by MTT assay after 72 h incubation. (b) Chemical structure of ocotillol. $^{*}P < 0.05$, compared with Dox group.

drugs [13]. Ginseng had a wide range of pharmacological actions, such as neuroprotective, cardioprotective, antioxidant, and anticancer properties, which were primarily attributable to the presence of different ginsenosides [14, 15]. Among which, Ginsenosides Rg3 and Rh2 were reported to enhance antitumor activity and/or decrease the toxic effects of several cytotoxic drugs, such as Dox, paclitaxel and cyclophosphamide [16–19]. As part of our continuing effort to discover novel agents from natural products to improve the therapeutic outcome of Dox, we tested the effects of several ginsenosides on its antitumor activity using MTT assay. Ocotillol (Figure 1(b)), a derivative of pseudoginsenoside F11 from American ginseng, was observed to significantly potentiate the cytotoxic activity of Dox (Figure 1(a)). In this study, we explored the effects of ocotillol on the potency of Dox and its associated mechanism of action.

2. Materials and Methods

2.1. Materials. Ocotillol, prepared from American ginseng by Shandong Engineering Research Center for Natural Drugs, was obtained as white powder and had the molecular formula $C_{30}H_{52}O_5$, MW 492. Purity of the compound used in present study was checked by HPLC and found to be higher than 98.5%. *In vitro*, Ocotillol, Dox (Zhejiang Hisun Pharmaceutical Co., Ltd., China), and pifithrin-α (Biyuntian, China) were dissolved in DMSO and stored at −20°C for less than one month before use. The vehicle, DMSO, was used as a control in all experiments at a maximum concentration of 0.1%. *In vivo*, Ocotillol and DOX were dissolved in 1% carboxymethyl cellulose sodium (CMCS) and 0.9% sodium chloride as proposed dose, respectively.

2.2. Cell Lines and Cell Culture. The human cancer cell lines A549, H1299, MCF7, and PC3 cells, were purchased from Cell Culture Center of Institute of Basic Medical Sciences, Chinese Academy of Medical Sciences. All the cancer cells were cultured in RPMI-1640 or DMEM medium supplemented with 10% fetal calf serum, penicillin (100 U/mL), and streptomycin (100 μg/mL; Gibco BRL, NY, USA) and incubated at 37°C in a humidified air atmosphere containing 5% CO_2. All cells were harvested in the exponentially growing phase.

2.3. Animals. Male nude mice (4~6 weeks old, BALB/c) were purchased from the Institute of Laboratory Animal Science, Chinese Academy of Medical Sciences, and Peking Union Medical College. All of the experiments were performed in accordance with the Guidelines for Care and Use of Experimental Animals of Experimental Animal Research Committee of Yantai University.

2.4. Cell Proliferation Assays. The viability of cell was evaluated using MTT assay as reported previously [20]. Briefly, cells were seeded into 96-well plates and then treated with tested articles at desired concentration for indicated time. MTT solution was added into the wells and incubated for 2 h. After the medium was removed, DMSO was added into each well. The plates were gently agitated until the color reaction was uniform and the OD_{570} was determined using a microplate reader (Wellscan MK3, Finland). Media-only treated cells served to indicate 100% cell viability, and the relative survival was defined as absorbance of treated wells divided by that of controls, in which the 50% inhibitory concentration (IC_{50}) was defined as the concentration that reduced the absorbance by 50% of the controls.

2.5. Flow Cytometry Assay. Cell apoptosis was determined by flow cytometry (FCM) as previously reported [21]. A549 cells were seeded into 6-well plates, and treatments were initiated

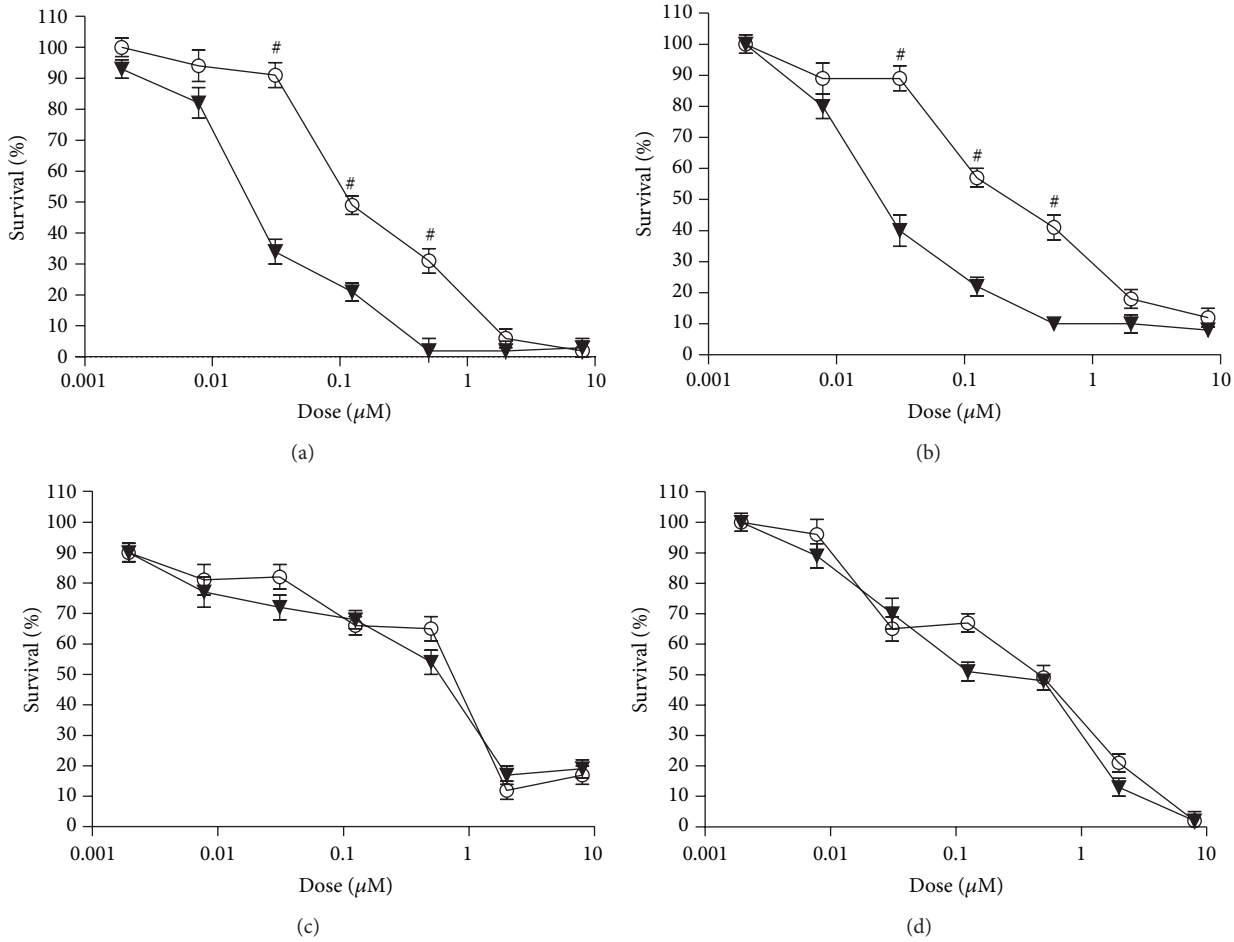

Figure 2: The effects of ocotillol on the cytotoxic activity of Dox in human cancer cells. A549 cells (a), MCF7 cells (b), PC3 cells (c), and H1299 cells (d) were seeded into 96-well plate and treated with Dox (○) or Dox + ocotillol (▼) as indicated. The cell viability was detected by MTT assay after 72 h incubation. $^{\#}P < 0.05$, compared with Dox group.

when cells were 60–70% confluent. Tested articles, diluted in medium, were added into the wells and incubated for 24 h, and then cells were harvested by digesting with trypsin/EDTA (Gibco BRL, NY, USA). After fixed with cold 70% ethanol, the cells were stained with propidium iodide (PI) solution (20 mg/mL PI and 20 mg/mL RNase A in PBS) for 30 min in 37°C. Samples were read on a Coulter Elite flow cytometer, and data were analyzed using Elite software program 4.0.

2.6. Hoechst 33342 Staining Assay. Effects of tested agents on apoptosis were visualized and quantified by immunofluorescence microscopy [22]. A549 cells were plated at 50,000 per well in 6-well cell culture plates with glass slides (Corning Incorporated, USA) and cultured overnight. Agents, diluted in medium, were added to desired concentrations. After 24 h exposure, cells were fixed with 3.7% formaldehyde in PBS for 10 min and stained with Hoechst 33342 solution (10 μg/mL). The slides were washed twice in PBS and fixed onto the microscopic slide. The cell images were taken with a Kodak fluorescence microscope, and the number of apoptosis cells was counted in random fields for at least 1000 cells each group.

2.7. Quantitative Reverse Transcription Polymerase Chain Reaction. Cells were lysed in TRIzol (Invitrogen, USA), and total RNA was prepared as previously described [21]. After reverse transcription using a first-strand cDNA synthesis kit (Fermentas, USA), the cDNA was subjected to real-time polymerase chain reaction (RT-PCR) assays using the ABI 7500 RT-PCR System. Primer sequences were as follows: *PUMA*, F: 5′-CCT GGA GGG TCC TGT ACA ATC T-3′, R: 5′-GCA CCT AAT TGG GCT CCA TCT-3′; *BAX*, F: 5′-TGG AGC TGC AGA GGA TGA TTG-3′, R: 5′-AAA CAT GTC AGC TGC CAC TCG-3′; *PIG3*, F: 5′-TTG AGG CAT CTG GAC ATG TG-3′, R: 5′-GGG TCA ATC CCT CTG GGA TAG-3′; *GADPH (control)*, F: 5′-CAT GTT CCA ATA TGA TTC CAC C-3′, R: 5′-GAT GGG ATT TCC ATT GAT GAC-3′.

2.8. Western Blotting Assay. Cells were collected and prepared for the lysates after incubation, and then the cell lysates were performed to detect the target protein as previously described [21]. Briefly, total cellular proteins were electrophoresed on 10% SDS-polyacrylamide gels, and then the proteins were transferred to a PVDF membrane (Millipore,

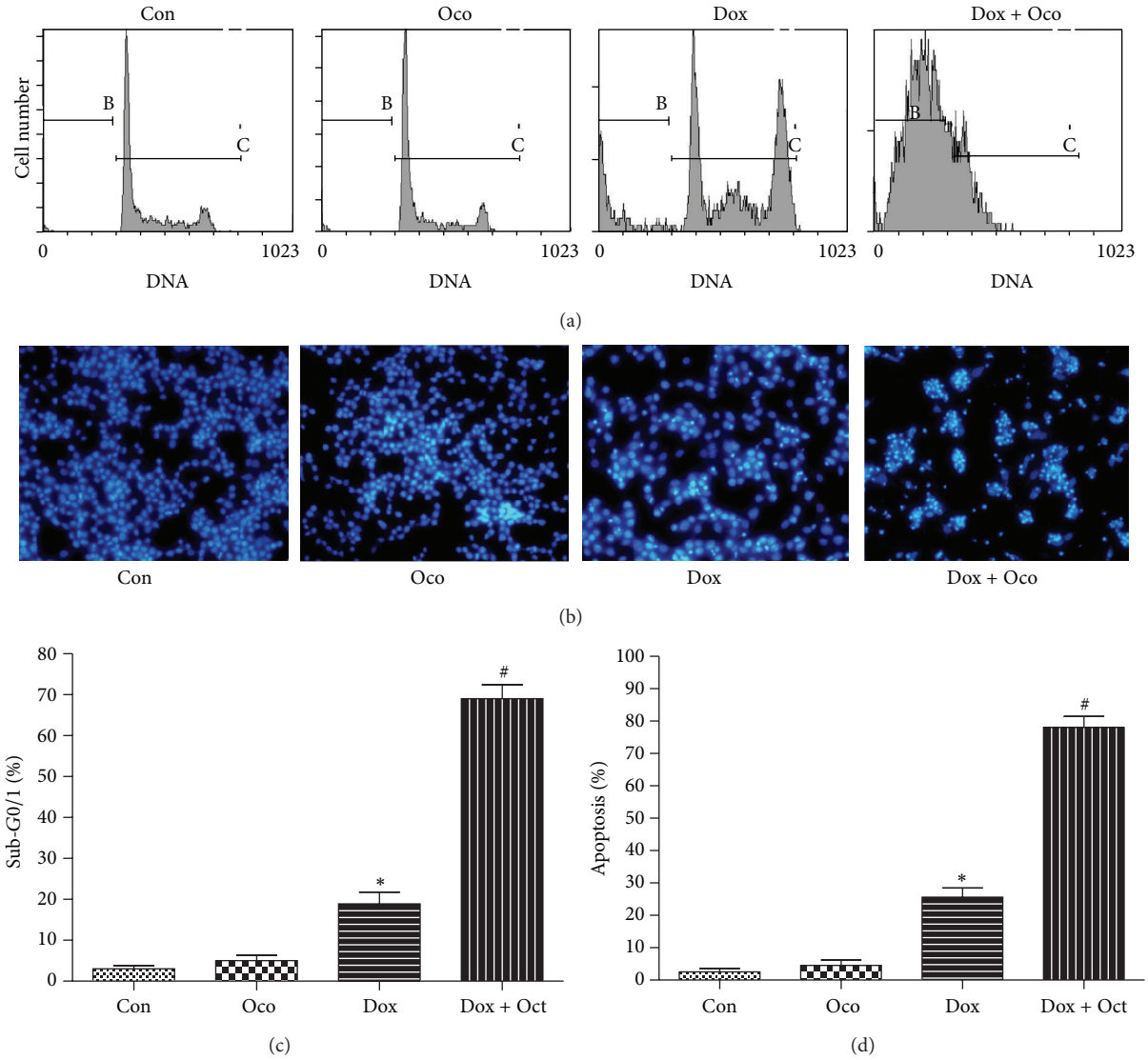

Figure 3: The effects of ocotillol on the cell apoptosis induced by Dox in A549 cells. A549 cells were seeded into 6-well plate and treated with Dox (0.5 μM), Oco (0.5 μM), or the combination for 24 h. The cells were then subjected to flow cytometry assay (a) to determine the percentages of apoptotic cells (c) or to Hoechst staining assays (b). At least 1000 cells were randomly chosen, and the numbers of apoptosis cells (determined by the morphologic observation) were counted (d). $^{*}P < 0.05$, compared with control group; $^{\#}P < 0.05$, compared with Dox group.

USA). After block, the membrane was incubated overnight with primary antibodies to P53 (Do-1, USA) and β-actin (C4, USA). The membranes were washed with TBS-0.05% Tween 20 for 5 min thrice and incubated with secondary antibodies and then visualized with an enhanced chemiluminescence detection kit (Amersham Life Sciences, USA). The film was developed, and the scanned pictures were shown.

2.9. Xenograft Tumor Model in Nude Mice. Male nude mice were introduced to establish xenograft tumor models of A549 as previously described [20]. Briefly, A549 cells were subcutaneously injected at the dorsum with 5×10^6 cells in 0.1 mL, and treatment was started when the tumors reached an average volume of 100~300 mm^3. Animals were randomized into 5 groups with 6 mice each group: (a) vehicle; (b) 10 mg/kg ocotillol; (c) 1.5 mg/kg Dox; (d) 10 mg/kg ocotillol plus 1.5 mg/kg Dox. Ocotillol was administrated by oral gavage, and Dox was injected intraperitoneally, which were at a volume of 10 mL/kg based on individual body weight. The mice were checked daily for toxicity/mortality relevant to treatment, and the tumor was measured with a caliper twice a week for up to endpoint days. The tumor volume in mm^3 was calculated by the formula: volume = (width)^2 $\times$ length/2, and the tumor growth curve was presented.

2.10. Data Analysis and Statistics. The results were presented as mean ± SD. Comparisons between more than 2 groups were performed by analysis of variance (one-way ANOVA),

Table 1: Inhibitory effects of Dox, Oco, or the combination on tumor cell lines.

Cell line	p53 status	IC_{50} (μM)		
		Dox	Dox + Oco 5 μM	Oco
A549	Wild type	0.16 ± 0.01	0.04 ± 0.01	>50
MCF7	Wild type	0.24 ± 0.03	0.05 ± 0.01	>50
PC3	Null	0.27 ± 0.03	0.24 ± 0.02	>50
H1299	Null	0.22 ± 0.04	0.16 ± 0.01	>50

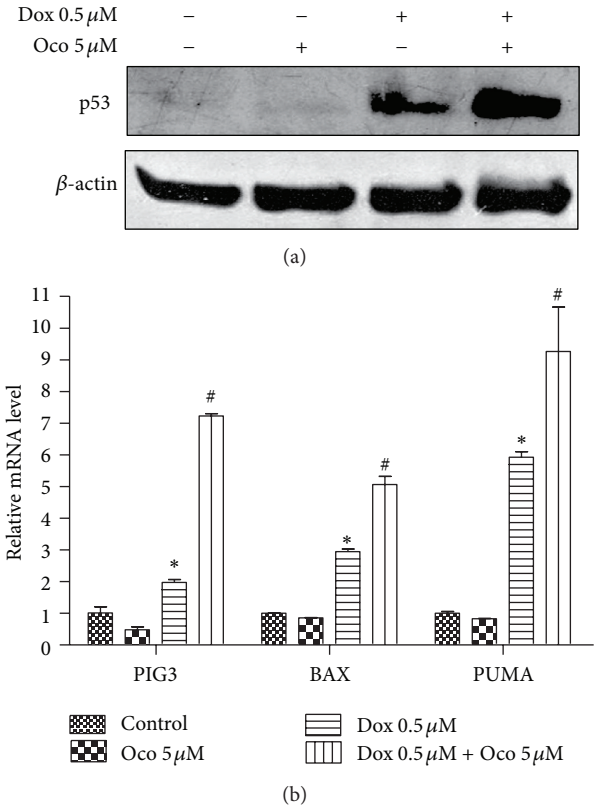

Figure 4: The effects of ocotillol on Dox-induced p53 activation. A549 cells were seeded into 6-well plate and treated with Dox (0.5 μM), Oco (0.5 μM), or the combination for 24 h. The cells were then lysed for immunoblotting to measure expression levels of p53 (a) or lysed for qRT-PCR assays to determine the *BAX*, *PUMA*, and *PIG3* mRNA levels. Data were depicted as average ± SD values of 3 determinations. $^{*}P < 0.05$, compared with control group; $^{\#}P < 0.05$, compared with Dox group.

followed by Students t-test. The level of statistical significance was defined as $P \leq 0.05$, unless indicated otherwise.

3. Results

3.1. Ocotillol Enhanced the Cytotoxic Activity of Dox in p53 Wild-Type Cancer Cells. A series of MTT assays were performed to explore the effect of ocotillol on the anti-tumor activity of Dox in four cancer cells, such as A549, MCF7, PC3, and H1299. After 72 h incubation, Dox did display robust cytotoxic effect against all the tested cells *in vitro* (Figure 2 and Table 1). Interestingly, cotreatment with ocotillol at concentration of 5 μM, which alone had no effect on cell proliferation, enhanced the cytotoxic effect of Dox in A549 and MCF7 cells (Figures 2(a) and 2(b)). The enhanced effects, however, were not observed in p53-null cells, such as PC3 and H1299 cell lines (Figures 2(c) and 2(d)). The IC_{50} values were calculated and shown in Table 1.

3.2. Ocotillol Potentiated Dox-Induced Cell Apoptosis. FCM and Hoechst staining assays were then performed to detect the effect of Dox-O on cell apoptosis in A549 cells. As shown by FCM, the ratio of cells in sub-G0 phase, in which they were considered to be undergoing apoptosis, was significantly increased after Dox treatment for 24 h (Figures 3(a) and 3(c)). Ocotillol (5 μM) alone had no effect on apoptosis but dramatically increased the ratio of cells in sub-G0 after being cotreated with Dox ($P < 0.01$, compared with the Dox only group). Similar results were found in Hoechst staining assay (Figure 3(b)), in which apoptotic cells were observed with characteristic morphologic characteristics, such as nucleic shrinkage. Apoptosis increased after Dox treatment for 24 h ($P < 0.01$, compared to control group); cells cotreated with Dox-O showed dramatically increased apoptosis (Figure 3(d), $P < 0.01$, compared to the Dox only group). Ocotillol alone had no effect on apoptosis at the tested concentration.

3.3. Dox with Ocotillol Enhanced the Activation of p53. Dox dramatically increased p53 protein levels in A549 cells (Figure 4(a)), which in turn increased the induction of its downstream target genes, such as *BAX*, *PUMA*, and *PIG3* (Figure 4(b), $P < 0.01$, compared with control group). However, DOX-O activated p53 to a greater extent, which enhanced mRNA expression of *PUMA*, *BAX*, and *PIG3* (Figure 4(b), $P < 0.01$, compared with Dox alone group). Ocotillol at tested concentration had no obviously effect on the mRNA expression of *PUMA*, *BAX* but decreased mRNA expression of *PIG3*.

3.4. Ocotillol Enhanced Potency of Dox in a p53-Dependent Pathway. Pifithrin-α, a p53 inhibitor, is often used to explore the p53 signal pathway [23]. As shown in Figure 5, the increased proapoptosis genes induced by Dox-O, such as *BAX*, *PUMA*, and *PIG3*, were significantly attenuated by being coincubated with pifithrin-α (Figure 5(a), $P < 0.01$, compared with Dox-O group). FCM (Figure 5(b)) and

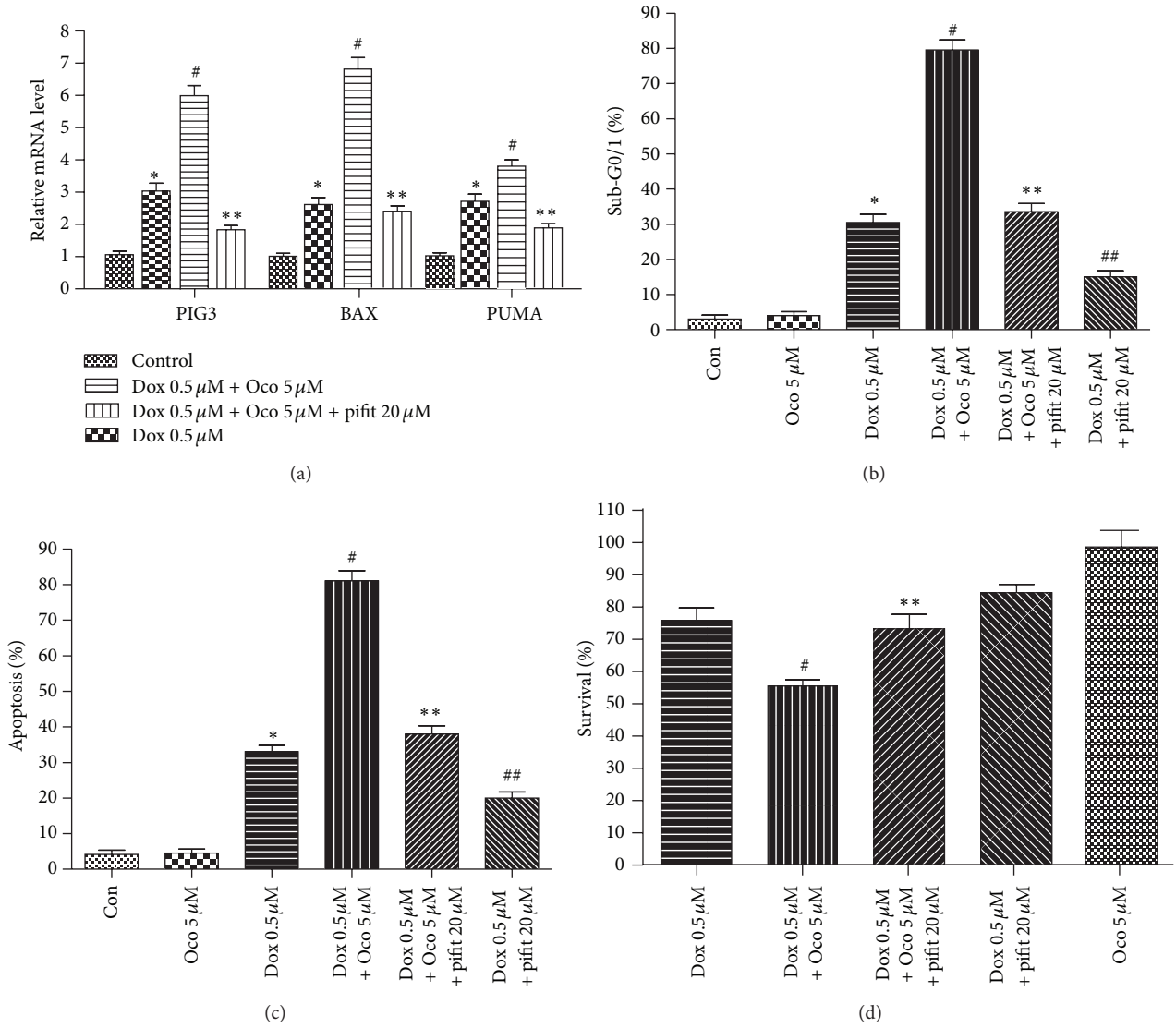

Figure 5: The effects of pifithrin-α on the cytotoxic activity of Dox-O in A549 cells. (a) A549 cells were seeded into 6-well plate and treated with as indicated for 24 h. The cells were then lysed for qRT-PCR assays to determine the *PUMA*, *PIG3*, and *BAX* mRNA levels. (b) and (c) A549 cells were treated as indicated for 24 h and subjected to flow cytometry (b) or Hoechst staining (c) to determine percentages of apoptotic cells. (d) A549 cells were treated as indicated, and the cell viability was detected by MTT assay after 24 h incubation. $^{*}P < 0.05$, compared with control group; $^{\#}P < 0.05$, compared with Dox group. $^{**}P < 0.05$, compared with Dox plus ocotillol group; $^{\#\#}P < 0.05$, compared with Dox group.

Hoechst staining (Figure 5(c)) showed pifithrin-α to significantly suppress the increased apoptosis in the Dox-O group ($P < 0.01$, compared with Dox-O group). As a result, the enhanced cytotoxic activity of Dox-O was dramatically attenuated when cotreated with pifithrin-α (Figure 5(d), $P < 0.01$, compared with Dox-O group).

3.5. Ocotillol Potentiated the Anti-Tumor Activity of Dox in Xenograft Tumor Model. A549 xenograft tumor was established, and the mice were treated with vehicle, ocotillol, Dox or Dox-O. As shown in Figure 6(a), ocotillol at dose of 10 mg/kg, which alone had no obvious effect on the tumor growth, could significantly increase the anti-tumor activity of Dox administrated every three days at dose of 1.5 mg/kg ($P < 0.01$, compared with Dox alone group). Little weight loss was observed (Figure 6(b)), and no animal was dead in all treated groups.

4. Discussions

Cancer was one of the major causes of death in the world, and its first-line and most salient treatment strategy still was the cytotoxic agent-based chemotherapy [2, 24]. Although Dox-based chemotherapy could increase patients' survival, side effects and acquisition of drug resistance severely limited its clinical effectiveness [25]. Therefore, novel therapeutic

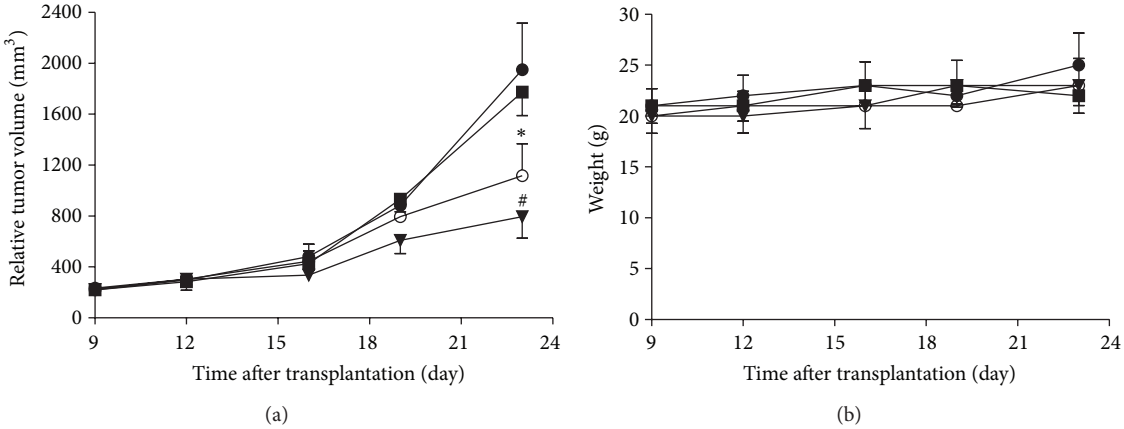

Figure 6: Effect of ocotillol on the antitumor activity of Dox on A549 xenograft tumors in nude mice. Tumor diameter was serially measured with a vernier caliper, the relative tumor volume was calculated, and the growth curve was drawn (a). The body weight changes of animals were recorded and shown (b). Vehicle (•); 10 mg/kg ocotillol (■); 1.5 mg/kg Dox (○); 1.5 mg/kg Dox plus 10 mg/kg Ocotillo (▼). $^{*}P < 0.05$, compared with control group; $^{\#}P < 0.05$, compared with Dox group.

strategies, in which cotreatment with a sensitizer could reduce the cumulative doses of Dox by enhancing the anti-tumor activities, needed to be developed. Here, we provided the first evidence that ocotillol could potentiate the cytotoxic activity of Dox via p53-dependent apoptosis.

In current study, ocotillol was observed to induce higher sensitization to Dox in p53 wild-type cell lines, not in p53-null cells (Figure 2), which indicated the enhancement of ocotillol on potency of Dox might be in a p53-dependent manner. Based on our previous data, ocotillol did not aggravate the cardiotoxicity of Dox in H9C2 cells [17]. Indeed, ocotillol could significantly enhance the anti-tumor activity of Dox in xenograft tumor models without apparently increasing its toxic effect, which was primarily evaluated by the animal survival and body weight (Figure 6). Dox-O combination therapy, therefore, could exert more robust anti-tumor effects and does not increase toxic effects, which might in turn decrease the cumulative toxic effects through reducing Dox dosage.

Inducing apoptosis was a common mechanism of anticancer drugs [26], in which the apoptotic cells were easily detected by several methods, such as FCM and Hoechst staining [27]. Stained apoptotic cells are showed with less nuclear PI dye and could be recorded as sub-G0 phase in FCM assay, and morphologic characteristics of apoptotic cells such as nucleus shrinkage and DNA breakage were shown after stained with Hoechst 33342. In the current study, both FCM and Hoechst staining showed proportions of apoptotic cells to be dramatically increased in the Dox-O group compared with the Dox alone group (Figure 3), indicating that ocotillol potentiated Dox cytotoxicity via promoting the cancer cells undergoing apoptosis.

As a transcription factor, p53 played an important role in many cancer drugs' anti-tumor effects, including both "cytotoxic drugs" and "target drugs" [28]. Doxorubicin, paclitaxel, etoposide, and cisplatin reportedly exerted cytotoxic activities through activating p53, resulting in increased expression of its target genes, such as *PUMA*, *PIG3*, and *BAX* [29]. In this study, mRNA expression *PUMA*, *PIG3* and *BAX* were increased following p53 activation after Dox treatment. Dox-O was seen to further increase mRNA expression of *PUMA*, *PIG3* and *BAX* (Figure 4), which were all known to be proapoptosis genes, induction of which led cells to undergo apoptosis. As a result, MTT assay detected this as decreased cell viability.

To verify that ocotillol's effect on the cytotoxicity of Dox was through p53 pathway, the p53 inhibitor pifithrin-α was used to block p53 transcription activity [23]. Indeed, pifithrin-α could significantly attenuated the increase of pro-apoptosis genes induced by Dox-O (Figure 5). As a result, the increased Dox-induced apoptosis in both the presence and absence of ocotillol was dramatically attenuated by co-administration with pifithrin-α. Consequently, the MTT assay showed that pifithrin-α repressed Dox cytotoxicity with and without ocotillol. The finding was consistent with the fact that Dox displayed anti-cancer activity through, or at least partially through, activating p53 [29]. All of these results showed clearly p53 played the major role in the effect of ocotillol on Dox potency, The exact molecular mechanisms of action, how Dox with ocotillol could further activate p53, and which regulator protein was involved were still needed to be explored.

5. Conclusion

We here reported for the first time that ocotillol enhanced Dox cytotoxicity apparently by inducing p53-dependent apoptosis. This implied that use of ocotillol with Dox could be an improved therapeutic strategy.

Authors' Contribution

Hongbo Wang, Pengfei Yu, and Jing Bai have contributed equally to this study.

Acknowledgments

This study was supported by Taishan Scholar Project, a Project of Shandong Province Higher Educational Science and Technology Program (J12LM53), and National Natural Science Foundation of China (no. 81202038). The authors thank Christopher Shih from Albany Pharmacy School (Albany, NY, USA) for critical reading of this paper.

References

[1] A. Jemal, F. Bray, M. M. Center, J. Ferlay, E. Ward, and D. Forman, "Global cancer statistics," *CA Cancer Journal for Clinicians*, vol. 61, no. 2, pp. 69–90, 2011.

[2] R. Lal, D. Enting, and H. Kristeleit, "Systemic treatment of non-small-cell lung cancer," *European Journal of Cancer*, vol. 47, no. 3, supplement, pp. S375–S377, 2011.

[3] D. R. Beil and L. M. Wein, "Sequencing surgery, radiotherapy and chemotherapy: insights from a mathematical analysis," *Breast Cancer Research and Treatment*, vol. 74, no. 3, pp. 279–286, 2002.

[4] C. Carvalho, R. X. Santos, S. Cardoso et al., "Doxorubicin: the good, the bad and the ugly effect," *Current Medicinal Chemistry*, vol. 16, no. 25, pp. 3267–3285, 2009.

[5] D. C. Drummond, O. Meyer, K. Hong, D. B. Kirpotin, and D. Papahadjopoulos, "Optimizing liposomes for delivery of chemotherapeutic agents to solid tumors," *Pharmacological Reviews*, vol. 51, no. 4, pp. 691–743, 1999.

[6] J. M. Scott, A. Khakoo, J. R. MacKey, M. J. Haykowsky, P. S. Douglas, and L. W. Jones, "Modulation of anthracycline-induced cardiotoxicity by aerobic exercise in breast cancer: current evidence and underlying mechanisms," *Circulation*, vol. 124, no. 5, pp. 642–650, 2011.

[7] G. Minotti, P. Menna, E. Salvatorelli, G. Cairo, and L. Gianni, "Anthracyclines: molecular advances and pharmacologie developments in antitumor activity and cardiotoxicity," *Pharmacological Reviews*, vol. 56, no. 2, pp. 185–229, 2004.

[8] J.-C. Marine, "Pharmacological rescue of p53 in cancer therapy: widening the sensitive tumor spectrum by targeting MDMX," *Cancer Cell*, vol. 18, no. 5, pp. 399–400, 2010.

[9] S. L. Harris and A. J. Levine, "The p53 pathway: positive and negative feedback loops," *Oncogene*, vol. 24, no. 17, pp. 2899–2908, 2005.

[10] H. Qian, Y. Yang, and X. Wang, "Curcumin enhanced adriamycin-induced human liver-derived Hepatoma G2 cell death through activation of mitochondria-mediated apoptosis and autophagy," *European Journal of Pharmaceutical Sciences*, vol. 43, no. 3, pp. 125–131, 2011.

[11] A. Spina, L. Sorvillo, F. Di Maiolo et al., "Inorganic phosphate enhances sensitivity of human osteosarcoma U2OS cells to doxorubicin via a p53-dependent pathway," *Journal of Cellular Physiology*, vol. 228, no. 1, pp. 198–206, 2012.

[12] X.-W. Yuan, X.-F. Zhu, X.-F. Huang et al., "Interferon-α enhances sensitivity of human osteosarcoma U2OS cells to doxorubicin by p53-dependent apoptosis," *Acta Pharmacologica Sinica*, vol. 28, no. 11, pp. 1835–1841, 2007.

[13] G. Schwartsmann, M. J. Ratain, G. M. Cragg et al., "Anticancer drug discovery and development throughout the world," *Journal of Clinical Oncology*, vol. 20, no. 18, pp. 47S–59S, 2002.

[14] M. Karmazyn, M. Moey, and X. T. Gan, "Therapeutic potential of ginseng in the management of cardiovascular disorders," *Drugs*, vol. 71, no. 15, pp. 1989–2008, 2011.

[15] L.-W. Qi, C.-Z. Wang, and C.-S. Yuan, "Ginsenosides from American ginseng: chemical and pharmacological diversity," *Phytochemistry*, vol. 72, no. 8, pp. 689–699, 2011.

[16] Z. Wang, Q. Zheng, K. Liu, G. Li, and R. Zheng, "Ginsenoside Rh2 enhances antitumour activity and decreases genotoxic effect of cyclophosphamide," *Basic and Clinical Pharmacology and Toxicology*, vol. 98, no. 4, pp. 411–415, 2006.

[17] H. Wang, P. Yu, and H. Gou, "Cardioprotective effects of 20(S)-ginsenoside Rh2 against doxorubicin-induced cardiotoxicity *in vitro* and *in vivo*," *Evidence-Based Complementary and Alternative Medicine*, vol. 2012, Article ID 506214, 8 pages, 2012.

[18] X. Xie, A. Eberding, C. Madera et al., "Rh2 synergistically enhances paclitaxel or mitoxantrone in prostate cancer models," *Journal of Urology*, vol. 175, no. 5, pp. 1926–1931, 2006.

[19] S.-W. Kim, H.-Y. Kwon, D.-W. Chi et al., "Reversal of P-glycoprotein-mediated multidrug resistance by ginsenoside Rg3," *Biochemical Pharmacology*, vol. 65, no. 1, pp. 75–82, 2003.

[20] H. Wang, H. Li, M. Zuo et al., "Lx2-32c, a novel taxane and its antitumor activities *in vitro* and *in vivo*," *Cancer Letters*, vol. 268, no. 1, pp. 89–97, 2008.

[21] H. Wang, X. Ma, S. Ren, J. K. Buolamwini, and C. Yan, "A small-molecule inhibitor of MDMX activates p53 and induces apoptosis," *Molecular Cancer Therapeutics*, vol. 10, no. 1, pp. 69–79, 2011.

[22] G. Lizard, V. Deckert, L. Dubrez, M. Moisant, P. Gambert, and L. Lagrost, "Induction of apoptosis in endothelial cells treated with cholesterol oxides," *American Journal of Pathology*, vol. 148, no. 5, pp. 1625–1638, 1996.

[23] P. G. Komarov, E. A. Komarova, R. V. Kondratov et al., "A chemical inhibitor of p53 that protects mice from the side effects of cancer therapy," *Science*, vol. 285, no. 5434, pp. 1733–1737, 1999.

[24] T. J. Rutkoski and R. T. Raines, "Evasion of ribonuclease inhibitor as a determinant of ribonuclease cytotoxicity," *Current Pharmaceutical Biotechnology*, vol. 9, no. 3, pp. 185–199, 2008.

[25] J. M. Appel, D. Nielsen, B. Zerahn, B. V. Jensen, and K. Skagen, "Anthracycline-induced chronic cardiotoxicity and heart failure," *Acta Oncologica*, vol. 46, no. 5, pp. 576–580, 2007.

[26] A. Ahmad, W. A. Sakr, and K. M. W. Rahman, "Anticancer properties of indole compounds: mechanism of apoptosis induction and role in chemotherapy," *Current Drug Targets*, vol. 11, no. 6, pp. 652–666, 2010.

[27] Z. Darzynkiewicz, S. Bruno, G. Del Bino et al., "Features of apoptotic cells measured by flow cytometry," *Cytometry*, vol. 13, no. 8, pp. 795–808, 1992.

[28] A. J. Levine and M. Oren, "The first 30 years of p53: growing ever more complex," *Nature Reviews Cancer*, vol. 9, no. 10, pp. 749–758, 2009.

[29] C. J. Brown, S. Lain, C. S. Verma, A. R. Fersht, and D. P. Lane, "Awakening guardian angels: drugging the P53 pathway," *Nature Reviews Cancer*, vol. 9, no. 12, pp. 862–873, 2009.

Hindawi Publishing Corporation
Evidence-Based Complementary and Alternative Medicine
Volume 2013, Article ID 943187, 10 pages
http://dx.doi.org/10.1155/2013/943187

Research Article

Butein Inhibits Angiogenesis of Human Endothelial Progenitor Cells via the Translation Dependent Signaling Pathway

Ching-Hu Chung,[1] Chien-Hsin Chang,[2] Shiou-Sheng Chen,[3,4] Hsueh-Hsiao Wang,[5] Juei-Yu Yen,[5] Che-Jen Hsiao,[6] Nan-Lin Wu,[7] Yen-Ling Chen,[8] Tur-Fu Huang,[2] Po-Chuan Wang,[9] Hung-I Yeh,[5,10] and Shih-Wei Wang[5]

[1] *Department of Pharmacology, Tzu Chi University, Hualien 970, Taiwan*
[2] *Institute of Pharmacology, College of Medicine, National Taiwan University, Taipei 100, Taiwan*
[3] *Division of Urology, Taipei City Hospital, Renai Branch, Taipei 106, Taiwan*
[4] *Department of Urology, National Yang-Ming University School of Medicine, Taipei 112, Taiwan*
[5] *Department of Medicine, Mackay Medical College, New Taipei City 252, Taiwan*
[6] *School of Respiratory Therapy, College of Medicine, Taipei Medical University, Taipei 110, Taiwan*
[7] *Department of Dermatology, Mackay Memorial Hospital, Hsinchu 300, Taiwan*
[8] *Department of Fragrance and Cosmetic Science, College of Pharmacy, Kaohsiung Medical University, Kaohsiung 807, Taiwan*
[9] *Department of Gastroenterology, Mackay Memorial Hospital, Hsinchu 300, Taiwan*
[10] *Department of Internal Medicine, Mackay Memorial Hospital, Taipei 104, Taiwan*

Correspondence should be addressed to
Po-Chuan Wang; a5965@ms7.mmh.org.tw and Shih-Wei Wang; shihwei@mmc.edu.tw

Received 27 March 2013; Accepted 9 May 2013

Academic Editor: Shun-Fa Yang

Compelling evidence indicates that bone marrow-derived endothelial progenitor cells (EPCs) can contribute to postnatal neovascularization and tumor angiogenesis. EPCs have been shown to play a "catalytic" role in metastatic progression by mediating the angiogenic switch. Understanding the pharmacological functions and molecular targets of natural products is critical for drug development. Butein, a natural chalcone derivative, has been reported to exert potent anticancer activity. However, the antiangiogenic activity of butein has not been addressed. In this study, we found that butein inhibited serum- and vascular endothelial growth factor- (VEGF-) induced cell proliferation, migration, and tube formation of human EPCs in a concentration dependent manner without cytotoxic effect. Furthermore, butein markedly abrogated VEGF-induced vessels sprouting from aortic rings and suppressed microvessel formation in the Matrigel implant assay *in vivo*. In addition, butein concentration-dependently repressed the phosphorylation of Akt, mTOR, and the major downstream effectors, p70S6K, 4E-BP1, and eIF4E in EPCs. Taken together, our results demonstrate for the first time that butein exhibits the antiangiogenic effect both *in vitro* and *in vivo* by targeting the translational machinery. Butein is a promising angiogenesis inhibitor with the potential for treatment of cancer and other angiogenesis-related diseases.

1. Introduction

Angiogenesis plays a critical role in physiological conditions such as embryonic development, reproduction, tissue repair, and bone remodeling. In contrast, angiogenesis is an important process for tumor progression and various inflammatory diseases [1]. Angiogenesis is the result of complex effect on cell-cell and cell-matrix interactions. This process mainly involves endothelial cells proliferation, migration, tube formation, and extracellular matrix (ECM) degradation [2]. Vascular endothelial growth factor (VEGF) is the most potent angiogenic factor, which is primarily secreted by cancer cells to mediate tumor angiogenesis via binding to VEGF receptor (VEGF-R). Therefore, targeting VEGF/VEGF-R axis to block

angiogenesis is currently an attractive therapeutic approach for cancer treatment [3, 4].

Circulating endothelial progenitor cells (EPCs) have been shown to play important roles in maintaining vascular integrity and facilitating tissue repair. Circulating EPCs are mobilized from the bone marrow into the bloodstream and induce neovascularization during tissue ischemia [5, 6]. Emerging evidence suggests that EPCs have the ability to self-renew, circulate, home to tumor sites, and differentiate into mature endothelial cells that contribute to angiogenesis and vasculogenesis during the growth and metastatic spread of tumors [7]. Tumor-derived cytokines, such as VEGF, regulate the mobilization of EPCs, which subsequently contribute to tumor angiogenesis and the growth of certain tumors [8]. EPCs reportedly mediate the progression of micrometastasis and subsequently promote tumor macrometastasis, as critical regulators of the angiogenic switch. These findings establish the role of EPCs in tumor angiogenesis and metastasis and support that selective targeting of EPCs may merit investigation for antiangiogenic treatment of metastatic cancer [9, 10].

Translational control has a crucial impact on cancer development and progression, directing both mRNA translation and protein synthesis that regulate tumor cell proliferation, transformation, angiogenesis, and metastasis [11]. Numerous molecular signals have been demonstrated to regulate translational signaling pathways. Earlier studies have shown that Akt and MAPK pathways regulate protein translation through its downstream mammalian target of rapamycin (mTOR) [12, 13]. In eukaryotes, 95–97% of total cellular mRNA translation is via cap-dependent pathway, and the others are through cap-independent pathway [14]. The best-understood roles of mTOR in mammalian cells are tightly associated with the control of cap-dependent mRNA translation. mTOR conducts this translational pathway through phosphorylation of two downstream effectors, the 70 kDa ribosomal protein S6 kinase (p70S6K) and eukaryotic initiation factor 4E binding protein 1 (4E-BP1) [15, 16]. P70 S6 kinase phosphorylates the 40S ribosomal subunit protein S6 and is involved in translational control of 5′ oligopyrimidine tract mRNAs. Unphosphorylated 4E-BP1 is a translational inhibitor that binds to eukaryotic initiation factor 4E (eIF4E) to repress translation initiation. The activation of mTOR leads to hierarchical phosphorylation of 4E-BP1, dislodging 4E-BP1 from eIF4E, and subsequently increasing cap-dependent translation [11]. mTOR-mediated translational signaling is important for cellular proliferation and growth in endothelial cells and various tumor cells [17, 18]. Deregulation of mTOR signaling is frequently associated with tumor growth and angiogenesis [16, 19]. Thus, mTOR signaling pathway is central to translational regulation and is a novel target for cancer therapeutics.

Butein (3,4,2′,4′-tetrahydroxychalcone), a type of chalcone derivative, has been identified from numerous plants including the heartwood of *Dalbergia odorifera* (namely, Jiangxiang in Chinese), the stem bark of cashews (*Semecarpus anacardium*), and the traditional Chinese and Tibetan medicinal herbs such as *Caragana jubata* and *Rhus verniciflua* Stokes. Previous reports have demonstrated that butein has various pharmacological effects, such as antioxidant and anti-inflammatory activities [20, 21], elicitation of endothelium-dependent vasodilation [22], antirestenosis effect [23], and anticancer effects in a variety of human cancer cells [24–29]. Several chalcones have been reported to exhibit antiangiogenic activity via blocking VEGF-induced angiogenesis [30, 31]. However, the antiangiogenesis property of butein is mostly unknown. In this study, we investigated the antiangiogenic activity of butein in both *in vitro* and *in vivo* assays and further elucidated its mechanism of action in human EPCs.

2. Materials and Methods

2.1. Materials. 3,4,2′,4′-Tetrahydroxychalcone (butein) was purchased from Extrasynthese Corporation (Genay, France). 3-[4,5-Dimethylthiazol-2-yl]-2,5-diphenyltetrazolium bromide (MTT), crystal violet, and other chemicals were purchased from Sigma (St Louis, MO). MV2 complete medium was purchased from PromoCell (Heidelberg, Germany). Defined fetal bovine serum (FBS) and all cultured reagents were purchased from HyClone (Logan, UT). Recombinant human VEGF was purchased from R&D Systems (Minneapolis, MN). Lactate dehydrogenase (LDH) assay reagents were purchased from Promega (Madison, WI). Antibodies to phospho-Akt (Ser473), Akt, phospho-mTOR (Ser2448), and phospho-eIF4E (Ser209) were purchased from Epitomics (Burlingame, CA). Antibodies to phospho-ERK1/2 (Thr202/Tyr204), ERK1/2, phospho-p70S6K (Thr389), phospho-4E-BP-1 (Thr37/46), and GAPDH were purchased from Cell Signaling Technologies (Boston, MA).

2.2. Isolation and Cultivation of EPCs. Ethical approval was granted by the Institutional Review Board of Mackay Medical College, New Taipei City, Taiwan (reference number: P1000002). Informed consent was obtained from healthy donors before the collection of peripheral blood (80 mL). The peripheral blood mononuclear cells (PBMCs) were fractionated from other blood components by centrifugation on Ficoll-Paque plus (Amersham Biosciences, Uppsala, Sweden) according to the manufacturer's instructions. CD34-positive progenitor cells were obtained from the isolated PBMCs using CD34 MicroBead Kit and MACS Cell Separation System (Miltenyi Biotec, Bergisch Gladbach, Germany). The isolation and maintenance of CD34-positive EPCs were performed as described previously [32, 33]. Briefly, human CD34-positive EPCs were maintained and propagated in MV2 complete medium consisting of MV2 basal medium and growth supplement, supplied 20% FBS. Cells were seeded onto 1% gelatin-coated plasticware and cultured in humidified air containing 5% CO2 at 37°C for further treatment. Characterization of EPCs was confirmed by UEA-1 binding, and surface marker staining of CD34, KDR, and CD31. (see Supplementary Figure 1 in Supplementary Material available online at http://dx.doi.org/10.1155/2013/943187). Experiments were conducted on EPCs between passages 8 and 12.

2.3. Cell Proliferation Assay. For crystal violet assay, EPCs (5×10^3 cells/well) were seeded onto 96-well plates. After

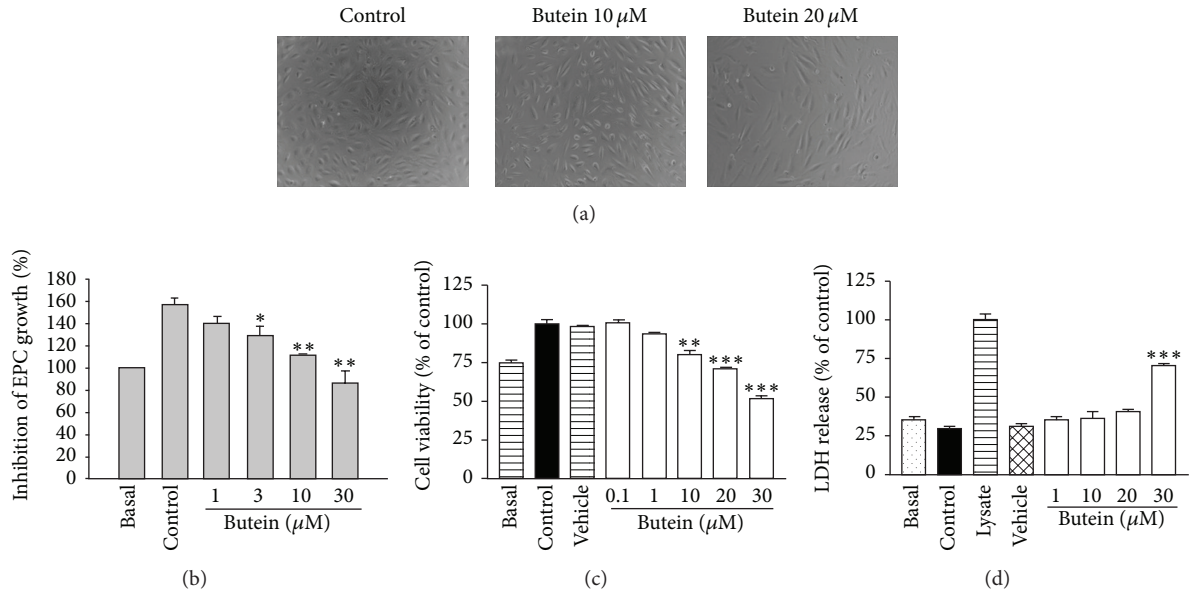

Figure 1: Effect of butein on cell proliferation and cytotoxicity of EPCs. Cells were seeded into a 96-well plate at 5000 cells per well overnight for attachment. After 72 h incubation with the indicated concentrations of butein in MV2 complete medium containing 10% FBS, cell morphology was detected by inverted phase contrast microscope (a), and cell proliferation was determined using crystal violet assay (b). Serum-starved cells were stimulated with or without VEGF (20 ng/mL) in the absence or presence of various concentrations of butein, and the cell growth and cytotoxicity were determined using MTT assay and LDH assay, respectively (c and d). Data are expressed as mean ± SEM of five independent experiments. $^{*}P < 0.05$, $^{**}P < 0.01$, and $^{***}P < 0.001$ compared with the control group.

24 h incubation, the culture medium was removed and cells were incubated with fresh MV2 complete medium containing 10% FBS for 72 h in the absence or presence of butein. Then, cell proliferation was determined by crystal violet staining, which was performed by staining with 0.5% crystal violet in 20% methanol. The dye was subsequently eluted in the solution containing 0.1 M sodium citrate and 75% ethanol, and absorbance was measured at 540 nm with ELISA-reader.

For MTT colorimetric assay, EPCs (5×10^3 cells/well) were incubated in 96-well plates and starved with MV2 complete medium for 16 h. Then, the culture medium was removed, and cells were incubated with fresh MV2 complete medium containing VEGF (20 ng/mL) for 48 h in the absence or presence of butein. Cells were incubated with MTT (0.5 mg/mL) for 2 h. Formazan crystal was lysed by dimethyl sulfoxide (DMSO), and absorbance was measured at 550 nm with ELISA-reader.

2.4. Cytotoxicity Assay. EPCs were seeded onto 96-well plates in a density of 5×10^3 cells per well and starved with MV2 complete medium for 16 h. Then, cells were treated with MV2 complete medium containing VEGF (20 ng/mL) for 48 h in the absence or presence of butein. The percentage of LDH release was calculated from the ratio of LDH activity in the medium to LDH activity in the cell lysate.

2.5. Cell Migration Assay. Cell migration assay was performed using Transwell chambers with 8.0 μm pore size (Coring, Coring, NY). EPCs (5×10^4 cells/well) were seeded onto the upper chamber with MV2 complete medium and then incubated in the bottom chamber with MV2 complete medium containing 10% FBS or VEGF (20 ng/mL) with the indicated concentrations of butein. After 16 h of treatment, cells on the upper side of the filters were mechanically removed, and those which migrated on the lower side were fixed with 4% formaldehyde then stained with 0.5% crystal violet for 10 min. Cell migration was quantified by counting the number of stained cells in 10 random fields with the inverted phase contrast microscope and photographed.

2.6. Capillary Tube Formation Assay. Matrigel (BD Biosciences, Bedford, MA), which was used to promote the differentiation of EPCs into a capillary tube-like structure, was added to 48-well plates. The Matrigel-coated 48-well plates were incubated at 37°C for 30 min to allow for polymerization. After gel formation, EPCs (6×10^4 cells) were seeded per well on the layer of polymerized Matrigel in MV2 complete medium containing 10% FBS or VEGF (20 ng/mL) with the indicated concentrations of butein, followed by incubation for 10–16 h at 37°C. Photomicrographs of capillary tube formation were taken with the inverted phase contrast microscope. Tube formation was quantified by measuring the long axis of each tube in 3 random fields per well by using Image-Pro Plus software.

2.7. Aortic Ring Sprouting Assay. Assay was performed as previously described with modification [34]. Aortas were

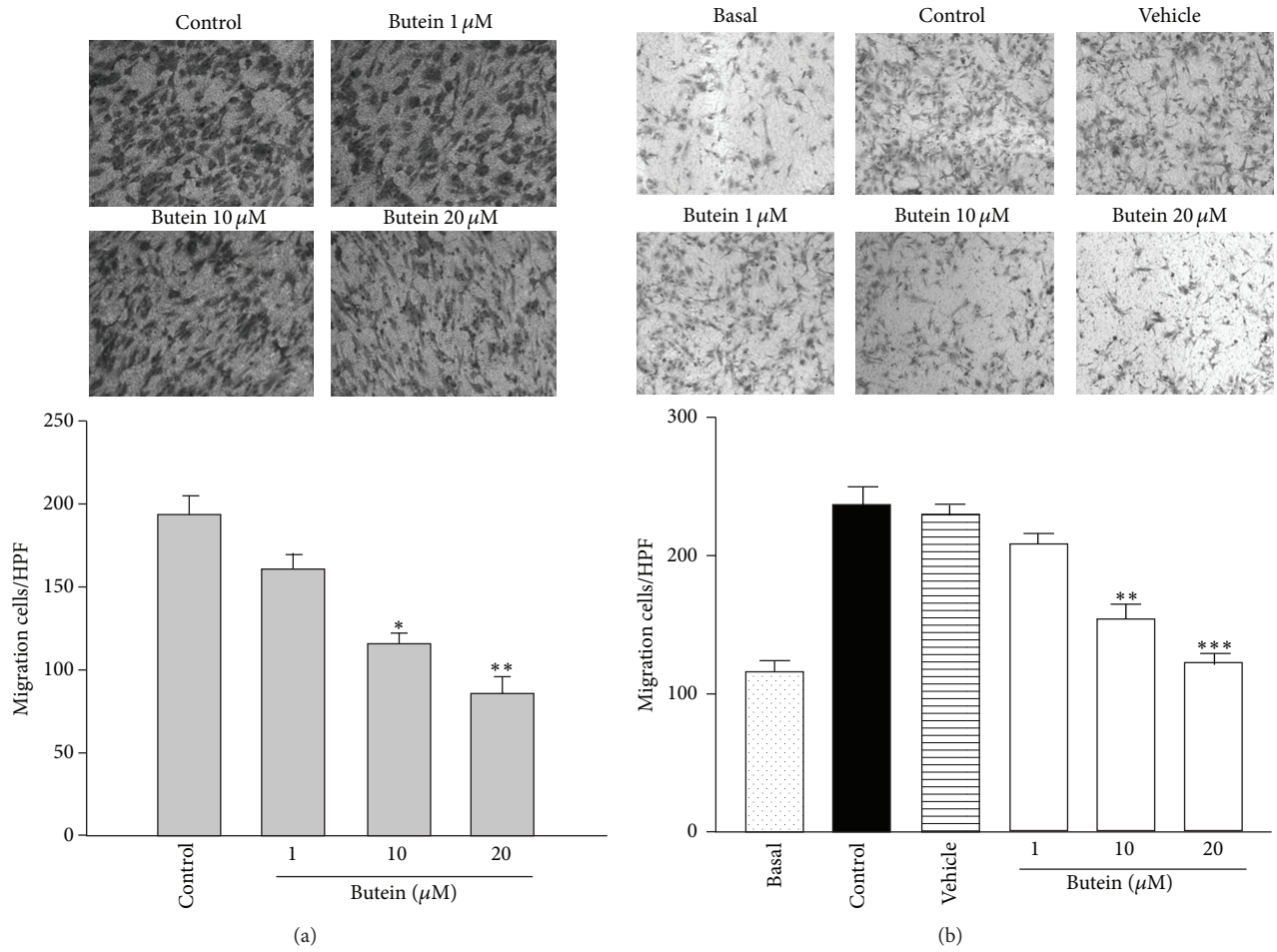

Figure 2: Effect of butein on cell migration of EPCs. Cells were seeded onto the upper chamber consisting of 8 mm pore-size filters and then treated with the indicated concentrations of butein in MV2 complete medium containing 10% FBS (a) or 20 ng/mL VEGF (b) as a chemoattractant in the lower chamber. Cells that invaded the filter were counted as mean ± SEM of five independent experiments. $^{*}P < 0.05$, $^{**}P < 0.01$, and $^{***}P < 0.001$ compared with the control group.

harvested from 8- to 10-week-old Sprague-Dawley rats. Following a complete washing, the aortas were cut into 1 mm ring segments. The aortic rings were placed in the 48-well plates which were precoated with 130 μL Matrigel and polymerized at 37°C. The wells were subsequently overlaid with another 50 μL Matrigel for sealing. VEGF (20 ng/mL) with or without butein was then added to the well. The cultured medium was changed every 3 days. Sprouting endothelial cells were observed and photographed on day 8. The area of sprouting vessels was measured quantitatively by Image-Pro Plus software.

2.8. Directed In Vivo Angiogenesis Assay (DIVAA). DIVAA was performed as described previously [35]. Briefly, sterile, surgical silicone tubes were filled at 4°C with matrigel containing VEGF with or without butein. Therefore, the dorsal haunches of the anesthetized mice (8- to 10-week-old female C57BL/6 mice) were shaved and sterile prepped. A 5 mm cutaneous incision was made, and a 10 mm deep subcutaneous pocket was created with a sterile hemostat. DIVAA tubes were incubated at 37°C for 1 hour to allow gel formation and then implanted into the dorsal flank of mice. After 15 days, DIVAA tubes were taken and photographed. Neovessels were quantified by measuring the hemoglobin of the plug with the Drabkin method and Drabkin reagent kit 525 (Sigma). The animals were maintained on a 12-hour light/dark cycle under controlled temperature (20 ± 1°C) and humidity (55 ± 5%). Animals were given continuous access to food and water. All procedures involving animal experiment were approved by the Institutional Animal Care and Use Committee at College of Medicine, Tzu Chi University.

2.9. Western Blot Analysis. Cells were lysed with lysis buffer as described previously [36]. Cell homogenates were diluted with loading buffer and boiled for 5 min for detecting phosphorylation and protein expression. Total protein was determined and equal amounts of protein were separated by 8–12% SDS-PAGE and immunoblotted with specific primary antibodies. Horseradish peroxidase-conjugated secondary antibodies (Santa Cruz Biotechnology, Santa Cruz, CA) were

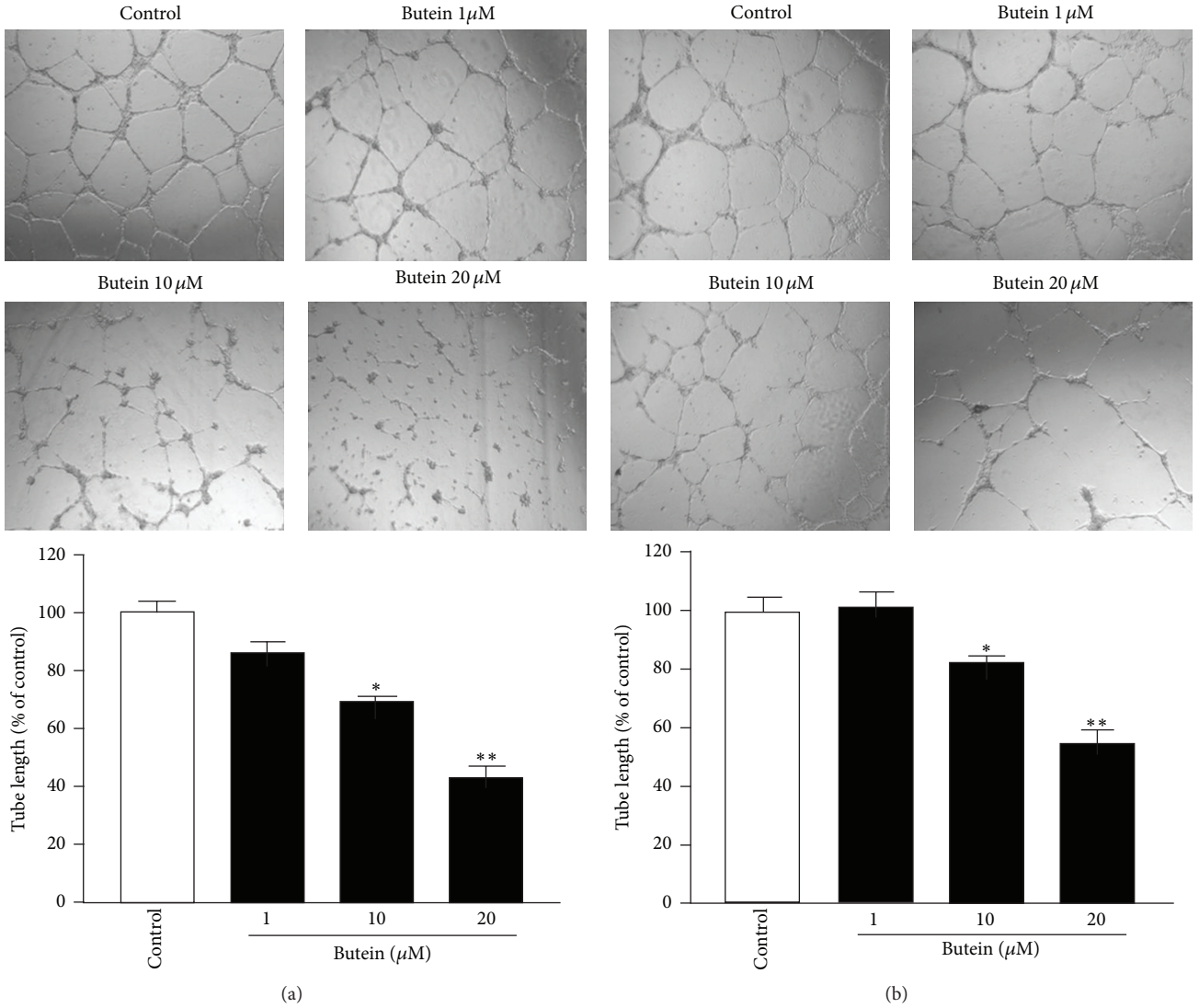

Figure 3: Effect of butein on tube formation of EPCs. Cells were plated on Matrigel-coated plates in the presence of MV2 complete medium containing 10% FBS (a) or 20 ng/mL VEGF (b) with various concentrations of butein, and tubular morphogenesis was recorded by the inverted phase contrast microscope. Tube formation was quantified by measuring the length of tubes in three random fields per well with the use of Image-Pro Plus and was calculated against DMSO control. Data are expressed as mean ± SEM of four independent experiments. $^{*}P < 0.05$, $^{**}P < 0.01$ compared with the control group.

used, and the signal was detected using an enhanced chemiluminescence detection kit (Amersham, Buckinghamshire, UK).

2.10. Statistical Analysis. Data are presented as the mean ± SEM for the indicated number of separate experiment. Statistical analyses of data were performed with one-way ANOVA followed by Student's t-test, and P values less than 0.05 were considered significant.

3. Results

3.1. Butein Inhibits Cell Proliferation of EPCs without Cytotoxicity. To assess the antiangiogenic activity of butein, we first evaluated the influence of butein on cell proliferation of EPCs. The results showed that butein induced the cytostatic effect in human EPCs (Figure 1(a)). Furthermore, butein suppressed serum- or VEGF-induced cell proliferation of EPCs in a concentration-dependent manner (Figures 1(b) and 1(c)). In order to investigate whether the effect of butein was due to its cytotoxicity, LDH assay was performed. There is no significant increase in LDH release when the concentration is lower than 20 μM. However, treatment of higher concentration of butein (30 μM) caused a significant LDH release (Figure 1(d)). Therefore, the concentration of butein used in the following research is less than 20 μM.

3.2. Butein Inhibits Cell Migration of EPCs. The migration of EPCs is an important step in angiogenesis. We investigated the chemotactic migration with Transwell chambers to

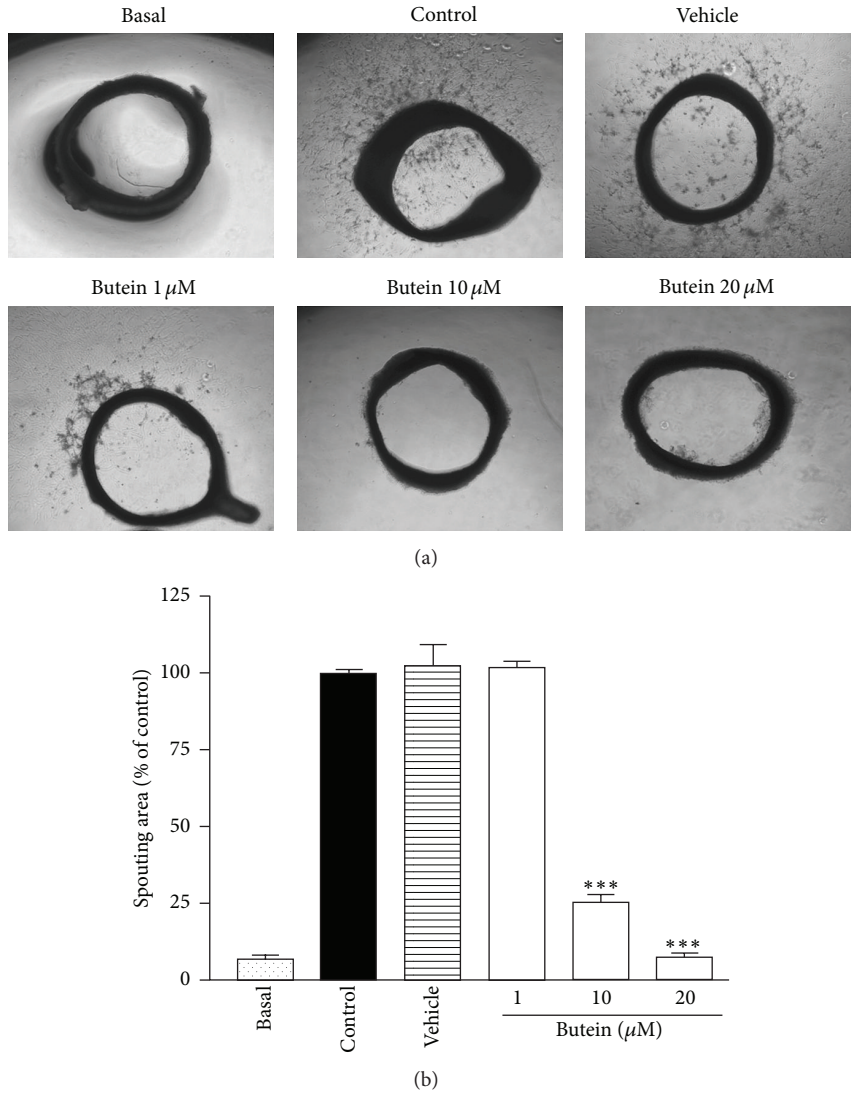

Figure 4: Effect of butein on VEGF-induced angiogenesis *ex vivo*. Aortas in Matrigel were treated with or without VEGF (20 ng/mL) in the absence or presence of various concentrations of butein. After 8 days, aortic rings were photographed. Experiments were repeated four times, and a representative result is shown. Data are expressed as mean ± SEM of four independent experiments. $^{***}P < 0.001$ compared with the control group.

examine the effect of butein on EPC migration toward serum or VEGF. As shown in Figure 2, serum and VEGF induced EPCs migration after 16 hr treatment. Butein significantly attenuated serum- and VEGF-induced cell migration.

3.3. Butein Inhibits Tube Formation of EPCs. In order to study the effect on EPCs differentiation and formation of capillary-like structure, we tested whether butein inhibited tube formation on Matrigel. The capillary tube-like structure was facilitated by angiogenic factors such as serum and VEGF. After 10 hours of treatment, butein exhibited the promising inhibitory effect on serum- or VEGF-induced tube formation (Figure 3). These results demonstrate that butein has the ability to block *in vitro* angiogenesis of EPCs.

3.4. Butein Inhibits Angiogenesis Ex Vivo and In Vivo. We further performed the aortic ring sprouting assay to evaluate *ex vivo* antiangiogenic effect of butein. As shown in Figure 4, VEGF apparently stimulated the vessels sprouting of the rat aortic ring, whereas butein significantly decreased the sprouting of VEGF-induced vessels in a concentration-dependent manner. To determine whether butein is capable of blocking angiogenesis *in vivo*, we used an *in vivo* mouse DIVAA model. An aliquot of growth factor-reduced Matrigel containing VEGF was filled into a sterile, surgical silicone tubing and then inoculated subcutaneously into mouse. New vessels were induced by VEGF and formed a capillary network in the DIVAA tubes. As shown in Figure 5, butein demonstrated the inhibitory effect of microvessel in growth into the DIVAA tubes. Quantification of angiogenesis by hemoglobin content

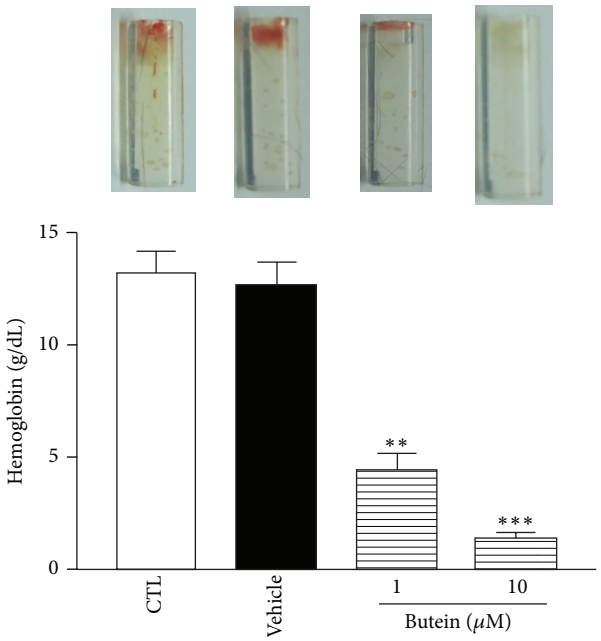

Figure 5: Effect of butein on VEGF-induced angiogenesis *in vivo*. Matrigel containing VEGF (200 ng/mL) with or without butein in sterile, surgical silicone tubes were subcutaneously placed into C57BL/6 mice. After 15 days, DIVAA tubes was taken and photographed. Hemoglobin was measured as an indication of blood vessel formation, using the Drabkin method. Data are presented as mean ± SEM of at least 3 mice per group. $^{**}P < 0.01$, $^{***}P < 0.001$ compared with control group.

revealed that butein significantly inhibited the angiogenic response in a dose-dependent manner. These results suggest that butein strongly blocks VEGF-induced angiogenesis *ex vivo* and *in vivo*.

3.5. Butein Inhibits the Translational Pathway in EPCs. Both phosphatidylinositol-3-kinase (PI3K)/Akt and extracellular signal-related kinase 1/2 (ERK1/2) signaling pathway play important roles in cell proliferation, survival, migration, and angiogenesis [18, 37]. Therefore, we investigated these molecular mechanisms underlying the effects of butein-mediated intracellular signal transduction in EPCs. As shown in Figure 6(a), phosphorylation of Akt and ERK1/2 were markedly increased after serum stimulation. Butein dramatically inhibited the phosphorylation of Akt in a concentration-dependent manner but did not significantly suppress the phosphorylation of ERK1/2 in EPCs. The important downstream effector of PI3K/Akt pathway termed mTOR is recognized to regulate the translational process through increased phosphorylation of p70S6K and 4E-BP1. In addition, mTOR and p70S6K signal have been indicated to regulate various biological functions of endothelial cells (ECs) for angiogenesis [17, 19]. Thus, we explored whether butein modulated these signaling pathways in EPCs. As shown in Figure 6(b), serum induced a significant increase in the phosphorylation of mTOR, p70S6K, 4E-BP1, and eIF4E. We found the phosphorylation of mTOR and the major downstream targets, p70S6K, 4E-BP1, and eIF4E, were significantly suppressed in EPCs by butein treatment. These results suggest that butein may inhibit angiogenesis probably through the inhibition of translational process.

4. Discussion

The development of new blood vessels from preexisting ones is generally referred to angiogenesis, which plays a critical role in tumor growth and metastasis. In recent years, anti-angiogenic agents have become attractive strategy for cancer treatment and provide some additional benefits, including fewer side effects and lower dosage of chemotherapy [3, 38]. Accumulating evidence indicates that tumor angiogenesis is also supported by the mobilization and functional incorporation of other cells such as endothelial progenitor cells (EPCs) [6]. Recently, EPCs have been proposed to improve early tumor growth and late tumor metastasis by intervening with the angiogenic switch; EPCs promote tumor neovessel formation through the production of angiogenic cytokines during tumor progression [8, 39]. Furthermore, several studies demonstrate that certain chemotherapy drugs can trigger circulating EPCs mobilization and subsequent tumor homing [10, 40]. Therefore, EPC-targeting therapies may be the promising strategy to block angiogenesis-mediated tumor growth. In this study, we used EPCs to investigate the effect of butein on angiogenesis. We found that butein inhibited serum- and VEGF-induced proliferation in a concentration-dependent manner (Figure 1). Tumor cells release chemoattractants, such as VEGF, into microenvironment and stimulate cell migration and angiogenic effects to form capillaries. We showed that butein reduced the ability of EPCs to migrate towards serum and VEGF (Figure 2). Butein markedly and concentration-dependently inhibited serum- and VEGF-induced capillary-like tubular formation of EPCs (Figure 3). Notably, we demonstrated the potent *ex vivo* and *in vivo* anti-angiogenic effect of butein, suggesting that butein may be a potential angiogenesis inhibitor (Figures 4 and 5).

Butein that is derived from numerous traditional herbal medicines displayed promising anticancer activities against a broad spectrum of human cancer cells via different mechanisms. Butein inhibited migration and invasion through the ERK1/2 and NF-Kb signaling pathways in bladder cancer cells [25]. Butein suppressed invasion and CXCR4 expression in breast and pancreatic cancer cells [26]. Butein was found to be an aromatase inhibitor with growth inhibitory effect in breast cancer cells [29]. In addition, butein inhibited cell growth and induced apoptosis in melanoma, leukemia, and hepatocellular carcinoma cells [24, 27, 28]. The concentration of butein for its anticancer effects varies from 5 to 200 μM depending on its mechanism, time treatment, and tumor cell type. Mostly, butein induced the growth inhibitory and apoptotic effects in cancer cells at a higher concentration around 25–200 μM. In the present study, the concentration of butein (<20 μM) did not induce LDH release of EPCs, indicating that this antiproliferation effect of butein was not due to its cytotoxicity (Figures 1(c) and 1(d)). Butein at a concentration of 10 μM significantly inhibited angiogenesis of human EPCs

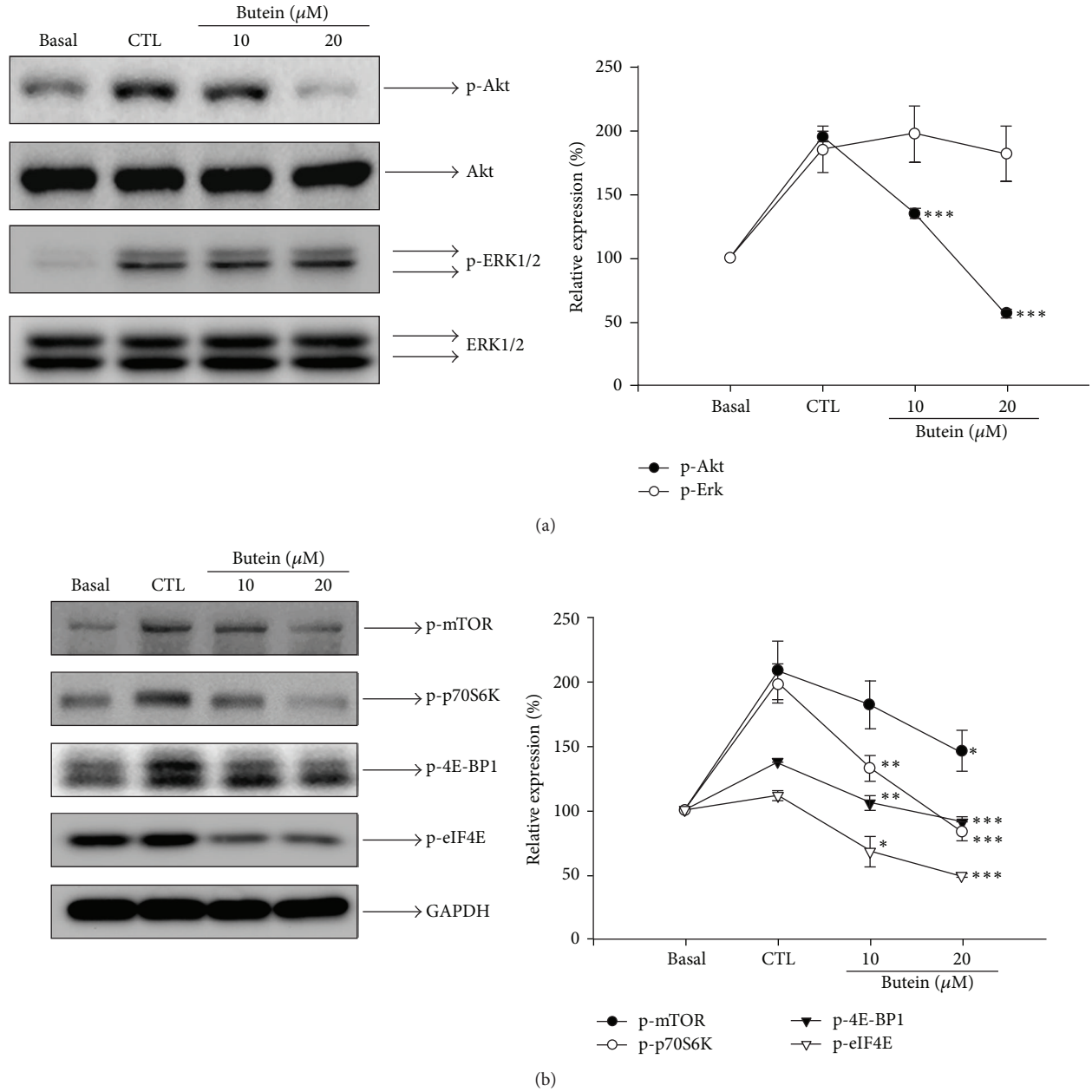

Figure 6: Effects of butein on the phosphorylation of Akt, ERK1/2, and translational regulatory proteins. Quiescent EPCs were treated with or without MV2 complete medium containing 10% FBS in the absence (control) or presence of butein (10 and 20 μM) for 15 min. Cells were harvested and lysed for the detection of p-Akt and p-ERK1/2 (a), p-mTOR, p-p70S6K, p-4E-BP1, and p-elf4E (b) by Western blot analysis. The quantitative densitometry of the relative level of protein was performed with Image-Pro Plus. Data are expressed as mean ± SEM of five independent experiments. $^{*}P < 0.05$, $^{**}P < 0.01$, and $^{***}P < 0.001$ compared with the control (CTL) group.

and human umbilical vein endothelial cells (HUVECs) (see Supplementary Figure 2). The growth inhibitory action of butein at low concentration (1–10 μM) is considered to be a more specific effect on endothelial cells that are stimulated by angiogenic growth factors. Taken together, we suggest that low concentration of butein exhibits novel anti-angiogenic activity and may contribute to suppress tumor growth and metastasis *in vivo*.

Importantly, our study is the first to show the effect of butein on AKT/mTOR-mediated translational pathway. Previous evidence implies that Akt and Erk signaling is the key mediator for vasculogenic functions, such as proliferation, survival, migration, and differentiation, which are activated by a variety of stimuli in endothelial cells and EPCs [37, 41]. Several studies showed that the inhibition of Akt and ERK1/2 signaling in tumor vasculature resulted

in vessel reduction and tumor growth suppression [42–44]. We found that butein significantly inhibited serum-induced Akt phosphorylation in a concentration-dependent manner, but not Erk1/2 phosphorylation in EPCs (Figure 6(a)). These results indicated that butein may suppress angiogenesis via inhibition of the Akt-dependent pathway. Akt signaling plays an important role in the activation of mTOR pathway, which has been indicated to regulate various biological functions of ECs for angiogenesis [13, 17]. Recent study also demonstrates that mTOR is involved in the control of cell growth in EPCs [45]. The mTOR signaling pathway is central to translational regulation and is a pivotal target in cancer therapeutics. Through activation of its downstream p70S6K and hyperphosphorylation of 4E-BP1, AKT/mTOR pathway coordinates and conducts cap-dependent mRNA translation in not only cell proliferation and growth, but also a crucial step leading to angiogenesis in the neoplastic and nonneoplastic processes [11, 46]. Our results showed that butein dramatically inhibited the mTOR signaling cascade, including mTOR, p70S6K, 4E-BP1, and elf4E in EPCs (Figure 6(b)). Thus, we suggest that anti-angiogenic activity of butein may be through the suppression of translation signaling pathway.

In conclusion, this study discovers a novel mechanism by which butein impairs angiogenesis *in vitro* and *in vivo*. We demonstrate that butein inhibits EPCs proliferation, migration, and tube formation by targeting the AKT/mTOR translation dependent signaling pathway. Since the contribution of EPCs during tumor angiogenesis is important for the initiation and promotion of tumor neovessel formation, our data provide evidence for butein that could be a potential candidate of angiogenesis inhibitor. Based on the findings herein, we suggest that butein is a promising natural product worthy of further development for the treatment of human cancer and other angiogenesis-related diseases.

Conflict of Interests

All authors have no financial or personal relationships with other people or organizations that could inappropriately influence their work.

Acknowledgment

This study was supported by research grants from the National Science Council of Taiwan (NSC 100-2320-B-715-001; NSC 101-2320-B-715-002 -MY3) awarded to S.-W. Wang.

References

[1] P. Carmeliet and R. K. Jain, "Angiogenesis in cancer and other diseases," *Nature*, vol. 407, no. 6801, pp. 249–257, 2000.

[2] A. S. Chung, J. Lee, and N. Ferrara, "Targeting the tumour vasculature: insights from physiological angiogenesis," *Nature Reviews Cancer*, vol. 10, no. 7, pp. 505–514, 2010.

[3] J. Folkman, "Angiogenesis: an organizing principle for drug discovery?" *Nature Reviews Drug Discovery*, vol. 6, no. 4, pp. 273–286, 2007.

[4] P. Carmeliet, "VEGF as a key mediator of angiogenesis in cancer," *Oncology*, vol. 69, supplement 3, pp. 4–10, 2005.

[5] T. Asahara, T. Murohara, A. Sullivan et al., "Isolation of putative progenitor endothelial cells for angiogenesis," *Science*, vol. 275, no. 5302, pp. 964–967, 1997.

[6] C. Urbich and S. Dimmeler, "Endothelial progenitor cells: characterization and role in vascular biology," *Circulation Research*, vol. 95, no. 4, pp. 343–353, 2004.

[7] B. A. Peters, L. A. Diaz, K. Polyak et al., ". Contribution of bone marrow-derived endothelial cells to human tumor vasculature," *Nature Medicine*, vol. 11, no. 3, pp. 261–262, 2005.

[8] F. Bertolini, Y. Shaked, P. Mancuso, and R. S. Kerbel, "The multifaceted circulating endothelial cell in cancer: towards marker and target identification," *Nature Reviews Cancer*, vol. 6, no. 11, pp. 835–845, 2006.

[9] D. Gao, D. J. Nolan, A. S. Mellick, K. Bambino, K. McDonnell, and V. Mittal, "Endothelial progenitor cells control the angiogenic switch in mouse lung metastasis," *Science*, vol. 319, no. 5860, pp. 195–198, 2008.

[10] Y. Shaked, E. Henke, J. M. L. Roodhart et al., "Rapid chemotherapy-induced acute endothelial progenitor cell mobilization: implications for antiangiogenic drugs as chemosensitizing agents," *Cancer Cell*, vol. 14, no. 3, pp. 263–273, 2008.

[11] D. Silvera, S. C. Formenti, and R. J. Schneider, "Translational control in cancer," *Nature Reviews Cancer*, vol. 10, no. 4, pp. 254–266, 2010.

[12] D. C. Fingar and J. Blenis, "Target of rapamycin (TOR): an integrator of nutrient and growth factor signals and coordinator of cell growth and cell cycle progression," *Oncogene*, vol. 23, no. 18, pp. 3151–3171, 2004.

[13] R. M. Memmott and P. A. Dennis, "Akt-dependent and -independent mechanisms of mTOR regulation in cancer," *Cellular Signalling*, vol. 21, no. 5, pp. 656–664, 2009.

[14] W. C. Merrick, "Cap-dependent and cap-independent translation in eukaryotic systems," *Gene*, vol. 332, no. 1-2, pp. 1–11, 2004.

[15] D. C. Fingar, S. Salama, C. Tsou, E. Harlow, and J. Blenis, "Mammalian cell size is controlled by mTOR and its downstream targets S6K1 and 4EBP1/eIF4E," *Genes and Development*, vol. 16, no. 12, pp. 1472–1487, 2002.

[16] Y. Mamane, E. Petroulakis, O. LeBacquer, and N. Sonenberg, "mTOR, translation initiation and cancer," *Oncogene*, vol. 25, no. 48, pp. 6416–6422, 2006.

[17] W. Li, M. Petrimpol, K. D. Molle, M. N. Hall, E. J. Battegay, and R. Humar, "Hypoxia-induced endothelial proliferation requires both mTORC1 and mTORC2," *Circulation Research*, vol. 100, no. 1, pp. 79–87, 2007.

[18] N. Hay, "The Akt-mTOR tango and its relevance to cancer," *Cancer Cell*, vol. 8, no. 3, pp. 179–183, 2005.

[19] L. Z. Liu, J. Z. Zheng, X. R. Wang, and B. H. Jiang, "Endothelial p70 S6 kinase 1 in regulating tumor angiogenesis," *Cancer Research*, vol. 68, no. 19, pp. 8183–8188, 2008.

[20] Z. J. Cheng, S. C. Kuo, S. C. Chan, F. N. Ko, and C. M. Teng, "Antioxidant properties of butein isolated from Dalbergia odorifera," *Biochimica et Biophysica Acta*, vol. 1392, no. 2-3, pp. 291–299, 1998.

[21] S. H. Lee, G. S. Seo, and D. H. Sohn, "Inhibition of lipopolysaccharide-induced expression of inducible nitric oxide synthase by butein in RAW 264.7 cells," *Biochemical and Biophysical Research Communications*, vol. 323, no. 1, pp. 125–132, 2004.

[22] S. M. Yu, Z. J. Cheng, and S. C. Kuo, "Endothelium-dependent relaxation of rat aorta by butein, a novel cyclic AMP-specific phosphodiesterase inhibitor," *European Journal of Pharmacology*, vol. 280, no. 1, pp. 69–77, 1995.

[23] Y. N. Chen, T. F. Huang, C. H. Chang et al., "Antirestenosis effect of butein in the neointima formation progression," *Journal of Agricultural and Food Chemistry*, vol. 60, no. 27, pp. 6832–6838, 2012.

[24] D. O. Moon, M. O. Kim, J. D. Lee, Y. H. Choi, and G. Y. Kim, "Butein suppresses c-Myc-dependent transcription and Akt-dependent phosphorylation of hTERT in human leukemia cells," *Cancer Letters*, vol. 286, no. 2, pp. 172–179, 2009.

[25] L. Zhang, W. Chen, and X. Li, "A novel anticancer effect of butein: inhibition of invasion through the ERK1/2 and NF-κB signaling pathways in bladder cancer cells," *FEBS Letters*, vol. 582, no. 13, pp. 1821–1828, 2008.

[26] A. W. L. Chua, H. S. Hay, P. Rajendran et al., "Butein downregulates chemokine receptor CXCR4 expression and function through suppression of NF-κB activation in breast and pancreatic tumor cells," *Biochemical Pharmacology*, vol. 80, no. 10, pp. 1553–1562, 2010.

[27] K. Iwashita, M. Kobori, K. Yamaki, and T. Tsushida, "Flavonoids inhibit cell growth and induce apoptosis in B16 melanoma 4A5 cells," *Bioscience, Biotechnology and Biochemistry*, vol. 64, no. 9, pp. 1813–1820, 2000.

[28] D. O. Moon, M. O. Kim, Y. H. Choi, J. W. Hyun, W. Y. Chang, and G. Y. Kim, "Butein induces G(2)/M phase arrest and apoptosis in human hepatoma cancer cells through ROS generation," *Cancer Letters*, vol. 288, no. 2, pp. 204–213, 2010.

[29] Y. Wang, F. L. Chan, S. Chen, and L. K. Leung, "The plant polyphenol butein inhibits testosterone-induced proliferation in breast cancer cells expressing aromatase," *Life Sciences*, vol. 77, no. 1, pp. 39–51, 2005.

[30] S. L. Lai, S. C. Cheah, P. F. Wong, S. M. Noor, and M. R. Mustafa, "*In vitro* and *in vivo* anti-angiogenic activities of panduratin a," *Plos One*, vol. 7, article e38103, 2012.

[31] J. S. Lee, Y. Kang, J. T. Kim, D. Thapa, E. S. Lee, and J. A. Kim, "The anti-angiogenic and anti-tumor activity of synthetic phenylpropenone derivatives is mediated through the inhibition of receptor tyrosine kinases," *European Journal of Pharmacology*, vol. 677, no. 1–3, pp. 22–30, 2012.

[32] H. H. Wang, C. A. J. Lin, C. H. Lee et al., "Fluorescent gold nanoclusters as a biocompatible marker for *in vitro* and *in vivo* tracking of endothelial cells," *ACS Nano*, vol. 5, no. 6, pp. 4337–4344, 2011.

[33] H. E. Tzeng, C. H. Tsai, Z. L. Chang et al., "Interleukin-6 induces vascular endothelial growth factor expression and promotes angiogenesis through apoptosis signal-regulating kinase 1 in human osteosarcoma," *Biochemical Pharmacology*, vol. 85, no. 4, pp. 531–540, 2013.

[34] R. F. Nicosia and A. Ottinetti, "Modulation of microvascular growth and morphogenesis by reconstituted basement membrane gel in three-dimensional cultures of rat aorta: a comparative study of angiogenesis in Matrigel, collagen, fibrin, and plasma clot," *In Vitro Cellular and Developmental Biology*, vol. 26, no. 2, pp. 119–128, 1990.

[35] L. Guedez, A. M. Rivera, R. Salloum et al., "Quantitative assessment of angiogenic responses by the directed *in vivo* angiogenesis assay," *American Journal of Pathology*, vol. 162, no. 5, pp. 1431–1439, 2003.

[36] S. W. Wang, H. H. Wu, S. C. Liu et al., "CCL5 and CCR5 interaction promotes cell motility in human osteosarcoma," *Plos One*, vol. 7, article e35101, 2012.

[37] R. Muñoz-Chápuli, A. R. Quesada, and M. Á. Medina, "Angiogenesis and signal transduction in endothelial cells," *Cellular and Molecular Life Sciences*, vol. 61, no. 17, pp. 2224–2243, 2004.

[38] K. M. Cook and W. D. Figg, "Angiogenesis inhibitors: current strategies and future prospects," *CA Cancer Journal for Clinicians*, vol. 60, no. 4, pp. 222–243, 2010.

[39] M. Seandel, J. Butler, D. Lyden, and S. Rafii, "A catalytic role for proangiogenic marrow-derived cells in tumor neovascularization," *Cancer Cell*, vol. 13, no. 3, pp. 181–183, 2008.

[40] Y. Shaked, A. Ciarrocchi, M. Franco et al., "Therapy-induced acute recruitment of circulating endothelial progenitor cells to tumors," *Science*, vol. 313, no. 5794, pp. 1785–1787, 2006.

[41] F. X. Ma and Z. C. Han, "Akt signaling and its role in postnatal neovascularization," *Histology and Histopathology*, vol. 20, no. 1, pp. 275–281, 2005.

[42] J. S. Sebolt-Leopold and R. Herrera, "Targeting the mitogen-activated protein kinase cascade to treat cancer," *Nature Reviews Cancer*, vol. 4, no. 12, pp. 937–947, 2004.

[43] C. Y. Peng, S. L. Pan, K. H. Lee, K. F. Bastow, and C. M. Teng, "Molecular mechanism of the inhibitory effect of KS-5 on bFGF-induced angiogenesis *in vitro* and *in vivo*," *Cancer Letters*, vol. 263, no. 1, pp. 114–121, 2008.

[44] A. C. Tsai, S. L. Pan, C. H. Liao et al., "Moscatilin, a bibenzyl derivative from the India orchid Dendrobrium loddigesii, suppresses tumor angiogenesis and growth *in vitro* and *in vivo*," *Cancer Letters*, vol. 292, no. 2, pp. 163–170, 2010.

[45] S. G. Miriuka, V. Rao, M. Peterson et al., "mTOR inhibition induces endothelial progenitor cell death," *American Journal of Transplantation*, vol. 6, no. 9, pp. 2069–2079, 2006.

[46] A. C. Hsieh, M. L. Truitt, and D. Ruggero, "Oncogenic AKTivation of translation as a therapeutic target," *British Journal of Cancer*, vol. 105, no. 3, pp. 329–336, 2011.

Hindawi Publishing Corporation
Evidence-Based Complementary and Alternative Medicine
Volume 2013, Article ID 718380, 13 pages
http://dx.doi.org/10.1155/2013/718380

Research Article

Inhibition of Metastatic Potential in Breast Carcinoma *In Vivo* and *In Vitro* through Targeting VEGFRs and FGFRs

Ming-Hsien Chien,[1,2] Liang-Ming Lee,[3] Michael Hsiao,[4] Lin-Hung Wei,[5] Chih-Hau Chen,[6] Tsung-Ching Lai,[4] Kuo-Tai Hua,[7] Min-Wei Chen,[5] Chung-Ming Sun,[6] and Min-Liang Kuo[7,8]

[1] *Graduate Institute of Clinical Medicine, College of Medicine, Taipei Medical University, Taipei 11031, Taiwan*
[2] *Wan Fang Hospital, Taipei Medical University, Taipei 116, Taiwan*
[3] *Department of Urology, Wan Fang Hospital, Taipei Medical University, Taipei 116, Taiwan*
[4] *The Genomics Research Center, Academia Sinica, Taipei 115, Taiwan*
[5] *Department of Oncology, National Taiwan University Hospital, Taipei 10041, Taiwan*
[6] *Department of Applied Chemistry, National Chiao Tung University, No. 1001 Ta Hsueh Road, Hsinchu 300-10, Taiwan*
[7] *Graduate Institute of Toxicology, College of Medicine, National Taiwan University, Taipei 100, Taiwan*
[8] *Graduate Institute of Biomedical Sciences, College of Life Science, National Taiwan University, No. 1, Section 4, Roosevelt Road, Taipei 106, Taiwan*

Correspondence should be addressed to Chung-Ming Sun; cmsun@mail.nctu.edu.tw
and Min-Liang Kuo; kuominliang@ntu.edu.tw

Received 22 March 2013; Accepted 20 April 2013

Academic Editor: Shun-Fa Yang

Angiogenesis and lymphangiogenesis are considered to play key roles in tumor metastasis. Targeting receptor tyrosine kinases essentially involved in the angiogenesis and lymphangiogenesis would theoretically prevent cancer metastasis. However, the optimal multikinase inhibitor for metastasis suppression has yet to be developed. In this study, we evaluated the effect of NSTPBP 0100194-A (194-A), a multikinase inhibitor of vascular endothelial growth factor receptors (VEGFRs)/fibroblast growth factor receptors (FGFRs), on lymphangiogenesis and angiogenesis in a mammary fat pad xenograft model of the highly invasive breast cancer cell line 4T1-Luc$^+$. We investigated the biologic effect of 194-A on various invasive breast cancer cell lines as well as endothelial and lymphatic endothelial cells. Intriguingly, we found that 194-A drastically reduced the formation of lung, liver, and lymph node metastasis of 4T1-Luc$^+$ and decreased primary tumor growth. This was associated with significant reductions in intratumoral lymphatic vessel length (LVL) and microvessel density (MVD). 194-A blocked VEGFRs mediated signaling on both endothelial and lymphatic endothelial cells. Moreover, 194-A significantly inhibited the invasive capacity induced by VEGF-C or FGF-2 *in vitro* in both 4T1 and MDA-MB231 cells. In conclusion, these experimental results demonstrate that simultaneous inhibition of VEGFRs/FGFRs kinases may be a promising strategy to prevent breast cancer metastasis.

1. Introduction

Tissue invasion and metastasis, which cause 90% of cancer deaths, are common features during the development of most types of human cancer. The distant settlements of tumor cells can be, in general, classified into hematogenous metastasis and lymphogenous metastasis. Although invasion and metastasis are exceedingly complex processes, recent advances in understanding the molecular mechanisms involved in angiogenesis and lymphangiogenesis have provided opportunities to develop new treatments to prevent metastasis.

Tumors express various angiogenic and lymphangiogenic factors. VEGF family, among all, is perhaps the most important one. VEGF-A, the founding member of the family, has emerged as the key mediator of neovascularization in cancer [1]. The biological functions of the VEGFs are mediated

by a family of cognate protein tyrosine kinase receptors (VEGFRs) [2–4]. VEGF-A binds to VEGFR-2 and VEGFR-1; VEGF-C and VEGF-D bind VEGFR-2 and VEGFR-3; PLGF and VEGF-B bind only to VEGFR-1; VEGF-E binds only to VEGFR-2. Signaling through VEGFR-2 and VEGFR-3 is crucial in the promotion of angiogenesis and lymphangiogenesis, respectively [5, 6]. In addition to the expression on endothelial cells/lymphatic endothelial cells, VEGFR-2/VEGFR-3 has been shown to be expressed in a variety of human malignancies, including breast carcinoma [7, 8].

Much research has determined that the VEGF-A/VEGFR-2 axis in cancer cells can promote growth of cancer cells [9], while the VEGF-C/VEGFR-3 axis enhances mobility of cancer cells and contributes to the promotion of metastasis in animals [10]. Given a significant role of VEGFR-2/VEGFR-3 in tumor development and progression, inhibition of both VEGF-A/VEGFR-2 and VEGF-C/VEGFR-3 signals has shown promising results in suppressing tumor progression and metastasis in preclinical studies [11].

Overexpression of fibroblast growth factor receptor (FGFR) tyrosine kinases has been found in human breast cancers and has been associated with poor patient prognosis [12, 13]. There are four FGFR genes (*FGFR1–FGFR4*) that encode receptors consisting of three extracellular immunoglobulin domains, a single-pass transmembrane domain, and a cytoplasmic tyrosine kinase domain [14]. In breast carcinoma, amplification and overexpression of FGFRs, including FGFR-1 (20%), FGFR-2 (12%), and FGFR-4 (30%), have been observed [15–17]. These FGFRs mediate signaling from their high-affinity ligands, fibroblast growth factors (FGFs) [18]. The FGFs/FGFRs signaling interferes with many cellular functions, such as cell proliferation, transformation, and angiogenesis [19]. In particular, recent advances have shown that FGFRs activity is linked to tumor growth, epithelial-mesenchymal transition, and distant metastasis and thus contributes to tumor progression [20–22]. Also, targeting FGFRs signaling has been shown to suppress tumor outgrowth and metastasis in pre-clinical models [23]. Therefore, blocking VEGFRs/FGFRs activities may be of clinical benefit in the management of patients with highly metastatic breast cancer.

We have recently discovered a low molecular weight synthetic receptor tyrosine kinase inhibitor with the 2H-indazole core [24]. We identified NSTPBP 0100194-A (194-A) as a compound with particularly strong inhibitory potency against VEGFR-3 and VEGFR-2 kinase activity. In addition, 194-A showed similar potency against FGFR-1, FGFR-2, and FGFR-4, but was largely inactive against other tyrosine kinases. The kinase inhibitory signature of 194-A prompted us to evaluate this compound as a therapeutic for VEGFRs/FGFRs-dependent malignancies. In this study, we determined the effect of 194-A on both angiogenesis and lymphangiogenesis using a 4T1 mammary fat pad model and found that inhibition of VEGFRs/FGFRs dramatically suppressed tumor metastasis to regional lymph nodes and distant organs, via angiogenic and lymphangiogenic inhibition as well as suppressing the metastatic potential of tumor cells.

2. Materials and Methods

2.1. Cell Lines. Human umbilical vein endothelial cells (HUVECs) and lymphatic endothelial cells (LECs) were purchased from PromoCell (Heidelberg, Germany). The high invasive breast cancer cell lines, 4T1 and MDA-MB231, were purchased from American Type Culture Collection (Manassas, VA, USA). These cells were cultured according to the vendor's guidelines. 4T1 cells were engineered to express the firefly luciferase protein for detection *in vivo* using Xenogen IVIS-100 imaging system. The luciferase positive population of 4T1 cells was selected in gentamicin (G418; Life Technologies). Bioluminescent, antibiotic resistant, and single-cell clones were amplified in culture and characterized for stable luminescence *in vitro,* and tumorigenic potential monitored *in vivo*.

2.2. Kinase Inhibitor. NSTPBP 0100194-A (194-A), 1-(2-cyclohexenylethyl)-2-(2-(3,3-diphenylpropyl)-2H-indazole-6-yl)-1H-benzo[d]imidazole-5-carboxylic acid (see Supplementary Figure 1 in Supplementary Material available online at http://dx.doi.org/10.1155/2013/718380) was provided by Dr. Chung-Ming Sun's laboratory at the Department of Applied Chemistry (National Chiao Tung University, Hsinchu, Taiwan). The synthetic routes were described elsewhere [24] and the kinase inhibitory profile was shown in Supplementary Table 1. For *in vitro* experiments, 194-A was dissolved in DMSO. For *in vivo* experiments, 194-A was prepared in a microemulsion containing 2 mg 194-A, 8.3 mg tricaprin, 50 mg Tween 80, and 20 mg propylene glycol in 1 mL PBS buffer.

2.3. Antibodies and Reagents. VEGF-C and VEGF-A_{165} were purchased from R&D Systems. The following primary antibodies were used: VEGFR-2, proliferating cell nuclear antigen (PCNA) (Upstate, Lake Placid, NY, USA); p-tyr1054 VEGFR-2 (Millipore); lymphatic vessel endothelial receptor 1 (LYVE-1) (R&D Systems); phosphorylated tyrosine (PY-99), VEGFR-3, phosphorylated extracellular signal-regulated kinase 1/2 (ERK1/2), ERK1/2, phosphorylated Akt, Akt, CD31 (Santa Cruz Biotechnology). Biotin-labeled donkey anti-goat IgG and TRITC-labeled donkey anti-goat IgG secondary antibody were purchased from Santa Cruz Biotechnology. 4′,6-Diamidino-2-phenylindole dihydrochloride (DAPI) was obtained from Sigma-Aldrich. Sunitinib and sorafenib were purchased from Pfizer and Bayer, respectively.

2.4. Immunoprecipitation and Western Blot. Protein lysates were prepared as previously described [25]. Western blotting was performed with primary antibodies for p-tyr1054 VEGFR-2, VEGFR-2, p-ERK1/2, ERK1/2, p-Akt, and Akt, as noted. For immunoprecipitation, protein lysates were incubated with VEGFR-3 antibody immobilized onto protein A-Sepharose (Sigma-Aldrich) for 1 h at 4°C with gentle rotation.

2.5. Endothelial Cell Proliferation. 5×10^3 HUVECs or LECs were seeded in collagen-coated 96-well plates and allowed

to attach overnight. The medium was replaced with serum-free medium containing 194-A or DMSO with 100 ng/mL VEGF-A or 500 ng/mL VEGF-C for 12 h. Cell proliferation was performed by MTS assay (Promega). Data were collected from three replicates.

2.6. Endothelial Cell Migration. Assessment of endothelial cell migratory activity was performed as described [26]. 3×10^4 HUVECs or LECs were suspended in serum-free media and seeded in the top chamber of a cell culture insert (Costar, Cambridge, MA, USA) after treatment with DMSO or 194-A for 30 min. The insert was placed in a 24-well plate containing serum-free medium with control protein, VEGF-A (100 ng/mL) or VEGF-C (500 ng/mL); the cells were incubated for 24 h and migrating cells were stained with crystal violet (Sigma, St Louis, MI, USA). The migratory activity was calculated as a percentage of migratory cells in the test samples versus control.

2.7. Invasion Assay. Invasion assays were done using modified Boyden chambers with Matrigel (30 μg, Collaborative Biomedical, Becton Dickinson Labware, San Jose, CA, USA) coated filter inserts for 24-well plates. Cells (1×10^5) were pretreated with DMSO or 194-A for 30 min and plated into 100 μL of low serum (1% FBS) RPMI or DMEM in the top chamber. The insert was placed in a 24-well plate containing low serum medium with control protein, FGF-2 (20 ng/mL) or VEGF-C (100 ng/mL) for 24 hr. The cells that invaded through the Matrigel and attached to the lower surface of the filter were stained with crystal violet and calculated.

2.8. In Vitro Cytotoxicity Assay. 4T-1 cells were plated in 96-well microtiter plates and treated with various concentrations (0, 1, 3, and 10 μM) of 194-A for 24 h, and cell viabilities were assessed using the MTS (Promega Corporation, Madison, WI, USA) assay. The absorbance (A) was read at 490 nm using an ELISA reader (MQX200; BioTek Instruments, Winooski, VT, USA).

2.9. 4T1 Tumor Model In Vivo. Female BALB/c mice were orthotopically injected with 2.5×10^5 4T1-Luc$^+$ cells, suspended in PBS, into the right fat pad. Tumors were measured every three days according to (tumor size = length $\times$ width^2 $\times$ 0.52). Mice were given 194-A, sorafenib (in cremophor EL/ethanol), or sunitinib (in citrate-buffer solution) as oral administrations of 50 mg/kg/day or other dosage, as noted. Treatment was initiated after tumors reached 75 mm^3 and lasted until the endpoint of the experiment. Mice were imaged once a week, by injecting 150 mg/kg luciferin i.p. and imaging the tumors using bioluminescence technology (Xenogen IVIS-100 imaging system). For primary tumors, the exposure time ranged from 5 seconds to 1 minute depending on the size of the tumor. For detection of metastatic tumor nodules, exposure time was extended to 5 minutes. To exclude treatment related toxicity, mice were weighted every two days. Lymph node, distal organs (lung and liver) metastasis, and primary tumor weights were excised at the end of the experiment. All experiments were repeated at least twice with a minimum of 5 mice per group.

2.10. Tumor Vascularity Detection In Vivo. Tumor vascularity was monitored by using non-contrast-enhanced flow-sensitive ultrasound (Vevo 770 micro-ultrasound system). Non-contrast-enhanced flow-sensitive ultrasound predominantly visualized the vessel networks on the tumor margins, some of which branched toward the tumor center. Tumor vascularity was quantified in power Doppler images by computing the color pixel density, which is equal to the percentage of image voxels within a region of interest that exhibits detectable flow.

2.11. Pharmacokinetics of p.o. 194-A Administration in Mice. BALB/C mice received a single dose of 50 mg/kg 194-A by oral gavage, and plasma samples were collected at different time points. The plasma samples were prepared for ultrahigh performance liquid chromatography coupled to tandem mass spectrometry (UPLC/MS/MS) analysis, by protein precipitation with two volumes of acetonitrile (100 μL) per 50 μL plasma sample. Pharmacokinetic parameters were determined by MassLynx 4.1 software.

2.12. Immunohistochemistry. Tumor tissues were processed for either paraffin or OCT sections as previously described [27]. CD31 and PCNA staining was detected using streptavidin-biotin peroxidase complex method by DAB Peroxidase Substrate Kit (SK-4100; Vector Laboratories). Detection of LYVE-1 was performed using TRITC-conjugated donkey anti-goat IgG secondary antibody under a Zeiss Axioskop fluorescence microscope. Microvessel density (MVD) and lymphatic vessel length (LVL) were quantified for each 200x field using ProImage software. For each tumor section, 3-4 fields were counted. The number of PCNA-positive cells, among at least 500 cells per field, was counted and expressed as percentage values.

2.13. In Vivo Cell Death Analysis. DeadEnd Fluorometric Terminal Deoxynucleotidyl Transferase-Mediated Nick-End Labeling System (Promega, Madison, WI) was used to evaluate the cell death in sections of 4T1 tumors obtained from control and test compounds-treated animals, according to the manufacturer's instructions.

2.14. Statistical Analysis. Differences between the means of unpaired samples were evaluated by the Student's t-test and differences in the median values between the two groups were evaluated by Wilcoxon rank-sum test using the SigmaPlot and SigmaStat programs. $P < 0.05$ was considered statistically significant. All statistical tests were of two sided.

3. Results

3.1. The In Vivo and In Vitro Antitumor Activity of 194-A in a Metastasis-Specific Mouse Mammary Carcinoma 4T1. To evaluate the antitumor activity of 194-A on primary tumor growth and metastasis, a mouse mammary carcinoma cell

line, 4T1, was used. 4T1 is a highly metastatic tumor cell that can metastasize to the lung, liver, and lymph nodes while the primary tumor is growing *in situ* [28]. 194-A was administered p.o. and evaluated in an orthotopic graft model. 4T1-Luc$^+$ cells were inoculated into the mammary fat pad and allowed to establish for 9 days before initiation of treatment. 4T1-Luc$^+$ orthotopic graft mice were treated with daily administrations of different dosages of 194-A (10~50 mg/kg) or vehicle control using oral gavage. Figure 1(a) showed the inhibitory potency of 194-A (50 mg/kg) on tumor growth after 10 days of treatment by photon emissions detection *in vivo*. The mean tumor volume from caliper measurement showed that treatment with 194-A resulted in a dose-dependent inhibition of tumor growth (Figure 1(b)). In 194-A-treated mice receiving 25 or 50 mg/kg daily, the mean tumor volume on day 30 was inhibited by 38% ($P < 0.05$) and 55% ($P < 0.01$), respectively, relative to the vehicle-treated 4T1 tumors (Figure 1(b)). Next, we examined the effects of 194-A on cell proliferation and apoptosis within the 4T1 tumors after 10 days of treatment. The immunohistochemical analysis of cell proliferation was performed using PCNA staining. The mean number of PCNA positive tumor cells was reduced with 60% after treatment with 194-A compared to control mice (Figure 1(c)). Additionally, the number of TUNEL positive cells was increased 4.3-fold in the 194-A treated group compared to the control group (Figure 1(d)). However, 194-A, at a concentration up to 10 μM for 24 h treatment, had no significant effect on 4T1 cells growth *in vitro* (Figure 1(e)). These experimental results clearly verify that 194-A can suppress *in vivo* tumor growth of 4T1 cells without significantly altering their *in vitro* growth rate. Pharmacokinetic studies revealed a maximal plasma concentration (C_{max}) ~7500 ng/mL at 0.75 hour, while the plasma levels were below 500 ng/mL at 12 hours after administration of 50 mg/kg 194-A. The p.o. bioavailability of 194-A in BALB/c mice was ~55%. The rapid reduction in 194-A levels implies that 194-A rapidly metabolize to another metabolite, but which metabolite exhibited antitumor activity *in vivo* must be further explored (Figure 1(f)).

3.2. The Antiangiogenesis Efficacy of 194-A in the 4T1 Tumor Model. 194-A exhibited significant activity against VEGFR-2 (Supplementary Table 1), the RTK known to promote angiogenesis. We, therefore, determined the effect of 194-A on intratumoral vasculature. We utilized a high frequency volumetric power Doppler ultrasound (HF-VPDU) to measure blood flow within large vessels of tumor vasculature with high flow velocities. Though HF-VPDU is a non-contrast-enhanced imaging, therapeutical effects can be recognized on the depicted vessels visually. Figure 2(a) showed that the intratumoral vascularity in orthotopic grafts was drastically decreased compared with control tumors after the 10-day 194-A treatment. The antiangiogenic effect of 194-A was also verified by immunohistochemical analysis with an endothelial cell marker, CD31, on primary tumor tissue (Figure 2(b), upper panel). Administration of 194-A at 50 mg/kg p.o. produced 64% inhibition of the microvessel density (MVD) relative to vehicle-treated 4T1 tumors (Figure 2(b), bottom panel). *In vitro*, a dose-dependent decrease in VEGF-A-induced HUVECs proliferation was observed upon addition of 194-A (Figure 2(c)). 194-A at 1 μM significantly inhibited VEGF-A-induced HUVECs proliferation. Similar inhibitory effect by 194-A on HUVECs migration was also observed (Figure 2(d)). Furthermore, we examined the effect of 194-A on VEGF-A-induced VEGFR-2 activity and their downstream signaling targets in primary HUVECs. 194-A at 1 μM inhibited VEGF-A-induced phosphorylation of VEGFR-2 (Tyr 1054), ERK1/2, and Akt significantly (Figure 2(e)). Overall, these data demonstrate that administration of 194-A suppresses angiogenesis in 4T1 tumors, which may account for the antitumor activity of 194-A.

3.3. Significant Antimetastatic and Antilymphangiogenic Effect of 194-A in the 4T1 Tumor Model. In contrast to modest tumor growth inhibition, formation of spontaneous lung metastasis was dramatically prevented by 194-A (~94% inhibition) as measured by luciferase expression (Figure 3(a)). Visual comparison of mouse lungs showed marked growth of lung metastasis in vehicle-treated group, but few established invasive metastasis in 194-A-treated group (Figure 3(a)). In addition, H&E staining revealed a significant reduction in the incidence of lung, liver, and lymph node tumor metastasis in response to 194-A treatment (Figures 3(b) and 3(c)). Metastasis to lymph nodes occurred in 8.5% ± 3.5% and to the lung in 25% ± 8% after 194-A treatment, whereas metastasis to the lymph nodes and lung occurred in 41.5 ± 8.5% and 100%, respectively, in vehicle-treated mice. Notably, immunofluorescent analysis with a lymph endothelial cell marker, LYVE-1, showed that the mean lymphatic vessel length (MLVL) was decreased by 194-A (~70% inhibition) compared to vehicle treatment (Figure 3(d)). *In vitro*, 194-A dose dependently inhibited VEGF-C-induced LECs proliferation and migration (Figures 3(e) and 3(f)). In parallel, the activation of VEGFR-3 and its downstream signaling pathway induced by VEGF-C were inhibited by 194-A in a dose-dependent manner and almost abolished by 194-A at 1 μM (Figure 3(g)). These experimental results demonstrated the antilymphangiogenesis efficacy of 194-A, which at least in part accounts for its antimetastatic effect.

3.4. 194-A Reduces the VEGF-C and FGF-2-Induced Invasive Effects of Mammary Carcinoma Cell Lines. Earlier studies of VEGFRs/FGFRs signaling on tumor cells have prompted us to evaluate whether 194-A would reduce the invasiveness of breast cancer cells [10, 20, 23, 29]. Here, we found that stimulation with VEGF-C in two VEGFR-3$^+$ mammary carcinoma cell lines, 4T1 (Supplementary Figure 2(a)) and MDA-MB231 [10], resulted in a significant increase of invasive ability (Figures 4(a) and 4(b)). A dose-dependent decrease in VEGF-C-induced invasion was observed upon addition of 194-A (Figures 4(a) and 4(b)). Furthermore, increased levels of FGFR-1 and FGFR-2 expression were observed in 4T1 (Supplementary Figure 2(b)) and MDA-MB231 cells [30]. FGF-2 stimulation substantially increased the invasiveness of MDA-MB231 and 4T1 cells. Likewise, 3 μM 194-A effectively suppressed the FGF-2 induced invasion of this two breast

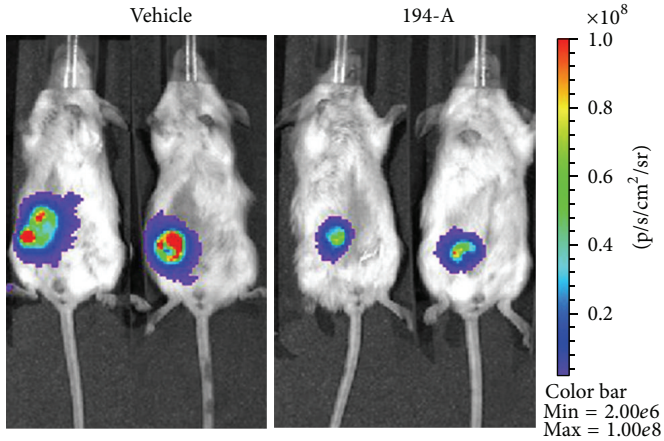

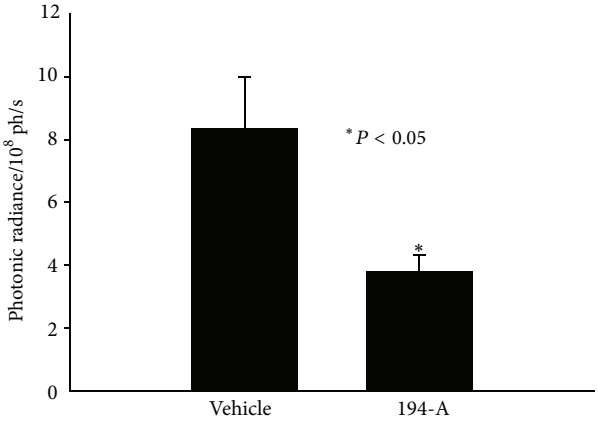

(a)

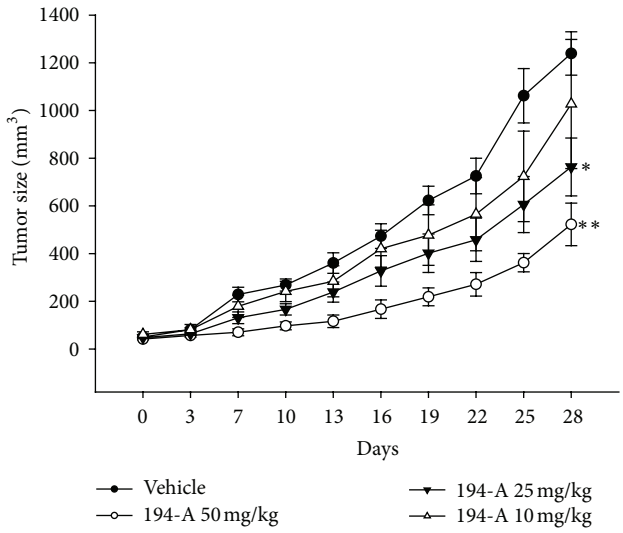

(b)

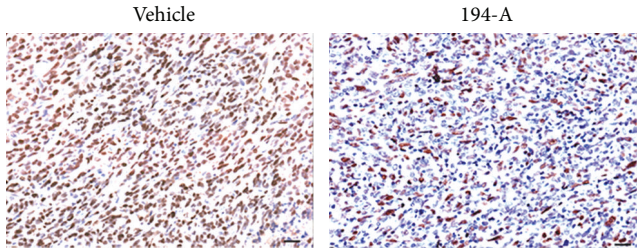

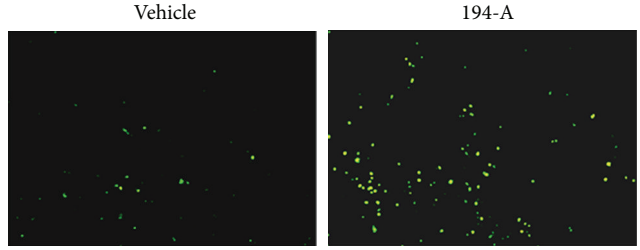

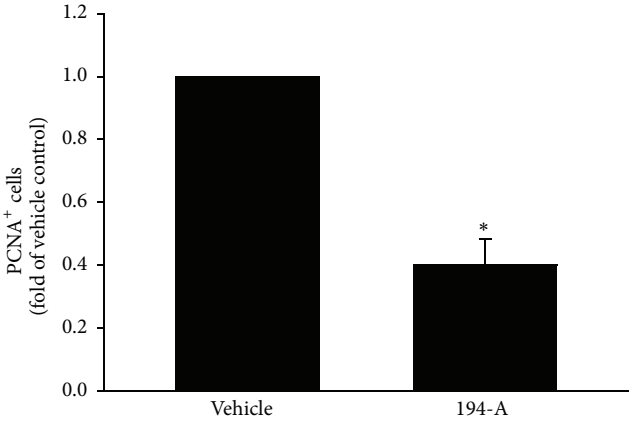

(c)

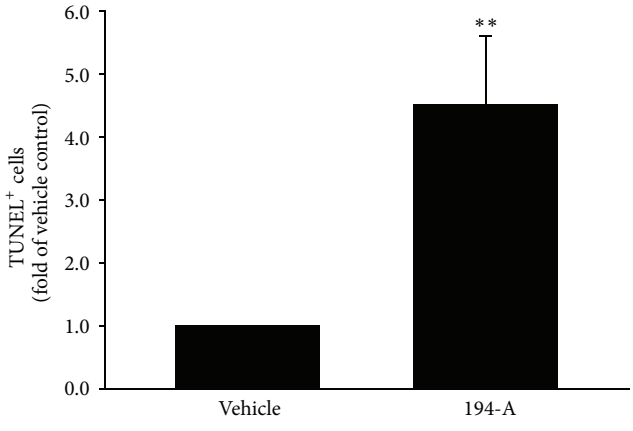

(d)

Figure 1: Continued.

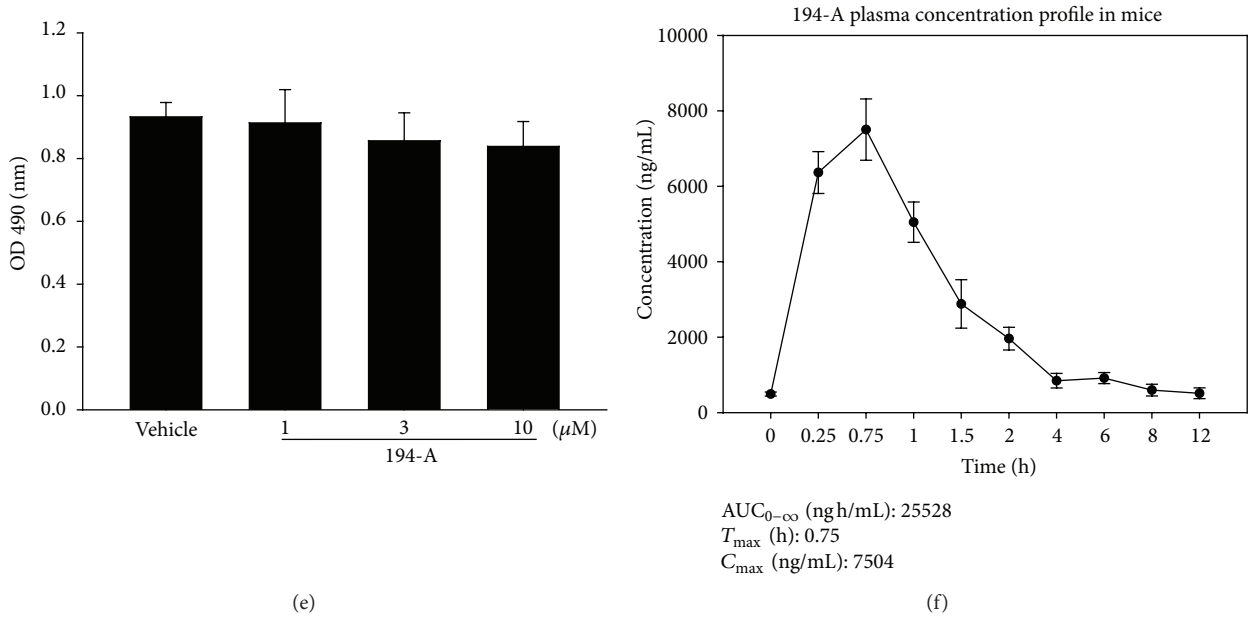

(e) (f)

FIGURE 1: The *in vivo* and *in vitro* antitumor activity of 194-A in the 4T1 orthotopic graft model. (a) and (b) Tumor growth inhibition after treatment with 194-A. 4T1-Luc$^+$ (5×10^5 cells/mouse) were orthotopically implanted into the fat pad of male BALB/c mice. The tumor growth inhibition by p.o. administration of 194-A at different dosages (10~50 mg/kg/day) was monitored based on emitted bioluminescence detection (a) or external measurement using a caliper (b). (c) and (d) 194-A induced inhibition of proliferation and induction of apoptosis in 4T1 orthotopic grafts. Proliferation index and apoptotic index were determined by PCNA immunohistochemical staining (c) and TUNEL assay (d), respectively, after 10-day 194-A treatment. PCNA-positive or TUNEL-positive cells were counted in five 200x fields per 4T1 tumor section ($n = 6$). The average number of PCNA-positive or TUNEL-positive cells in each section was normalized to vehicle control. (e) 194-A (1~10 μM) have no significant effects on 4T1 cells proliferation as measured by MTS analysis. *Lines* or *columns*, mean ($n = 6$); *bars*, SE. $^*P < 0.05$; $^{**}P < 0.01$ as compared to the vehicle control group. Scale bar, 20 μm. (f) 194-A plasma concentration in mice after a single p.o. dose of 50 mg/kg ($n = 3$).

cancer cell lines (Figures 4(c) and 4(d)). These works further support the anti-metastatic potential of 194-A by targeting VEGFRs/FGFRs signaling.

3.5. The Antimetastatic Effects of 194-A Are Comparable with Sunitinib and Sorafenib. Given our observations that inhibition of VEGFRs/FGFRs signaling caused significant metastasis inhibition, we compared the therapeutic effects of 194-A, sunitinib, and sorafenib on metastasis of 4T1 to distant lung. Sunitinib and sorafenib are clinically used VEGFRs/PDGFR inhibitors with stronger potency than 194-A in inhibiting VEGFRs [31, 32]. We treated tumor-bearing mice using oral gavage with 50 mg/kg 194-A, sunitinib, or sorafenib daily starting 9 days after inoculation and administered for 30 days. While 194-A significantly reduced the primary tumor growth by 50% compared to the vehicle control ($P = 0.047$), sunitinib and sorafenib were shown to be more effective than 194-A ($P = 0.009$ and 0.048) (Figure 5(a)). Of note, using photon emissions detection of lung metastasis, we found that 194-A has comparable potency to sunitinib and sorafenib in preventing 4T1 metastasis to lung at the end of treatment ($P = 0.75$ and 0.92). Figure 5(b) showed that the median value of photon emissions from the lungs was 2.9×10^5 (for 194-A), 1.9×10^5 (for sunitinib), 2.5×10^5 (for sorafenib), and 1.4×10^6 (for vehicle). No significant difference in body weight was detected among these four groups (Figure 5(c)). These experimental results suggest that the kinase inhibitory profile of 194-A (VEGFRs/FGFRs) might be feasible for preventing breast cancer metastasis.

4. Discussion

Much research has determined the requirement of angiogenesis for growth and progression of dormant lesions. It is of particular interest to determine whether antiangiogenic approach will not only reduce tumor growth but also block the progression of dormant lesions into aggressive cancers or metastasis in high-risk cancer patients. The multikinase inhibitor 194-A was an equally potent inhibitor of VEGFRs and FGFRs in cell-free assay (Supplementary Table 1). Administration of 194-A (p.o.) partially reduced tumor growth of 4T1 cells injected into the mammary fat pad and drastically reduced metastasis to distal organs. Histological analyses revealed decreased angiogenesis and lymphangiogenesis in tumor section from 194-A-treated mice, highlighting the impact of angiogenesis and lymphangiogenesis on tumor development and progression. 194-A treatment substantially reduced breast cancer cell motility and invasive ability associated with VEGFRs/FGFRs. The anti-metastatic potency of 194-A can be attributed by the synergistic inhibitory effects, which are achieved by targeting different signaling circuits, not only in endothelial cells, but also

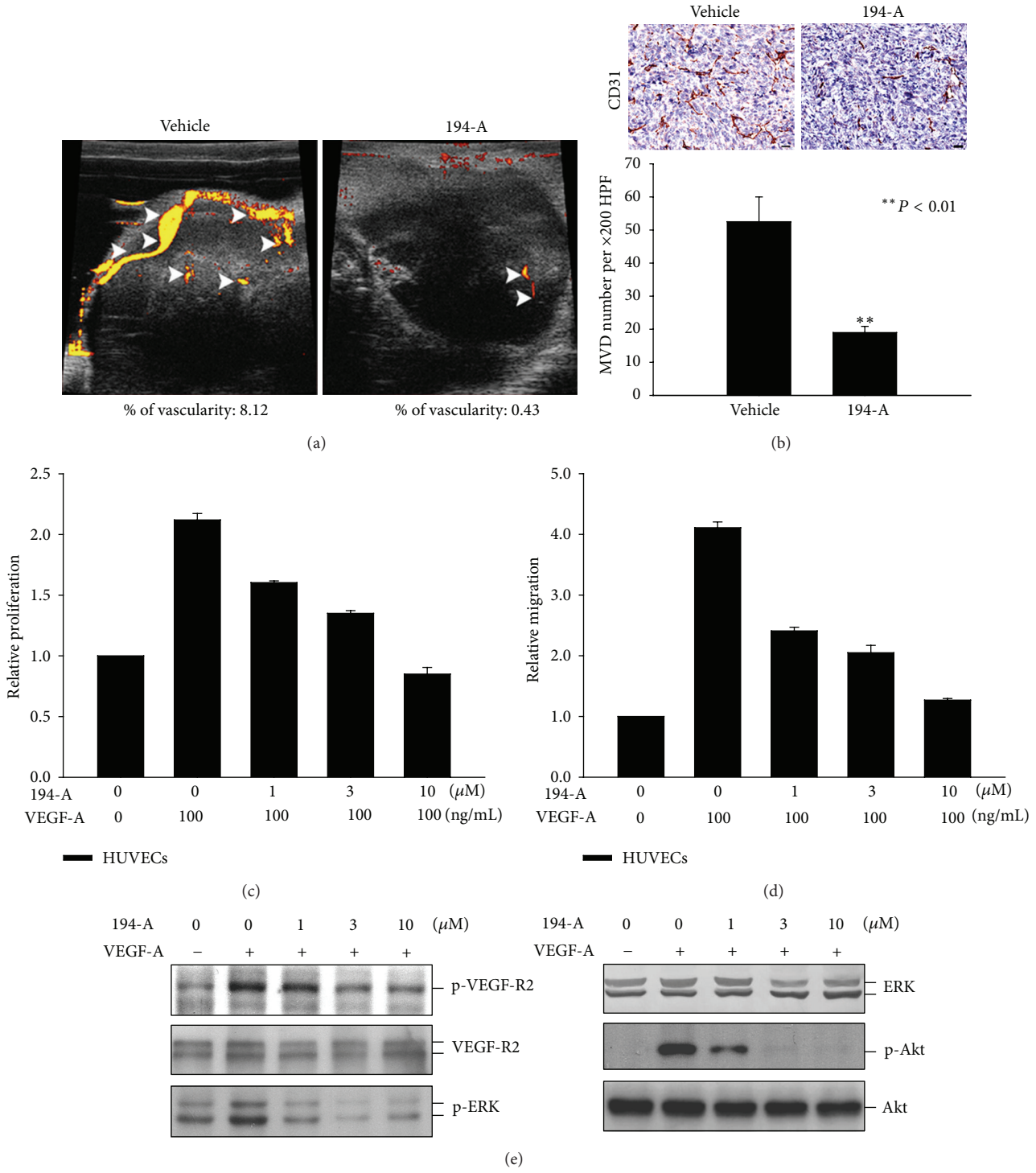

Figure 2: The antiangiogenesis efficacy of 194-A in the 4T1 orthotopic graft model. (a) Tumor vascularity was monitored after 10 days of 194-A (50 mg/kg) p.o. treatment, by using non-contrast-enhanced flow-sensitive ultrasound (Vevo 770 micro-ultrasound system). (b) Immunohistochemical staining of 4T1 tumor sections with CD31 antibody, counterstained with hematoxylin. Vessel density per 200x field was assessed from 3 to 4 fields per tumor section. *Columns*, mean ($n = 6$); *bars*, SE. $^{**}P < 0.01$ as compared to the vehicle control group. Scale bar, 20 μm. (c) Relative proliferation of HUVECs grown in serum-free media supplemented with 100 ng/mL of VEGF-A as indicated. Proliferation was reduced in a dose-dependent manner in response to 194-A treatment. Mean values of three replicates, normalized to the untreated controls; *bars*, SE. (d) Treatment with increasing concentrations of 194-A reduced VEGF-A-induced migration in HUVECs. The number of migrating cells was normalized to DMSO control and values are displayed as mean values from three independent experiments. (e) 194-A inhibited VEGF-A-induced activation of VEGFR-2 and its common downstream signaling molecules. Serum-starved HUVECs were pretreated with 194-A for 30 min and then stimulated with 100 ng/mL VEGF-A for 10 min. Lysates were resolved in SDS-PAGE and probed with specific antibodies against p-Tyr1054 VEGFR-2, VEGFR-2, p-ERK1/2, ERK1/2 p-Akt, and Akt.

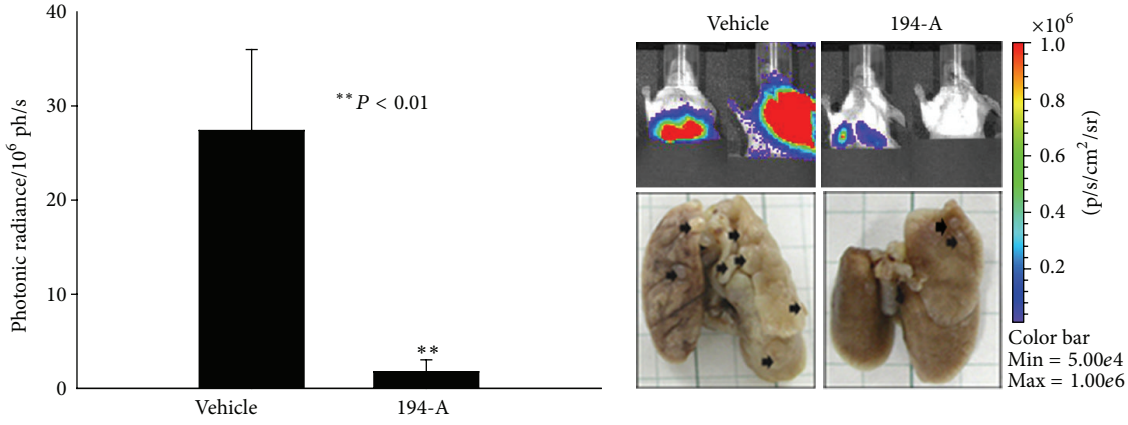

(a)

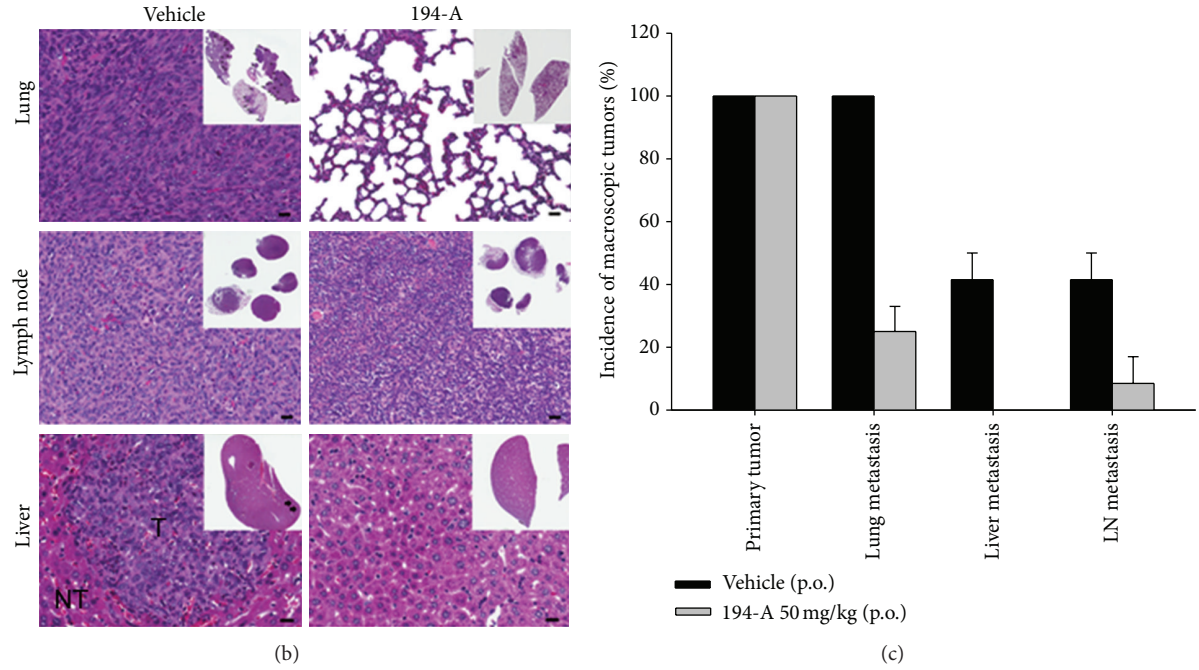

(b) (c)

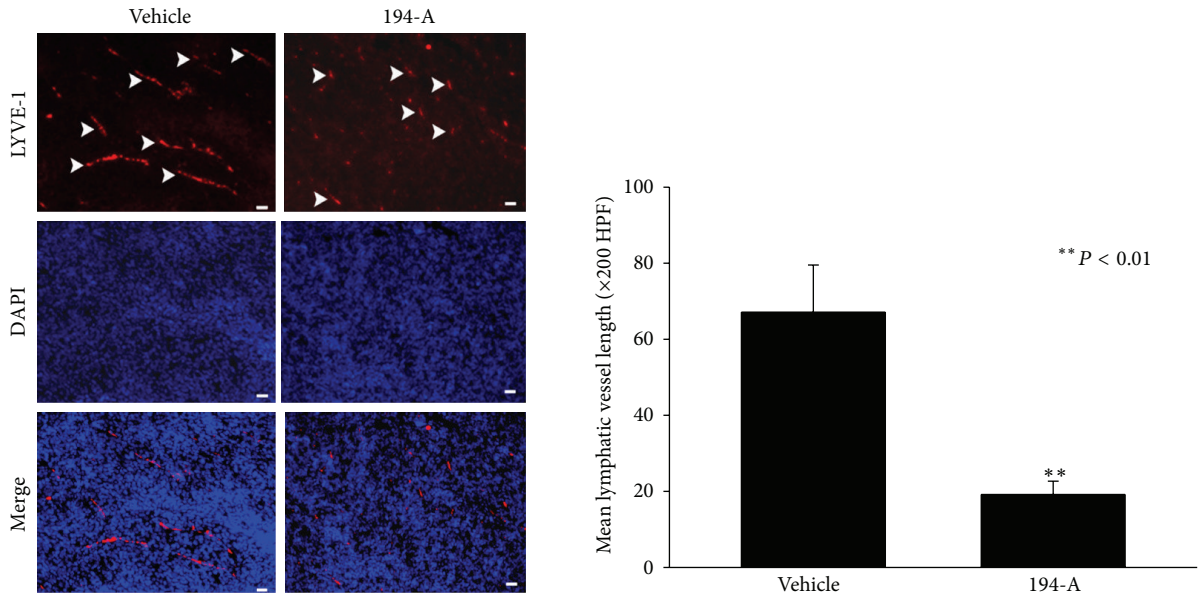

(d)

Figure 3: Continued.

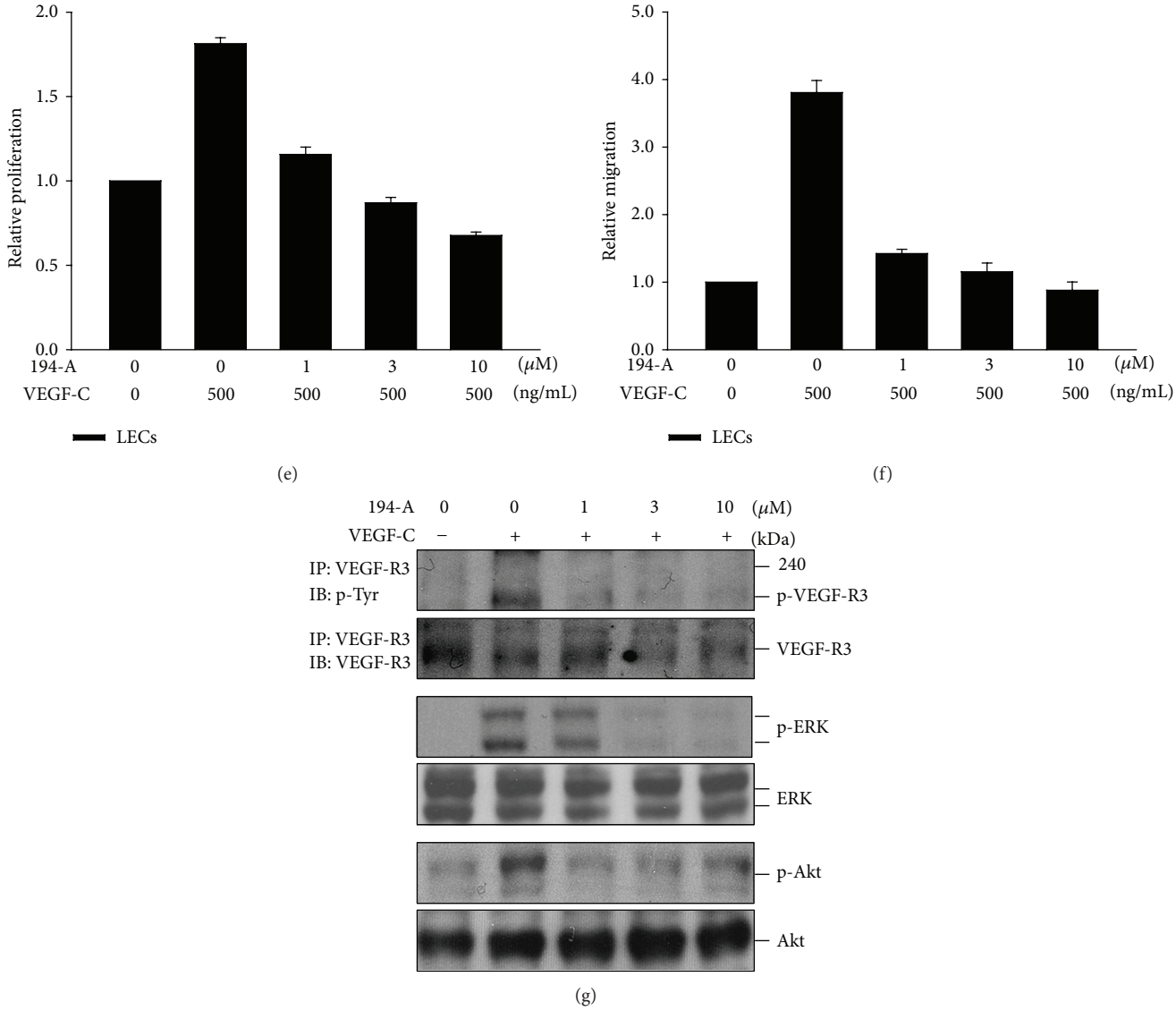

Figure 3: Significant antimetastatic and antilymphangiogenic effect of 194-A in the 4T1 orthotopic graft model. (a) 4T1-Luc$^+$ (5×10^5 cells/mouse) were orthotopically implanted into the fat pad of male BALB/c mice. Mice were p.o. administered with 50 mg/kg/day of 194-A or vehicle control for 30 days. At the end of the study, lung metastasis was measured by *in vivo* bioluminescent signals and *ex vivo* visualization. Arrow indicates metastatic tumor nodules. (b) Histological analyses of lung, liver, and lymph node metastasis from vehicle or 194-A-treated group. T, tumor part; NT, nontumor part. (c) The incidence of tumor metastasis was evaluated by histological analyses of the lung, liver, and lymph node. Mean values of two replicates; *bars*, SE. (d) Cryostat sections of 4T1 tumors, from mice treated with 194-A or vehicle control, were stained against LYVE-1 for the quantification of the mean lymphatic vessel length (LVL). Vessel length per 200x field was assessed from 3 to 4 fields per tumor section. *Columns*, mean ($n = 6$); *bars*, SE. $^{**}P < 0.01$ as compared to the vehicle control group. Scale bar, 20 μm. (e) and (f) Relative proliferation or migration of LECs grown in serum-free media supplemented with 500 ng/mL of VEGF-C as indicated. Proliferation (e) or migration (f) was reduced in a dose-dependent manner in response to 194-A treatment. Mean values of three replicates, normalized to the untreated controls; *bars*, SE. (g) 194-A inhibited VEGF-C-induced activation of VEGFR-3 and its common downstream signaling molecules. Serum-starved LECs were pretreated with 194-A for 30 min and then stimulated with 100 ng/mL VEGF-C for 10 min. Lysates were subjected to immunoprecipitation (IP) with VEGFR-3-specific antibody and resolved in SDS-PAGE, or resolved in SDS-PAGE directly and probed with specific antibodies against p-Tyr, VEGFR-3, p-ERK1/2, ERK1/2 p-Akt, and Akt.

in cancer cells. Furthermore, we confirmed the effect of 194-A on tumor growth and metastasis using xenograft models of two highly metastatic cell lines, Lewis lung carcinoma, and B16/F10 (data not shown). These studies implicate the pivotal role of VEGFRs/FGFRs in cancer progression and metastasis.

Angiogenesis itself is a complex, multistep process that follows stage- and tissue-specific regulations. Various angiogenic factors have been identified that form an intimate network regulating angiogenesis. The most successful anti-angiogenic approaches are likely to involve combinatorial

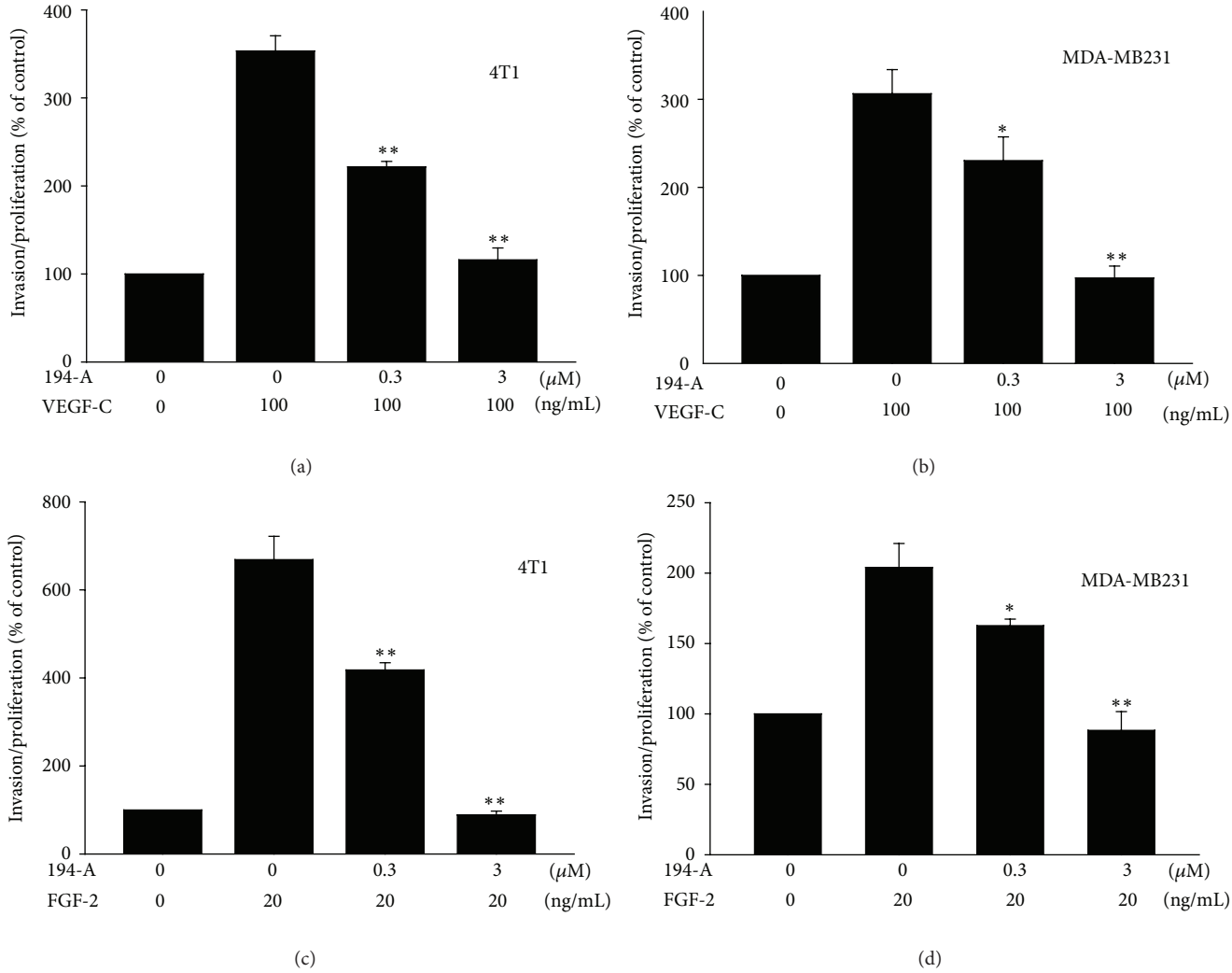

Figure 4: Effect of 194-A on VEGF-C or FGF-2-induced invasive effects in mammary carcinoma cells. Relative invasion of 4T1 and MDA-MB231 grown in low-serum (1% FBS) media supplemented with 100 ng/mL of VEGF-C (a) or 20 ng/mL FGF-2 (b) as indicated. Invasive ability was reduced in a dose-dependent manner in response to 194-A treatment. Mean value of three replicates, normalized to the untreated controls; *bars*, SE. $^{*}P < 0.05$; $^{**}P < 0.01$ as compared to the VEGF-C or FGF-2 treatment group.

strategies to target the angiogenic factors appearing on the central stage of the angiogenesis network, such as VEGF, FGF, and PDGF. Some dual-action inhibitors have emerged that are more effective in restraining cancer growth. For example, sunitinib inhibits PDGF and VEGF receptors [33]; ZD6474 inhibits VEGFR and EGFR [34]; VX-322 inhibits FLT-3 and c-KIT [35]. Both VEGF and FGF are potent angiogenic factors. An intimate crosstalk exists among FGF-2 and the different members of the VEGF family during angiogenesis and lymphangiogenesis [36]. Previous reports have demonstrated that combinatory inhibition of VEGFR-1 and FGFR-1 produced an enhanced suppression of tumor growth in different types of cancer [37]. Our observation is in line with these studies, suggesting that blockade of both VEGFRs and FGFRs would efficiently inhibit angiogenesis.

Preventative antiangiogenic strategies could be especially useful in patients who are at high risk for developing metastasis. Few experimental studies in animals, as well as in clinical trials, have already shown promising results. For example, angiostatin and endostatin reduced the formation of metastasis in the murine Lewis lung carcinoma model [38, 39]. Additionally, regional lymph nodes are often the primary sites for metastasis, emphasizing the importance of the lymphatic system in metastatic process. Blocking the lymphangiogenic process has reduced metastasis to both the lymph node and distant organs [40]. Dual inhibition of both VEGFR-3 and VEGFR-2 appeared to be a better strategy to suppress tumor metastasis as both VEGFR-2 and VEGFR-3 are essentially involved in tumor angiogenesis and lymphangiogenesis. Supportive evidence from previous report showed that combination treatment using anti-VEGFR-2 and anti-VEGFR-3 antibodies more potently decreased lymph node and lung metastasis than each antibody treated alone [41]. The results of our study also highlight the significance

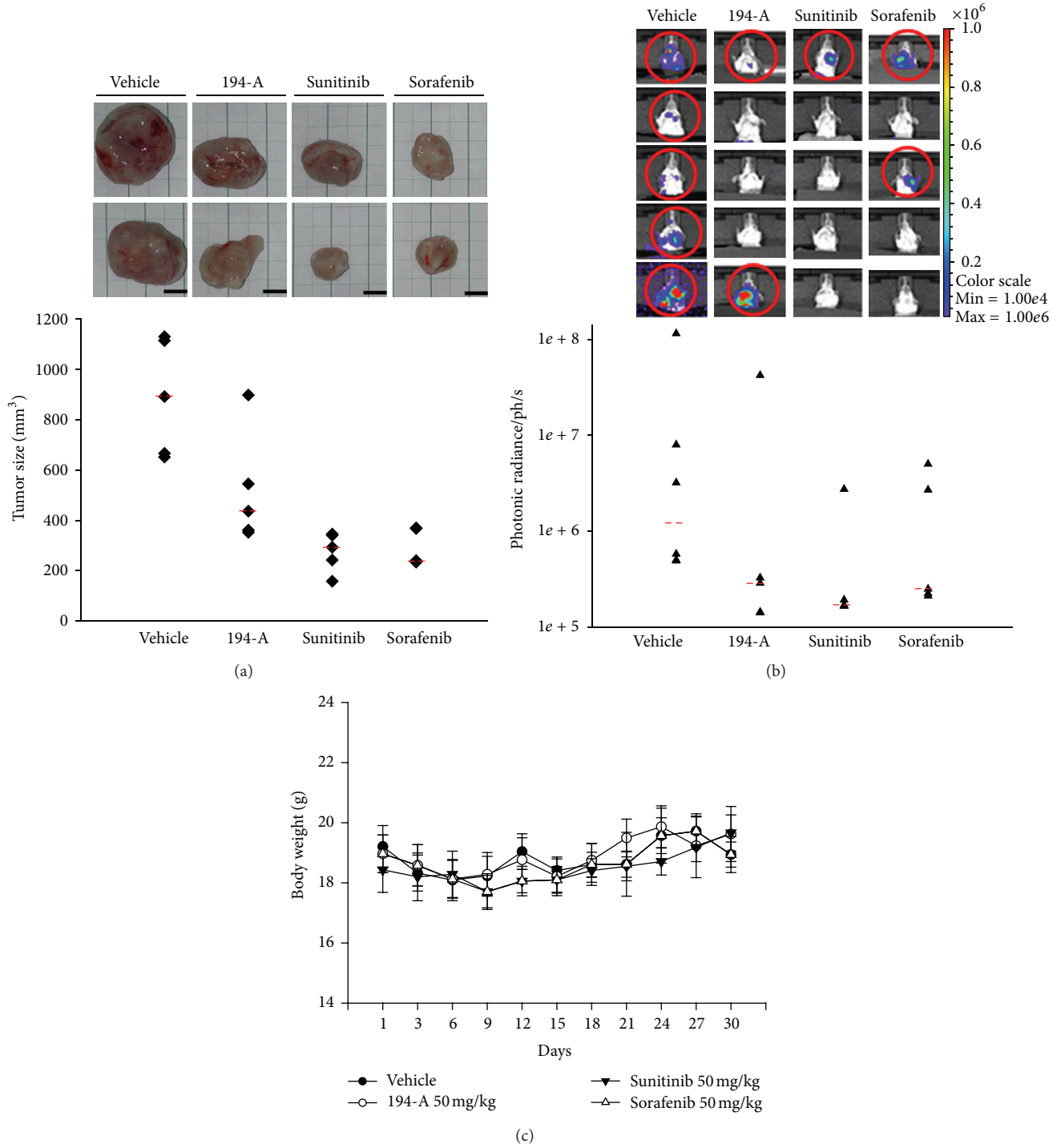

FIGURE 5: Comparison of the antitumor activity of 194-A with sunitinib or sorafenib in the 4T1 orthotopic graft model. (a) At the end of study, the tumor volume in mice treated with vehicle, 50 mg/kg/day 194-A (p.o.), sunitinib (p.o.), or sorafenib (p.o.) was measured by using a caliper. The median value of tumor volume was indicated. (b) Lung metastasis was measured at the end of study by *in vivo* bioluminescent signals. The median value of photon emissions was indicated. *Bars*, median values ($n = 5$). (c) 194-A, sunitinib, or sorafenib treatment did not affect the body weights significantly. *Lines*, mean ($n = 5$); *bars*, SE.

of inhibition of VEGFR-3 and VEGFR-2 kinases in lymphatic and vascular endothelial cells, which reduced lymphangiogenesis and angiogenesis, resulted in inhibition of regional lymph node and distal organs metastasis.

The invasive ability of tumor cell is a critical determinant of the metastatic phenotype of human cancers. Several sets of growth factors and their cognate receptors have been reported to be importantly involved in the regulation of

tumor invasion and metastasis [42]. Earlier, we have demonstrated that the VEGF-C/VEGFR-3 signal directly promote cancer cells invasion and increase both lymph node and lung metastasis in xenograft model of human lung adenocarcinoma [10]. Treatment with a soluble form of VEGFR-3 (Flt4/Fc) suppressed lung and lymph node metastasis of two distinct lung tumor cell lines (A549 cells and VEGF-C-overexpressing H928 cells) [10]. 194-A might, therefore, directly inhibit VEGFR-3 in tumor cells, to down-regulate invasive activity and suppress tumor metastasis. Furthermore, it has also been demonstrated that FGFRs can mediate cell proliferation and the invasive ability of breast cancer cells [20, 29]. Indeed, both 4T1 (Supplementary Figure 2(b)) and MDA-MB-231 [30] cells expressed high levels of FGFR-2. We found that 194-A inhibited FGF-2-induced invasive ability of 4T1 cells more significantly than other chemoattractant (fibronectin) (data not shown). These observations suggest that the antitumor metastasis activity of 194-A *in vivo* might be, at least in part, attributed to reduced tumor cell invasiveness via inhibition of VEGFR-3- and FGFRs-mediated signaling on tumor cells.

Multiple pathways promote tumor angiogenesis and lymphangiogenesis. To restrict the metastatic spread of cancer, the ideal drug should counteract the essential angiogenic and lymphangiogenic factors produced by cancer cells and/or stromal cells during tumor progression. Clinically, VEGFRs/FGFRs expression is associated with poor prognosis in multiple cancer type.

5. Conclusion

This study has validated the VEGFRs/FGFRs-mediated signaling pathways as a potential therapeutic target for inhibiting the metastatic spread of tumor cells. These encouraging data support further evaluation of VEGFRs/FGFRs inhibition for the treatment of highly metastatic cancer. It will also be tempting to determine whether this inhibition combined with conventional cytotoxic therapy could result in added efficacy without drawbacks in the near future.

Conflict of Interests

None of the authors have any conflict of interests regarding this research.

Authors' Contribution

Ming-Hsien Chien and Liang-Ming Lee contributed equally to this work.

Acknowledgments

This work was supported by research grants from the National Science Council of the Republic of China (NSC97-2323-B-002-011) to Min-Liang Kuo, Taipei Medical University-Wan Fang Hospital, Taiwan, (102 TMU-WFH-04) to Ming-Hsien Chien.

References

[1] N. Ferrara and T. Davis-Smyth, "The biology of vascular endothelial growth factor," *Endocrine Reviews*, vol. 18, no. 1, pp. 4–25, 1997.

[2] G. H. Fong, J. Rossant, M. Gertsenstein, and M. L. Breitman, "Role of the Flt-1 receptor tyrosine kinase in regulating the assembly of vascular endothelium," *Nature*, vol. 376, no. 6535, pp. 66–70, 1995.

[3] F. Shalaby, J. Rossant, T. P. Yamaguchi et al., "Failure of blood-island formation and vasculogenesis in Flk-1 deficient mice," *Nature*, vol. 376, no. 6535, pp. 62–66, 1995.

[4] D. J. Dumont, L. Jussila, J. Taipale et al., "Cardiovascular failure in mouse embryos deficient in VEGF receptor-3," *Science*, vol. 282, no. 5390, pp. 946–949, 1998.

[5] A. K. Olsson, A. Dimberg, J. Kreuger, and L. Claesson-Welsh, "VEGF receptor signalling—in control of vascular function," *Nature Reviews Molecular Cell Biology*, vol. 7, no. 5, pp. 359–371, 2006.

[6] T. Mäkinen, L. Jussila, T. Veikkola et al., "Inhibition of lymphangiogenesis with resulting lymphedema in transgenic mice expressing soluble VEGF receptor-3," *Nature Medicine*, vol. 7, no. 2, pp. 199–205, 2001.

[7] J. L. Su, C. J. Yen, P. S. Chen et al., "The role of the VEGF-C/VEGFR-3 axis in cancer progression," *British Journal of Cancer*, vol. 96, no. 4, pp. 541–545, 2007.

[8] N. R. Smith, D. Baker, N. H. James et al., "Vascular endothelial growth factor receptors VEGFR-2 and VEGFR-3 are localized primarily to the vasculature in human primary solid cancers," *Clinical Cancer Research*, vol. 16, no. 14, pp. 3548–3561, 2010.

[9] Z. Von Marschall, T. Cramer, and M. Höcker, "De novo expression of vascular endothelial growth factor in human pancreatic cancer: evidence for an autocrine mitogenic loop," *Gastroenterology*, vol. 119, no. 5, pp. 1358–1372, 2000.

[10] J. L. Su, P. C. Yang, J. Y. Shih et al., "The VEGF-C/Flt-4 axis promotes invasion and metastasis of cancer cells," *Cancer Cell*, vol. 9, no. 3, pp. 209–223, 2006.

[11] J. Matsui, Y. Funahashi, T. Uenaka, T. Watanabe, A. Tsuruoka, and M. Asada, "Multi-kinase inhibitor E7080 suppresses lymph node and lung metastases of human mammary breast tumor MDA-MB-231 via inhibition of vascular endothelial growth factor-receptor (VEGF-R) 2 and VEGF-R3 kinase," *Clinical Cancer Research*, vol. 14, no. 17, pp. 5459–5465, 2008.

[12] S. Elbauomy Elsheikh, A. R. Green, M. B. Lambros et al., "FGFR1 amplification in breast carcinomas: a chromogenic in situ hybridisation analysis," *Breast Cancer Research*, vol. 9, no. 2, p. R23, 2007.

[13] D. Meijer, A. M. Sieuwerts, M. P. Look, T. Van Agthoven, J. A. Foekens, and L. C. J. Dorssers, "Fibroblast growth factor receptor 4 predicts failure on tamoxifen therapy in patients with recurrent breast cancer," *Endocrine-Related Cancer*, vol. 15, no. 1, pp. 101–111, 2008.

[14] M. Mohammadi, S. K. Olsen, and O. A. Ibrahimi, "Structural basis for fibroblast growth factor receptor activation," *Cytokine and Growth Factor Reviews*, vol. 16, no. 2, pp. 107–137, 2005.

[15] J. Adnane, P. Gaudray, C. A. Dionne et al., "BEK and FLG, two receptors to members of the FGF family, are amplified in subsets of human breast cancers," *Oncogene*, vol. 6, no. 4, pp. 659–663, 1991.

[16] S. Jaakkola, P. Salmikangas, S. Nylund et al., "Amplification of fgfr4 gene in human breast and gynecological cancers," *International Journal of Cancer*, vol. 54, no. 3, pp. 378–382, 1993.

[17] F. Penault-Llorca, F. Bertucci, J. Adelaide et al., "Expression of FGF and FGF receptor genes in human breast cancer," *International Journal of Cancer*, vol. 61, no. 2, pp. 170–176, 1995.

[18] D. M. Ornitz and N. Itoh, "Fibroblast growth factors," *Genome Biology*, vol. 2, no. 3, article 3005, 2001.

[19] R. Grose and C. Dickson, "Fibroblast growth factor signaling in tumorigenesis," *Cytokine and Growth Factor Reviews*, vol. 16, no. 2, pp. 179–186, 2005.

[20] K. Suyama, I. Shapiro, M. Guttman, and R. B. Hazan, "A signaling pathway leading to metastasis is controlled by N-cadherin and the FGF receptor," *Cancer Cell*, vol. 2, no. 4, pp. 301–314, 2002.

[21] V. D. Acevedo, R. D. Gangula, K. W. Freeman et al., "Inducible FGFR-1 activation leads to irreversible prostate adenocarcinoma and an epithelial-to-mesenchymal transition," *Cancer Cell*, vol. 12, no. 6, pp. 559–571, 2007.

[22] R. Sharpe, A. Pearson, M. T. Herrera-Abreu et al., "FGFR signaling promotes the growth of triple-negative and basal-like breast cancer cell lines both in vitro and in vivo," *Clinical Cancer Research*, vol. 17, no. 16, pp. 5275–5286, 2011.

[23] J. H. Dey, F. Bianchi, J. Voshol, D. Bonenfant, E. J. Oakeley, and N. E. Hynes, "Targeting fibroblast growth factor receptors blocks PI3K/AKT signaling, induces apoptosis, and impairs mammary tumor outgrowth and metastasis," *Cancer Research*, vol. 70, no. 10, pp. 4151–4162, 2010.

[24] K. Chanda, B. Maiti, G. S. Yellol, M. H. Chien, M. L. Kuo, and C. M. Sun, "Polymer supported synthesis of novel benzoxazole linked benzimidazoles under microwave conditions: in vitro evaluation of VEGFR-3 kinase inhibition activity," *Organic and Biomolecular Chemistry*, vol. 9, no. 6, pp. 1917–1926, 2011.

[25] M. T. Lin, R. C. Lee, P. C. Yang, F. M. Ho, and M. L. Kuo, "Cyclooxygenase-2 inducing Mcl-1-dependent survival mechanism in human lung adenocarcinoma CL1.0 cells: involvement of phosphatidylinositol 3-kinase/Akt pathway," *Journal of Biological Chemistry*, vol. 276, no. 52, pp. 48997–49002, 2001.

[26] J. D. Shields, M. S. Emmett, D. B. A. Dunn et al., "Chemokine-mediated migration of melanoma cells towards lymphatics—a mechanism contributing to metastasis," *Oncogene*, vol. 26, no. 21, pp. 2997–3005, 2007.

[27] C. Cursiefen, U. Schlötzer-Schrehardt, M. Küchle et al., "Lymphatic vessels in vascularized human corneas: immunohistochemical investigation using LYVE-1 and podoplanin," *Investigative Ophthalmology and Visual Science*, vol. 43, no. 7, pp. 2127–2135, 2002.

[28] C. J. Aslakson and F. R. Miller, "Selective events in the metastatic process defined by analysis of the sequential dissemination of subpopulations of a mouse mammary tumor," *Cancer Research*, vol. 52, no. 6, pp. 1399–1405, 1992.

[29] M. Koziczak, T. Holbro, and N. E. Hynes, "Blocking of FGFR signaling inhibits breast cancer cell proliferation through down-regulation of D-type cyclins," *Oncogene*, vol. 23, no. 20, pp. 3501–3508, 2004.

[30] V. Nurcombe, C. E. Smart, H. Chipperfield, S. M. Cool, B. Boilly, and H. Hondermarck, "The proliferative and migratory activities of breast cancer cells can be differentially regulated by heparan sulfates," *Journal of Biological Chemistry*, vol. 275, no. 39, pp. 30009–30018, 2000.

[31] D. B. Mendel, A. Douglas Laird, X. Xin et al., "In vivo antitumor activity of SU11248, a novel tyrosine kinase inhibitor targeting vascular endothelial growth factor and platelet-derived growth factor receptors: determination of a pharmacokinetic/pharmacodynamic relationship," *Clinical Cancer Research*, vol. 9, no. 1, pp. 327–337, 2003.

[32] S. M. Wilhelm, C. Carter, L. Tang et al., "BAY 43-9006 exhibits broad spectrum oral antitumor activity and targets the RAF/MEK/ERK pathway and receptor tyrosine kinases involved in tumor progression and angiogenesis," *Cancer Research*, vol. 64, no. 19, pp. 7099–7109, 2004.

[33] R. Roskoski, "Sunitinib: a VEGF and PDGF receptor protein kinase and angiogenesis inhibitor," *Biochemical and Biophysical Research Communications*, vol. 356, no. 2, pp. 323–328, 2007.

[34] S. R. Wedge, D. J. Ogilvie, M. Dukes et al., "ZD6474 inhibits vascular endothelial growth factor signaling, angiogenesis, and tumor growth following oral administration," *Cancer Research*, vol. 62, no. 16, pp. 4645–4655, 2002.

[35] D. K. Heidary, G. Huang, D. Boucher et al., "VX-322: a novel dual receptor tyrosine kinase inhibitor for the treatment of acute myelogenous leukemia," *Journal of Medicinal Chemistry*, vol. 55, no. 2, pp. 725–734, 2012.

[36] M. Presta, P. Dell'Era, S. Mitola, E. Moroni, R. Ronca, and M. Rusnati, "Fibroblast growth factor/fibroblast growth factor receptor system in angiogenesis," *Cytokine and Growth Factor Reviews*, vol. 16, no. 2, pp. 159–178, 2005.

[37] T. Ogawa, K. Takayama, N. Takakura, S. Kitano, and H. Ueno, "Anti-tumor angiogenesis therapy using soluble receptors: enhanced inhibition of tumor growth when soluble fibroblast growth factor receptor-1 is used with soluble vascular endothelial growth factor receptor," *Cancer Gene Therapy*, vol. 9, no. 8, pp. 633–640, 2002.

[38] M. S. O'Reilly, "Angiostatin: an endogenous inhibitor of angiogenesis and of tumor growth," *EXS*, vol. 79, pp. 273–294, 1997.

[39] M. S. O'Reilly, T. Boehm, Y. Shing et al., "Endostatin: an endogenous inhibitor of angiogenesis and tumor growth," *Cell*, vol. 88, no. 2, pp. 277–285, 1997.

[40] S. A. Stacker, M. E. Baldwin, and M. G. Achen, "The role of tumor lymphangiogenesis in metastatic spread," *The FASEB Journal*, vol. 16, no. 9, pp. 922–934, 2002.

[41] N. Roberts, B. Kloos, M. Cassella et al., "Inhibition of VEGFR-3 activation with the antagonistic antibody more potently suppresses lymph node and distant metastases than inactivation of VEGFR-2," *Cancer Research*, vol. 66, no. 5, pp. 2650–2657, 2006.

[42] G. Christofori, "New signals from the invasive front," *Nature*, vol. 441, no. 7092, pp. 444–450, 2006.